Norwegian University of Life Sciences
Faculty of Science and Technology

Philosophiae Doctor (PhD)
Thesis 2024:5

Comprehensive phenotypic characterization of newly isolated cold-adapted bacteria from Antarctic temporary meltwater ponds

Omfattende fenotypisk karakterisering av nylig isolerte kuldetilpassede bakterier fra midlertidige smeltevannsbassenger i Antarktis

Volha Akulava

Comprehensive phenotypic characterization of newly isolated cold-adapted bacteria from Antarctic temporary meltwater ponds

Omfattende fenotypisk karakterisering av nylig isolerte kuldetilpassede bakterier fra midlertidige smeltevannsbassenger i Antarktis

Philosophiae Doctor (PhD) Thesis

Volha Akulava

Norwegian University of Life Sciences
Faculty of Science and Technology

Ås 2023

Thesis number 2024:5
ISSN 1894-6402
ISBN 978-82-575-2122-6

Supervisors and Evaluation Committee

Main supervisor:	Assoc. Prof. Dr. Volha Shapaval Norwegian University of Life Sciences Faculty of Science and Technology
Co-supervisors:	Prof. Dr. Achim Kohler Norwegian University of Life Sciences Faculty of Science and Technology
	Assoc. Prof. Dr. Uladzislau Miamin Belarussian State University Faculty of Biology
	Assoc. Prof. Dr. Leonid Valentovich Institute of Microbiology
Evaluation committee:	Prof. Dr. Gianluigi Cardinali University of Perugia
	Dr. Francesca Di Bartolomeo SINTEF
Coordinator:	Associate Professor Zakhar Maletskyi Norwegian University of Life Sciences Faculty of Science and Technology

Table of Contents

Acknowledgements

The present PhD study has been conducted from 2018 to 2023 at the Faculty of Science and Technology (REALTEK), Norwegian University of Life Sciences (NMBU), in the Biospectroscopy and Data Modeling group (BioSpec), in collaboration with the Faculty of Biology, Belarussian State University (BSU). This research was supported by the project "Belanoda—Multidisciplinary graduate and post-graduate education in big data analysis for life sciences" (CPEA-LT-2016/10126) and the "Belanoda—Digital learning platform for boosting multidisciplinary education in data analysis for life sciences in the Eurasia region" (CPEA-STA-2019/10025) funded by the Eurasia program, Norwegian Agency for International Cooperation and Quality Enhancement in Higher Education (Diku).

I would like to express my gratitude to my primary supervisor, Assoc. Prof. Volha Shapaval, and my co-supervisor, Prof. Achim Kohler, for their unwavering guidance and invaluable expertise throughout my Ph.D. journey. Their availability and support, even amidst their busy schedules, have been truly appreciated. I am thankful for the engaging discussions, their significant contributions, their respectful and empathetic approach, and for giving me the opportunity to be a part of the BioSpec group. Thank you for helping me to get truly multidisciplinary experience in many directions like biotechnology, spectroscopy and data analysis and teaching me how to study biology through the prism of spectroscopy. I would like to extend my gratitude to my co-supervisors, Assoc. Prof. Leonid Valentovich, for his patience and unwavering support, thank you for opening a big scientific world for me and sharing with me valuable knowledge in molecular biology and always supporting my ideas. I would also like to thank my co-supervisor, Assoc. Prof. Vladislau Miamin for all his scientific contributions and support along the entire PhD journey. Many thanks to Dana Byrtusova, Boris Zimmerman, Valeria Tafintseva, Margarita Smirnova, Vlad Blazhko, Dag Ekeberg, and Andrey Dolgih for your time and

expertise which contributed to the publications presented in this thesis are highly appreciated.

I want to extend my deep appreciation to Vlad Blazhko for his unwavering support. His problem-solving skills are nothing short of magical. Thank you, Dana, for always being near and supporting me and for all amazing trips. I would like to thank Margarita Smirnova for the wonderful times we've had in the lab, to Cristian Bolano Losada for being a valuable scientific expert and for his invaluable advice and enjoyable conversations, to Simona Dzurendova, you have been the best office mate and for helping and sharing her experience in many fields. Miriam Aledda, Clementine Isembart, Ondrej Slany and Benjamin Xavier Dupuy, it has been a pleasure sharing the lab with you. I would like to acknowledge the entire Biospec and our neighbour Robotics group for fostering a friendly and collaborative working environment, for sharing their knowledge and for constant support. It has been five incredible years filled with unforgettable moments. I also want to thank Berit Hauger Lindstad for her invaluable assistance in coordinating my PhD journey.

Certainly, life is not only work. I want to express my deep gratitude to my family and friends for their unwavering love, constant support, and for reminding me of life's essential things. They have always believed in me, and for that, I am truly grateful.

Volha Akulava

Ås, November 2023

Abstract

Antarctic meltwater ponds are unique unexplored biotopes characterized by a high complexity of microbiota and affected by ever-changing ecological factors. Cold-adapted bacteria isolated from Antarctic meltwater ponds represent excellent model organisms to study climate change induced stress adaptation. Moreover, these bacteria may possess biotechnologically relevant properties and can be used for production of valuable chemicals.

The main aim of this PhD work was to perform comprehensive phenotypic characterization of newly isolated cold-adapted bacteria from unexplored sea-affected meltwater ponds in the Thala Hills Oasis (Enderby Land, East Antarctica). As a first step of the PhD work, physicochemical and biological analysis of water from the studied meltwater ponds as well as isolation and identification of bacteria, their physiological characterization and evaluation of their antibiotic susceptibility was performed in **Paper I**. It has been shown that the meltwater ponds have water with alkaline pH and can be characterized by a relatively high bacterial activity. In total of twenty-nine bacterial isolates were retrieved from the meltwater samples. By using 16S rRNA gene sequencing, the isolated bacteria were classified as Proteobacteria, Actinobacteria, Firmicutes, and Bacteroidetes, belonging to 12 genera where *Pseudomonas* was the predominant genus. Many isolates were psychrotrophic, capable of producing pigments and extracellular enzymes, where lipases and proteases were prevalent. Antibiotic susceptibility testing revealed a presence of resistance to at least one antibiotic for most of the isolates and seven isolates showed multi-resistance.

Alterations in cellular lipids are considered as one of the adaptation strategies to harsh environmental conditions. Temperature is one of the most important factors inducing tremendous biochemical changes in bacterial cells. Temperature-induced changes of cellular lipids and other biomolecules in the isolated Antarctic meltwater bacteria were studied in

Paper II. A distinct change in fatty acid profile for different Gram-groups, phyla, genera, and species was observed. Notably, most bacteria increased their lipid content when grown at lower temperatures. Fourier-transform infrared spectroscopy (FTIR) analysis highlighted temperature-triggered alterations in lipids, proteins and polysaccharides, where the most significant changes were observed in the polysaccharide region at 1200-900 cm^{-1}, particularly for the peak at 1083 cm^{-1}, related to phosphodiester groups mainly from phospholipids (for Gram-negative bacteria) and teichoic /lipoteichoic acids (for Gram-positive bacteria).

In order to further understand temperature-induced cellular biochemical responses in Antarctic meltwater bacteria, profiling of the total cellular biochemical profile of bacteria grown at different temperatures and in various forms of culture medium was performed in **Paper III**. The obtained results showed that overall variability of cell chemistry was lower when bacteria were cultivated on agar. The effect of temperature appeared to be specie-specific with the biggest alterations detected for the bacteria with a wide growth temperature range. Lipids were least affected while polysaccharides were the most affected by the temperature.

In **Paper I** it was observed that several of the newly isolated cold-adapted bacteria were pigmented. Therefore, in **Paper IV** pigment production was studied using FT-Raman spectroscopy and reference analytical techniques. High-throughput screening performed by FT-Raman indicated that from twenty-nine tested bacteria seven Antarctic meltwater bacteria were characterized by pigments production. Among pigments identified in the meltwater bacteria, several have industrial importance – such as β-carotene, canthaxanthin, lycopene, and zeaxanthin. A subset of the pigment producing meltwater bacteria was further studied to evaluate pigment production and biomass productivity under blue-light exposition. Due to that bacterial pigments have been suggested to be used in solar cells dyeing or dye-synthesized solar cells, a photostability of intact pigment bacterial biomass was investigated.

Overall, this PhD work provided comprehensive knowledge on the biochemical characterization and biotechnological potential of the

Antarctic meltwater pound bacteria. It was shown that isolates from Antarctic MPs may have biotechnological potential and could be used as bioindicators to track antibiotic resistance spreading and the impact of human or animal presence in polar regions. This PhD work showed that Antarctic meltwater bacteria change their total biochemical profile in response to different temperatures and this change is species-specific. Several meltwater bacterial isolates showed to be promising producers of industrially relevant pigments. Finally, this PhD work showed remarkable effectiveness of high-throughput FTIR and FT-Raman spectroscopy for screenings, bioprospecting, and biochemical characterization of newly isolated bacteria.

Norsk sammendrag

Antarktiske smeltevannsdammer er unike og uutforskede biotoper kjennetegnet av høy kompleksitet av mikrobiota og påvirket av stadig skiftende økologiske faktorer. Kaldtilpassede bakterier isolert fra Antarktis' smeltevannsdammer representerer utmerkede modellorganismer for å studere tilpasning til klimaendringer. Videre kan disse bakteriene inneha bioteknologisk relevante egenskaper og brukes til produksjon av verdifulle kjemikalier.

Hovedmålet med denne doktorgradsoppgaven var å utføre omfattende fenotypisk karakterisering av nylig isolerte kaldtilpassede bakterier fra uutforskede smeltevannsdammer som er påvirket av havet i Thala Hills Oasis (Enderby Land, Øst-Antarktis). Som det første trinnet i doktorgradsoppgaven ble fysisk-kjemisk og biologisk analyse av vann fra de studerte smeltevannsdammene, samt isolasjon og identifikasjon av bakterier, fysiologisk karakterisering og evaluering av deres antibiotikaresistens utført i **Artikkel I**. Det ble vist at smeltevannsdammene har vann med alkalisk pH og kan kjennetegnes av en relativt høy bakteriell aktivitet. Totalt ble tjueni bakterieisolater isolert fra prøvene. Ved hjelp av 16S rRNA-genavlesning ble de isolerte bakteriene klassifisert som Proteobakterier, Actinobakterier, Firmicutes og Bacteroidetes, som tilhører tolv slekter, hvor *Pseudomonas* var den dominerende slekten. Mange isolater var psykrotrofe, i stand til å produsere pigmenter og ekstracellulære enzymer, hvor lipaser og proteaser var mest fremtredende. Testing for antibiotikaresistens avslørte tilstedeværelsen av resistens mot minst ett antibiotikum for de fleste isolatene, og syv isolater viste multiresistens.

Endringer i cellulære lipider betraktes som en av tilpasningsstrategiene til tøffe miljøforhold. Temperatur er en av de viktigste faktorene som utløser betydelige biokjemiske endringer i bakterieceller. Temperaturinduserte endringer i cellulære lipider og andre biomolekyler i de isolerte Antarktis-smeltevannsbakteriene ble studert i **Artikkel II**. Det ble observert en tydelig

endring i fettsyreprofilen for forskjellige Gram-grupper, filer, slekter og arter. Spesielt økte de fleste bakteriene lipidinnholdet når de ble dyrket ved lavere temperaturer. Fouriertransform infrarød spektroskopi (FTIR) analyserte temperaturinduserte endringer i lipider, proteiner og polysakkarider, der de mest betydningsfulle endringene ble observert i polysakkaridområdet ved 1200-900 cm^{-1}, spesielt for toppen ved 1083 $cm^{-1,}$ relatert til fosfodiestergrupper hovedsakelig fra fosfolipider (for Gram-negative bakterier) og teikosyre/lipoteikosyre (for Gram-positive bakterier).

For å bedre forstå temperaturinduserte cellulære biokjemiske responser hos bakterier i antarktisk smeltevann, ble profilering av den totale cellulære biokjemiske profilen til bakterier dyrket ved ulike temperaturer og i ulike former for dyrkningsmedium utført i **Papir III**. De oppnådde resultatene viste at den generelle variasjonen i cellekjemien var lavere når bakteriene ble dyrket på agar. Effekten av temperaturen syntes å være arts-spesifikk, med de største endringene påvist hos bakteriene med et bredt temperaturområde for vekst. Lipider ble minst påvirket, mens polysakkarider var mest påvirket av temperaturen.

Som observert i **Artikkel I**, var noen bakterier pigmenterte, dette ble videre undersøkt i **Artikkel IV**, der pigmentproduksjon ble studert ved hjelp av FT-Raman spektroskopi og referanseanalytiske teknikker. Høykapasitets-screening utført med FT-Raman indikerte at av de tjueni testede bakteriene ble syv Antarktis-smeltevannsbakterier karakterisert av pigment-produksjon. Blant pigmentene som ble identifisert i smeltevanns-bakteriene, hadde flere industriell betydning, som β-karoten, kanthaxantin, lycopen og zeaxantin. En del av de pigmentproduserende smeltevannsbakteriene ble ytterligere studert for å evaluere pigmentproduksjon og biomasseproduktivitet under eksponering for blått lys. Siden bakteriepigmenter har blitt foreslått å bli brukt i farging av solceller eller solcelle-dyeing, ble fotostabiliteten til intakt pigmentbakteriebiomasse undersøkt.

Totalt sett ga dette doktorgradsarbeidet omfattende kunnskap om den biokjemiske karakteriseringen og bioteknologiske potensialet til Antarktis-

smeltevannsbakterier. Det ble vist at isolater fra Antarktis' smeltevannsdammer kan ha bioteknologisk potensiale og kan brukes som bioindikatorer for å spore spredning av antibiotikaresistens og innvirkningen av menneskers eller dyrs tilstedeværelse i polarområdene. Dette doktorgradsarbeidet viste at Antarktis-smeltevannsbakterier endrer sin totale biokjemiske profil som svar på forskjellige temperaturer, og denne endringen er artsavhengig. Flere isolater av smeltevannsbakterier viste seg å være lovende produsenter av industrielt relevante pigmenter. Til slutt viste denne doktorgradsstudien en bemerkelsesverdig effektivitet av høykapasitets FTIR og FT-Raman spektroskopi for screening, bioprospektering og biokjemisk karakterisering av nylig isolerte bakterier.

List of papers

Paper I

Volha Akulava, Uladzislau Miamin, Katsiaryna Akhremchuk, Leonid Valentovich, Andrey Dolgikh, Volha Shapaval. **Isolation, Physiological Characterization, and Antibiotic Susceptibility Testing of Fast-Growing Bacteria from the Sea-Affected Temporary Meltwater Ponds in the Thala Hills Oasis (Enderby Land, East Antarctica).** *Biology* (Basel). 2022 Jul 29;11(8):1143. doi: 10.3390/biology11081143.

Paper II

Volha Akulava, Margarita Smirnova, Dana Byrtusova, Boris Zimmermann, Dag Ekeberg, Achim Kohler, Uladzislau Miamin, Leonid Valentovich, Volha Shapaval. **Explorative characterization and taxonomy-aligned comparison of alterations of lipids and other biomolecules in Antarctic bacteria grown at different temperatures.** *Environmental Microbiology, Under revision.*

Paper III

Volha Akulava, Valeria Tafintseva, Uladzislau Blazhko, Achim Kohler, Uladzislau Miamin, Leonid Valentovich, Volha Shapaval. **Global biochemical profiling of fast-growing bacteria from Antarctic meltwater ponds by high-throughput FTIR spectroscopy.** *Manuscript.*

Paper IV

Volha Akulava, Dana Byrtusova, Boris Zimmermann, Achim Kohler, Uladzislau Miamin, Leonid Valentovich, Volha Shapaval. **Screening for pigment production and characterization of pigment profile and photostability in cold-adapted Antarctic bacteria using FT-Raman spectroscopy.** *Journal of Photochemistry and Photobiology B: Biology, Submitted.*

Additional scientific contributions

Research publications

Keerthikka Ravi, Nicole R. Falkowski, Brittan S. Scales, Volha D. Akulava, Leonid N. Valentovich, Gary B. Huffnagle. **The Psychrotrophic *Pseudomonas lundensis*, a Non-aeruginosa Pseudomonad, Has a Type III Secretion System of the Ysc Family, Which Is Transcriptionally Active at 37°C.** *mBio.* 2022 Jan-Feb; 13(1): e03869-21. DOI: 10.1128/mbio.03869-21

Margarita Smirnova, Cristian Bolaño Losada, Volha Akulava, Volha Shapaval. **New cold-adapted bacteria for efficient hydrolysis of feather waste at low temperature.** *Bioresource Technology Reports* 23:101530. DOI: 10.1016/j.biteb.2023.101530

Oral and poster presentations as a main presenting author

Volha Akulava, Uladzislau Miamin, Katsiaryna Akhremchuk, Leonid Valentovich, Andrey Dolgikh, Volha Shapaval. **Comprehensive characterization of the fast-growing bacteria isolated from the meltwater ponds in the Thala Hills oasis (Enderby Land, East Antarctica).** Tvärminne Symposium on Polar Microbes and Viruses; 3^{d}-6th May 2022, Finland. Oral.

Volha Akulava, Boris Zimmermann, Margarita Smirnova, Achim Kohler Uladzislau Miamin, Volha Shapaval. **Profiling pigments in the psychrotrophic Antarctic bacteria by FT-Raman spectroscopy.** The 9th International Conference on Polar and Alpine Microbiology; 9th-14thOctober, Germany. Oral.

Volha Akulava, Achim Kohler, Leonid Valentovich, Uladzislau Miamin, Volha Shapaval. **High-throughput biochemical phenotyping of bacteria isolated from the coastal area of East Antarctica by PCA analysis of FTIR spectra.** Workshop on Machine Learning and Chemometrics in Biospectroscopy; 18th-19th August 2019, Belarus. Poster.

List of main abbreviations

BHIA	brain heart infusion agar
BHIB	brain heart infusion broth
br-SFA	branched saturated fatty acids
DNA	deoxyribonucleic acid
EMSC	extended multiplicative signal correction
EPS	exopolysaccharides
FA	fatty acid
FAME	fatty acid methyl esters
FTIR	Fourier transform infrared spectroscopy
FT-Raman	Fourier transform Raman spectroscopy
GC	gas chromatography
GC-FID	gas chromatography system equipped with a flame ionization detector
HTS	high-throughput setup
IR	infrared
IS	internal standard
MP	meltwater pond
MPA	meat peptone agar
MTPS	microtiter plate system
n-MUFA	normal/linear chain monounsaturated fatty acid
n-SFA	non-branched saturated fatty acid
Hydroxy -FA	hydroxy fatty acid
PC	principal components
PCA	principal component analysis
PCR	polymerase chain reaction
PHA	polyhydroxyalkanoate
PUFA	polyunsaturated fatty acid
rRNA	ribosomal ribonucleic acid
SG	Savitzky-Golay
TLC	thin layer chromatography

Aim of the thesis

The main aim of the thesis was to perform comprehensive phenotyping and characterization of cold-adapted bacteria, newly isolated from Antarctic meltwater ponds located in the Western part of Enderby Land, East Antarctica.

The sub-goals were:

1. To perform an overall physiological characterization and antibiotic susceptibility testing of cold-adapted bacteria **(Paper I)**

2. To perform characterization of temperature-associated alterations in lipids and other biomolecules in cold-adapted bacteria **(Paper II)**

3. To perform global biochemical phenotyping using FTIR spectroscopy of cold-adapted bacteria **(Paper III)**

4. To characterize carotenoids producing Antarctic bacteria and evaluate pigment stability using FT-Raman spectroscopy **(Paper IV)**

1 Introduction

1.1 Meltwater ponds – unique unexplored biotopes

Meltwater ponds (MPs) are temporary aquatic biotopes that form on the surface of glaciers and ice sheets (ice shelf MPs) [1] or rugged terrain, often between rocky ridges (terrestrial MPs) [2] when ice melts during the warmer months in polar and alpine regions such as Antarctica, Arctica [3, 4], Greenland [5] and others cold regions [6] (Figure 1.1). MPs exhibit considerable variation in size from small puddles to large, interconnected water bodies depending on their location and presence of slopes, and can be flowing, low-flowing, or non-flowing [7].

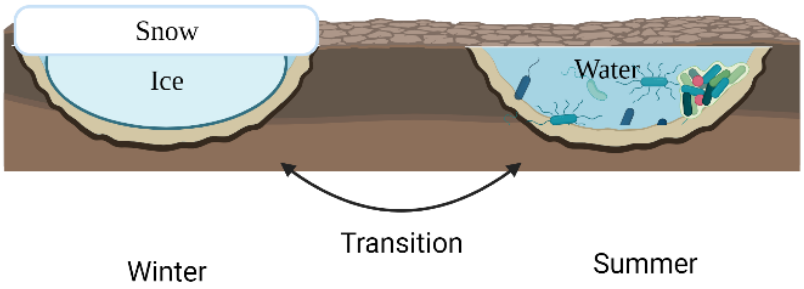

Figure 1.1. Formation of MPs

MPs are characterized by a high complexity of ever-changing ecological factors, such as (i) abiotic (temperature, freeze-thaw cycles, nutrient availability, abrupt chemical gradients, salinity, etc.), (ii) biotic (presence of plants, animals, microorganisms), and (iii) anthropogenic. The physicochemical (abiotic) factors affecting MPs vary widely depending on the size of a pond, surrounding mineral formations, and weather conditions. The most characteristic physicochemical abiotic factors [8-15] affecting MPs include the following:

(1) *Salinity:* MPs can be salty, with a salinity that is often higher than in seawater. The salinity of MPs is determined by the amount of salt in surrounding ice and rocks, as well as the amount of freshwater entering the pond.

(2) *pH:* the pH of MPs varies widely, with values ranging from neutral to alkaline (7-11.2) and it is influenced by the presence of organic matter, amount of dissolved gases, and weather conditions.
(3) *Temperature:* The temperature of water in MPs varies significantly depending on the depth of a pond and the season.
(4) *Nutrients availability:* Nutrients availability is essential for the MPs' microbiota diversity, and it varies depending on the surrounding geology and the amount of organic matter in the water. A presence of birds (skuas) and marine mammals close to MPs can significantly affect nutrients availability.
(5) *Dissolved oxygen:* The amount of dissolved oxygen in MPs is influenced by temperature, salinity, and the number of photosynthetic organisms occurring in the water.
(6) *Turbidity:* The number of suspended particles in water affects the turbidity of MPs.
(7) *Solar radiation:* Light intensity affects the temperature, algae growth, and chemical reactions in MPs, influencing their physicochemical parameters. It can also impact ice melting rates, microbial activity, and overall biological productivity in these aquatic biotopes.

MPs are often exposed to a series of biotic factors and are characterized by the presence of various microorganisms, invertebrates, and even visiting vertebrates like migratory birds [16] and mammals. Occasionally, migratory birds and seals visit these ponds for water and food, introducing nutrients and potentially affecting local ecology. Local human activities in the Antarctic environment have the potential to cause significant impacts, despite the continent's remote and pristine nature [17].

Antarctic MPs are affected by a high variety of abiotic and biotic factors and, therefore, considered as unique biotopes to explore. During the last decade, Antarctica has received a significant attention due to its vulnerability to ice sheet instability [18]. MPs observed in the East Antarctica in the areas of the McMurdo Ice Shelf (MIS) and Dry Valleys have been extensively studied [8-10, 12-15, 19] (Figure 1.2). MPs located in the north of the East Antarctica are not well explored. Most studies done so far

focused on the glaciology or geology of MPs occurring from surface ice melting on the Amery Ice Shelf [20], on Vestfold Hills [10] and Thala Hills [7] (Figure 1.2). The microbial diversity of MPs in the north of East Antarctica was studied to a very little extent.

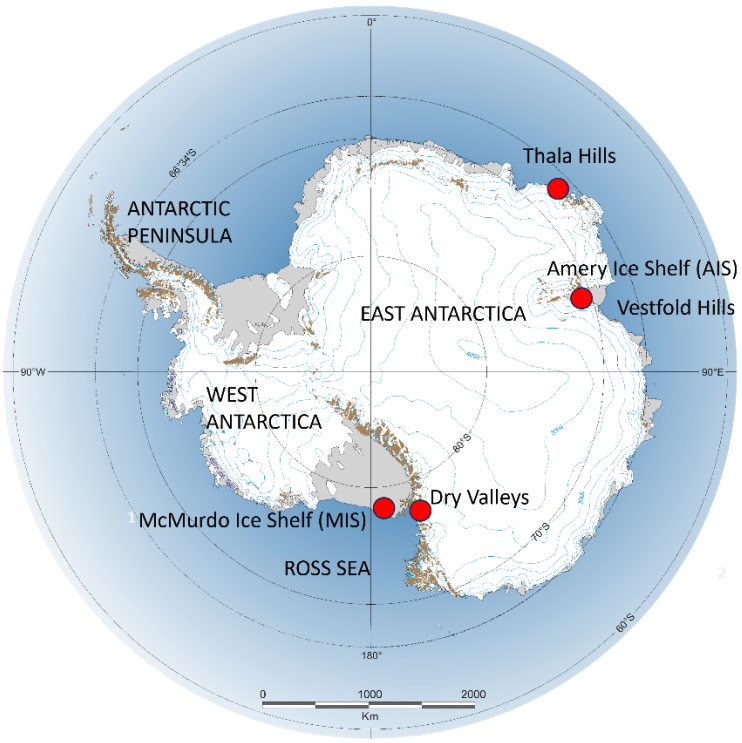

Figure 1.2. Antarctica regions with the studied MPs.

1.2 Microbiota of Antarctic meltwater ponds

Due to the exposure to a wide range of ecological factors, Antarctic MPs are considered as biotopes with **highly diverse microbiota of cold-adapted psychrophilic and psychrotrophic microorganisms** [12, 15, 21, 22].

According to previously reported studies which assessed the overall microbial diversity using a cultivation-independent approach, bacteria are the most prevalent group of microorganisms present in Antarctic environments. The abundance of either fungi or archaea varies depending

on the specific environmental sample being evaluated [23]. It has been reported that **Cyanobacteria and Proteobacteria** are the predominant type of microorganisms found in Antarctic MP mats and sediments, and glacial meltwater [10, 14, 24, 25]. Interestingly, Cyanobacteria are dominating also in Arctic [4] and other extreme ecosystems such as hot springs and desert crusts [10]. Commonly reported microorganisms found in MPs are **cyanobacteria**: *Nostoc*, *Phormidium*, *Oscillatoria*, *Leptolyngbya* and *Gloeocapsa* [4, 10], **bacteria**: Actinobacteria, Bacteroidetes, Acidobacteria, Firmicutes, Chloroflexi, Verrucomicrobia and Planctomycetes [14, 26, 27], **archaea**: Euryarcheaota and Crenarcheota [4], **fungi**: Ascomycota and Chytridiomycota [23, 28, 29], **yeast**: *Cryptococcus victoriae*, *Cryptococcus friedmannii*, *Leucosporidium scottii*, and *Rhodotorula glacialis* [30]. Overall, a high microbiota diversity was reported between different ponds, and it was highly pond-specific [17]. Geochemically stratification inside of each meltwater ponds and especially pH and conductivity gradients are key factors contributing to variations of the bacterial community inside each pond [31].

Research on microbiota of the Antarctic meltwater ponds offers an opportunity to gain insights into resilience of microbial life in extreme environments. In order to understand the impact of climate change on the Antarctic ice sheets, it is important to comprehend these distinctive ecosystems. The significant variations observed in MPs' geochemistry and microbial diversity make these ponds exceptionally valuable as a scientific resource for fundamental and applied microbiology and biotechnology.

In this PhD work microbiota of the nine MPs in the Thala Hills Oasis (Enderby Land, East Antarctica) was studied with a focus on the isolation, identification and comprehensive characterization of fast-growing bacteria.

1.3 Metabolic plasticity of cold-adapted bacteria

Metabolic plasticity enables microorganisms to select their metabolic mode according to environmental conditions and it's a main driving force in adaptation and survival of microorganisms in different environments [32] (Figure 1.3). In polar regions, temperature is the most significant factor

affecting microbial life due to its impact on biochemical reactions, gas solubility, solute transport, and osmotic stress, leading to adverse effects on cellular processes [33]. In addition to temperature, polar regions are characterized by harsh UV radiation, limited water availability and nutrient deficiency conditions [27, 34]. Antarctic bacteria thrive in these environments characterized by these extreme and constantly changing physicochemical and ecological conditions, they possess extraordinarily high metabolic plasticity. Metabolic activity of cold-adapted bacteria is expressed in a number of structural and biochemical changes [35]. The examples of these changes are shown on the Figure 1.3.

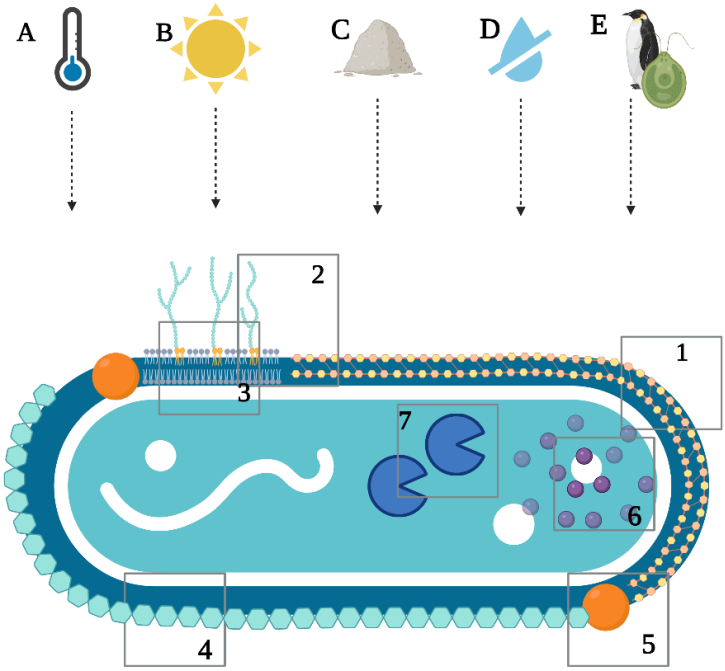

Figure 1.3. Environmental factors affecting bacteria (A-Temperature, B- Solar radiation, C-chemical gradients (nutrients, pH, salts), D-limited water availability, E- interactions with other organisms) and examples of metabolic plasticity of cold-adapted bacteria (1-changes in peptidoglycan layer, 2-changes in lipopolysaccharides, 3- changes in FA, 4- production of exopolysaccharides, 5- synthesis of pigments, 6 - accumulation of osmolytes, 7- production of specific proteins and changes in proteins activity.

In the literature, the variation in the cellular and extracellular structures such as changes in cell envelope are referred to as **structural changes** [36]. The bacterial cell envelope has a complex structure enabling efficient protection of inner cellular structures and allowing to resist to certain physicochemical stress factors [34, 36]. For example, Gram-positive cold-adapted bacteria are often characterized by a thicker outer peptidoglycan layer (Figure 1.3-1) and Gram-negative by changes in the composition and fluidity of lipopolysaccharides and production of exopolysaccharides [36] (Figure 1.3-2) that is enhancing their resistance against low temperatures and protects from intracellular ice formation [34, 36]. It has been reported that cold-adapted bacteria can produce unique **polysaccharides** as one of the strategies to survive in extreme cold and nutrient-limited environments [34, 36] (Figure 1.3-4). Extracellular polysaccharides or **exopolysaccharides (EPS)** are secreted into the surrounding environment of bacterial cells and can function as ice recrystallization inhibitors under cold temperatures [37]. They form a protective matrix around the cells, providing resistance to desiccation, freezing, and other environmental stress factors. EPS production is vital for maintaining the integrity of microbial aggregates, essential for bacterial survival [38]. In cold environments, EPS function as osmo-protectants and providing cryoprotection [39]. EPS also play a crucial role in enhancing biofilm formation, which in turn improves access to nutrients and the survival of cells [34].

Among the **biochemical changes**, alterations in composition and/or production of specific chemicals are typical for cold-adapted bacteria (Figure 1.3-3). **Lipids** are one of the main temperature sensitive biomolecules in bacterial cells which accounts approximately for 10– 15 % (w/w) of cell dry weight [40]. They are localized mainly in the form of phospholipids in the cell membrane [41] or can be accumulated in the form of acyl glycerides, wax esters and/or free FA in lipid droplets in some bacteria [42]. Lipids play multiple roles in bacterial cells. They have a role in the regulation of membrane fluidity and selective membrane permeability [43]. For cold-adapted bacteria, temperature-associated alterations in the amount of lipids, in the ratio between different types of lipids, and in the FA profile have been reported previously [44]. Thus, an

increased production of saturated fatty acids (SFAs) and cyclopropane fatty acids can increase rigidity and can lower permeability of the membrane bilayer, while high presence of cis-unsaturated fatty acids (cis-UFAs) and polyunsaturated fatty acids (PUFAs) lead to a higher fluidity and permeability of the membrane [45]. Changes in branched-chain fatty acids can affect membrane fluidity, where increase in anteiso-FA results in a more fluid membrane structure than for iso-FA [45-47]. The ratio between long- and short-chain FA can also regulate membrane fluidity under unfavorable temperature conditions [47].

Production and accumulation of **osmolytes** (glycine betaine, trehalose, glycerol, sucrose, mannitol etc.) (Figure 1.3-6), and various specific **proteins** (Figure 1.3-7) appear also as a metabolic response to temperature fluctuations for cold-adapted bacteria. Compatible osmolytes prevent cell shrinkage and enhance osmotic balance [34]. Cold-adapted bacteria can synthesize ice-binding proteins (Figure 1.3-8) that inhibit ice crystal growth at lower freezing temperatures [37]. Cold shock proteins facilitate growth at low temperatures, and they are activated during cold exposure [48].

As a response to extreme UV radiation conditions, low temperatures, freezing and thawing cycles, bacteria from cold polar regions often exhibit an ability to produce **pigments,** mainly carotenoids [49-53] followed by violaceins, tetrapyrroles, indolic bichromes and heterocyclic biochromes, and others [52] (Figure 1.3- 5). Carotenoids are the most diverse group of natural pigments [54], most of carotenoids consist of eight isoprene units, creating a C40 backbone with β-cyclization and their yellow-to-red color results from a polyene chain's conjugated double bond system [54], which absorbs blue light with a maximum capacity of 440 to 520 nm [55]. In addition to C40 carotenoids, certain bacteria have the capacity to produce C30 carotenoids and, to a lesser extent, carotenoids of varying chain lengths, such as C45, C50, and C60 [54, 56]. Carotenoids play a crucial role in the adaptability of polar cold-adapted bacteria, and they act as photoprotectors, antioxidants, and they are involved in maintaining membrane fluidity [62].

1.4 Environmental importance and biotechnological potential of cold-adapted bacteria from Antarctic meltwater ponds

Antarctic cold-adapted bacteria from MPs play an important role in carbon and nutrient cycling [5, 57], by breaking down organic matter and converting nitrogen- and phosphorus-containing compounds into forms which can be used by organisms [5]. Additionally, they contribute to weathering rock surfaces and releasing minerals into surrounding environment [58]. These bacteria can influence ice melt rates through the albedo effect [59]. They also can be involved in bioremediation, detoxification of pollutants, and act as indicators of environmental changes, helping researchers to assess ecosystem health and human activities in the Antarctic ecosystem [60]. Furthermore, it is well known that cold-adapted bacteria can be utilized as microbial cell factories for the production of biotechnologically valuable bio-based chemicals [34, 52, 55, 61-65] (Figure 1.4), as for example:

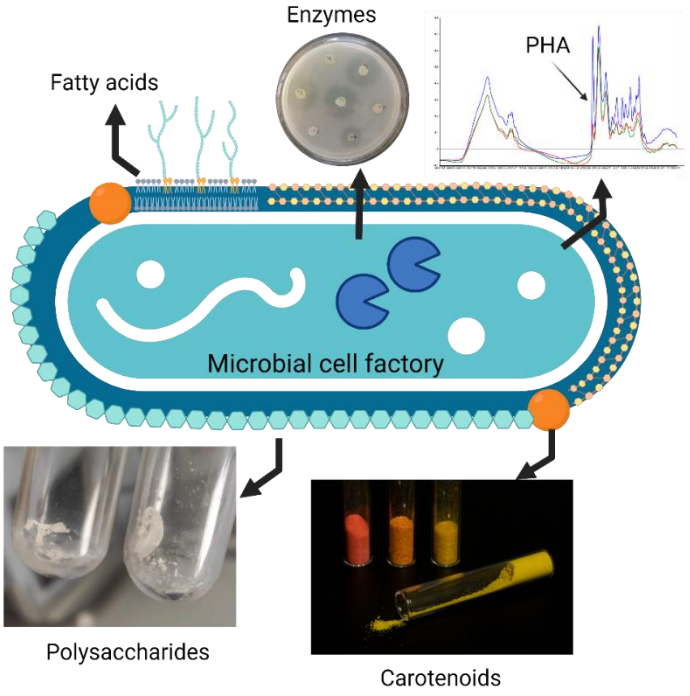

Figure 1.4. Biotechnological potential of Antarctic cold-adapted bacteria from MPs

- **Fatty acids:** Polyunsaturated fatty acids (PUFAs) have various applications in food, pharmaceutical, and cosmetic industries. Antarctic cold-adapted bacteria are known to produce a variety of PUFAs. They can be a source of omega-3 FA, such as eicosapentaenoic acid (EPA) and docosahexaenoic acid (DHA) [64]. Antarctic bacteria from different genera, including *Shewanella, Pseudoalteromonas, Psychrobacter, Colwellia, Moritella* have been identified as able to produce PUFAs [66-68].
- **Extracellular polysaccharides:** EPS are high molecular weight biopolymers primarily composed of homo- or hetero-polysaccharides. They can be either covalently bound (forming capsular polysaccharides that protect cells) or loosely attached (as slime polysaccharides released into the environment) to the cell surface [69]. For instance, cold-adapted bacteria like *Pseudoalteromonas*, *Winogradskyella*, *Colwellia, Shewanella* and *Marinobacter* are able to produce high concentrations of EPSs at low temperatures [33, 69]. EPS are known for emulsification, cryoprotection, biofilm formation, and heavy metal binding properties and have a potential for being used in cosmetics, environmental and food biotechnology as alternatives to conventional commercial polymers [69].
- **Carotenoids:** Carotenoids are pigments which can be naturally synthesized by organisms including bacteria. Due to their potent coloration, low toxicity, stability, and antioxidant properties, natural carotenoids find commercial application in food, feed, cosmetics, and pharmaceuticals [56]. Since Antarctic cold-adapted bacteria originate from extreme environmental conditions including low temperatures, high UV radiation, and nutrient limitations, it is particular interesting to perform bioprospecting for carotenoids production. Some studies have shown that bacteria isolated from Antarctic soil and marine environments are capable of producing carotenoids, including astaxanthin, zeaxanthin, canthaxanthin, decaprenoxanthin, echinenone, beta-carotene, etc. [52]. Research on bacterial species from Antarctica revealed a predominance of pigmented bacteria, primarily belonging to the following genera: *Agrococcus, Arthrobacter,*

Brachybacterium, Cryobacterium, Leifsonia, Micrococcus, Paeniglutamicibacter, Rhodococcus, Salinibacterium, *Sphingobacterium* and *Flavobacterium* [52, 55, 70-72].

- **Enzymes:** Cold-adapted bacteria deploy highly catalytic enzymes to thrive in low-temperature environments. Psychrophilic enzymes are adapted to function in cold environments. At low temperatures they show an about tenfold higher specific activity to compensate for slower reaction rates. However, they are less stable and can unfold and become inactive at milder temperatures. This high activity at low temperatures is achieved by destabilizing the active site or the entire protein, making the catalytic center more flexible [73]. Consequently, cold-adapted bacteria favor highly active enzymes in frigid conditions [33]. Antarctic bacteria are considered as a promising source of biotechnologically attractive enzymes (e.g., proteases, lipases, amylases, ureases, nucleases, β-galactosidases, and keratinases) [74-78]. The bacterial isolates exhibiting the highest enzymatic activities were identified as *Pseudomonas*, *Psychrobacter, Arthrobacter, Bacillus*, *Flavobacterium* and *Carnobacterium* [63, 79, 80]. They exhibit a potential to be used in various fields, including food processing, pharmaceuticals, brewing, bioremediation, and molecular biology [73].
- **Polyhydroxyalkanoates (PHAs):** PHAs are biodegradable polymers produced by microorganisms, including Antarctic bacteria [61, 81]. They are produced as intracellular storage material under unbalanced growth conditions in a high access of carbon and nitrogen limitation [82]. PHAs structures vary and are composed of repeating units (monomers) of 3-hydroxy fatty acid monomers connected by ester bonds [83]. The properties of PHAs can be adjusted by varying monomer composition, tailoring them for specific applications [84]. Potential PHAs producers belong mainly to *Pseudomonas* and *Janthinobacterium* genera [61, 83, 85].

In this PhD work characterization of lipids, pigments, enzymatic activity and total cellular biochemical profile of the fast-growing bacteria, newly isolated from the MPs in the Thala Hills Oasis (Enderby Land, East Antarctica) was performed.

1.5 Isolation, identification and morpho-physiological characterization of bacteria from Antarctic meltwater ponds studied in the PhD work

1.5.1 Sampling sites of the meltwater ponds in Antarctica

Antarctic bacteria studied in this PhD work, were obtained from water samples that were collected during the 5th Belarusian Antarctic Expedition in the austral summer season (January 2013) from the middle part of the water column of nine non-flowing MPs located in rock baths (0.1–3 m diameter, 2–100 m distance from the shoreline, 0.1–0.5 m deep, and 0–10 m above sea level). The sampling sites were located 800 m from the Belarussian Antarctic Station "Vechernyaya" and 2.7 km from the Adelie penguin colony at the Azure Cape (67°39'22.7"S 46°10'30.2"E) of the Vecherny region of the Thala Hills oasis in the central part of Enderby Land (East Antarctica) (Figure 1.5).

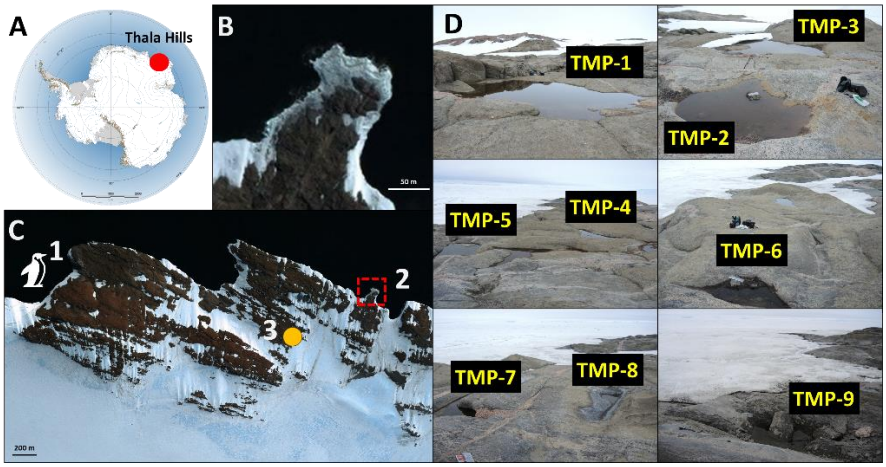

Figure 1.5. Sampling sites. (A) Location of the Thala Hills oasis in the coastal area of East Antarctica (marked by the red circle). (B-C) Satellite image of the eastern part of the Thala Hills oasis (1—Adelie penguin colony area, 2—sampling sites area, 3—location of the Belarussian Antarctic Station "Vechernyaya" in the eastern part of the Thala Hills oasis), (D) Photos of the studied MPs.

Physicochemical parameters (pH, TDS, temperature) were measured *in situ* at different time points (11 January 2013, 14 January 2013, 17 January 2013, and 26 January 2013) using portable pH/Conductivity/TDS Testers.

Bacterioplankton analysis involved collecting water samples in sterile polythene tubes and preserving them with 4% formalin and subsequnetly storing at 4 °C. For the quantitative bacterioplankton assessment the BN—bacterial cell number $\times 10^6$ cells/mL was calculated for the samples sampled 11 January 2013 by using Equation 1:

$$BN = S \times 10^6 \times \frac{a}{s} \times V \times 10 \quad (1)$$

where **S** is the filter area in mm; **10^6** is the recalculation of mm in µm; **a** is the sum of counted cells; **s** is the grid area in µm; **V** is the volume of the filtered sample in mL; and 10 is a number of fields of view. The number of bacterial cells was determined via the acridine orange staining method [86] using an epifluorescence microscope, and imaging data were processed with Image-Pro Plus. The biomass was calculated according to the size of each bacterial cell.

1.5.2 Cultivation approaches and media for isolation, identification and characterization of Antarctic bacteria

Cultivation approaches and systems. Cultivation of bacteria can be done in solid and liquid media, in the presence or absence of oxygen and using various cultivation systems such as Petri dishes, glass tubes, flasks, microplates, bioreactors etc. Cultivation in Petri dishes uses solid media solidified with agar and reveals distinct bacterial populations, each originating from a single cell. Agar-based cultivation are often used for isolation, colony characterization, antibiotic susceptibility testing, enzymatic assays, screening for pigments production etc. [87]. The agar plate screening method is time-consuming, low throughput, and low precision in detecting the target molecules. In contrast, submerged screening methods provide superior control over culture conditions, leading to increased production of target molecules. They enable high-throughput screening of numerous samples simultaneously. Furthermore, these methods enhance specificity and sensitivity in identifying target molecules compared to agar plate screening. Additionally, liquid media screening mimics industrial submerged culture conditions, which is ideal

for discovering potential microbes for industrial use [88]. Cultivation in liquid media is characterized by the relatively faster growth of bacterial cells and often used for biochemical characterization of bacteria as well as for developing biotechnological production of bacteria-based chemicals [89]. Currently, the use of microplates is considered as the most versatile approach for cultivation as microplates allow performing high-throughput studies [90]. There are mainly two types of microplates used for cultivation of bacteria: (i) 100-well honeycomb microplates, which are used for the cultivation in Bioscreen C (Oy Growth Curves Ab Ltd., Finland) and BioLector incubator systems (Beckman Coulter, USA); (ii) 96-, 24-, 12- and 6-well (low or deep) microtiter plates which can be used in a shaking platform consisting of an incubator and shaker. An example for such a system is the Duetz Microtiter plate cultivation system [91] (Duetz-MTPS) (Enzyscreen, Netherlands) which was used in this PhD work for bacterial screening and biochemical profiling (Figure 1.6). Each MTP is closed with a composite sandwich cover, incorporating a soft silicone layer at the base, a 0.3-micron expanded polytetrafluoroethylene (ePTFE) layer, and a microfiber filter in the middle to facilitate efficient gas exchange. Additionally, it features a stainless-steel lid equipped with pinholes at the apex, as illustrated on Figure 1.6. The sandwich cover system serves the dual purpose of minimizing solvent evaporation and preventing cross-contamination between individual wells during the cultivation process. The robust attachment of the sandwich cover to the microtiter plate is ensured by a specialized clamp system (Figure 1.6). The culture volume of the Duetz-MTPS exhibits flexibility, spanning from 0.1 mL in the case of a 96-low well MTPs to 35 mL for 6-well MTPs. Recent studies have successfully demonstrated the scalability of cultivations in the Duetz-MTPS to larger systems, including Erlenmeyer shake flasks, 1.5 L and 25 L bioreactors [90]. One of the limitations of the Duetz-MTPS is the absence of integrated monitoring capabilities for parameters such as pH, dissolved oxygen, and optical density which is possible for flasks cultivation [92].

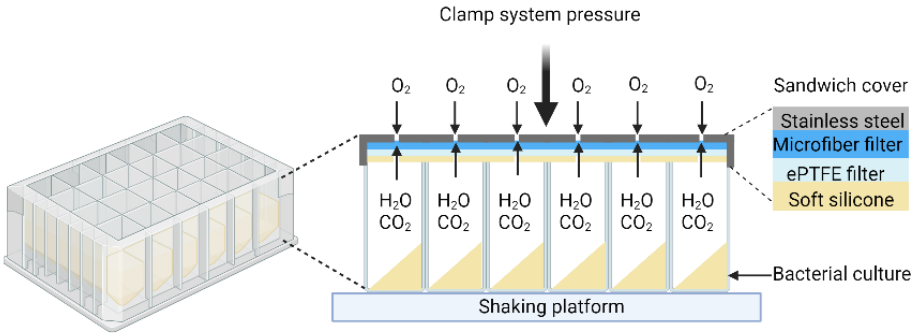

Figure 1.6. Duetz MTPS system: microplate and sandwich cover layers.

In this PhD work, agar-based cultivation was used for the isolation, morphological characterization and antibiotic susceptibility testing in **Paper I.** Broth-based cultivation using Duetz-MTPS was performed for explorative characterization and taxonomy-aligned comparison of alterations in lipids and other biomolecules in **Paper II.** The impact of various temperatures and cultivation on two forms of BHI medium (agar and broth-based) on total cellular biomolecular profiling of Antarctic bacteria was evaluated in **Paper III.** Duetz-MTPS system was used for high-throughput screening and characterization of pigment producing bacteria in **Paper IV**. Flask cultivation was used to get appropriate amounts of biomass for pigments analysis and to cultivate bacteria under blue light exposure in **Paper IV**.

In this PhD study, complex nutrient-rich media meat peptone agar (MPA) was used for the isolation of bacteria and brain heart infusion agar (BHIA) for morphological characterization in **Paper I.** BHIA and brain heart infusion broth BHIB was used for the total cellular biomolecular profiling in **Paper III.** BHIB was used for profiling lipids and pigments in **Paper II, IV**. Mueller-Hinton Agar (MHA) was used for antimicrobial susceptibility assessments in **Paper I**. A set of media with different substrates was used for the detection of enzymatic activity of bacterial strains by the plate-method in **Paper I**.

1.5.3 Isolation and purification of bacteria from the Antarctic MPs

For this PhD work, bacteria were isolated by collecting water samples from the MPs in sterile tubes, stored at 4°C. Water samples were taken in duplicates, and then plated in triplicates on MPA and cultivated for 14 days at 5°C and 18°C for isolating psychrophilic and psychrotolerant bacteria, respectively (**Paper I**). Single colonies with different morphology, size and color, observed after 2-6 days of cultivation, were transferred onto new MPA dishes for purification. Isolates forming single colonies after 2–6 days of cultivation were considered fast-growing [93, 94].

In total, twenty-nine fast-growing bacteria with different colony types (colony morphology, size, and pigmentation) were isolated from nine MPs located in the Vecherny region of the Thala Hills oasis in the central part of Enderby Land (East Antarctica) (**Paper I**). Fourteen isolates were isolated after incubation at 5°C and fifteen isolates were isolated after incubation at 18°C. For long-term storage, the isolated purified bacteria were grown on MPA and the obtained single colonies were suspended in meat peptone broth (MPB) and glycerol, and transferred into cryo-vials for the storage at -80°C. All the isolates were deposited in the Belarusian Collection of Non-pathogenic Microorganisms at the Institute of Microbiology of the National Academy of Sciences of Belarus (Minsk, Belarus).

1.5.4 Identification of bacteria by 16S rRNA gene sequencing

The 16S rRNA gene sequencing is a traditional approach for identification of bacteria and archaea [95, 96]. The 16S rRNA gene is highly conserved across bacterial species, but it also contains variable regions that can be used to differentiate between different taxa [97]. By analyzing these variable regions, evolutionary relationships between newly isolated bacteria and previously identified reference strains can be identified. The identification of newly isolated bacteria by 16S rRNA gene sequencing involved the following steps [97]: (1) Cultivation of bacteria, (2) DNA extraction, (3) Polymerase Chain Reaction (PCR) amplification of specific gene regions (e.g., 16S rRNA [98]), (4) DNA sequencing (Sanger sequencing

[99] and other methods [100]) and (5) Data analysis and comparing the obtained nucleotide sequences of the 16S rRNA gene with the reference databases to build phylogenetic trees. Databases such as SILVA (16S Ribosomal RNA Sequences Database) [60], EZBioCloud 16S Database [61], and NCBI GenBank (National Center for Biotechnology Information - GenBank) can assist in taxonomic classification and identification. Once the taxonomic classification and identification is complete, sequences of the studied bacteria and their closest neighbors in the database can be exported for visualization and building a phylogenetic tree. Molecular Evolutionary Genetics Analysis (MEGA) software allows researchers to align the 16S rRNA gene sequences and construct phylogenetic trees based on different algorithms as for example Maximum Likelihood or Neighbor-Joining (NJ) [101]. These trees are a model of the evolutionary relationships between different taxa, suggesting phylogenetic relationships of the studied bacteria.

In this PhD work, twenty-nine bacteria isolated from the Antarctic MPs were cultured on MPA agar at 18°C for 7-10 days. DNA was extracted using the Jena Biosciences' DNA Preparation Kit PP-206 and the 16S rDNA fragment was amplified with universal bacterial primers 8f (5'-AGAGTTTGATCCTGGCTCAG-3') and 1492r (5'-GGTTACCTTGTTACGACTT-3'). Sequencing was performed using the Sanger method with Jena Bioscience's DNA Cycle Sequencing Kit PCR-401S and Primers: 926R-seq (5'-CCGTCAATTCATTTGAGTTT-3'), 336F-seq (5'-ACGGYCCAGACTCCTACG-3'), 522R-seq (5'-TATTACCGCGGCTGCTGGCAC-3'), and 918F-seq (5'-ACTCAAAKGAATTGACGGG-3'). Sequencing products were analyzed with the LI-COR Biosciences "4300 DNA Analyzer". The obtained 16S rRNA data were preprocessed by editing and rendering in FASTA format using the e-Seq™ software V. 3.1.10 (LI-COR Biosciences, Lincoln, NE, USA). The obtained sequences were compared to those available in the EzBioCloud database (ChunLab Inc., Seoul, Korea) [39] to choose reference sequences for the phylogenetic analyses and to find similarities with the known strains (Table 1.1). The phylogenetic tree was reconstructed using the MEGA 11 program [40] (Figure 1.7).

Figure 1.7. Phylogenetic tree based on 16S rDNA sequences of the MPs isolates.

Table 1.1. 16S rRNA gene sequence affiliation to the closest phylogenetic neighbors of the bacteria isolated from Antarctic MPs.

Isolate code [Pond №]	Collection number	Gen Bank Accession number	Nearest taxonomic neighbor by EzBioCloud alignment (Organisms, Accession number)	Identity (%)
TMP1[1]	BIM B-1565	ON248060	*Shewanella baltica* NCTC 10735	100
TMP5[2]	BIM B-1557	ON248064	*Shewanella baltica* NCTC 10735	99.72
TMP11[5]	BIM B-1561	ON248069	*Shewanella baltica* NCTC 10735	99.66
TMP14[5]	BIM B-1563	ON248072	*Shewanella* WE21	99.38
			Shewanella baltica NCTC 10735	99.04
TMP6[3]	BIM B-1558	ON248065	*Acinetobacter lwoffii* NCTC 5866	99.79
TMP2[1]	BIM B-1554	ON248061	*Pseudomonas lundensis* DSM 6252	99.86
TMP3[2]	BIM B-1555	ON248062	*Pseudomonas lundensis* DSM 6252	99.86
TMP4[2]	BIM B-1556	ON248063	*Pseudomonas lundensis* DSM 6252	99.79
TMP7[4]	BIM B-1559	ON248066	*Pseudomonas leptonychotis* CCM 8849	99.93
TMP18[6]	BIM B-1568	ON248076	*Pseudomonas leptonychotis* CCM 8849	100
TMP19[6]	BIM B-1566	ON248077	*Pseudomonas leptonychotis* CCM 8849	100
TMP9[4]	BIM B-1560	ON248067	*Pseudomonas peli* R-20805	99.52
TMP17[6]	BIM B-1569	ON248075	*Pseudomonas peli* R-20805	99.38
TMP20[7]	BIM B-1546	ON248078	*Pseudomonas peli* R-20805	99.52
TMP22[9]	BIM B-1552	ON248080	*Pseudomonas peli* R-20805	99.52
TMP25[9]	BIM B-1542	ON248083	*Pseudomonas peli* R-20805	99.52
TMP26[9]	BIM B-1548	ON248084	*Pseudomonas peli* R-20805	99.11
TMP13[5]	BIM B-1562	ON248071	*Flavobacterium degerlachei* DSM 15718	98.47
TMP10[4]	BIM B-1539	ON248068	*Sporosarcina globispora* DSM 4	99.59
			Sporosarcina psychrophila IAM 12468	99.59
TMP12[5]	BIM B-1540	ON248070	*Carnobacterium inhibens* subsp. *inhibens* DSM 13024	100
TMP27[9]	BIM B-1541	ON248085	*Carnobacterium funditum* DSM 5970	100
TMP28[9]	BIM B-1544	ON248086	*Carnobacterium iners* LMG 26642	99.86
TMP29[8]	BIM B-1577	ON248087	*Facklamia tabacinasalis* CCUG 30090	99.46
TMP15[5]	BIM B-1549	ON248073	*Arthrobacter* ERGS4:06	98.97
			Arthrobacter PAMC25486	98.90
			Arthrobacter alpinus DSM 22274	98.70
			Arthrobacter glacialis HLT2-12-2	98.70
TMP24[9]	BIM B-1543	ON248082	*Arthrobacter agilis* DSM 20550	100
TMP16[6]	BIM B-1571	ON248074	*Brachybacterium paraconglomeratum* LMG19861	99.93
TMP21[7]	BIM B-1545	ON248079	*Micrococcus luteus* NCTC 2665	99.58
TMP23[9]	BIM B-1547	ON248081	*Agrococcus citreus* IAM 15145	99.50
TMP30[8]	BIM B-1567	ON248088	*Leifsonia* PHSC20C1	99.59
			Leifsonia rubra CMS 76R	99.45

1.5.5 Morpho-physiological characterization

Morpho-physiological characterization of newly isolated bacteria usually involves determination of (i) cell and colony morphology, (ii) optimal growth conditions (temperature, pH, NaCl), (iii) enzymatic activities, (iv) carbon source utilization, (v) antibiotic susceptibility. The shape and size of the bacterial cells can be observed by staining and subsequent microscopic examination. Gram staining is commonly used to classify bacteria into Gram-positive and Gram-negative groups based on the cell wall structure [102]. The determination of the optimal growth conditions includes cultivation of bacteria at different temperatures what is especially relevant for cold- adapted bacteria in order to differentiate between psychrophiles and psychrotrophs [103]. Enzymatic activity are assessed through substrate breakdown and product formation evaluated by visual analysis, spectrophotometry, fluorescence and radiolabeling [104]. The susceptibility of bacteria to different antibiotics is determined by using disk diffusion methods, minimum inhibitory concentration assays or genetic methods [105-107]. The most traditional and widely used antibiotic susceptibility testing methods predominantly rely on detecting antibiotic resistance through the measurement of bacterial growth on the presence of antibiotics [108]. Antibiotic resistance is a natural protective mechanism in bacteria, and it can be exacerbated by to the transportation of antibiotic resistant bacteria to Antarctic areas by atmospheric and oceanic currents from outside the Antarctic region [109]. In addition, an increase in the selective pressure of anthropogenic and animal activity in Antarctica may result in the spread of resistant bacteria [60, 110], leading to the appearance of multi-resistant strains in Antarctic region [60].

Morpho-physiological characterization of the Antarctic bacteria in this PhD work included determination of cell morphology, optimal growth conditions, enzymatic activity and susceptibility towards antibiotics (Figure 1.8), which is reported in **Paper I** and **Paper II**. Cell morphology was assessed via Gram staining and microscopy (**Paper II**). Bacterial isolates were cultured at 18°C on BHIA until single colonies were observed. Gram staining was done following the protocol of the three-step Gram stain procedure kit (Merck KGaA, Germany). The stained cells were examined

using a Leica DM4 B light microscope with a 100× immersion lens. In order to evaluate thermotolerance, the bacterial isolates were grown on BHIA at 4, 10, 18, 25, 30, and 37 °C for up to 10 days with daily visual inspections of the cultures (**Paper I**). Various plate-based assays were employed to evaluate production of extracellular enzymes using selective media (**Paper I**).

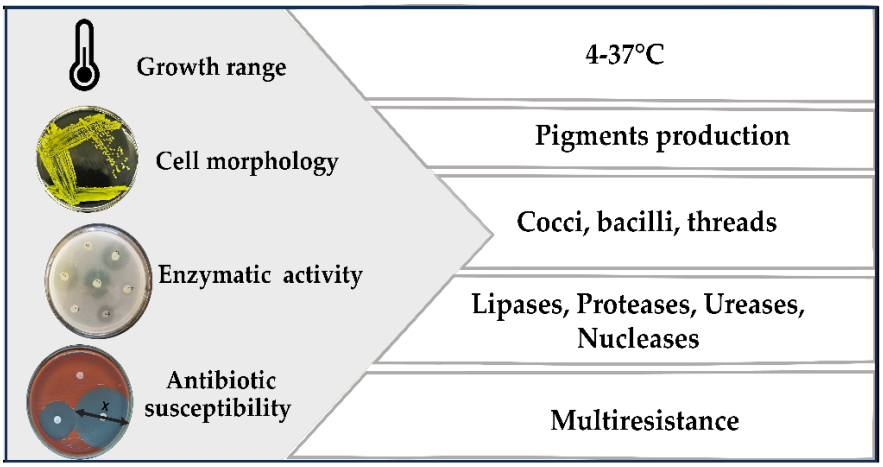

Figure 1.8. Schematic overview of the morpho-physiological characterization of the Antarctic bacteria performed in this PhD work.

Antibiotic susceptibility was evaluated by applying the Kirby–Bauer disc diffusion method [111] using Mueller–Hinton agar (Merck, Darmstadt, Germany) and commercial disks for susceptibility testing (Bio-Rad, Hercules, CA, USA) (**Paper I**). Antibiotic susceptibility tests involved 18 antibiotics and 5 antibacterial agents. The strains *Escherichia coli* ATCC 25922, *Pseudomonas aeruginosa* ATCC 27853, and *Staphylococcus aureus* ATCC 29213 were used as controls. The data analysis for the control cultures was performed according to the breakpoints established by the European Committee on Antimicrobial Susceptibility Testing [105] and Clinical and Laboratory Standards Institute [106] documents. The data analysis of the susceptibility testing of the Antarctic bacterial isolates was performed as described by Daniela et al. [60].

1.6 Targeted and total cellular biochemical profiling

Biochemical characterization of microorganisms can be targeted or non-targeted. For the targeted characterization a wide range of analytical techniques can be applied depending on the chemical of interest. Among targeted analytical techniques, the following are considered as reference: (i) High-Performance Liquid Chromatography-Mass Spectrometry (HPLC-MS) is used for the analysis of polysaccharides and pigments [112, 113], (ii) gas chromatography (GC) is used for the analysis of lipids, lipidic compounds and polyhydroxyalkanoates [114, 115], (iii) matrix-assisted laser desorption ionization–time of flight mass spectrometry (MALDI-ToF MS) is used for the analysis of protein profile [116]. The choice of technique depends on the type of analysis required and the nature of the sample. Non-targeted characterization provides a comprehensive analysis of the entire sample without predefining the analytes and allowing to obtain a total cellular biochemical profile in a single measurement run. Vibrational spectroscopy has been positioned as a powerful technologies for non-targeted biochemical profiling and investigation of microorganisms [117].

In this PhD work, bacterial biomass was separated from the growth medium after cultivation using centrifugation, followed by washing and freeze-drying. The prepared biomass was then used for targeted and non-targeted biochemical characterization. Characterization of the total lipid content and FA profile was done using GC-FID (**Paper II**). The pigment profile was assessed using HPLC-MS (**Paper IV**). FTIR spectroscopy was used for the explorative characterization and taxonomy-aligned comparison of alterations of lipids and other biomolecules in **Paper II**, and global cellular biochemical profiling in **Paper III**. Screening for pigment production and characterization of pigment profile and photostability of Antarctic bacteria from MPs was done by FT-Raman spectroscopy in **Paper IV**.

1.6.1 Reference analysis of lipids and pigments

In this PhD work, prior to lipid and pigment analysis using reference wet-chemistry techniques, the targeted molecules were extracted using a previously described method for lipids [66] with some modifications and

for previously described method for pigments [118]. Thin layer chromatography (TLC) was used to separate single pigments.

Analysis of lipids (Paper II): For lipid analysis, the extracted lipids were converted into fatty acid methyl esters (FAME) according to El Razak et al. [66]. Gas chromatography equipped with a flame ionization detector (GC-FID) was utilized for the estimation of the total lipid content and FAs profile. For the identification and quantification of FAs, the C4–C24 FAME mixture (Supelco, St. Louis, MO, USA) and the bacterial acid methyl esters (BAME) mixture (Matreya LLC, High Tech Road, State College, PA 16803 USA) were used as an external standard, in addition to the C19:0 1,2-dinonadecanoyl-sn-glycero-3-phosphocholine internal standard (IS) as was previously described [119]. For the estimation of the FA profile, all significant peaks in the chromatogram were automatically integrated by the software Agilent OpenLAB CDS (EZChrom Edition, USA). The calculation of the relative response factor (RRF) was done using FA concentration from the C4-C24 FAME mix that is given by the manufacturer according to:

$$RRF_{FA} = \frac{areaFA_{FAME\ MIX}}{c\ FA_{FAME\ MIX}} \times \frac{c\ C19{:}0_{FAME\ MIX}}{area\ C19{:}0_{FAME\ MIX}} \quad (2).$$

The estimation of weight of individual FAs was based on peak area, relative response factor (RRF) and C19:0 internal standard as follows:

$$weigh\ FA_{sample} = \frac{weight\ C19{:}0\ (IS)}{area\ C19{:}0\ (IS)} \times \frac{area\ FA_{sample}}{RRF_{FA}} \quad (3).$$

To estimate weight percentages of single FA for each sample, the weights of each FA was used according to

$$\%\ FA_{sample} = \frac{weight\ FA_{sample}}{\sum weight\ FA_{sample} - weight\ C19{:}0\ (IS)} \quad (4)$$

The total weight of FAs in the sample was adjusted by adding the weight of the internal standard. The weight percentage of FAME content in the sample (L/X %) was calculated according to:

$$\frac{L}{X}\ \% = \frac{\sum weight\ FA_{sample} - weight\ C19{:}0\ (IS)}{weight\ of\ dry\ biomass} \quad (5)$$

The total lipid content of bacterial biomass was estimated in percentage (%) as a sum of FAMEs (the weight of C19:0 was subtracted) divided by the weight of freeze-dried biomass. In addition to total lipid content and fatty acid profile, parameters related to fatty acids structural characteristics were calculated and for this detected fatty acids were grouped into the following groups: (1) PUFAs (summed polyunsaturated fatty acids), (2) n-SFAs (summed non-branched saturated fatty acids), (3) br-SFAs (summed branched saturated fatty acids), (4) n-MUFAs (summed non-branched monounsaturated fatty acids), (5) hydroxy-FAs (summed hydroxy fatty acids), (6) cyclic-FAs (summed cyclic fatty acids), (7) summed cis-FAs/trans-FAs and (8) iso-FAs /anteiso-FAs [45].

Analysis of pigments (Paper IV): The extracted pigments were analysed by HPLC-MS. The samples in a volume of 5 µL were injected into a Thermo Fisher Scientific Hypersil GOLD 1.9 µm HPLC analytical column. The stepped linear gradient of buffers A (0.1% formic acid (VWR chemicals, USA) in water) and B (0.1% formic acid and 99.9% acetonitrile) (Sigma-Aldrich, Germany) was distributed as follows: 00-05 min – 50% buffer A and 50% buffer B, 05-40 min – gradient from 50-100% buffer B, 40-45 min – 100% buffer B. The separation of components was monitored using a photodiode array detector at the 190-600 nm range and a mass spectrometer tandem quadrupole-time-of-flight at the 50-1700 m/z range. A positive electrospray ionization mode with a time-of-flight detector was used.

1.6.2 Biochemical profiling by vibrational spectroscopy

Traditional analytical approaches for the chemical analysis of bacterial metabolites, such as liquid or gas chromatography, offer detailed information on individual analytes but these methods are often time-consuming and require extraction protocols, making them suboptimal for high-throughput screening. In this PhD project, both traditional analytical methods for identification of lipids (**Paper II**) and pigments (**Paper IV**) in combination with two vibrational spectroscopy techniques –FTIR spectroscopy and FT-Raman spectroscopy, which provide complementary

biochemical information were used. FTIR and IR-Raman spectroscopy was previously applied for analysis of bacteria [40, 117, 120-125] including some studies performed on Antarctic bacteria: (i) for detection and characterization of exopolysaccharides [38], biosurfactants [126], nanoparticles etc. (ii) analysis of low-temperatures degradation of microplastic [127], feather [79], and petroleum [128].

In this PhD work FTIR spectroscopy was used for biochemical characterization of bacteria isolated from the Antarctic MPs (**Paper II**, **Paper III**) and FT-Raman spectroscopy was used for analysis of pigments production and photostability of pigments (**Paper IV**). Vibrational spectroscopy is an analytical technology that enables high-throughput biochemical fingerprinting and quantitative or semi-quantitative analysis of all major intracellular and extracellular bacteria metabolites in a one measurement run. Notably, vibrational spectroscopy analysis requires little to no sample preparation [117].

The main principle of vibrational spectroscopy is based on the interaction between light and vibrational modes of molecules. Molecules can absorb mid-infrared radiation (FTIR), where the absorbed energy or frequency is characteristic for molecular bonds and structure of molecules. In FT-Raman spectroscopy a near-infrared laser is used, where molecules interact with the laser radiation such that the molecule either absorbs part of the incoming radiation or transfers part of the molecule's vibrational energy to the incoming radiation. In both cases, in FTIR and FT-Raman spectroscopy, the interactions between the radiation and the molecule reveal specific information about molecular vibrations and structures [124, 129].

Fourier Transform infrared spectroscopy (FTIR) technique: In mid- infrared (mid -IR) spectroscopy, a broad spectrum of infrared light is passed through a sample. A sample absorbs specific frequencies of infrared radiation that correspond to the vibrational energy levels of the molecules present in the sample. The fundamental absorption phenomena related to molecular vibrations appear in the so-called mid-IR spectral region of 4000-400 cm^{-1} (2.5 to 25 micrometer), which is the region mostly covered by FTIR techniques.

During an FTIR transmission measurements, infrared radiation is directed through a thin sample of few micrometers. Within this process, the IR radiation is partially absorbed by the chemical bonds of the molecules within the sample. The acquired spectrum is typically represented in a unitless parameter called "absorbance," which is plotted against wavenumbers (cm^{-1}). Distinct absorbance bands correspond to specific chemical constituents within the sample. The precise position of these bands and the probability of absorption depends on the polarity and strength of chemical bonds and can be affected by the surrounding molecular environment. As a result, the FTIR spectrum reflects both intermolecular and intramolecular influences [130].

The measured signal was represented as the absorbance (A), since the absorbance is approximately proportional to the concentration of chemical components present in the sample. The absorbance is calculated as (Equation 6):

$$A = log\frac{1}{T} \qquad (6)$$

where T denotes transmittance. The transmittance is the ratio of the intensity of the IR beam after it has passed through the sample (I_S) to the intensity of the IR beam before entering the sample (I_R) (Equation 7):

$$T = \frac{I_S}{I_R} \qquad (7)$$

The initial IR beam intensity before interacting with the sample can be established through free channel measurements, which are conducted without the sample. A Fourier transform spectrometer has its name from the fact that it uses a principle that requires a Fourier transform of the measured signal, the so-called interferogram to obtain the intensity.

The absorbed energy causes the molecular bonds to vibrate, resulting in characteristic absorption bands in the infrared spectrum. Different types of vibrational modes can be observed in the infrared spectrum [129]:

(i) *Stretching vibrations*, which occur when the bond length between two atoms changes.

(ii) *Bending vibrations (deformations)*, which occur when there is a change in the bond angle between three or more atoms. They may appear as scissoring, bending in or out of plane, rocking and wagging.

The positions and intensities of the absorption peaks provide descriptive information about the functional groups present in the molecule and its overall structure. A vibrational transition is infrared active, if the molecule changes the dipole moment during the vibration. Thus, infrared spectroscopy is highly sensitive to vibrations of polar functional groups, such as carbonyl (C=O), hydroxyl (O-H), and amino (N-H) groups .

In this PhD work, for performing cellular biochemical profiling by FTIR spectroscopy (**Paper II** and **Paper III**), bacterial biomass was separated from the growth medium by centrifugation and washed with distilled water three times (Figure 1.10). 10 µL of the homogenized bacterial suspension was pipetted onto the IR-light-transparent silicon 384-well silica microplates (Bruker Optics GmbH, Ettlingen, Germany) in three technical replicates, and dried at room temperature for at least 2 hours before the analysis (Figure 1.10). FTIR transmittance spectra were measured using a high-throughput screening extension unit (HTS-XT) coupled to the Vertex 70 FTIR spectrometer (both Bruker Optik, Germany). The FTIR system was equipped with a globar mid-IR source and a deuterated L-alanine doped triglycine sulfate (DLaTGS) detector. The HTS-FTIR spectra were recorded with a total of 64 scans, using Blackman-Harris 3-Term apodization, spectral resolution of 6 cm^{-1}, and digital spacing of 1.928 cm^{-1}, over the range of 4000–400 cm^{-1}, and an aperture of 6 mm.

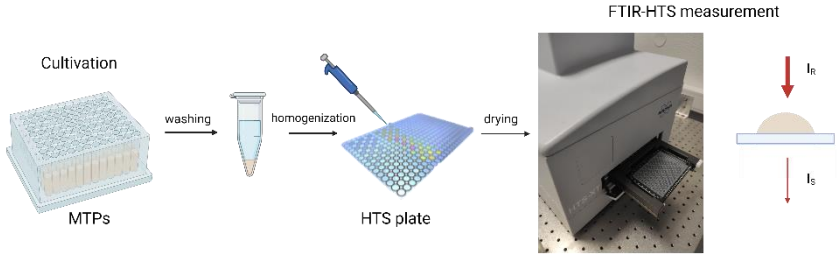

Figure 1.10. The workflow of biomass preparation and FTIR-HTS measurement.

Fourier Transform Raman Spectroscopy (FT-Raman): In FT-Raman spectroscopy, monochromatic light emerging from an excitation laser in the near infrared – usually at 1064 nm is directed onto the sample [129]. When the photons interact with the molecules, most of them scatter elastically, resulting in no change in their energy. However, a small fraction of photons undergoes inelastic scattering, which is the so-called Raman effect, and which means they either gain or lose energy due to the interactions with molecules. The Raman effect is based on the energy difference between the incident photons and the scattered photons, which corresponds to the vibrational energy change of the molecules [129]. The Raman spectrum is obtained by measuring the intensity of scattered light at different frequencies, relative to the incident light. A vibrational transition is Raman active, if the molecule changes polarizability during the vibration.

In this PhD work, FT-Raman spectroscopy was applied to perform semi-quantitative screening of pigment production in Antarctic bacteria and library-dependent analysis using an in-house library of pigments for comparison with pigment profiles in pigment producing bacteria (**Paper IV**). Prior FT-Raman analysis, bacterial biomass was freeze-dried (Figure 1.11A). Approximately 5-10 mg of the biomass was transferred to flat-bottom 400 µL glass inserts (Agilent, USA), covering the bottom of the vial. The glass inserts were then placed in a 96-well multi-well holder, and measurements were conducted using a high-throughput setting stage

measurement accessory. To perform FT-Raman analysis of the pigments' extracts, the extracts were deposited on TLC plates, where single pigments were separated. The separated pigments and standards were measured by FT-Raman (Figure 1.11B). After the solvent was evaporated, the plate was placed on a Z-motorized stage measurement accessory for further measurements (Figure 1.11C). Measurements were performed using a MultiRAM FT-Raman spectrometer (Bruker Optic GmbH, Germany) with an neodymium-doped yttrium aluminum garnet (Nd:YAG) 1064 nm excitation laser. The spectra were recorded in the region between 3785 – 45 cm^{-1} with a spectral resolution of 8 cm^{-1} and with 2048 scans per sample. MultiRAM FT-Raman spectrometer (Bruker Optik GmbH, Germany) equipped germanium detector cooled with liquid nitrogen.

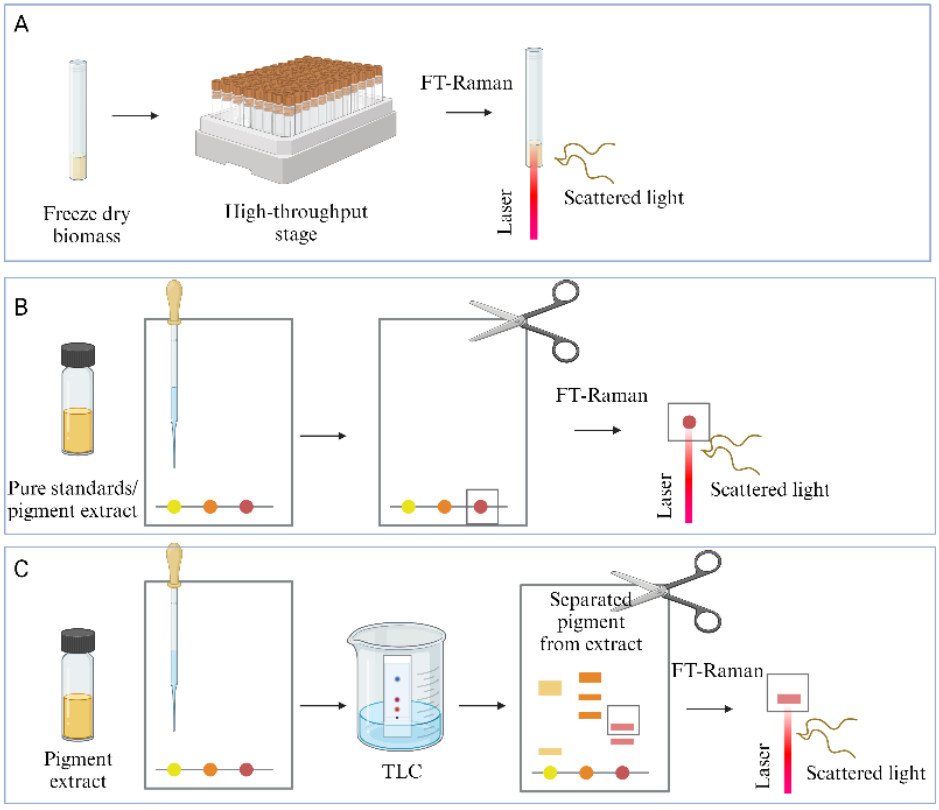

Figure 1.11. Sample preparation for TLC coupled with FT-Raman spectroscopy.

The comparison of FTIR and FT-Raman spectroscopies

Both infrared and Raman spectroscopy methods are highly complementary, providing a comprehensive analysis of molecular vibrations and structures (Figure 1.12, Table 1.2). Although there can be overlap in the vibrational modes captured by Raman and IR spectroscopy, Raman spectroscopy is most effective for detecting vibrations within non-polar groups, while IR spectroscopy is most sensitive for the vibrations of polar groups [129].

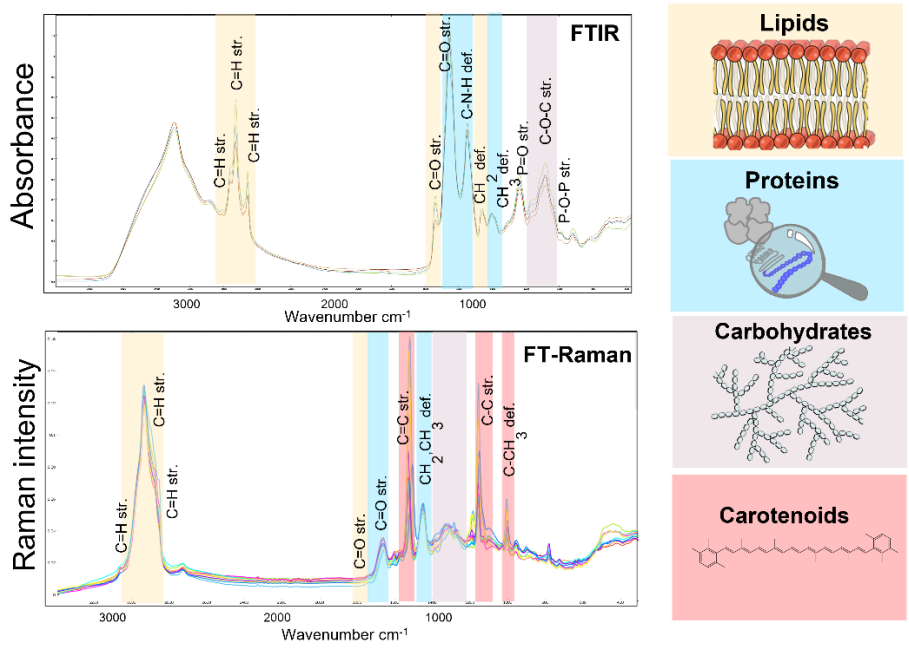

Figure 1.12. Representative FTIR-HTS and FT-Raman spectra of bacterial biomass.

Table 1.2 – Band assignment for the FTIR and FT-Raman. Peak frequencies have been obtained from second derivative spectra. Abbreviations: asym, antisymmetric; sym, symmetric; str, stretching; defederation [120, 121, 123, 131-134].

FTIR-HTS cm^{-1}	FT-Raman cm^{-1}	Molecular vibration	Cell component
Lipids			
3006	3008	=C-H str	Polyunsaturated lipids

2960/2875	2933/2895	-C-H (CH_3) str	Mainly unsaturated lipids, little contribution from proteins, carbohydrates, nucleic acids
2925 /2853	2855	-C-H (CH_2) str	
1742	1740	>C= O str	Acyl glycerides, esters, lipids
Proteins			
1693	1660	-C=O str C=C str	Amide I
1656			
1636			
1548		C-N-H def	Amid II
1311	1310-1250	C-N-H def	Amide III band
Mixed			
1466	1460-1440	CH_2 def	Lipids and protein
1453		CH_3 def	
1240	1165	P=O asymmetric str. of $>PO_2$	Phosphodiesters, phospholipids, nucleic acids
1222			
Carbohydrates			
1083		C–O str of glycogen PO^{-2} symmetric str	Phosphodiesters, phospholipids, nucleic acids, teichoic acids, glycogen
1200-1000	1200-1150	C-O-C str, C-O-H def, COH	Carbohydrates
Carotenoids			
Not detectable	1500-1550	C=C str.	Carotenoids
	1100-1120	C-C str.	
	1000-1010	C-CH_3 str	

1.7 Data analysis

In this PhD work the following types of data were generated: (i) univariate data such as biomass weight (g/L), ratio values, antibiotic susceptibility zones (mm) (**Paper I- IV**), and (ii) multivariate data such as genetic data (**Paper I**), GC-FID data of fatty acid profile and total lipid content (%) (**Paper II**) and FTIR and FT-Raman spectral data (**Paper II-IV**).

1.7.1 Analysis of univariate data

For the univariate data the average of biological replicates was calculated, and the standard deviation was estimated**.**

1.7.2 Analysis of multivariate data

Principal component analysis (PCA), cluster analysis and correlation analysis were employed to analyze complex GC-FID data and spectral data to uncover patterns, correlations, and relationships between the measured

variables [135]. Multivariate spectral data require preprocessing prior the analysis to remove unwanted variation.

Preprocessing

GC -FID data preprocessing include normalization by using autoscaling with mean-centring, followed by the division of each column (variable) by the standard deviation.

Different preprocessing methods were used for the elimination of physical effects and unwanted variations from the **spectral data**, ensuring that only chemical information is extracted for further analysis. By addressing baseline shifts, mitigating background noise, and compensating for scattering effects, preprocessing serves the purpose of eliminating extraneous non-chemical factors that may obscure or distort the genuine spectral signatures [136]. The specific preprocessing procedures applied in IR and Raman spectroscopy are contingent upon the data's characteristics and the nature of the sample but most pre-processing methods used for IR spectra are generally applicable to Raman spectra [137].

In the context of infrared spectra preprocessing, techniques such as Extended Multiplicative Signal Correction (EMSC) are used to enhance data quality [138]. EMSC effectively rectifies baseline offsets and normalizes spectra by scaling facilitating the identification of chemical differences between samples. The implementation of filters like the Savitzky-Golay filter achieves noise reduction without compromising essential spectral features [139]. The selection of specific wavelengths or regions of interest narrows the focus on the biomolecules of interest [140]. Detection and removal of outliers enhances the reliability of the dataset [137]. Furthermore, the application of second derivative transformation improves baseline correction by removing constant background signals, enhances peak resolution and aids in distinguishing overlapping bands [137].

In this PhD work before conducting data analysis, quality test (Figure 1.13A) was performed on the spectra using a test developed by Tafintseva et al. [141] for FTIR spectra (**Paper II-III**). To ensure the quality of the FT-Raman

spectra, a quality assessment was conducted as follows: Peak maximum values within the biomass region (1430-1470 cm-1) and the non-informative region (1800-2000 cm-1) were identified and calculated the ratio between these maximum values (**Paper IV**)**.** Spectra with low signal-to-noise ratio were removed from analysis (**Paper IV**). Spectra that passed the quality test were preprocessed in the following way (**Paper II-IV**): (1) averaging of technical replicates for each sample by calculating arithmetic mean in **Paper III**; (2) applying Savitzky−Golay algorithm with second polynomial degree and different window sizes depending on the spectral region where 9 points were used for lipid region, 19 points for protein region and 13 for carbohydrate region or 11 points for the whole spectral region for FTIR spectra (**Paper II, III**) or area normalization for FT-Raman spectra (**Paper IV**) (Figure 1.13A); (3) splitting the data according to the informative regions based on the type of macromolecules: 3050–2800 cm^{-1} and 1800–1700 cm^{-1} for lipids, 1700–1500 cm^{-1} for proteins, mixed region at 1500–1200 cm^{-1} and 1200–700 cm^{-1} for polysaccharides for FTIR spectra (**Paper III**) or using the whole spectral region (**Paper II and IV**) (4) EMSC was applied for second-derivative spectra for each region separately to separate informative signals from physical effects such as variability due to light scattering or sample thickness for FTIR spectra (**Paper II, III**).

After preprocessing, ratio of peak intensities and multivariate data analysis techniques such as PCA and correlation PCA analysis were applied in **Paper II-IV** to analyze the total cellular biochemical profile of the studied bacteria (Figure 1.13B). For PCA, the complete mid-infrared region (**Paper II**) as well as single spectral regions of lipids, proteins and polysaccharides were used (**Paper III**)**.** Correlation analysis between variables and PCA scores was used to investigate the temperature effect on biochemical profile measured by FTIR-HTS spectroscopy in **Paper III** that resulted in correlation loading plots showing a subset of the most relevant spectral variables (peaks) and temperature. Pearson correlation coefficient (r) was calculated to examine the relationship between the L/P ratio and total lipid content in **Paper II** (Figure 1.13B).

Assessment of relative peak heights. Ratio of peak intensities at specific wavelengths facilitates a deeper understanding of relative chemical composition of a sample [142]. This is valuable for studying drug effects, stress responses, or adaptation mechanisms [122, 123, 143] (Figure 1.13B). For the evaluation of temperature-induced changes in bacterial cells, ratios between lipids, polysaccharides and proteins were estimated using FTIR spectra in **Paper II**. The protein Amide I peak at 1656 cm^{-1} was selected as a relatively stable reference band due to the possibly low variation of protein content in bacterial cells. Ratiometric analysis was used to evaluate effect of temperature and light on pigments production in **Paper IV.** For estimating the relative content of pigments, the ratio between peak maxima in the range of 1500-1540 cm^{-1} (indicating the presence of carbon-carbon double bonds within the carotenoid molecule) and peak maxima of the biomass in the range of 1430-1470 cm^{-1} (related to total biomass) was calculated.

Principal Component Analysis (PCA). PCA is a widely used unsupervised data analysis method for exploring multivariate data, primarily employed to reveal underlying patterns [144]. Its objective is to visually represent the positions of data points in fewer dimensions, preserving maximum information, and investigating relationships among dependent variables [144]. Score plots visualize data points in the reduced space, highlighting clustering and outliers. A loading plot in PCA displays the relationships between the original variables and the PC. Each principal component is represented as a vector pointing to the direction of its highest variation in the space of the original variables. The contribution of each variable to the vector indicates the variable's contribution to the principal component's variance. Loading plots help to identify which original variables are driving the observed patterns and they provide insights into the underlying structure of the data. Correlation loading plots display the variable impact on PC, aiding in identifying influential factors.

The Unscrambler, V10.01 (CAMO PROCESS AS, Oslo, Norway) and algorithms in Matlab, V12.a (The Mathworks, Inc., Natick, MA) were used to perform the analysis in **Paper III.** Quasar or Orange-Spectroscopy data

mining toolbox version 3.31.1 (University of Ljubljana, Ljubljana, Slovenia) was used for the preprocessing spectral analysis, ratiometric analysis, PCA analysis [145-147] in **Paper II-IV**.

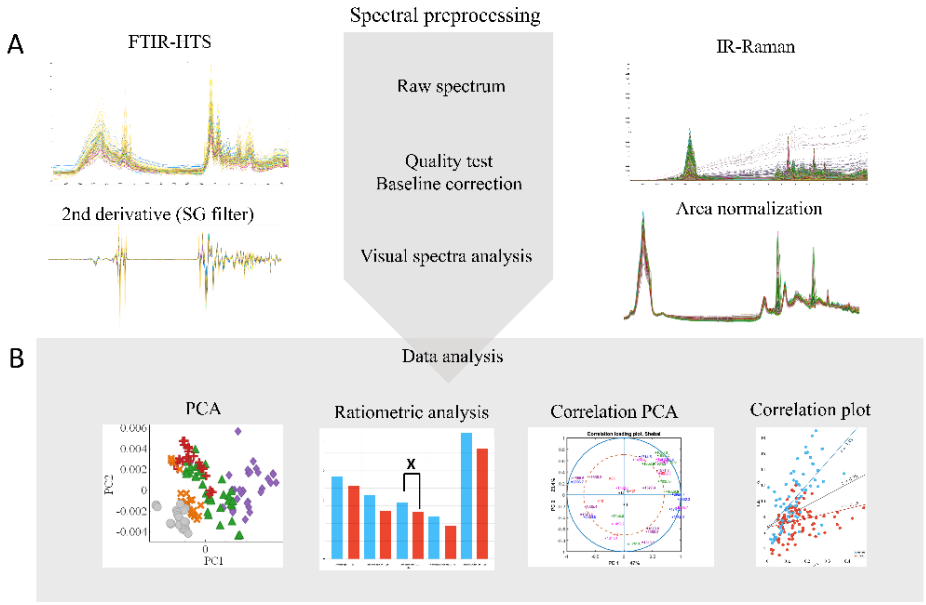

Figure 1.13. Overview of A- spectral preprocessing methods and B- data analysis methods used in the PhD work.

2 Main results and discussion

2.1 Paper I: Isolation, Physiological Characterization, and Antibiotic Susceptibility Testing of Fast-Growing Bacteria from the Sea-Affected Temporary Meltwater Ponds in the Thala Hills Oasis (Enderby Land, East Antarctica)

Paper I presents an assessment of bacterial diversity for nine temporary meltwater ponds located in the Vecherniy district of the Tala Hills oasis in the Western part of Enderby Land in East Antarctica. This study includes physicochemical and biological analysis of water samples and analyses of the genotypic and physiological traits of twenty-nine fast-growing bacteria isolated from these ponds. **Paper I** also includes a large study on the antibiotic susceptibility using eighteen antibiotics (3 of which were used at two concentrations) and five antibacterial agents.

The 16S rRNA gene was amplified and sequenced, and the resulting sequences were compared to databases for the taxonomic classification and phylogenetic tree construction. The isolated Antarctic meltwater bacteria were identified as related to four phyla, Proteobacteria, Actinobacteria, Firmicutes, and Bacteroidetes, and represented by twelve genera. Proteobacteria was the first predominant phylum among the isolates, and it was represented by three genera: *Pseudomonas*, *Shewanella*, and *Acinetobacter*. Actinobacteria was the second predominant phylum, and it was represented by five genera: *Arthrobacter*, *Brachybacterium*, *Micrococcus*, *Agrococcus*, and *Leifsonia*. The Firmicutes phylum was represented by three genera: *Carnobacterium*, *Sporosarcina*, and *Facklamia*. The Bacteroidetes phylum was represented by only one isolate belonging to the genus *Flavobacterium*.

For the majority of the isolates the optimal growth temperature was 18°C, while many isolates tolerated 4°C to 25°C, 30°C, and 37°C. Among various tested enzymatic activities, lipolytic and proteolytic activities were the most predominant. Some isolates expressed deoxyribonuclease, amylase activity and β-galactosidase and catalase activity. The highest enzymatic activity was detected for *Brachybacterium paraconglomeratum* BIM B-

1571, *Micrococcus luteus* BIM B-1545, for several *Pseudomonas lundensis* and for *Shewanella baltica* isolates.

Evaluation of antibiotic susceptibility was performed using the Kirby-Bauer disk diffusion method at temperatures 18°C and 25°C for eighteen antibiotics. Twenty-five isolates were resistant to at least one antibiotic, and seven isolates showed different levels of multi-resistance (Figure 2.1). Many isolates (>10) were resistant to ampicillin, cefuroxime, amoxicillin-clavulanic acid, and trimethoprim. A few isolates (<3) were resistant to imipenem, ciprofloxacin, high concentrations of rifampicin 30 µg, 120 µg of gentamicin, 300 µg of streptomycin, and doxycycline. None of the isolates was resistant to a high concentration of streptomycin. Most of the Gram-negative isolates were resistant to β-lactam-type antibiotics such as ampicillin, amoxicillin-clavulanic acid, cefuroxime, and trimethoprim. Among the Gram-negative isolates, *Acinetobacter lwoffii* BIM B-1558 and all *Pseudomonas lundensis* isolates showed multiple antibiotic resistance and were resistant to ten and more antibiotics. For Gram-positive isolates, the highest level of resistance was detected against aminoglycoside antibiotics (tobramycin, kanamycin, and low concentrations of streptomycin) and trimethoprim. Gram-positive bacterial isolates such as *Brachybacterium paraconglomeratum* BIM B-1571, *Agrococcus citreus* BIM B-1547, *Carnobacterium inhibens* BIM B-1540, and *Facklamia tabacinasalis* BIM B-1577 were resistant to five and more antibiotics, mostly aminoglycosides and trimethoprim. The isolates *Pseudomonas peli* BIM B-1560 and BIM B-1542 and *Sporosarcina* sp. BIM B-1539 were susceptible to all tested antibiotics (Figure 2.1).

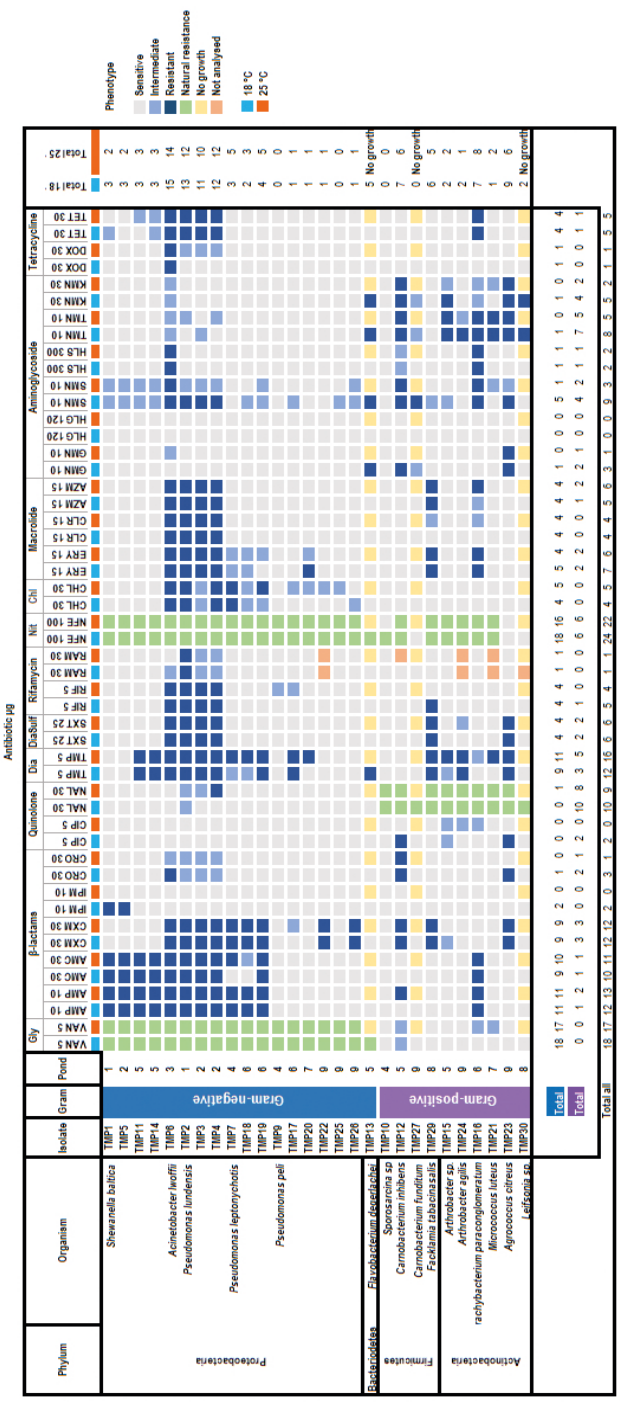

Figure 2.1. Antimicrobial susceptibility profiles of bacterial isolates from MPs at 18 and 25°C.

2.2 Paper II: Explorative characterization and taxonomy-aligned comparison of alterations of lipids and other biomolecules in Antarctic bacteria grown at different temperatures

In **Paper II** an exploratory characterization and taxonomy-aligned comparison of temperature-induced changes in cellular biomolecules, including lipids, proteins, and polysaccharides for the newly isolated cold-adapted meltwater bacteria was conducted.

The effect of temperature on the total lipid content in bacterial cells was species-specific. The majority of the isolates showed an increase in total lipid content at lower temperatures. The total lipid content differed significantly for two Gram groups, where Gram-negative bacteria exhibited in average a higher total lipid content compared to Gram-positive bacteria. Proteobacteria displayed the highest total lipid content. The main variability in total lipid content was observed among different species (Figure 2.2). It was observed that total lipid content in bacteria related to genus *Pseudomonas* considerably varied from 6 to 19 % w/w between different species and was high for *Pseudomonas peli* strains from 14% up to 19%.

The analysis of the structural characteristics of the fatty acid profile showed that all Gram-positive Actinobacteria and Firmicutes from genera *Facklamia* and *Carnobacterium* had br-SFAs as a major group of fatty acids, while Gram-negative Proteobacteria, except *Shewanella*, had n-MUFAs and n-SFAs at all studied temperatures. Interestingly, bacteria from genera *Shewanella* and *Flavobacterium* had br-SFAs present in their profile, which were not detected for other Gram-negative bacteria (Figure 2.3). Temperature induced changes of the fatty acid profile were registered for all studied bacteria. Gram-positive bacteria demonstrated alterations in both quantity and type (anteiso-/iso-) of methyl branching, as well as changes in chain length and unsaturation, while Gram-negative bacteria showed alterations only in unsaturation and acyl chain length when grown at low temperature.

Long-chain fatty acids (LCFAs) were predominant (60-98%) in all studied Antarctic bacteria, while medium-chain fatty acids (MCLFAs) were found in smaller amounts (3-11%) in some *Pseudomonas* and *Flavobacterium* isolates and increased at higher growth temperatures. Very long-chain fatty acids (VLCFAs) were detected in lowest amount (up to 7%) mainly for Actinobacteria grown at higher temperatures, and short-chain fatty acids (SCFAs) were present in negligible amount.

FTIR analysis of the intact bacterial biomass obtained from cultivation at different temperatures indicated the impact of temperature on the whole cellular biochemical profile, where the most pronounced changes were recorded for the mixed spectral region at 1500-900 cm^{-1} where peaks related to carbohydrates, nucleic acids and phosphates are present. The effect of temperature on this spectral region was considerable for all taxonomic groups. Thus, an increase in intensity for several peaks in the mixed region (1400 cm^{-1}, 1240 cm^{-1} and 1083 cm^{-1}) along with temperature decrease was recorded for the majority of Proteobacteria, Bacteroidetes and Actinobacteria isolates, while changes for Firmicutes were less intense (Figure 2.4). The most significant changes in the mixed spectral region were detected for *Pseudomonas*, *Shewanella*, *Acinetobacter* and *Leifsonia*. FTIR spectra of nearly all bacteria showed alterations in a peak at 1083 cm^{-1} related to phosphodiester groups mainly from phospholipids (for Gram-negative bacteria) and teichoic /lipoteichoic acids (for Gram-positive bacteria), which was significantly higher for lower temperatures. The ester peak at 1743 cm^{-1} was increased for lower temperature for Gram-positive Actinobacteria. Temperature-induced changes in the protein region (1700-1500 cm^{-1}) were mainly associated with a shift of Amide I peak at 1640 cm^{-1} related to β-sheet structures of proteins. A shift of the Amide I peak at 1640 cm^{-1} to lower wavenumbers was recorded for Proteobacteria from the genera *Shewanella* and *Pseudomonas* and from Firmicutes isolates from the genus *Carnobacterium* grown at higher growth temperature.

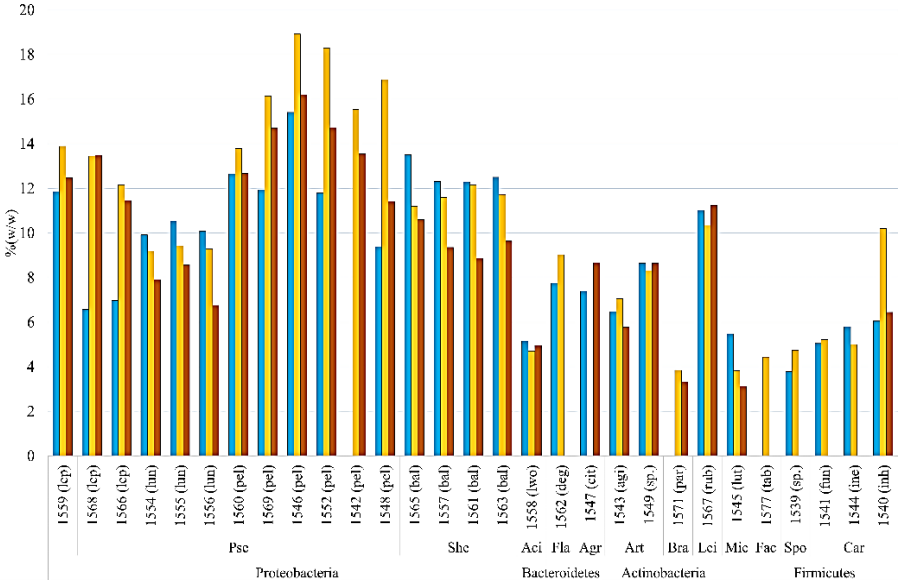

Figure 2.2. Total lipid content (%, w/w) of bacterial biomass of different genera grown at different temperatures (blue – 5°C, yellow – 15°C and orange – 25°C)

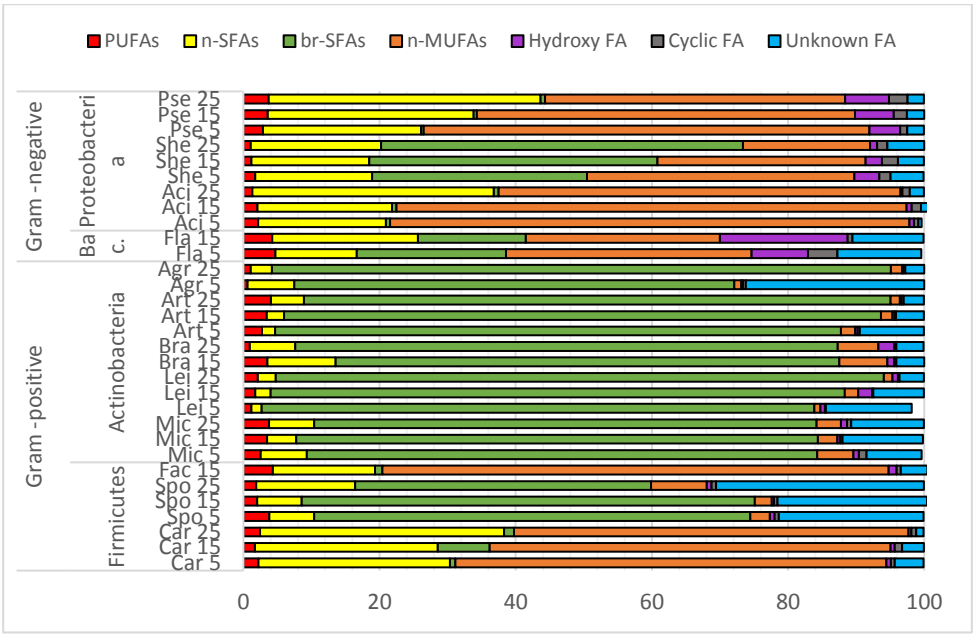

Figure 2.3 Fatty acid profile of bacteria grown at different temperatures (%, w/w)

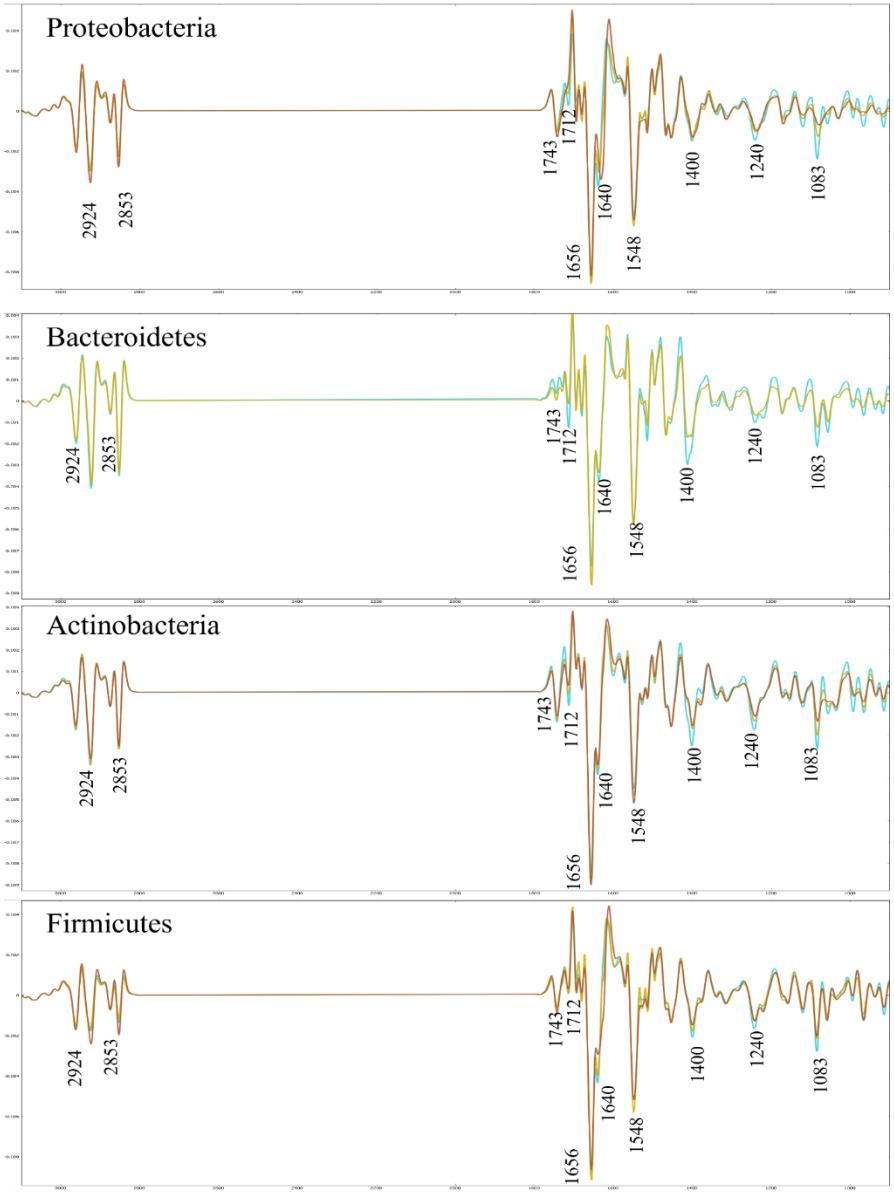

Figure 2.4. Second derivative FTIR spectra of bacterial biomass of different phyla averaged for different temperatures (blue – 5°C, yellow – 15°C and orange – 25°C).

2.3 Paper III: Global biochemical profiling of fast-growing Antarctic bacteria isolated from meltwater ponds by high-throughput FTIR spectroscopy

In **Paper III** a characterization of the total cellular biochemical profile of the Antarctic meltwater bacteria grown in different cultivation media and at different temperatures was performed by FTIR spectroscopy.

FTIR profiling revealed distinct chemical differences in biochemical profile for the bacteria grown on agar and broth, where agar provided better phylogeny-aligned clustering than broth (Figure 2.5). Lipid spectral region showed to be the most discriminative and provided the best phylogeny-aligned clustering. Cultivation on agar also provided the most stable biochemical profile characterized by the low variability. FTIR biochemical spectral profiles distinguished significant chemical variations between Gram groups, notably in lipid content and phosphodiesters. Additionally, variations in protein structure were observed, with Gram-positive bacteria exhibiting higher intensities in α-helical and β-pleated sheet structures.

The effect of temperature on the profile was lower than effect of media and provided better phylogeny-aligned clustering (Figure 2.6). The impact of temperature on the cellular biochemical profile of the studied bacteria was specie-specific, where polysaccharides were the most affected cellular component while lipids stayed the most unchanged. The most consistent FTIR biochemical profile for all studied species was at 18°C while growth at 25°C triggered changes for *Pseudomonas, Flavobacterium* and *Arthrobacter* strains where each specie had specific responses. The growth at higher temperatures 30°C and 37°C was affecting only bacteria from genus *Shewanella* and *Pseudomonas lundensis,* with *Acinetobacter lwoffii* BIM B – 1558 strains, respectively, where the main changes were associated with proteins and polysaccharides (Figure 2.7A). Low temperatures 4°C and 10°C showed to have the highest effect on the majority of studied species, except all *Pseudomonas* species, *Arthrobacter alpinus* BIM B – 1549, *Carnobacterium iners* BIM B – 1544 (Figure 2.7B). Correlation analysis showed that *Micrococcus luteus* BIM B – 1545 and

Leifsonia sp. BIM B – 1567 have consistent biochemical profile not affected by the temperature (Figure 2.7C).

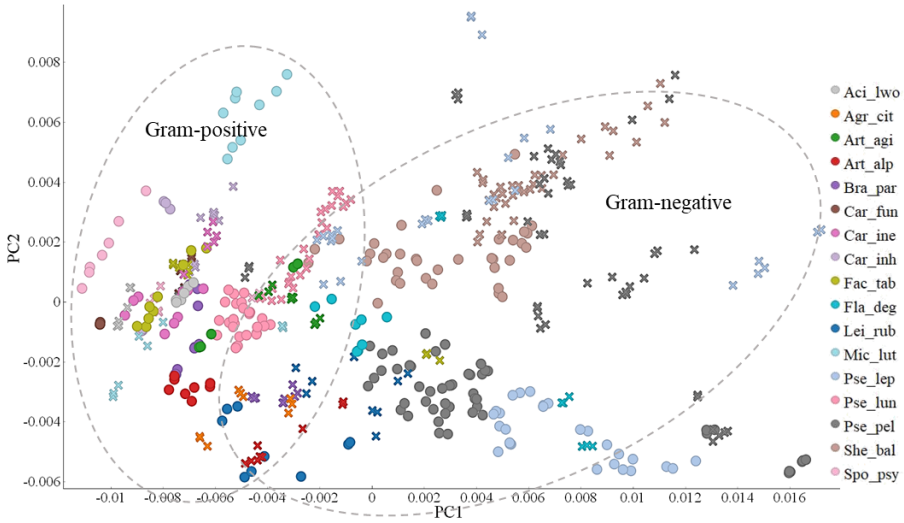

Figure 2.5. PCA scatter plot of Antarctic bacteria cultivated on one temperature 18°C and different media BHIA and BHIB ('●' – Agar, '✕' – Broth), colors represent specie.

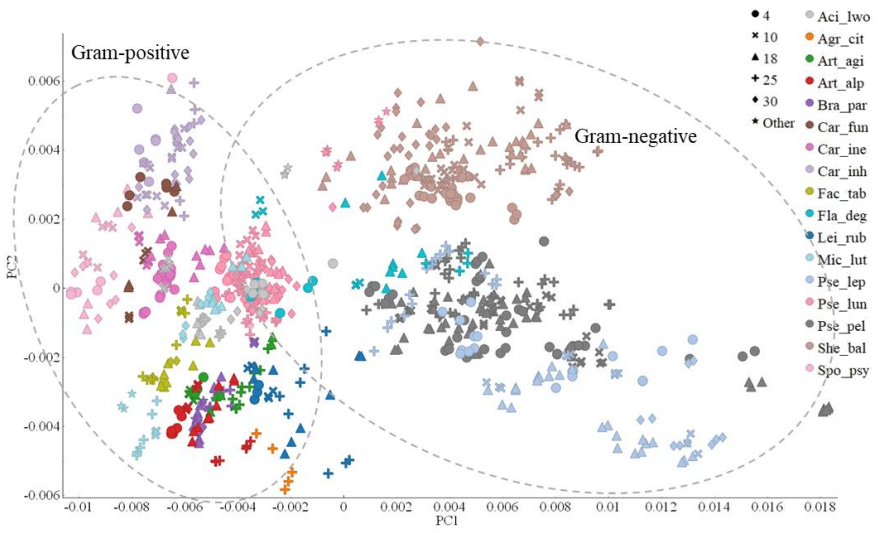

Figure 2.6. PCA scatter plot of Antarctic bacteria cultivated on different temperatures 4, 10, 18, 25, 30 and 37°C media agar and broth, colors represent specie.

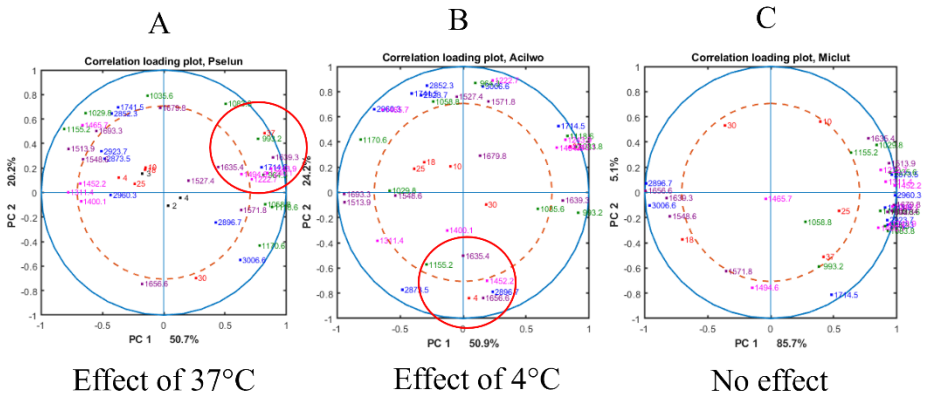

Figure 2.7. Correlation loading plot based on PCA analysis of FTIR-HTS with: A- effect of 37°C on the profile of Pseudomonas lundensis strains, B- effect of 4°C on the profile of Acinetobacter lwoffii BIM B – 1558 strain and C- no effect of temperature on the profile of Micrococcus luteus BIM B – 1545.

2.4 Paper IV: Screening for pigment production and characterization of pigment profile and photostability in cold-adapted Antarctic bacteria using FT-Raman spectroscopy

In **Paper IV,** screening for pigment production and characterization of the pigment profile and photostability of intact pigmented biomass was performed. FT-Raman spectroscopy combined with PCA, and analysis of relative band intensities was used to identify pigment producing Antarctic meltwater bacteria. For estimating the relative content of pigments, carotenoid-to-biomass ratio (C/B) was calculated. Specifically, the ratio between peak maxima in the range of 1500-1540 cm^{-1} (related to C=C stretching in polyene chain of carotenoids) and peak maxima in the range of 1430-1470 cm^{-1} (related to CH_2 and CH_3 deformations of lipids, proteins, and carbohydrates, thus serving as proxy signal for total biomass) was calculated (Figure 2.8). Among the studied twenty-nine bacterial strains, production of pigments was detected for six strains related to the Actinobacteria phylum (*Agrococcus, Arthrobacter, Brachybacterium, Leifsonia, Micrococcus*) and one genus of the Bacteroidetes phylum (*Flavobacterium*) (Figure 2.8). Growth of bacteria at different temperatures resulted in a species-specific effect where for *Flavobacterium degerlachei* BIM B-1562, *Arthrobacter* sp. BIM B-1549, *Leifsonia* sp. BIM B-1567 relative pigment content increased with temperature increase, and the opposite was observed for the other studied bacteria (Figure 2.8). The pigment profile detected by FT-Raman was based on the position of peak maxima of the C=C stretching vibrations in carotenoids, and it was species-specific. Reference HPLC-MS analysis revealed the presence of a complex carotenoid profile of Antarctic bacteria. For example, *Flavobacterium degerlachei* BIM B-1562 from the Bacteroidetes phylum, showed a distinctive pigment profile characterized by the presence of C40 ehinenone, canthaxanthin, and zeaxanthin as the main carotenoids. *Leifsonia rubra* BIM B-1567 exhibited C40 lycopene and phytoene as the main carotenoids. The strain *Agrococcus citreus* BIM B-1547 exhibited relatively low levels of carotenoids, with only C45 and C50 variants being detected

Based on FT-Raman screening and HPLC-MS data, five bacterial isolates have been identified as promising pigment producers marked with stars in Figure 2.8. These isolates were further tested for their biomass production and the induction of pigment production when they are exposed to blue light. It has been observed that blue light induced pigment production in all tested bacterial isolates except *Arthrobacter* sp. BIM B-1549 (Figure 2.9). According to the results for biomass productivity and relative pigment content estimated as carotenoids/biomass ratio using FT-Raman spectra, the most promising pigment producers were *Flavobacterium degerlachei* BIM B-1562, *Arthrobacter* sp. BIM B-1549 and *Leifsonia rubra* BIM B-1567 (Figure 2.9).

Pronounced photodegradation effects on pigments was observed in the pigmented bacterial biomass after exposure to light with 900 lux for 60 hours. The results from photostability testing showed that the lowest degradation rate of pigment was observed for *Arthrobacter agilis* BIM B-1543, where C50 carotenoids are predominant (Figure 2.10). FT-Raman showed to be a powerful analytical tool to assess both relative pigment content and the pigment profile using a spectral library of pigment standards.

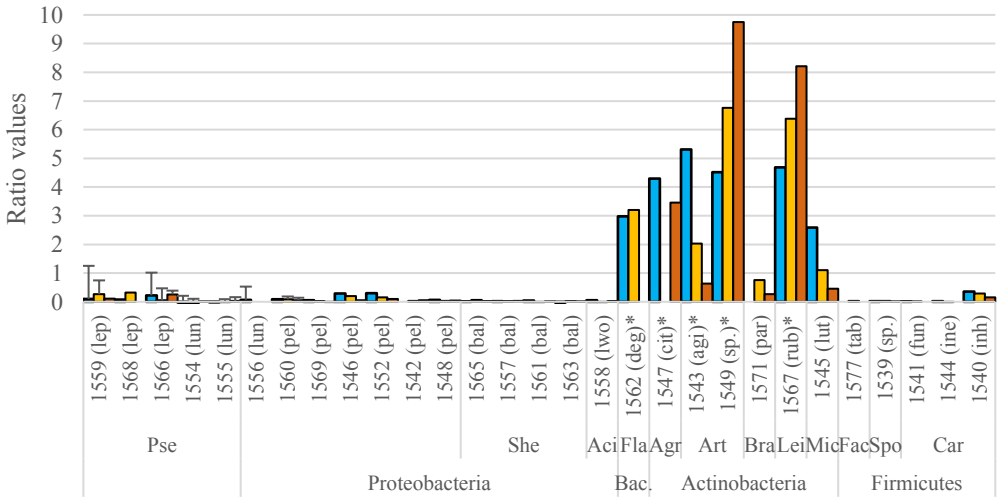

*Figure 2.8. Analysis of relative band ratios in FT-Raman spectra of pigmented bacterial biomass obtained after cultivation at different temperatures (blue – 5°C, yellow – 15°C, and orange – 25°C). Genera: Agr-Agrococcus, Art-Arthrobacter, Bra-Brachybacterium, Fla-Flavobacterium, Lei-Leifsonia, Mic-Micrococcus, Pse-Pseudomonas, She-Shewanella. * - strains selected for detail analysis.*

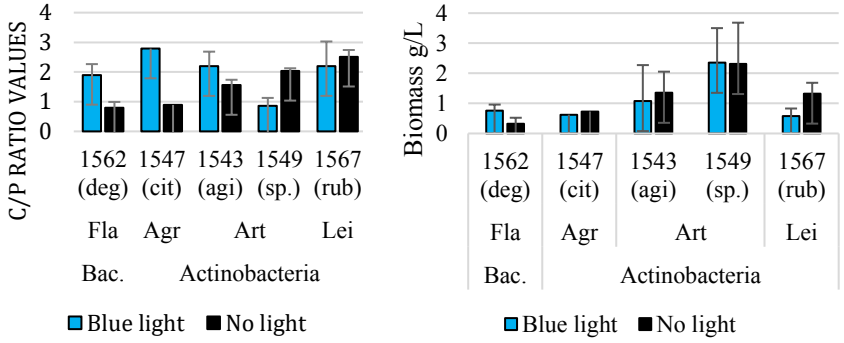

Figure 2.9. Relative pigment amount at 15°C under blue light exposure and no light exposition (control) measured by quantifying the C/P ratio of the freeze-dried biomass and biomass production (g/L) at 15°C. Genera: Fla-Flavobacterium, Agr-Agrococcus, Art-Arthrobacter, Lei-Leifsonia.

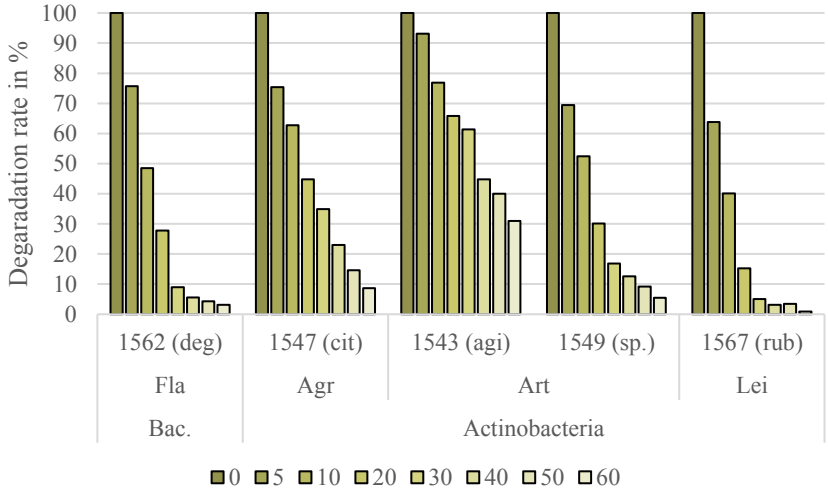

Figure 2.10. Analysis of relative band ratios in FT-Raman spectra of the freeze-dried bacterial biomass exposed by light. Colors represent exposition time (h), Genera: Fla-Flavobacterium, Agr-Agrococcus, Art-Arthrobacter, Lei-Leifsonia.

3 Conclusion and future prospects

In this PhD work, for the first time, isolation, identification and global phenotypic characterization of twenty-nine newly isolated cold-adapted bacteria from temporary meltwater ponds located in the Western part of Enderby Land, East Antarctica was performed. The impact of temperature on cellular lipids, pigments and total cellular biochemical profile of the isolated Antarctic meltwater bacteria was in a special focus of this PhD work. Vibrational spectroscopy techniques FT-IR and FT-Raman spectroscopy were used for biochemical profiling, library-independent estimation of the relative total piment content and library-dependent estimation of pigment profile.

The physiological characterization and evaluation of antibiotic susceptibility performed in **Paper I** showed that the isolated meltwater bacteria are psychrotrophic, can possess multiple enzymatic activities and some of them have antibiotic multi-resistance. The recorded physiological characteristics and antibiotic resistance may be associated with animal activity close to the meltwater ponds. The fact that several isolated bacteria showed a high level of multi-resistance would be important to consider when predicting the effect of climate change and anthropogenic activity in Antarctic regions.

This PhD work showed that the cellular response of the meltwater bacteria to temperature fluctuation in Antarctica is driven by changes in alteration in many biochemical components of their cells. Thus, in **Paper II** it was shown that changes in lipids as well as proteins, phosphorus containing compounds and polysaccharides were triggered by temperature fluctuations. Thus, it was observed that the changes in lipids and proteins are more specie-specific, while changes in carbohydrates, nucleic acids and phosphates were detected for all taxonomy groups. Additionally high lipids amount up to 19% was reported for some *Pseudomonas peli* strains that could have a possible biotechnological potential. **Paper III**, for the first time, reports the total cellular biochemical profile of the Antarctic meltwater bacteria as well as its variation under different cultivation

conditions. The results suggest that agar is the best form of BHI medium for understanding biochemical nature of phylogenetic relations and studying effect of abiotic factors on cell chemistry. Temperature-induced changes in biochemical composition were species-specific, with the most significant effects observed in bacteria with a broad growth temperature range. Interestingly, the biochemical profile of *Micrococcus luteus* BIM B – 1545 was little affected by temperature but extensively affected by the form of cultivation medium.

Paper IV demonstrated the importance of screening and studying polar bacteria for identifying new potential pigment producers. Some Antarctic bacteria related to *Flavobacterium, Arthrobacter* and *Leifsonia* genera exhibited the high levels of pigment content achieved under non-optimized cultivation conditions. Interesting observation was made for *Arthrobacter agilis* BIM B-1543 showed that the lowest degradation rate of pigment what could be important for considering of using it for solar cells. In addition, it was demonstrated that FT-Raman spectroscopy is a truly powerful analytical tool for both semi-qualitative screenings and descriptive analysis of pigmented microorganisms.

Overall, the findings from this PhD work have a significant contribution to understanding microbiota of polar regions. This work deepens our understanding of the importance and potential of Antarctic bacteria and sheds light on their cellular responses to temperature which is considered as one of the main environmental factors affecting survival and adaptation of microorganisms. In addition, this PhD work clearly demonstrates the analytical benefits and potential of vibrational spectroscopy techniques for total biochemical characterization as well as semi-quantitative chemical analysis of single biochemical components in bacterial cells. The comprehensive knowledge obtained in this PhD work can be used as a background to further explore some of the isolated Antarctic meltwater bacteria, for example, for production of pigments and lipids. More research to uncover the genetic and metabolic basis of multi-resistance for some isolates needs to be performed in order to understand the consequences

and potential risks that may arise when these isolates spread due to a climate change.

4 References

1. Kingslake, J., J.C. Ely, I. Das, and R.E. Bell, *Widespread movement of meltwater onto and across Antarctic ice shelves.* Nature, 2017. **544**(7650): p. 349-352.
2. Kakareka, S.V., et al., *Chemical characteristics of antarctic lakes of the Thala Hills.* Arctic and Antarctic Research, 2019. **65**(4): p. 422-437.
3. Aspmo, K., et al., *Mercury in the atmosphere, snow and melt water ponds in the North Atlantic Ocean during Arctic summer.* Environmental science & technology, 2006. **40**(13): p. 4083-4089.
4. Jungblut, A.D., D. Mueller, and W.F. Vincent, *Arctic ice shelf ecosystems.* Arctic ice shelves and ice islands, 2017: p. 227-260.
5. Wilkins, D., et al., *Key microbial drivers in Antarctic aquatic environments.* FEMS Microbiology Reviews, 2013. **37**(3): p. 303-335.
6. Liu, Y., et al., *Culturable bacteria in glacial meltwater at 6,350 m on the East Rongbuk Glacier, Mount Everest.* Extremophiles, 2009. **13**: p. 89-99.
7. Miamin, V.E., et al., *Microbiology investigation in the Vechernyy region, Tala Hills (East Antarctica)*, Belarus State University Annual, 2014. **9**: p. 58-67.
8. De Mora, S., R.F. Whitehead, and M. Gregory, *The chemical composition of glacial melt water ponds and streams on the McMurdo Ice Shelf, Antarctica.* Antarctic Science, 1994. **6**(1): p. 17-27.
9. Healy, M., J. Webster-Brown, K. Brown, and V. Lane, *Chemistry and stratification of Antarctic meltwater ponds II: Inland ponds in the McMurdo Dry Valleys, Victoria Land.* Antarctic Science, 2006. **18**(4): p. 525-533.
10. Jungblut, A.D., et al., *Diversity within cyanobacterial mat communities in variable salinity meltwater ponds of McMurdo Ice Shelf, Antarctica.* Environmental microbiology, 2005. **7**(4): p. 519-529.
11. Schmidt, S., et al., *Limnological properties of Antarctic ponds during winter freezing.* Antarctic Science, 1991. **3**(4): p. 379-388.

12. Wait, B., et al., *PChemistry and stratification of Antarctic meltwater ponds I: coastal ponds near Bratina Island, McMurdo Ice Shelf.* Antarctic Science, 2006. **18**(4): p. 515-524.
13. Archer, S.D., I.R. McDonald, C.W. Herbold, and S.C. Cary, *Characterisation of bacterioplankton communities in the meltwater ponds of Bratina Island, Victoria Land, Antarctica.* FEMS Microbiology Ecology, 2014. **89**(2): p. 451-464.
14. Archer, S.D., et al., *Benthic microbial communities of coastal terrestrial and ice shelf Antarctic meltwater ponds.* Frontiers in microbiology, 2015. **6**: p. 485.
15. Wait, B., R. Nokes, and J. Webster-Brown, *Freeze-thaw dynamics and the implications for stratification and brine geochemistry in meltwater ponds on the McMurdo Ice Shelf, Antarctica.* Antarctic Science, 2009. **21**(3): p. 243-254.
16. Keatley, B.E., et al., *Impacts of seabird-derived nutrients on water quality and diatom assemblages from Cape Vera, Devon Island, Canadian High Arctic.* Hydrobiologia, 2009. **621**: p. 191-205.
17. Tin, T., et al., *Impacts of local human activities on the Antarctic environment.* Antarctic Science, 2009. **21**(1): p. 3-33.
18. Noble, T., et al., *The sensitivity of the Antarctic ice sheet to a changing climate: past, present, and future.* Reviews of Geophysics, 2020. **58**(4): p. e2019RG000663.
19. Jackson, E.E., I. Hawes, and A.D. Jungblut, *16S rRNA gene and 18S rRNA gene diversity in microbial mat communities in meltwater ponds on the McMurdo Ice Shelf, Antarctica.* Polar Biology, 2021. **44**(4): p. 823-836.
20. Spergel, J.J., et al., *Surface meltwater drainage and ponding on Amery Ice Shelf, East Antarctica, 1973–2019.* Journal of Glaciology, 2021. **67**(266): p. 985-998.
21. Dieser, M., et al., *Physicochemical and biological dynamics in a coastal Antarctic lake as it transitions from frozen to open water.* Antarctic Science, 2013. **25**(5): p. 663-675.
22. Hogg, I.D., et al., *Biotic interactions in Antarctic terrestrial ecosystems: are they a factor?* Soil Biology and Biochemistry, 2006. **38**(10): p. 3035-3040.
23. Rosa, L.H., *Fungi of antarctica: Diversity, ecology and biotechnological applications*. 2019: Springer.
24. Kleinteich, J., et al., *Diversity of toxin and non-toxin containing cyanobacterial mats of meltwater ponds on the Antarctic Peninsula: a pyrosequencing approach.* Antarctic Science, 2014. **26**(5): p. 521-532.

25. Vincent, W.F., *Cyanobacterial dominance in the polar regions*, in *The ecology of cyanobacteria: Their diversity in time and space*. 2000, Springer. p. 321-340.
26. Smith, H.J., et al., *Relationship between dissolved organic matter quality and microbial community composition across polar glacial environments.* FEMS Microbiology Ecology, 2018. **94**(7): p. fiy090.
27. Maccario, L., L. Sanguino, T.M. Vogel, and C. Larose, *Snow and ice ecosystems: not so extreme.* Research in microbiology, 2015. **166**(10): p. 782-795.
28. Baublis, J.A., R.A. Wharton Jr, and P.A. Volz, *Diversity of micro-fungi in an Antarctic dry valley.* Journal of Basic Microbiology, 1991. **31**(1): p. 1-12.
29. Ilicic, D., et al., *Antarctic glacial meltwater impacts the diversity of fungal parasites associated with Benthic diatoms in shallow coastal zones.* Frontiers in microbiology, 2022. **13**: p. 805694.
30. Ferreira, E.M.S., F.M.P. de Sousa, L.H. Rosa, and R.S. Pimenta, *Taxonomy and richness of yeasts associated with angiosperms, bryophytes, and meltwater biofilms collected in the Antarctic Peninsula.* Extremophiles, 2019. **23**: p. 151-159.
31. Archer, S.D.J., I.R. McDonald, C.W. Herbold, and S.C. Cary, *Characterisation of bacterioplankton communities in the meltwater ponds of Bratina Island, Victoria Land, Antarctica.* FEMS Microbiology Ecology, 2014. **89**(2): p. 451-464.
32. Comte, J., L. Fauteux, and P.A.d. Giorgio, *Links between metabolic plasticity and functional redundancy in freshwater bacterioplankton communities.* Frontiers in microbiology, 2013. **4**: p. 112.
33. Lauritano, C., C. Rizzo, A. Lo Giudice, and M. Saggiomo, *Physiological and molecular responses to main environmental stressors of microalgae and bacteria in polar marine environments.* Microorganisms, 2020. **8**(12): p. 1957.
34. Ramasamy, K.P., et al., *Comprehensive insights on environmental adaptation strategies in Antarctic bacteria and biotechnological applications of cold adapted molecules.* Frontiers in Microbiology, 2023. **14**: p. 1197797.
35. Dasila, H., D. Maithani, D.C. Suyal, and P. Debbarma, *Cold-Adapted Microorganisms: Survival Strategies and Biotechnological Significance.* Survival Strategies in Cold-adapted Microorganisms, 2022: p. 357-378.

36. Tribelli, P.M. and N.I. López, *Reporting key features in cold-adapted bacteria.* Life, 2018. **8**(1): p. 8.
37. Rizzo, C. and A. Lo Giudice, *Life from a Snowflake: Diversity and Adaptation of Cold-Loving Bacteria among Ice Crystals.* Crystals, 2022. **12**(3): p. 312.
38. Mancuso Nichols, C., et al., *Production of exopolysaccharides by Antarctic marine bacterial isolates.* Journal of Applied Microbiology, 2004. **96**(5): p. 1057-1066.
39. Deming, J.W. and J.N. Young, *The role of exopolysaccharides in microbial adaptation to cold habitats.* Psychrophiles: from biodiversity to biotechnology, 2017: p. 259-284.
40. Naumann, D., *Infrared spectroscopy in microbiology.* Encyclopedia of analytical chemistry, 2000. **102**: p. 131.
41. Sohlenkamp, C. and O. Geiger, *Bacterial membrane lipids: diversity in structures and pathways.* FEMS microbiology reviews, 2016. **40**(1): p. 133-159.
42. Wältermann, M., et al., *Mechanism of lipid-body formation in prokaryotes: how bacteria fatten up.* Molecular microbiology, 2005. **55**(3): p. 750-763.
43. Chattopadhyay, M. and M. Jagannadham, *Maintenance of membrane fluidity in Antarctic bacteria.* Polar Biology, 2001. **24**(5): p. 386-388.
44. Hassan, N., et al., *Temperature driven membrane lipid adaptation in glacial psychrophilic bacteria.* Frontiers in Microbiology, 2020. **11**: p. 824.
45. Mező, E., et al., *Effect of Culture Conditions on Fatty Acid Profiles of Bacteria and Lipopolysaccharides of the Genus Pseudomonas—GC-MS Analysis on Ionic Liquid-Based Column.* Molecules, 2022. **27**(20): p. 6930.
46. Russell, N., *Functions of lipids: structural roles and membrane functions.* Microbial lipids, 1989. **2**: p. 279-365.
47. Denich, T., L. Beaudette, H. Lee, and J. Trevors, *Effect of selected environmental and physico-chemical factors on bacterial cytoplasmic membranes.* Journal of microbiological methods, 2003. **52**(2): p. 149-182.
48. Phadtare, S., J. Alsina, and M. Inouye, *Cold-shock response and cold-shock proteins.* Current opinion in microbiology, 1999. **2**(2): p. 175-180.

49. Dieser, M., M. Greenwood, and C.M. Foreman, *Carotenoid Pigmentation in Antarctic Heterotrophic Bacteria as a Strategy to Withstand Environmental Stresses.* Arctic, Antarctic, and Alpine Research, 2010. **42**(4): p. 396-405.
50. Fong, N.J.C., M.L. Burgess, K.D. Barrow, and D.R. Glenn, *Carotenoid accumulation in the psychrotrophic bacterium Arthrobacter agilis in response to thermal and salt stress.* Applied Microbiology and Biotechnology, 2001. **56**(5-6): p. 750-756.
51. Órdenes-Aenishanslins, N., et al., *Pigments from UV-resistant Antarctic bacteria as photosensitizers in dye sensitized solar cells.* Journal of Photochemistry and Photobiology B: Biology, 2016. **162**: p. 707-714.
52. Silva, T.R.E., et al., *Pigments from Antarctic bacteria and their biotechnological applications.* Critical Reviews in Biotechnology, 2021. **41**(6): p. 809-826.
53. Styczynski, M., et al., *Genome-based insights into the production of carotenoids by Antarctic bacteria, Planococcus sp. ANT_H30 and Rhodococcus sp. ANT_H53B.* Molecules, 2020. **25**(19): p. 4357.
54. Maoka, T., *Carotenoids as natural functional pigments.* Journal of natural medicines, 2020. **74**(1): p. 1-16.
55. Sajjad, W., et al., *Pigment production by cold-adapted bacteria and fungi: colorful tale of cryosphere with wide range applications.* Extremophiles, 2020. **24**(4): p. 447-473.
56. López, G.-D., et al., *Bacterial carotenoids: Extraction, characterization, and applications.* Critical Reviews in Analytical Chemistry, 2023. **53**(6): p. 1239-1262.
57. Smith, H.J., et al., *Microbial formation of labile organic carbon in Antarctic glacial environments.* Nature Geoscience, 2017. **10**(5): p. 356-359.
58. Sajjad, W., et al., *Endolithic microbes of rocks, their community, function and survival strategies.* International Biodeterioration & Biodegradation, 2022. **169**: p. 105387.
59. Huovinen, P., J. Ramírez, and I. Gómez, *Remote sensing of albedo-reducing snow algae and impurities in the Maritime Antarctica.* ISPRS Journal of Photogrammetry and Remote Sensing, 2018. **146**: p. 507-517.
60. Daniela Jara, et al., *Antibiotic resistance in bacterial isolates from freshwater samples in Fildes Peninsula, King George Island, Antarctica.* Scientific Reports, 2020. **10**(1).

61. Ciesielski, S., et al., *The diversity of bacteria isolated from Antarctic freshwater reservoirs possessing the ability to produce polyhydroxyalkanoates.* Current microbiology, 2014. **69**: p. 594-603.
62. Al-Maqtari, Q.A., A. Waleed, and A.A. Mahdi, *Cold-active enzymes and their applications in industrial fields-A review.* Int. J. Res. Agric. Sci, 2019. **6**(4): p. 2348-3997.
63. Loperena, L., et al., *Extracellular enzymes produced by microorganisms isolated from maritime Antarctica.* World journal of microbiology and biotechnology, 2012. **28**: p. 2249-2256.
64. Jadhav, V.V., et al., *Fatty acid profiles of PUFA producing Antarctic bacteria: correlation with RAPD analysis.* Annals of microbiology, 2010. **60**: p. 693-699.
65. Nichols, D., et al., *Developments with Antarctic microorganisms: culture collections, bioactivity screening, taxonomy, PUFA production and cold-adapted enzymes.* Current Opinion in Biotechnology, 1999. **10**(3): p. 240-246.
66. El Razak, A.A., A.C. Ward, and J. Glassey, *Screening of Marine Bacterial Producers of Polyunsaturated Fatty Acids and Optimisation of Production.* Microbial Ecology, 2014. **67**(2): p. 454-464.
67. Nichols, D.S., P.D. Nichols, and T.A. McMeekin, *Polyunsaturated fatty acids in Antarctic bacteria.* Antarctic Science, 1993. **5**(2): p. 149-160.
68. Russell, N.J. and D.S. Nichols, *Polyunsaturated fatty acids in marine bacteria—a dogma rewritten.* Microbiology, 1999. **145**(4): p. 767-779.
69. Caruso, C., et al., *Production and biotechnological potential of extracellular polymeric substances from sponge-associated Antarctic bacteria.* Applied and environmental microbiology, 2018. **84**(4): p. e01624-17.
70. Leiva, S., et al., *Diversity of pigmented Gram-positive bacteria associated with marine macroalgae from Antarctica.* FEMS Microbiology Letters, 2015. **362**(24): p. fnv206.
71. Vila, E., et al., *Carotenoids from heterotrophic bacteria isolated from fildes peninsula, king george island, antarctica.* Biotechnology Reports, 2019. **21**: p. e00306.

72. Jagannadham, M.V., et al., *Carotenoids of an Antarctic psychrotolerant bacterium, Sphingobacterium antarcticus, and a mesophilic bacterium, Sphingobacterium multivorum.* Archives of microbiology, 2000. **173**: p. 418-424.
73. Hamid, B., et al., *Cold-active enzymes and their potential industrial applications—A Review.* Molecules, 2022. **27**(18): p. 5885.
74. Ferrés, I., V. Amarelle, F. Noya, and E. Fabiano, *Identification of Antarctic culturable bacteria able to produce diverse enzymes of potential biotechnological interest.* Advances in Polar Science, 2015. **26**: p. 71-79.
75. Morozova, O.V., et al., *Antibiotic resistance and cold-adaptive enzymes of antarctic culturable bacteria from King George Island.* Polar Science, 2022. **31**: p. 100756.
76. Piegza, M., W. Łaba, and M. Kačániová, *New Arctic Bacterial Isolates with Relevant Enzymatic Potential.* Molecules, 2020. **25**(17): p. 3930.
77. Rizzo, C., et al., *Cultivable Bacterial Communities in Brines from Perennially Ice-Covered and Pristine Antarctic Lakes: Ecological and Biotechnological Implications.* Microorganisms, 2020. **8**(6): p. 819.
78. Santiago, M., C.A. Ramírez-Sarmiento, R.A. Zamora, and L.P. Parra, *Discovery, molecular mechanisms, and industrial applications of cold-active enzymes.* Frontiers in microbiology, 2016. **7**: p. 1408.
79. Smirnova, M., et al., *New cold-adapted bacteria for efficient hydrolysis of feather waste at low temperature.* Bioresource Technology Reports, 2023: p. 101530.
80. Lo Giudice, A. and C. Rizzo, *Bacteria associated with marine benthic invertebrates from polar environments: unexplored frontiers for biodiscovery?* Diversity, 2018. **10**(3): p. 80.
81. Smirnova, M., et al., *Temperature- and Nutrients-Induced Phenotypic Changes of Antarctic Green Snow Bacteria Probed by High-Throughput FTIR Spectroscopy.* Biology, 2022. **11**(6): p. 890.
82. Ayub, N.D., P.M. Tribelli, and N.I. López, *Polyhydroxyalkanoates are essential for maintenance of redox state in the Antarctic bacterium Pseudomonas sp. 14-3 during low temperature adaptation.* Extremophiles, 2009. **13**: p. 59-66.

83. Anderson, A.J. and E. Dawes, *Occurrence, metabolism, metabolic role, and industrial uses of bacterial polyhydroxyalkanoates.* Microbiological reviews, 1990. **54**(4): p. 450-472.
84. Chai, J.M., et al., *Surface-modified highly biocompatible bacterial-poly (3-hydroxybutyrate-co-4-hydroxybutyrate): a review on the promising next-generation biomaterial.* Polymers, 2020. **13**(1): p. 51.
85. Goh, Y.S. and I.K.P. Tan, *Polyhydroxyalkanoate production by antarctic soil bacteria isolated from Casey Station and Signy Island.* Microbiological research, 2012. **167**(4): p. 211-219.
86. Hobbie, J.E., R.J. Daley, and S. Jasper, *Use of nuclepore filters for counting bacteria by fluorescence microscopy.* Applied and environmental microbiology, 1977. **33**(5): p. 1225-1228.
87. Sanders, E.R., *Aseptic laboratory techniques: plating methods.* JoVE (Journal of Visualized Experiments), 2012(63): p. e3064.
88. Ali, N.S., F. Huang, W. Qin, and T.C. Yang, *A high throughput screening process and quick isolation of novel lignin-degrading microbes from large number of natural biomasses.* Biotechnology Reports, 2023. **39**: p. e00809.
89. Bonnet, M., J.C. Lagier, D. Raoult, and S. Khelaifia, *Bacterial culture through selective and non-selective conditions: the evolution of culture media in clinical microbiology.* New microbes and new infections, 2020. **34**: p. 100622.
90. Kosa, G., et al., *Assessment of the scalability of a microtiter plate system for screening of oleaginous microorganisms.* Applied Microbiology and Biotechnology, 2018. **102**(11): p. 4915-4925.
91. Duetz, W.A., et al., *Methods for Intense Aeration, Growth, Storage, and Replication of Bacterial Strains in Microtiter Plates.* Applied and Environmental Microbiology, 2000. **66**(6): p. 2641-2646.
92. Schneider, K., V. Schütz, G.T. John, and E. Heinzle, *Optical device for parallel online measurement of dissolved oxygen and pH in shake flask cultures.* Bioprocess and biosystems engineering, 2010. **33**: p. 541-547.
93. Kato, S., et al., *Isolation of previously uncultured slow-growing bacteria by using a simple modification in the preparation of agar media.* Applied and environmental microbiology, 2018. **84**(19): p. e00807-18.
94. Smirnova, M., et al., *Isolation and characterization of fast-growing green snow bacteria from coastal East Antarctica.* MicrobiologyOpen, 2021. **10**(1).

95. Kim, M. and J. Chun, *16S rRNA gene-based identification of bacteria and archaea using the EzTaxon server*, in *Methods in microbiology*. 2014, Elsevier. p. 61-74.
96. Janda, J.M. and S.L. Abbott, *16S rRNA gene sequencing for bacterial identification in the diagnostic laboratory: pluses, perils, and pitfalls.* Journal of clinical microbiology, 2007. **45**(9): p. 2761-2764.
97. Clarridge III, J.E., *Impact of 16S rRNA gene sequence analysis for identification of bacteria on clinical microbiology and infectious diseases.* Clinical microbiology reviews, 2004. **17**(4): p. 840-862.
98. Lane, D., *16S/23S rRNA sequencing.* Nucleic acid techniques in bacterial systematics, 1991.
99. Sanger, F., S. Nicklen, and A.R. Coulson, *DNA sequencing with chain-terminating inhibitors.* Proceedings of the national academy of sciences, 1977. **74**(12): p. 5463-5467.
100. Satam, H., et al., *Next-generation sequencing technology: Current trends and advancements.* Biology, 2023. **12**(7): p. 997.
101. Tamura, K., G. Stecher, and S. Kumar, *MEGA11: molecular evolutionary genetics analysis version 11.* Molecular biology and evolution, 2021. **38**(7): p. 3022-3027.
102. Beveridge, T.J., *Use of the Gram stain in microbiology.* Biotechnic & Histochemistry, 2001. **76**(3): p. 111-118.
103. Morita, R.Y., *Psychrophilic bacteria.* Bacteriological reviews, 1975. **39**(2): p. 144-167.
104. Gunjal, A., M. Waghmode, N. Patil, and N. Nawani, *Significance of soil enzymes in agriculture*, in *Smart bioremediation technologies*. 2019, Elsevier. p. 159-168.
105. *The European Committee on Antimicrobial Susceptibility Testing. Breakpoint tables for interpretation of MICs and zone diameters, version 12.0, 2022. http://www.eucast.org."*. 30 May 2022].
106. *CLSI document M100. In Performance Standards for Antimicrobial. Susceptibility Tests, 30th ed.; Wayne, PA, USA, 2020, CLSI: Clinical and Laboratory Standards Institute*CLSI: Clinical and Laboratory Standards Institute
107. Cockerill III, F.R., *Genetic methods for assessing antimicrobial resistance.* Antimicrobial agents and chemotherapy, 1999. **43**(2): p. 199-212.
108. March-Rosselló, G.A., *Rapid methods for detection of bacterial resistance to antibiotics.* Enfermedades infecciosas y microbiologia clinica (English ed.), 2017. **35**(3): p. 182-188.

109. Martínez, J.L., *Natural antibiotic resistance and contamination by antibiotic resistance determinants: the two ages in the evolution of resistance to antimicrobials.* Frontiers in microbiology, 2012. **3**: p. 1.
110. Van Goethem, M.W., et al., *A reservoir of 'historical' antibiotic resistance genes in remote pristine Antarctic soils.* Microbiome, 2018. **6**(1).
111. Bauer, A.W., W.M. Kirby, J.C. Sherris, and M. Turck, *Antibiotic susceptibility testing by a standardized single disk method.* Am J Clin Pathol, 1966. **45**(4): p. 493-6.
112. Schöner, T.A., et al., *Aryl polyenes, a highly abundant class of bacterial natural products, are functionally related to antioxidative carotenoids.* ChemBioChem, 2016. **17**(3): p. 247-253.
113. Asker, D., *High throughput screening and profiling of high-value carotenoids from a wide diversity of bacteria in surface seawater.* Food chemistry, 2018. **261**: p. 103-111.
114. Godbole, S., *Methods for identification, quantification and characterization of polyhydroxyalkanoates-a review.* International Journal of Bioassays, 2016. **5**(4): p. 2016.
115. Sasser, M., *Identification of bacteria by gas chromatography of cellular fatty acids*. 1990, MIDI technical note 101. Newark, DE: MIDI inc.
116. Angeletti, S., *Matrix assisted laser desorption time of flight mass spectrometry (MALDI-TOF MS) in clinical microbiology.* Journal of microbiological methods, 2017. **138**: p. 20-29.
117. Harz, M., P. Rösch, and J. Popp, *Vibrational spectroscopy—A powerful tool for the rapid identification of microbial cells at the single-cell level.* Cytometry Part A: The Journal of the International Society for Analytical Cytology, 2009. **75**(2): p. 104-113.
118. Byrtusová, D., et al., *Rhodotorula kratochvilovae CCY 20-2-26—The source of multifunctional metabolites.* Microorganisms, 2021. **9**(6): p. 1280.
119. Quideau, S.A., et al., *Extraction and Analysis of Microbial Phospholipid Fatty Acids in Soils.* Journal of Visualized Experiments, 2016(114).
120. Garip, S., A.C. Gozen, and F. Severcan, *Use of Fourier transform infrared spectroscopy for rapid comparative analysis of Bacillus and Micrococcus isolates.* Food Chemistry, 2009. **113**(4): p. 1301-1307.

121. Girardeau, A., et al., *Insights into lactic acid bacteria cryoresistance using FTIR microspectroscopy.* Analytical and Bioanalytical Chemistry, 2022. **414**(3): p. 1425-1443.
122. Jehlička, J., et al., *Potential and limits of Raman spectroscopy for carotenoid detection in microorganisms: implications for astrobiology.* Philosophical Transactions of the Royal Society A: Mathematical, Physical and Engineering Sciences, 2014. **372**(2030): p. 20140199.
123. Kochan, K., et al., *Vibrational spectroscopy as a sensitive probe for the chemistry of intra-phase bacterial growth.* Sensors, 2020. **20**(12): p. 3452.
124. Siebert, F. and P. Hildebrandt, *Vibrational spectroscopy in life science*. 2008: John Wiley & Sons.
125. Zarnowiec, P., L. Lechowicz, G. Czerwonka, and W. Kaca, *Fourier transform infrared spectroscopy (FTIR) as a tool for the identification and differentiation of pathogenic bacteria.* Current medicinal chemistry, 2015. **22**(14): p. 1710-1718.
126. Jadhav, V.V., et al., *Studies on biosurfactant from Oceanobacillus sp. BRI 10 isolated from Antarctic sea water.* Desalination, 2013. **318**: p. 64-71.
127. Habib, S., et al., *Biodeterioration of untreated polypropylene microplastic particles by Antarctic bacteria.* Polymers, 2020. **12**(11): p. 2616.
128. Yi-bin, W., et al., *Low-temperature degradation mechanism analysis of petroleum hydrocarbon-degrading Antarctic psychrophilic strains.* J Pure Appl Microbiol, 2014. **8**(1): p. 47-53.
129. Larkin, P., *Infrared and Raman spectroscopy: principles and spectral interpretation*. 2017: Elsevier.
130. Barth, A., *Infrared spectroscopy of proteins.* Biochimica et Biophysica Acta (BBA)-Bioenergetics, 2007. **1767**(9): p. 1073-1101.
131. Garip, S., F. Bozoglu, and F. Severcan, *Differentiation of mesophilic and thermophilic bacteria with Fourier transform infrared spectroscopy.* Applied spectroscopy, 2007. **61**(2): p. 186-192.
132. Kochan, K., et al., *In vivo atomic force microscopy–infrared spectroscopy of bacteria.* Journal of The Royal Society Interface, 2018. **15**(140): p. 20180115.

133. Maquelin, K., et al., *Identification of medically relevant microorganisms by vibrational spectroscopy.* Journal of microbiological methods, 2002. **51**(3): p. 255-271.
134. Chisanga, M., H. Muhamadali, D.I. Ellis, and R. Goodacre, *Surface-enhanced Raman scattering (SERS) in microbiology: illumination and enhancement of the microbial world.* Applied spectroscopy, 2018. **72**(7): p. 987-1000.
135. Hair, J.F., *Multivariate data analysis: An overview.* International encyclopedia of statistical science, 2011: p. 904-907.
136. Afseth, N.K. and A. Kohler, *Extended multiplicative signal correction in vibrational spectroscopy, a tutorial.* Chemometrics and Intelligent Laboratory Systems, 2012. **117**: p. 92-99.
137. Lasch, P., *Spectral pre-processing for biomedical vibrational spectroscopy and microspectroscopic imaging.* Chemometrics and Intelligent Laboratory Systems, 2012. **117**: p. 100-114.
138. Kohler, A., et al., *Model-based pre-processing in vibrational spectroscopy.* 2020.
139. Savitzky, A. and M.J. Golay, *Smoothing and differentiation of data by simplified least squares procedures.* Analytical chemistry, 1964. **36**(8): p. 1627-1639.
140. Wang, R. and Y. Wang, *Fourier transform infrared spectroscopy in oral cancer diagnosis.* International journal of molecular sciences, 2021. **22**(3): p. 1206.
141. Tafintseva, V., V. Shapaval, M. Smirnova, and A. Kohler, *Extended multiplicative signal correction for FTIR spectral quality test and pre-processing of infrared imaging data.* Journal of Biophotonics, 2020. **13**(3).
142. Jamieson, L.E., A. Li, K. Faulds, and D. Graham, *Ratiometric analysis using Raman spectroscopy as a powerful predictor of structural properties of fatty acids.* Royal Society open science, 2018. **5**(12): p. 181483.
143. Mukherjee, R., T. Verma, D. Nandi, and S. Umapathy, *Understanding the effects of culture conditions in bacterial growth: A biochemical perspective using Raman microscopy.* Journal of biophotonics, 2020. **13**(1): p. e201900233.
144. Syms, C., *Principal components analysis*. 2008, Elsevier.
145. Demšar, J., et al., *Orange: data mining toolbox in Python.* The Journal of Machine Learning Research, 2013. **14**(1): p. 2349-2353.

146. Toplak, M., et al., *Infrared orange: connecting hyperspectral data with machine learning.* Synchrotron Radiation News, 2017. **30**(4): p. 40-45.
147. Toplak, M., S.T. Read, C. Sandt, and F. Borondics, *Quasar: easy machine learning for biospectroscopy.* Cells, 2021. **10**(9): p. 2300.

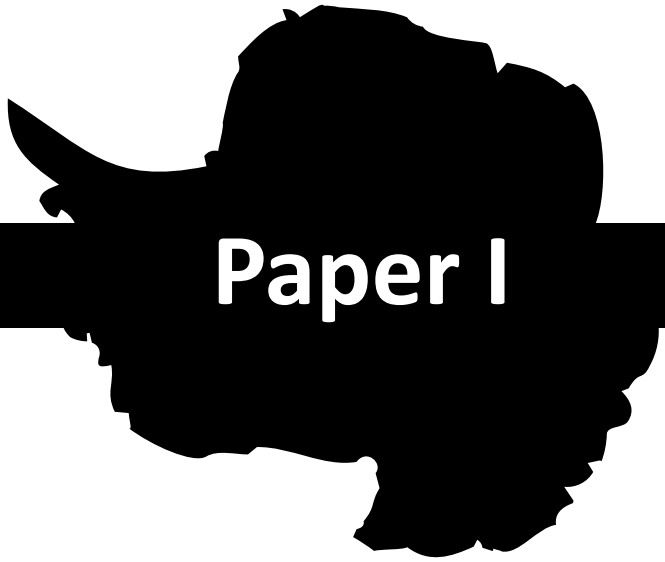

Paper I

biology

MDPI

Article

Isolation, Physiological Characterization, and Antibiotic Susceptibility Testing of Fast-Growing Bacteria from the Sea-Affected Temporary Meltwater Ponds in the Thala Hills Oasis (Enderby Land, East Antarctica)

Volha Akulava [1,2,*], Uladzislau Miamin [2,3], Katsiaryna Akhremchuk [4], Leonid Valentovich [2,4], Andrey Dolgikh [5] and Volha Shapaval [1]

[1] Faculty of Science and Technology, Norwegian University of Life Sciences, 1432 Ås, Norway; volha.shapaval@nmbu.no
[2] Faculty of Biology, Belarusian State University, 220030 Minsk, Belarus; vladmiamin@mail.ru (U.M.); valentovich@bio.bsu.by (L.V.)
[3] Scientific and Practical Center of the National Academy of Sciences of Belarus for Bioresources, 220072 Minsk, Belarus
[4] Institute of Microbiology, National Academy of Sciences of Belarus, 220141 Minsk, Belarus; katerina_akhr@bio.bsu.by
[5] Institute of Geography, Russian Academy of Sciences, 119017 Moscow, Russia; dolgikh@igras.ru
* Correspondence: volha.akulava@nmbu.no

Citation: Akulava, V.; Miamin, U.; Akhremchuk, K.; Valentovich, L.; Dolgikh, A.; Shapaval, V. Isolation, Physiological Characterization, and Antibiotic Susceptibility Testing of Fast-Growing Bacteria from the Sea-Affected Temporary Meltwater Ponds in the Thala Hills Oasis (Enderby Land, East Antarctica). *Biology* **2022**, *11*, x. https://doi.org/10.3390/xxxxx

Academic Editors: Chrissoula Voidarou, Athina S. Tzora, Georgios Rozos and Pierangelo Luporini

Received: 2 June 2022
Accepted: 25 July 2022
Published: 29 July 2022

Publisher's Note: MDPI stays neutral with regard to jurisdictional claims in published maps and institutional affiliations.

Copyright: © 2022 by the authors. Licensee MDPI, Basel, Switzerland. This article is an open access article distributed under the terms and conditions of the Creative Commons Attribution (CC BY) license (https://creativecommons.org/licenses/by/4.0/).

Simple Summary: The characterization of microbial communities from Antarctic temporary meltwater ponds is limited, while they could serve as a source of biotechnologically interesting microorganisms. In this study, we characterized a set of bacteria isolated from the sea-affected temporary meltwater ponds in the East Antarctica area of the Vecherny region of the Thala Hills Oasis, Enderby Land. The isolated meltwater bacteria were identified as Proteobacteria, Actinobacteria, Firmicutes, and Bacteroidetes, where Proteobacteria and Actinobacteria were predominant. The isolated bacteria were able to grow in a relatively wide temperature range between 4 °C and 37 °C, with an optimal temperature range of 18–25 °C. Further, most of the isolates showed an ability to secrete lipases and proteases, and several of them were pigmented. Bacterial isolates from the genera *Pseudomonas* and *Acinetobacter* exhibited multi-resistance against β-lactams, sulfonamide, macrolide, diaminopyrimidines, and chloramphenicol antibiotics. This study shows that bacterial communities from the temporary meltwater ponds in East Antarctica consist of metabolically versatile bacteria that might be defined by their location near the sea and the close presence of animals, penguins and skuas in particular.

Abstract: In this study, for the first time, we report the identification and characterization of culturable fast-growing bacteria isolated from the sea-affected temporary meltwater ponds (MPs) in the East Antarctica area of the Vecherny region (− 67.656317, 46.175058) of the Thala Hills Oasis, Enderby Land. Water samples from the studied MPs showed alkaline pH (from 8.0 to 10.1) and highly varied total dissolved solids (86–94,000 mg/L). In total, twenty-nine bacterial isolates were retrieved from the studied MPs. The phylogenetic analysis based on 16S rRNA gene sequence similarities showed that the isolated bacteria belong to the phyla Proteobacteria, Actinobacteria, Firmicutes, and Bacteroidetes and the twelve genera *Pseudomonas*, *Shewanella*, *Acinetobacter*, *Sporosarcina*, *Facklamia*, *Carnobacterium*, *Arthrobacter*, *Brachybacterium*, *Micrococcus*, *Agrococcus*, *Leifsonia*, and *Flavobacterium*. Most of the isolated bacteria were psychrotrophs and showed the production of one or more extracellular enzymes. Lipolytic and proteolytic activities were more prevalent among the isolates. Five isolates from the Actinobacteria phylum and one isolate from the Bacteroidetes phylum had strong pigmentation. Antibiotic susceptibility testing revealed that most of the isolates are resistant to at least one antibiotic, and seven isolates showed multi-resistance.

Keywords: meltwater ponds; Antarctic bacteria; 16S rRNA gene sequencing; plate-based assays; thermotolerance; enzymatic activity; antibiotic resistance

1. Introduction

Due to the weather peculiarities, the polar region is considered to be one of the most versatile environments. During the summer period in polar areas, there are numerous temporary meltwater ponds (MPs) appearing as a result of snow and ice melting [1]. MPs are formed on the rough terrain, often between rocky ridges where there are conditions for the accumulation of the melted snow and snow-glacial water [2]. MPs sizes varies significantly depending on the location, presence of slopes, etc., and they can be flowing, low-flowing, or non-flowing and characterized by different physical parameters and chemical compositions providing individually distinct geochemical environments [3]. MPs are very dynamic and strongly connected with snow and ice since they appear for a short period due to snow and ice melting during the Antarctic summer (October–February). Temporary water reservoirs located on Antarctica's shore are constantly exposed to various environmental abiotic (temperature fluctuations, freeze-thaw cycles, nutrient deficiency, abrupt chemical gradients, and increased salinity in habitats), biotic (plants and animals), and anthropogenic factors, and therefore, they usually have microbiota consisting of diverse cold-adapted organisms [4–6].

According to the authors' knowledge, the microbial communities from Thala Hills oasis MPs are the least studied biotopes, and only MPs in the regions of the McMurdo Ice Shelf (MIS) and Dry Valleys have been described to some certain extent, with the main focus on the geochemistry of the water column [7–9], the microbial diversity of microbial mats [10] and sediments [11], surface water samples [12], and the water column [13]. Little attention has been given to the isolation and characterization of bacteria inhabiting MPs in Thala Hills oasis. Only a few recent studies that focused on the terrestrial biology, geology, and diversity of eukaryotes and prokaryotes in the snow and soil from this region are available [14–17]. Moreover, recently the characterization and biopotential of yeast cultures isolated from soil samples of East Antarctica were evaluated [18]. Due to the fact that bacteria in Antarctic meltwater ponds are important for driving biogeochemical cycles, sustaining essential chemical processes, and participating in a carbon sink and because they are able to tolerate environmental fluctuations, studying them could be especially useful for understanding environmental and ecological changes in Antarctica as well as discovering new microbial cell factories for modern biotechnology and biorefinery applications. For example, biotechnologically attractive enzymes (e.g., proteases, lipases, amylases, ureases, nucleases, β-galactosidases, and keratinases) [14,19–25] and pigments (e.g., carotenoids) [19,26–31] can be synthesized by culturable psychrophilic and psychrotrophic bacteria [32].

Approaches for investigating microbiota from a given ecosystem can be either culture-dependent or culture-independent. Despite the advantages of the culture-independent method, which provides more informative data on the diversity of microbial communities, the culture-dependent method, which leads to the isolation of culturable bacteria, remains a part of a traditional bioprospecting strategy in biotechnology [19]. In the present study, the culture-dependent methods were used.

Antibiotic resistance is a natural defense mechanism in bacteria [33], but it can be exacerbated due to the transportation of antibiotics to Antarctic areas by atmospheric and oceanic currents from outside the Antarctic region [33]. In addition, increasing the selective pressure of the anthropogenic and animal activity in Antarctica results in the spread of resistant strains [34], which may lead to the appearance of multi-resistant strains [35]. In order to understand to what extent meltwater bacteria possess antibiotic resistance, we

performed antibiotic susceptibility testing for a total of twenty-three antibiotics and antimicrobial agents.

The main aim of this study was to identify and characterize the fast-growing bacteria isolated from MPs in the Vecherny region of the Thala Hills Oasis, Enderby Land, which has limited anthropic pressure and is affected by the sea and the presence of animals, penguins and skuas in particular. To the authors' knowledge, this is the first study reporting the identification and characterization of the culturable fast-growing bacteria isolated from the temporary meltwater ponds of Enderby Land, East Antarctica.

2. Materials and Methods

2.1. Sampling Sites and Sampling Procedure

Water samples were collected during the 5th Belarusian Antarctic Expedition in the austral summer season (January 2013) from the middle part of the water column of nine non-flowing MPs located in rock baths (0.1–3 m diameter, 2–100 m distance from the shoreline, 0.1–0.5 m deep, and 0–10 m above sea level). The key sampling site was located 800 m from the Belarussian Antarctic Station "Vechernyaya", 14 km from the Russian Antarctic Station Molodezhnaya, and 2.7 km from the Adelie penguin colony at the Azure Cape (−67.656317, 46.175058) of the Vecherny region of the Thala Hills oasis in the central part of Enderby Land (East Antarctica) (Figure 1).

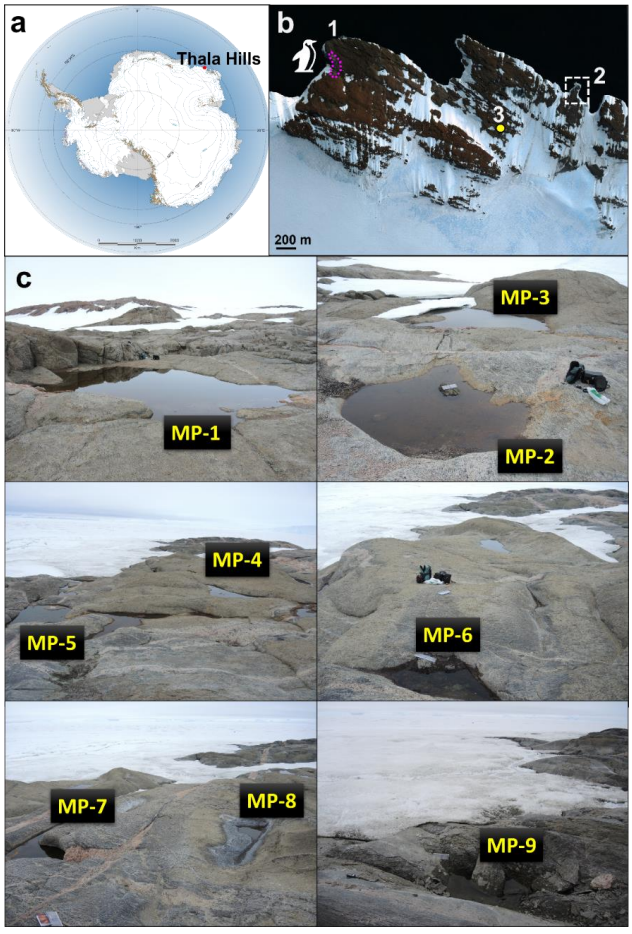

Figure 1. Sampling sites. (**a**) Location of the Thala Hills oasis in the coastal area of East Antarctica (marked by the red circle). (**b**) Satellite image of the eastern part of the Thala Hills oasis (1—Adelie penguin colony area, 2—sampling sites area, 3—location of the Belarussian Antarctic Station "Vechernyaya" in the eastern part of the Thala Hills oasis (marked by the yellow circle)) (**c**) Photos of the studied temporary meltwater ponds (MPs).

For the isolation of the fast-growing bacteria, water samples were collected in 20 mL sterile polypropylene tubes and kept at 4 °C before the isolation. For bacterioplankton analysis, water samples were collected in 100 mL sterile polythene bottles. Then, formalin, until a final concentration of 4%, was added to each sample for preservation. The collected samples were stored at 4 °C. For the physicochemical analysis, samples were collected in 100 mL non-sterile polythene bottles. All water samples were collected in two replicates on the same day.

2.2. Bacterioplankton and Physicochemical Analysis of Water Samples

Physicochemical parameters such as pH, total dissolved solids (TDS), and temperature were measured in situ at different time points (Day 1—11 January 2013, Day 2—14 January 2013, Day 3—17 January 2013, and Day 4—26 January 2013) with portable Combo pH/Conductivity/TDS Testers (HI98129 Low Range, HI98130 High Range) (Hanna Instruments, Kungsbacka, Sweden).

For the evaluation of the quantitative parameters of bacterioplankton, samples collected on the first day (Day 1—11 January 2013) were used. The bacterial cell number was determined using the acridine orange method according to Hobbie et al. [36], and the measurements were taken with an Axiovert 25 epifluorescence inverted microscope (Carl Zeiss, Berlin, Germany) equipped with a Nuclepore filter with a pore diameter of 0.2 μm and an AxioCam MRc camera (Carl Zeiss, Berlin, Germany). Water samples were examined under the 100× immersion lens. Pictures for each water sample were recorded in Carl Zeiss AxioVision Rel. 4.4 software (Carl Zeiss, Berlin, Germany) (10 in parallel from each filter (data not shown)). The processing of the obtained imaging data was conducted in the Image-Pro Plus program (Media Cybernetics, Rockville, MD, USA).

The correction of color and tone for the fluorescence images and the counting of objects (bacterioplankton) with the output of their geometric characteristics was performed by automated processing using an in-house algorithm created in the built-in Image-Pro Plus macro language. After the preliminary counting, the algorithm makes it possible to manually correct the counted objects (the separation of merged objects the removal of image artifacts from the counted objects, and the removal of wrongly identified objects). The estimation of the bacterioplankton was carried out using the corrected data. For the estimation of the bacterial cell number (BN), the following formula was used: $BN = S \times 10^6 \times a/s \times V \times 10$, where S is the filter area, mm; 10^6 is the recalculation of mm in μm; a is the sum of counted cells; s is the grid area, μm; V is the volume of the filtered sample; and 10 is a number of fields of view. The biomass was calculated according to the size of each bacterial cell. An in-house algorithm in Microsoft Excel was used to automatically enter the conversion formula in a spreadsheet and form an array of processing results.

2.3. Isolation of the Fast-Growing Bacteria

The isolation of the fast-growing bacteria was performed by the spread plating of 0.1 mL of each water sample in triplicates on meat peptone agar (MPA) (5.0 g/L peptone, 1.5 g/L meat extract, 1.5 g/L yeast extract, and 20.0 g/L agar, pH 7.0 ± 0.2) and cultivating for 14 days at 5 °C and 18 °C for isolating psychrophilic and psychrotolerant bacteria, respectively. Bacterial colonies that differed in phenotypic traits (the form of colonies, growth rate, and pigmentation) were selected for further purification. The growth rate was determined visually by daily observation, and we selected the colonies appearing at various time points during the first 2–6 days of the cultivation. The obtained single colonies were transferred onto new Petri dishes with MPA to obtain pure cultures. Isolated pure cultures were preserved in the following way: (1) the cultures were grown on the slanting full-fledged MPA agar in tubes for 6 days at 18 °C; (2) the obtained cells were washed and suspended in a mixture of meat peptone broth (MPB) (5.0 g/L peptone, 1.5 g/L meat extract, 1.5 g/L yeast extract, and 5.0 g/L NaCl with a final pH of 7.0 ± 0.2) and glycerol (20% of the final volume) with the ratio 1:1; (3) the suspended cells were stored at −80 °C.

2.4. Total DNA Extraction, Amplification, and Sequencing

For 16S rDNA sequencing, bacteria were cultivated on MPA agar for 7 to 10 days at 18 °C. Bacterial DNA was extracted using a DNA Preparation Kit PP-206 (Jena Biosciences, Jena, Germany). The extracted and purified DNA was stored at −20 °C. The fragment of 16S rDNA was amplified using universal bacterial primers 8f (5′-AGAGTTTGATCCTGGCTCAG-3′) and 1492r (5′-GGTTACCTTGTTACGACTT-3′) (Primetech, Minsk, Belarus), described previously [37]. Each 25 μL of the reaction mixture contained 10 μL of 2.5 × Flash buffer (ArtBioTech, Minsk, Belarus), 0.2 μL of each primer with the final concentration of 0.4 mM, 1 μL (≈10 ng) of bacterial DNA matrix, 0.25 μL of Flash polymerase (high-performance Pfu-polymerase, 2 U/μL) (ArtBioTech, Minsk, Belarus), and H_2O (deionized) up to 25 μL. For the negative control, deionized water was added in an equivalent amount instead of the DNA matrix. Polymerase chain reaction (PCR) was performed in a SureCycler 8800 thermocycler (Agilent Technologies, Santa Clara, CA, USA). The initial denaturation was performed at 98 °C for 3 min, and 30 cycles of amplification consisted of denaturation at 98 °C for 30 s, annealing at 51 °C for 30 s, and elongation at 72 °C for 1 min, and the final extension phase was performed at 72 °C for 4 min.

The sequencing of 16S rRNA genes was carried out according to the Sanger method [38], and it was performed using the DNA Cycle Sequencing Kit PCR-401S (Jena Bioscience, Jena, Germany) and the following primers (Primetech, Minsk, Belarus): 926R-seq (5′-CCGTCAATTCATTTGAGTTT-3′), 336F-seq (5′-ACGGYCCAGACTCCTACG-3′), 522R-seq (5′-TATTACCGCGGCTGCTGGCAC-3′), and 918F-seq (5′-ACTCAAAKGAATTGACGGG-3′). All reactions were run according to the manufacturer's protocols. The products of the sequencing reaction were detected using the automatic sequencer «4300 DNA Analyzer» (LI-COR Biosciences, Lincoln, NE, USA).

2.5. Analysis of 16S rRNA Sequencing Data

The obtained 16S rRNA data were preprocessed by editing and rendering in FASTA format using the e-Seq™ software V. 3.1.10 (LI-COR Biosciences, Lincoln, NE, USA). To obtain consensus sequences, all sequences for each isolate were aligned using AlignIR 2.1 (LI-COR Biosciences, Lincoln, NE, USA). The obtained sequences were compared to those available in the EzBioCloud database (ChunLab Inc., Seoul, Korea) [39] to choose reference sequences for the phylogenetic analyses and find similarities with the known strains. The phylogenetic tree was reconstructed using the MEGA 11 program [40]. The CLUSTAL W algorithm was used to align the sequences with the most similar orthologous sequences from the EzBioCloud database. The phylogenetic distance tree was inferred using the neighbor-joining analysis (NJ, *p*-distance matrix). The optimal mathematical model of nucleotide substitutions with the lowest Bayesian information criterion score was selected

for the construction of the phylogenetic tree. The evolutionary history was inferred using the maximum likelihood method and the Tamura–Nei model [41]. To evaluate the confidence limits of the branching, a bootstrap analysis was performed on a 1000 replicate data set [42]. Bootstrap values greater than 70% of confidence are shown at the branching points. The strain archaea *Methanosarcina barkeri* Schnellen 1947 was chosen as a root for the phylogenetic tree. The obtained 16S rRNA sequences are deposited in the GenBank nucleotide sequence database (National Center for Biotechnology Information, Bethesda, MD, USA) under the accession numbers ON248060-ON248088.

2.6. Thermotolerance and Enzymatic Activity

To study thermotolerance, the bacterial isolates were grown on BHI (brain heart infusion) agar (Sigma Aldrich, St. Louis, MI, USA) at 4 °C, 10 °C, 18 °C, 25 °C, 30 °C, and 37 °C for up to 10 days with daily visual inspections of the cultures.

The production of the extracellular enzymes was evaluated by applying various plate-based assays using specific substrates—solid basal media containing: (1) for lipolytic activity, 10 g/L peptone, 5 g/L NaCl, 0.1 g/L $CaCl_2 \cdot 2H_2O$, g/L 20 agar, and 10 mL (*v*/*v*) of Tween 80, pH 7.4; (2) for amylolytic activity, 10 g/L peptone, 5 g/L KH_2PO_4, 20 g/L agar, and 0.2% (*w*/*v*) soluble starch; (3) for protease activity, 6 g/L NaCl, 1.3% (*w*/*v*) nutrient broth, and 15% gelatin or calcium–casein agar (Condalab, Torrejón de Ardoz, Spain); (4) for DNase activity, DNase test agar (Condalab, Torrejón de Ardoz, Spain); (5) for urease activity, 1 g/L peptone, 5 g/L NaCl, 1 g/L glucose, 2 g/L KH_2PO_4, 0.012 g/L phenol red, 20 g/L agar, and 20 g/L urea, pH 6.8 +/− 0.2 (at 25 °C); (6) for β-galactosidase (β-GAL) activity, Luria broth agar with X-Gal (5-bromo-4-chloro-3-indolyl-β- D-galactopyranoside) and IPTG (isopropyl β- D-1-thiogalactopyranoside); and (7) for keratinase activity, 15 g/L chicken feather meal powder, 0.5 g/L NaCl, 0.3 g/L K_2HPO, 0.4 g/L KH_2PO_4, and 15 g/L agar, pH 7.2. All plate-based assays were performed in duplicates at 18 °C for up to 10 days. The enzymatic activity was evaluated by estimating the colony growth, the formation of enzyme-specific zones, and/or the presence of media changes: (1) white precipitation zones of calcium salts around colonies for lipolytic activity; (2) clearance zones after flooding with iodine solution for amylolytic activity; (3) clearance zones for protease activity; (4) colorful zones for DNase activity; (5) the intensity of the pink color of the medium for urease activity; (6) the intensity of blue-colored colonies for β-galactosidase (β-GAL) activity; (7) the presence of a hydrolysis halo around the colony for keratinase activity. Catalase activity was determined by using the slide-drop method, where immediate bubble formation was observed after mixing a small amount of bacterial biomass with 3% H_2O_2.

2.7. Antibiotic Susceptibility Testing

Antibiotic susceptibility was evaluated by the Kirby–Bauer disc diffusion method [43] using Mueller–Hinton agar (Merck, Darmstadt, Germany), and it was performed in duplicates. The isolate *Carnobacterium iners* TMP 28 was excluded from the experiment due to weak growth. Based on the predominance of psychrotrophic bacteria and their optimal growth temperature in the range of 18–25 °C, two temperatures, 18 °C and 25 °C, were selected for the test. Susceptibility was evaluated for 18 antibiotics (3 of which were presented in two different concentrations) and 5 antibacterial agents. The following commercial disks for susceptibility testing (Bio-Rad, Hercules, CA, USA) were used: glycopeptide antibiotic (5 μg of vancomycin), β-lactam antibiotics (10 μg of ampicillin, 20 μg of amoxicillin, 10 μg of clavulanic acid, 30 μg of cefuroxime, 10 μg of imipenem, and 30 μg of ceftriaxone), quinolones (5 μg of ciprofloxacin and 30 μg of nalidixic acid), diaminopyrimidines (5 μg of trimethoprim) and diaminopyrimidine coupled with sulfonamide (1.25 μg of trimethoprim and 23.75 μg of sulfamethoxazole), rifamycin antibiotics (5/30 μg of rifampicin), macrolide antibiotic (15 μg of erythromycin, 15 μg of clarithromycin, and 15

μg of azitromycin), aminoglycoside antibiotic (10/120 μg of gentamicin, 10 μg of tobramycin, 10/300 μg of streptomycin, and 30 μg of kanamicyn), tetracycline antibiotics (30 μg of doxycycline and 30 μg of tetracycline), 30 μg of chloramphenicol, and 100 μg of nitrofurantoin. The strains *Escherichia coli* ATCC 25922, *Pseudomonas aeruginosa* ATCC 27853, and *Staphylococcus aureus* ATCC 29213 were used for the quality control of the antibiotic assays. The data analysis for the control cultures was performed according to the breakpoints established by the EUCAST [44] and CLSI [45] documents. The data analysis for the Antarctic bacterial isolates was performed as described by Daniela et al. [35]. The inhibition zones ≤15 mm in diameter (including the disc) were considered as a breakpoint to define the resistance, and zones ≤20 mm were defined as intermediate.

3. Results

3.1. Physicochemical Characterization of Water Samples from Meltwater Ponds

Size, depth, and physicochemical parameters such as pH, temperature (T), and total dissolved solids (TDS) were measured for all MPs on different days to follow changes over time. The pH values of all water samples were alkaline (from 8.0 to 10.1). TDS varied considerably from 86 mg/L to 94,000 mg/L. An increases in TDS for all samples were recorded over time because of the evaporation process. The temperature of the water samples was between 12 °C and 17.5 °C (Table 1). All ponds were characterized by the absence of water flow.

The quantitative characteristics of bacterioplankton varied from $0.95 \pm 0.12 \times 10^6$ to $4.52 \pm 0.67 \times 10^6$ cells/mL, and the biomass was in a range from 0.151 ± 0.034 to 0.939 ± 0.280 mg/L (Table 1). For all ponds, a predominance of orange or brown benthos was visually observed. The presence of clean water in the upper layer was observed for all ponds except for MP-1 and MP-7, which had considerable water blooms. The presence of organic clusters of biomass with a diameter of ≈0.5 cm was observed in MP-1 and MP-6. Ponds MP-1 and MP-2 were located 30 m from the skua nest and served as swimming places for skuas. For the pond MP-8, a white salt crust formation along the edges was observed (Figure 1).

Table 1. Visual observation and physicochemical parameters measured in situ at different time points and morphometric parameters of bacterioplankton.

	Day	Temporary Meltwater Pond Number															
		MP-1		**MP-2**		**MP-3**		**MP-4**		**MP-5**		**MP-6**		**MP-7**		**MP-8**		**MP-9**	
Physicochemical parameters																			
Size, m	Day 1 *	5 × 5		4 × 5		1.5 × 2		2 × 2		3 × 2		1 × 0.5		1.5 × 1		0.5 × 0.5		1 × 1	
Depth, m		0.3		0.3		0.2		0.25		0.25		0.3		0.5		0.1		0.2	
pH		10.1		9.8		8.0		10.0		9.6		9.9		9.5		8.3		10.0	
TDS *, mg/L T, °C		TDS	T	TDS	T	TDS	T	TDS	T	TDS	T	TDS	T	TDS	T	TDS	T	TDS	T
	Day 1	271	13	631	14	86	16	458	16	580	13	1902	13	4470	12	94,000	12	1640	13
	Day 2	ND	ND	859	18	122	17.5	585	17.3	730	14.4			ND	ND				
	Day 3	364	9.3	940	11.4	163	12.3	740	10.5	1006	8.9	PD*	PD	5684	10.2	PD	PD	PD	PD
	Day 4	401	ND	1209	ND	355	ND	1126	ND	790	ND			6385	ND				
Visual observation																			
WB	Day 1	+		−		−		−		−		−		+		−		−	
BC		B		O, B		O		O, G, B		O, G		B		O		Gr, B		−	
OC		+		−		−		−		−		+		−		−		−	
Skuas		+		+		−		−		−		−		−		−		−	
Salt		−		−		−		−		−		−		−		+		−	
Bacterioplankton parameters																			
BN	Day 1	4.52 ± 0.67		1.32 ± 0.17		1.52 ± 0.26		3.01 ± 0.36		0.95 ± 0.12		2.82 ± 0.41		2.22 ± 0.28		4.46 ± 0.40		2.02 ± 0.32	
BB		0.47 ± 0.17		0.16 ± 0.06		0.32 ± 0.12		0.27 ± 0.12		0.15 ± 0.03		0.50 ± 0.14		0.31 ± 0.11		0.94 ± 0.28		0.77 ± 0.20	
NBI		2		3		1		3		5		4		2		2		7	

* Day 1—11 January 2013, Day 2—14 January 2013, Day 3—17 January 2013, and Day 4—26 January 2013; T—temperature, TDS—total dissolved solids, PD—pond dried; ND—not determined; WB—Water bloom; OC—Organic matter clusters; Skuas—Skuas observed; Salts—Salt on the edges; BC—Benthos color: B—brown, O—orange, G—green, Gr—gray; "−"—not observed, "+"—observed; BN—bacterial cell number $\times 10^6$ cells/mL, BB—bacterial biomass, mg/L; NBI—number of bacterial isolates

3.2. Isolation and Phylogenetic Characterization of the Meltwater Fast-Growing Bacteria

Due to the fact that the isolation of bacteria was conducted for two weeks and all selected isolates retrieved within this time were able to produce single colonies within 2–6 days, we concluded that these isolated bacteria could be considered to be fast-growing [14,46,47]. In total, twenty-nine fast-growing bacteria with different colony types (colony morphology, size, and pigmentation) and growth rates were isolated from nine MPs of East Antarctica. The highest numbers of bacterial isolates were obtained from the ponds MP-9 (7 isolates), MP-5 (5 isolates), and MP-6 (4 isolates), while other ponds were characterized by 1 to 3 bacterial isolates (Table 1). Five isolates showed strong pigmentation: *Flavobacterium degerlachei* TMP13, *Arthrobacter* sp. TMP15, *Agrococcus citreus* TMP23, and *Leifsonia* sp. TMP30 showed a strong yellow color, and isolate *Arthrobacter agilis* TMP24 had a salmon color (Figure 2). All isolates were deposited in the Belarusian Collection of Non-pathogenic Microorganisms at the Institute of Microbiology of the National Academy of Sciences of Belarus (Minsk, Belarus) (Table 2).

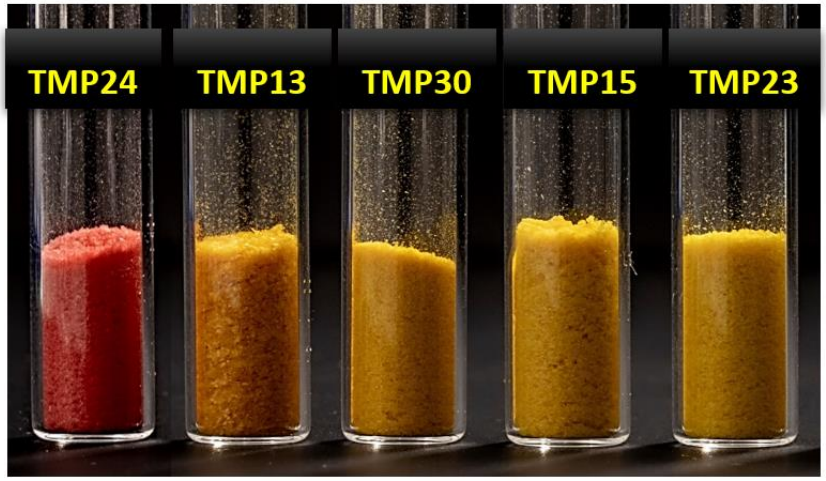

Figure 2. Freeze-dried biomass of pigmented isolates: *Flavobacterium degerlachei* TMP13, *Arthrobacter* sp. TMP15, *Agrococcus citreus* TMP23, *Arthrobacter agilis* TMP24, and *Leifsonia* sp. TMP30.

16S rRNA sequencing was used to study the phylogenetic relationships of the isolated fast-growing bacteria. A comparative 16S rRNA gene sequence analysis revealed the similarity of the isolate sequences to the EzBioCloud database sequences, with high similarity percentages from 98.47% to 100 % (Table 2). The isolated culturable fast-growing bacteria were phylogenetically related to four phyla, Proteobacteria, Actinobacteria, Firmicutes, and Bacteroidetes, and represented twelve genera. Proteobacteria was the first predominant phylum among the isolates (17 out of 29 isolates), and it was represented by three genera: *Pseudomonas* (12/17), *Shewanella* (4/17), and *Acinetobacter* (1/17). Actinobacteria was the second predominant phylum (6/29), and it was represented by five genera: *Arthrobacter* (2/6), *Brachybacterium* (1/6), *Micrococcus* (1/6), *Agrococcus* (1/6), and *Leifsonia* (1/6). The Firmicutes phylum (5/29) was represented by three genera: *Carnobacterium* (3/5), *Sporosarcina* (1/6), and *Facklamia* (1/6). The Bacteroidetes phylum was represented by only one isolate belonging to the genus *Flavobacterium*. Isolates from the Proteobacteria phylum were detected in all studied ponds except MP-8, while isolates of the other phyla were detected only in ponds MP-4–MP-9 (Table 2).

Table 2. 16S rRNA gene sequence affiliation to the closest phylogenetic neighbors, isolation temperature, and physiological parameters of the bacteria isolated from Antarctic temporary meltwater ponds.

Isolate Code [MP*]	Collection Number	Gen Bank Accession Number	Nearest Taxonomic Neighbor by EzBioCloud Alignment	Identity (%)	Isolation Temperature (°C)	Thermotolerance (°C)	Enzymatic Activity at 18 °C
Proteobacteria							
TMP1 [1]	BIM B-1565	ON248060	*Shewanella baltica* NCTC 10735	100	5	4–30	L *; Gel; D; C
TMP5 [2]	BIM B-1557	ON248064	*Shewanella baltica* NCTC 10735	99.72	18	4–30	L; Gel; D; C
TMP11 [5]	BIM B-1561	ON248069	*Shewanella baltica* NCTC 10735	99.66	5	4–30	L; Gel; D
TMP14 [5]	BIM B-1563	ON248072	*Shewanella* WE21	99.38	5	4–30	L; Gel; D
			Shewanella baltica NCTC 10735	99.04			
TMP6 [3]	BIM B-1558	ON248065	*Acinetobacter lwoffii* NCTC 5866	99.79	18	4–37	L; C
TMP2 [1]	BIM B-1554	ON248061	*Pseudomonas lundensis* DSM 6252	99.86	18	4–37	Cas; Gel; U; C
TMP3 [2]	BIM B-1555	ON248062	*Pseudomonas lundensis* DSM 6252	99.86	5	4–37	Cas; Gel; U; C
TMP4 [2]	BIM B-1556	ON248063	*Pseudomonas lundensis* DSM 6252	99.79	18	4–37	Cas; Gel; U; C
TMP7 [4]	BIM B-1559	ON248066	*Pseudomonas leptonychotis* CCM 8849	99.93	5	4–37	L; Cas
TMP18 [6]	BIM B-1568	ON248076	*Pseudomonas leptonychotis* CCM 8849	100	18	4–30	L; Cas
TMP19 [6]	BIM B-1566	ON248077	*Pseudomonas leptonychotis* CCM 8849	100	18	4–30	L; Cas
TMP9 [4]	BIM B-1560	ON248067	*Pseudomonas peli* R-20805	99.52	5	4–25	L
TMP17 [6]	BIM B-1569	ON248075	*Pseudomonas peli* R-20805	99.38	5	4–25	L
TMP20 [7]	BIM B-1546	ON248078	*Pseudomonas peli* R-20805	99.52	5	4–25	L
TMP22 [9]	BIM B-1552	ON248080	*Pseudomonas peli* R-20805	99.52	5	4–25	L
TMP25 [9]	BIM B-1542	ON248083	*Pseudomonas peli* R-20805	99.52	18	4–25	L
TMP26 [9]	BIM B-1548	ON248084	*Pseudomonas peli* R-20805	99.11	5	4–25	L
Bacteroidetes							
TMP13 [5]	BIM B-1562	ON248071	*Flavobacterium degerlachei* DSM 15718	98.47	18	4–25	C
Firmicutes							
TMP10 [4]	BIM B-1539	ON248068	*Sporosarcina globispora* DSM 4	99.59	18	4–30	U; C
			Sporosarcina psychrophila IAM 12468	99.59			
TMP12 [5]	BIM B-1540	ON248070	*Carnobacterium inhibens* subsp. *inhibens* DSM 13024	100	5	4–30	L
TMP27 [9]	BIM B-1541	ON248085	*Carnobacterium funditum* DSM 5970	100	18	4–18	ND
TMP28 [9]	BIM B-1544	ON248086	*Carnobacterium iners* LMG 26642	99.86	18	4–18	ND

TMP29 [8]	BIM B-1577	ON248087	*Facklamia tabacinasalis* CCUG 30090	99.46	18	10–30	ND
			Actinobacteria				
TMP15 [5]	BIM B-1549	ON248073	*Arthrobacter* ERGS4:06	98.97	5	4–25	C
			Arthrobacter PAMC25486	98.90			
			Arthrobacter alpinus DSM 22274	98.70			
			Arthrobacter glacialis HLT2-12-2	98.70			
TMP24 [9]	BIM B-1543	ON248082	*Arthrobacter agilis* DSM 20550	100	18	4–25	L; C
TMP16 [6]	BIM B-1571	ON248074	*Brachybacterium paraconglomeratum* LMG19861	99.93	5	10–37	Cas; A; U; BG; C
TMP21 [7]	BIM B-1545	ON248079	*Micrococcus luteus* NCTC 2665	99.58	5	10–37	L; Cas; Gel; A; C
TMP23 [9]	BIM B-1547	ON248081	*Agrococcus citreus* IAM 15145	99.50	18	18–25	C
TMP30 [8]	BIM B-1567	ON248088	*Leifsonia* PHSC20C1	99.59	18	4–25	C
			Leifsonia rubra CMS 76R	99.45			

* MP — meltwater pond number, L—lipolytic activity (Twin 80), Cas—protease activity (Calcium–casein agar), Gel—protease activity (Gelatin), A—amylolytic activity, U—urease activity, D—DNase activity, BG—β-galactosidase (β-GAL) activity, C—catalase activity, ND—not determined.

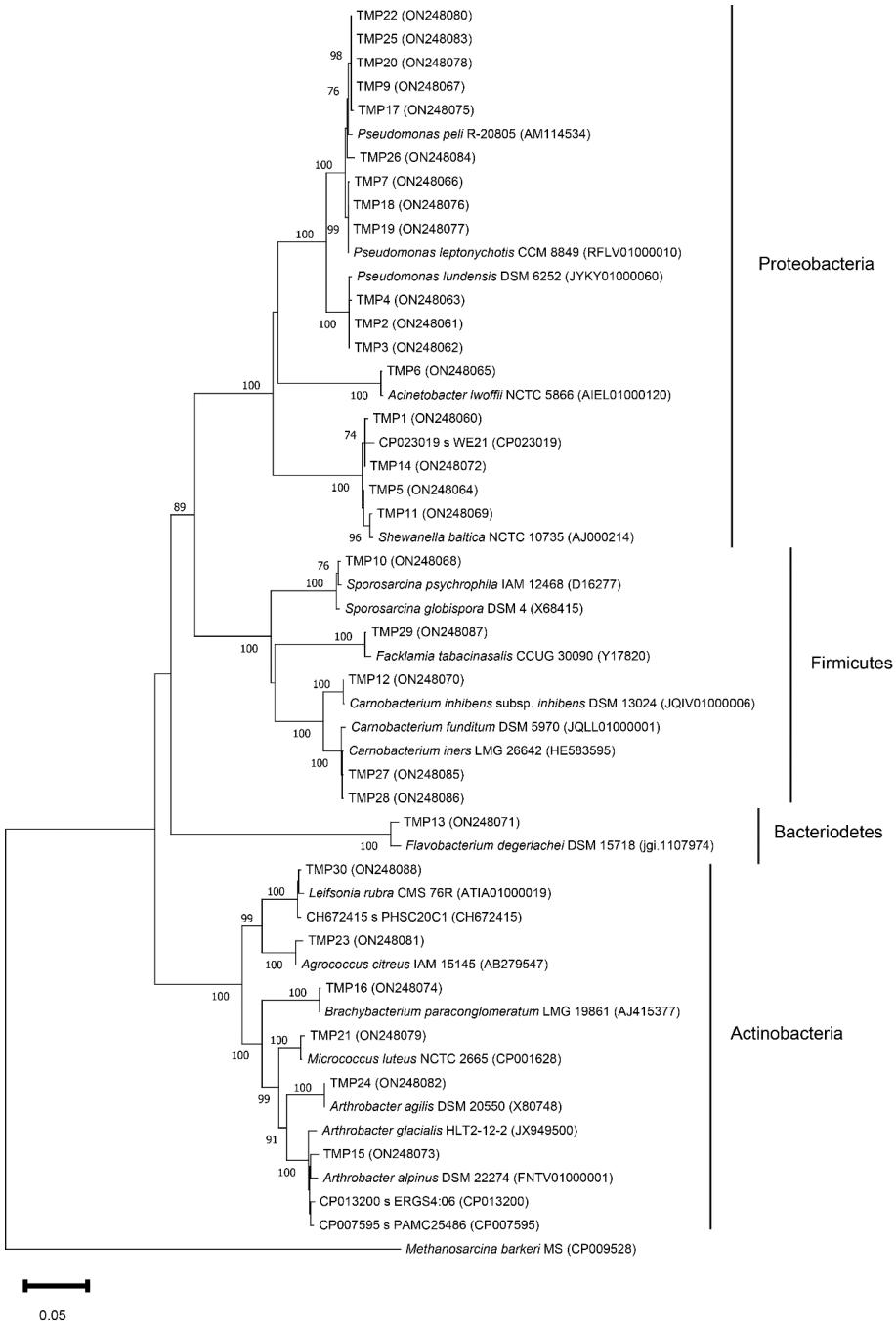

Figure 3. Phylogenetic tree based on 16S rDNA sequences of the MP isolates. Evolutionary history was inferred using the maximum likelihood method and the Tamura–Nei model. The node numbers represent the percentage of bootstrap replicates of 1000 resamplings (values below 70% are not

shown). The scale bar represents substitutions per nucleotide position. All accession numbers are in parentheses following the bacterial strain.

Isolates belonging to the genera *Pseudomonas*, *Carnobacterium*, and *Arthrobacter* were represented by several species such as *P. lundensis*, *P. peli*, *P. leptonychotis*, *C. funditum*, *C. iners*, *C. inhibens*, *Arthrobacter* sp., and *Ar. agilis*. Isolates from the genera *Shewanella*, *Acinetobacter*, *Sporosarcina*, *Facklamia*, *Flavobacterium*, *Brachybacterium*, *Micrococcus*, *Agrococcus*, and *Leifsonia* were represented by the species *S. baltica*, *Ac. lwoffii*, *S. globispora*, *F. tabacinasalis*, *F. degerlachei*, *B. paraconglomeratum*, *M. luteus*, *Ag. citreus*, and *Leifsonia* sp., respectively. Due to the low resolution of 16S rRNA gene sequence analysis, the species affiliation for some isolates of the genera *Pseudomonas*, *Arthrobacter*, and *Leifsonia* could not be determined (Table 2).

3.3. Thermotolerance and Enzymatic Activity

To evaluate the thermotolerance and identify the optimal growth temperature, bacterial isolates were cultivated at six temperatures (4 °C, 10 °C, 18 °C, 25 °C, 30 °C, and 37 °C). The majority of the isolates were found to be psychrotolerant, with an optimal growth temperature of 18 °C, but were able to grow at 4 °C to 25 °C, 30 °C, and 37 °C. All bacterial isolates (28/29) except *Agrococcus citreus* TMP23 grew at 10 °C and 18 °C, and most of the strains (23/29) were able to grow at 4 °C. Four isolates, *Pseudomonas lundensis* TMP2, TMP3, and TMP4 and isolate *Acinetobacter lwoffii* TMP6, were able to grow at all tested temperatures. Bacterial isolates *Facklamia tabacinasalis* TMP29, *Brachybacterium paraconglomeratum* TMP16, and *Micrococcus luteus* TMP21 did not grow at 4 °C but were able to grow at 30 °C or 37 °C. Two isolates, *Carnobacterium funditum* TMP27 and *Carnobacterium iners* TMP28, were able to grow at 4 °C but not at 25 °C and could be considered psychrophiles (Table 2).

Most of the isolated fast-growing meltwater bacteria showed one or more enzymatic activities, except the isolates *Carnobacterium funditum* TMP27, *Carnobacterium iners* TMP28, and *Facklamia tabacinasalis* MP29, which showed slow growth on minimal selective media. A high level of enzymatic activity (three or more enzymes) was detected for *Brachybacterium paraconglomeratum* TMP16 and *Micrococcus luteus* TMP21 and for all isolates of *Pseudomonas lundensis* and *Shewanella baltica*. Lipolytic activity was the most common enzymatic activity among the isolates, where all strains of *Shewanella baltica*, *Pseudomonas leptonychotis*, *Pseudomonas peli*, and *Acinetobacter lwoffii* TMP6, *Carnobacterium inhibens* TMP12, *Arthrobacter agilis* TMP24, and *Micrococcus luteus* TMP21 showed an ability to hydrolyze Tween 80. Proteolytic activity was detected for twelve isolates. The degradation of both casein and gelatin were detected for all isolates of *Pseudomonas lundensis* and *Micrococcus luteus* TMP21. The utilization of gelatin was observed for all isolates of *Shewanella baltica*, while casein was degraded by all isolates of *Pseudomonas leptonychotis* and *Brachybacterium paraconglomeratum* TMP16. Five isolates, *Pseudomonas lundensis* TMP2, TMP3, TMP4, *Sporosarcina globispora* TMP10, and *Brachybacterium paraconglomeratum* TMP16, showed urease activity. Amylase activity was detected only for two isolates, *Brachybacterium paraconglomeratum* TMP16 and *Micrococcus luteus* TMP21. The production of deoxyribonuclease was detected for all isolates of *Shewanella baltica*. β-galactosidase activity was detected only for *Brachybacterium paraconglomeratum* TMP16. Catalase activity was determined for all isolates from the phyla Bacteroidetes and Actinobacteria and for several Proteobacteria isolates. The production of keratinase was not detected for the isolated bacteria (Table 2).

3.4. Antibiotic Susceptibility

In total, twenty-eight isolated meltwater bacteria were tested for susceptibility towards twenty-three antibiotics and antibacterial agents, where twenty of them were broad-spectrum antibiotics, one was an antibiotic against Gram-positive bacteria (Vancomycin), one was an antibacterial agent active against Gram-negative bacteria (Nalidixic

acid), and one was an antibacterial against most Gram-positive cocci and *E. coli* (Nitrofurantoin). Rifampicin, gentamicin, and streptomycin were presented in two concentrations (Figure 4). Due to the absence of growth on Mueller–Hinton agar at 25 °C, the susceptibility screening for isolates *Flavobacterium degerlachei* TMP13, *Carnobacterium funditum* TMP27, and *Leifsonia* sp. TMP30 was conducted only at 18 °C. We observed that among the tested bacteria many were not susceptible to nitrofurantoin (24 and 22 isolates at 18 and 25 °C, respectively), and all Gram-negative and Gram-positive bacteria were resistant to vancomycin and nalidixic acid, respectively, due to natural resistance. These data were not included in the calculation of the susceptibility profile of the analyzed bacteria. The studied bacteria showed higher susceptibility towards the evaluated antibiotics at 25 °C than at 18 °C. For some isolates, temperature-induced changes in antibiotic susceptibility were observed (Figure 4).

Twenty-five isolates were resistant to at least one antibiotic, and seven isolates showed different levels of multi-resistance. Many isolates (> 10) were resistant to ampicillin, cefuroxime, amoxicillin-clavulanic acid, and trimethoprim. Very few isolates (< 3) were resistant to imipenem, ciprofloxacin, 30 μg of rifampicin, 120 μg of gentamicin, 300 μg of streptomycin, and doxycycline. Variation in the resistance was detected towards antibiotics present in different concentrations (gentamicin, streptomycin, and rifampicin), and resistance was lower for higher concentrations. None of the isolates were resistant to a high concentration of streptomycin (Figure 4).

Most of the Gram-negative isolates were resistant to β-lactam-type antibiotics such as ampicillin, amoxicillin-clavulanic acid, cefuroxime, and trimethoprim. Among the Gram-negative isolates, *Acinetobacter lwoffii* TMP6 and all *Pseudomonas lundensis* isolates showed multiple antibiotic resistance to more than ten antibiotics from the classes β-lactams, sulfonamide, macrolide, and chloramphenicol. Among the Gram-positive isolates, the highest level of resistance was detected against aminoglycoside antibiotics (tobramycin, kanamycin, and low concentrations of streptomycin) and trimethoprim. Isolates *Brachybacterium paraconglomeratum* TMP16, *Agrococcus citreus* TMP23, *Carnobacterium inhibens* TMP12, and *Facklamia tabacinasalis* TMP29 were resistant to five and more antibiotics, mostly aminoglycosides and trimethoprim. Isolates *Pseudomonas peli* TMP9 and TMP25 and *Sporosarcina* sp. TMP10 were susceptible to all tested antibiotics (Figure 4).

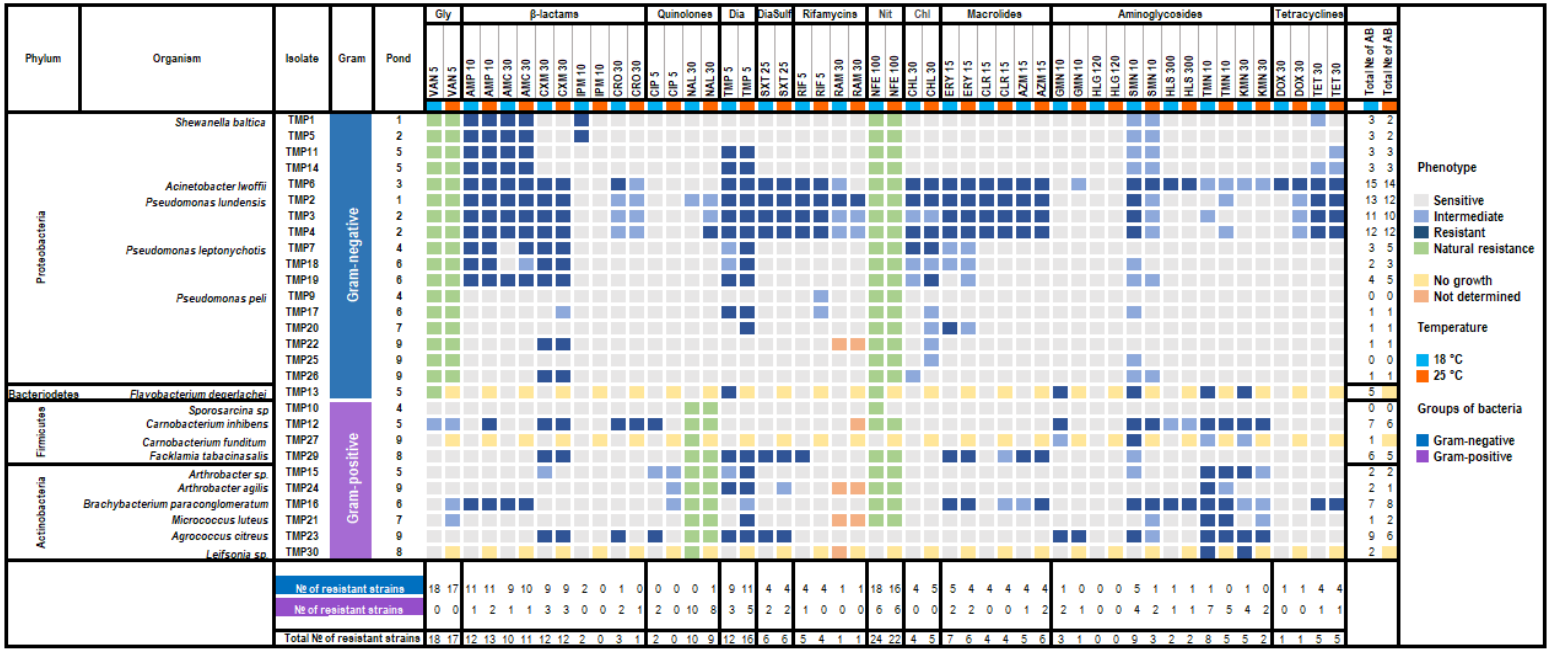

Figure 4. Heatmap of the antimicrobial susceptibility profiles of bacterial isolates from temporary meltwater ponds. Antibiotics and antibacterial agents (AB): Gly—Glycopeptide, Dia—Diaminopyrimidines, Sulf—Sulfanilamide, Nit—Nitrofurantoin, Chl—Chloramphenicol; VAN = 5μg of vancomycin, AMP = 10 μg of ampicillin, AMC = 20 μg of amoxicillin + 10 μg of clavulanic acid, CXM = 30 μg of cefuroxime, IMP = 10 μg of imipenem, CRO = 30 μg of ceftriaxone, CIP = 5 μg of ciprofloxacin, NAL = 30 μg of nalidixic acid, TMP = 5 μg of trimethoprim, SXT = 1.25 μg of trimethoprim + 23.75 μg of sulfamethoxazole, RIF = 5 μg of rifampicin, RAM = 30 μg of rifampicin, ERY = 15 μg of erythromycin, CLR = 15 μg of clarithromycin, AXM = 15 μg of azithromycin, GMN = 10 μg of gentamicin, HGL = 120 μg of gentamicin, TMN = 10 μg of tobramycin, SMN = 10/300 μg of streptomycin, HLS = 300 μg of streptomycin, KMN = 30 μg of kanamycin, DOX = 30 μg of doxycycline, TET = 30 μg of tetracycline, CHL = 30 μg of chloramphenicol, NFE = 100 μg of nitrofurantoin. For each isolate, the total number of antibiotics to which it showed resistance was estimated separately for different temperatures (18 °C and 25 °C) and these values are shown in the second last two right columns. For each antibiotic, the total number of resistant strains was estimated separately for Gram-positive and Gram-negative bacteria and total number and shown in the last three rows.

4. Discussion

In the framework of this study, we, for the first time, characterized bacteria isolated from the sea-affected terrestrial temporary non-flowing meltwater ponds in the Thala Hills oasis (Enderby Land, East Antarctica), which are small water reservoirs formed on the unevenness of the terrain due to snow and ice melting.

A physicochemical characterization of the water samples showed that the water in these MPs has a high alkaline pH that can possibly be explained by the photosynthetic activity of cyanobacteria [48]. We observed high variability in TDS, the number of bacteria, and the productivity of bacterioplankton between different ponds, which can be due to the absence of water flow, small size (diameter 0.1–3 m), low depth (0.1–0.5 m), chemical composition of rock-forming minerals, water evaporation process, and effect of sea aerosols due to the location along the shoreline. A similar variability in TDS was reported for meltwater ponds from other Antarctic regions [7,49]. A previous study of the temporary meltwater ponds of the same area in East Antarctica [3] showed that the maximum number of bacterial cells and microbial biomass in non-flowing ponds (which we study in this paper) are higher than in flowing and weakly flowing ponds and were closer to the number measured for the green snow sample taken in the same area [14]. Thus, when calculating the biomass of bacterioplankton per 1 L, it can be concluded that the productivity of bacterioplankton in stagnant water ponds is the highest, more than 20 times higher than the productivity of bacterioplankton in flowing water ponds, and comparable to the productivity of surface snow samples.

Physicochemical parameters such as salinity and pH can have significant direct and indirect impacts on the formation of microbial communities as well as their diversity and ecological responses [50]. Combining culture-based and non-culture-based approaches is desirable for describing novel microbial communities, but in this study, one of the aims was to isolate culturable bacteria that could be further used in bioprospecting for the production of different valuable products. Therefore, the culture-based approach was applied. For example, the production of pigments such as carotenoids is common among Antarctic bacteria because they play a key role in the adaptation to the cold environment through the modulation of membrane fluidity and protect bacterial cells against ultraviolet radiation [26–28,30,31]. Thus, at a very first step, in order to isolate bacterial isolates from different taxonomic groups, bacterial colonies with considerably different phenotypic traits (shape and size of colonies, growth rate, pigmentation) were selected, resulting in twenty-nine fast-growing bacterial isolates.

16S rRNA sequencing indicated the presence of similar types of bacteria as reported for other meltwater ponds and environments in Antarctica. The isolated meltwater bacteria were identified as Proteobacteria, Actinobacteria, Firmicutes, and Bacteroidetes, in accordance with the previously reported studies [23,51,52]. Among the isolated bacteria, Proteobacteria (with the predominance of the genus *Pseudamonas*) were the dominating group, with seventeen isolates that were isolated from all meltwater ponds except MP- 8. Proteobacteria bacteria may dominate in culture-based studies due to their ability to grow rapidly on nutrient-rich media such as MPA and effectively compete in heterotrophic conditions [23,53]. Proteobacteria are often identified as the dominating member of Antarctic microbial communities [11,51,52]. The predominance of Proteobacteria and their presence in almost all studied ponds may have a connection to the alkaline pH and small depth of the ponds since it was previously reported that Proteobacteria are the dominant phylum in the samples taken from the bottom of water bodies, while Bacteroidetes are predominant in surface water samples [13]. The second most abundant phylum was Actinobacteria, with genus *Arthrobacter* dominating. The isolation of *Arthrobacter* and *Leifsonia* was shown for green snow samples from Antarctica [14]. Such genera as *Agrococcus*, *Arthrobacter*, *Brachybacterium*, and *Micrococcus* were found in an association with marine macroalgae from Antarctica [54], and they are often retrieved from different Antarctic samples using culture-based techniques [55]. The presence of Actinobacteria members

may lead to their co-existence with marine macroalgae and high adaptability since they can tolerate a wide range of environmental gradients, such as temperature, pH, and salinity [56]. The production of pigments by Actinobacteria may be promising for biotechnological applications [31,54]. The genera *Carnobacterium* and *Sporosarcina* were predominant from the Firmicutes phylum and were previously isolated from other Antarctic environments (lakes, ponds, and permafrost ice) [23]. Retrieving Firmicutes bacteria could be explained by their ability to form endospores, which are extremely resistant to adverse environments [57]. Bacteroidetes were represented by only one isolate, which may be due to the low selectivity of the medium used and the overall predominance of Proteobacteria, as reported by Carmen et. al. [23]. Our results indicate that the isolated microbial communities from MPs vary, and a similar observation was shown before for the microbial communities of water bodies from the Ross Sea region, where the abundance of Proteobacteria, Bacteroidetes, and Actinobacteria within different ponds was highly variable between years, with a link to climate-driven factors [12].

Interestingly, that bacterial species isolated from MPs in this study were previously found in both cold and non-cold environments, while most of the isolated bacterial species were similar to those found in other types of samples from cold polar and non-polar regions. For example, other researchers isolated *Shewanella baltica* [58], *Pseudomonas lundensis* [59,60], *Pseudomonas leptonychotis* [61], *Carnobacterium funditum* [62], *Carnobacterium iners*, *Flavobacterium degerlachei* [63], *Arthrobacter agilis* [64], *Micrococcus luteus* [21], and *Leifsonia rubra* [14,65] from water, soil, and animal samples of polar origin. The species *Pseudomonas lundensis*, *Pseudomonas peli* [25], *Acinetobacter lwoffii* [66], *Sporosarcina globispora* [67], *Carnobacterium inhibens* [68], *Arthrobacter alpinus* [69,70], and *Arthrobacter agilis* were isolated from cold non-polar environments such as frozen food, non-polar permafrost sediments, glaciers, glacial currents, a subglacial lake in the Himalayas, and Siberian permafrost. Since in this study we isolated bacteria that were previously found in cold polar and non-polar regions, it could be hypothesized that these species have especially flexible metabolic machinery that allows them to adapt and survive in distinct cold regions [51].

Screening for thermotolerance showed that many of the isolated bacteria are psychrotrophs and can grow within a wide temperature range from 4 up to 25, 30, or 37 °C, and only two isolates, *C. funditum* TMP27 and *C. iners* TMP28, were classified as psychrophilic since they could grow at 18 °C but not at 25 °C [29,71]. The appearance of psychrotrophs is common in cold environments, as they have well-developed metabolic responses and nutrient adaptability to the wide temperature fluctuation common for Antarctica, as previously reported [22,72–74].

The production of a wide range of enzymes by cold-adapted psychotropic and psychrophilic bacteria was reported before, and a similar observation was obtained in this study. Screening for enzymatic activity at the optimal growth temperature of 18 °C showed that most of the isolates (predominantly from the *Pseudamonas* genus) possess lipolytic activity that is in accordance with previous studies [19,75,76]. In oligotrophic Antarctic water ecosystems, characterized by low temperatures and low light intensity, phytoplankton stores up to 80% of available carbohydrates and other C-sources in the form of lipids, which leads to an increase in the production of lipase/esterase enzymes by the microbes present in these ecosystems [19,77]. Some isolates have shown urease activity that could be explained by the presence of seals close to the sampling sites or by the presence of other natural sources of urea, as described by Tara et. al. [78]. Urea could be an important source of nitrogen in polar systems [78]. Urease activity correlates with antibiotic multi-resistance, which is often explained by the presence of the ABC transporter system used for the transportation of urea inside cells [79] and antibiotics outside [34]. *Shewanella* isolates showed DNase activity, and this is in accordance with the previous results where it was shown that *Shewanella* can utilize DNA as a sole source of carbon, nitrogen, and phosphorus in media that is lacking these nutrients under aerobic and anaerobic con-

ditions [80]. The production of catalase, protecting cells from the toxic stress-induced reactive oxygen species (ROS) [20], was detected for more than half of the isolates. Keratinolytic activity was not possessed by any of the studied isolates, while the production of keratinases by Antarctic bacteria was previously reported [81]. The production of extracellular enzymes such us lipases, proteases, urease, and DNases by isolates from MPs indicates that these microbes play an important role in the breakdown and subsequent mineralization of MP organic matter. Bacteria could contribute to the biotransformation of organic carbon, sulfur, and nitrogenous compounds and may play a key role in the food webs and nutrient cycling of the pond's ecosystem [82,83].

As the studied MPs are (1) located in the shore area and affected by the sea, (2) characterized by average human activity (3–10 people per season), and (3) the presence of birds (penguins and skuas) and sea animal (seals), their microbial communities potentially could be affected by the transport of resistance genes. Therefore, we decided to evaluate the antibiotic susceptibility of the bacteria isolated from these MPs. We recorded a relatively high level of resistance among the tested isolates (more than six resistant isolates) towards β-lactams (ampicillin, amoxicillin-clavulanic acid, and cefuroxime), macrolide (erythromycin), aminoglycoside antibiotic (streptomycin (in low concentrations) and tobramycin), trimethoprim and trimethoprim with sulfamethoxazole. Similar results were reported for the bacterial isolates from other Antarctic environments [20,35,72,84,85]. The presence of migratory birds in the studied area could generate a selective pressure on the local microbiota and contribute to the spreading of antibiotic resistance [35]. Thus, one of the most resistant isolates was from the species *Pseudomonas lundensis*, showing a high level of resistance to thirteen antibiotics, was isolated from MP- 1 and MP-2, which was located 30 m from the skua nest and served as a swimming place for skuas. Other isolates with low levels of resistance were from meltwater pounds MP-3, MP-5, MP-6, MP-8, and MP-9, which did not serve as a swimming places for skuas. Isolates of *Acinetobacter lwoffii* TMP6 were resistant to fifteen antibiotics, *Brachybacterium paraconglomeratum* TMP16 and *Agrococcus citreus* TMP23 were resistant to nine antibiotics, and *Facklamia tabacinasalis* TMP29 and *Carnobacterium inhibens* TMP12 were resistant to six and seven antibiotics, respectively. Isolates from ponds MP-4 and MP-7 showed high levels of susceptibility towards the tested antibiotics. Its known that bacteria from the phyla Proteobacteria, Firmicutes, and Actinobacteria could encode multiple resistance mechanisms [34]. One of the most common resistance strategies in bacteria is multidrug efflux pumps. Multidrug efflux pumps have broad specificity and confer resistance to a wide range of antibiotics [34,84]. It was also shown that due to the presence of many antibiotic resistance genes Proteobacteria could have taxonomic dominance in microbial communities. Interestingly, in this study, the resistance of bacterial isolates from the phylum Proteobacteria varied a lot—from isolates with multi-resistance to isolates susceptible to all tested antibiotics. Summarizing our observations, the bacterial communities of MPs could be used as bioindicators in Antarctica to track antibiotic resistance gene mobilization to the polar regions and the impact of human or animal presence.

5. Conclusions

Based on the obtained results, we can hypothesize that the bacterial communities of the temporary meltwater ponds in East Antarctica include metabolically versatile bacteria, as among the isolated species, many are commonly found in both polar and non-polar cold regions. The isolated bacteria were shown to be psychrotrophic and were able to grow at a wide range of the temperatures from 4 to 37 °C, and the optimal temperature varied from 18 to 25 °C. It seems that the physiological properties, such as the enzymatic activity and antibiotic susceptibility, of the isolated meltwater bacteria are defined by the location of animals, penguins and skuas in particular, close to the MPs. The production of enzymes and pigments detected in this study may be promising for biotechnological applications. Antibiotic susceptibility testing revealed that most of the isolates were resistant to at least one antibiotic, and seven isolates showed multi-resistance from six to fifteen out

of twenty-three tested antibiotics and antibacterial agents. In summary, isolates from Antarctic MPs may have biotechnological potential and could be used as bioindicators to track antibiotic resistance gene mobilization and the impact of human or animal presence in polar regions.

Author Contributions: Conceptualization, V.S., V.A. and L.V.; methodology, V.A., L.V., V.S. and U.M.; formal analysis, V.A. and L.V.; investigation, V.A., K.A., L.V., U.M. and A.D.; resources, U.M., L.V., and V.S.; data curation, V.A., L.V. and K.A.; writing—original draft preparation, V.A.; writing—review and editing, V.S., V.A., L.V., U.M., K.A. and A.D.; visualization, V.A. and A.D.; supervision, V.S., L.V. and U.M.; project administration, V.S.; funding acquisition, V.S. All authors have read and agreed to the published version of the manuscript.

Funding: This research was supported by the project "Belanoda—Multidisciplinary graduate and post-graduate education in big data analysis for life sciences" (CPEA-LT-2016/10126), funded by the Eurasia program, Norwegian Agency for International Cooperation and Quality Enhancement in Higher Education (Diku), and the Belanoda Digital learning platform for boosting multidisciplinary education in data analysis for life sciences in the Eurasia region (CPEA-STA-2019/10025).

Institutional Review Board Statement: Not applicable.

Informed Consent Statement: Not applicable.

Data Availability Statement: The data that support the findings of this study are available from the corresponding author upon reasonable request.

Conflicts of Interest: The authors declare no conflict of interest.

References

1. Wilkins, D.; Yau, S.; Williams, T.J.; Allen, M.A.; Brown, M.V.; Demaere, M.Z.; Lauro, F.M.; Cavicchioli, R. Key microbial drivers in Antarctic aquatic environments. *FEMS Microbiol. Rev.* **2013**, *37*, 303–335. https://doi.org/10.1111/1574-6976.12007.
2. Kakareka, S.V.; Kukharchyk, T.I.; Kokosh, Y.G.; Kudrevich, M.A.; Giginyak, Y.G.; Myamin, V.E. Chemical characteristics of antarctic lakes of the Thala Hills. *Arct. Antarct. Res.* **2019**, *65*, 422–437. https://doi.org/10.30758/0555-2648-2019-65-4-422-437.
3. Miamin, V.E.; Nikitina, L.V.; Charniauskaya, M.I.; Zaniuk, A.A.; Titok, M.A.; Laziuk, S.K.; Sidarenka, A.V.; Valentovich, L.N.; Dolgikh, A.V. Microbiology investigation in the Vechernyy region, Tala Hills (East Antarctica). *Belarus State Univ. Annu. Physiol. Biochem. Mol. Base Biosyst. Funct.* **2014**, *9*, 58–67.
4. Dieser, M.; Foreman, C.M.; Jaros, C.; Lisle, J.T.; Greenwood, M.; Laybourn-Parry, J.; Miller, P.L.; Chin, Y.-P.; McKnight, D.M. Physicochemical and biological dynamics in a coastal Antarctic lake as it transitions from frozen to open water. *Antarct. Sci.* **2013**, *25*, 663–675. https://doi.org/10.1017/s0954102013000102.
5. Hogg, I.D.; Cary, S.C.; Convey, P.; Newsham, K.K.; O'Donnell, A.G.; Adams, B.J.; Aislabie, J.; Frati, F.; Stevens, M.I.; Wall, D.H. Biotic interactions in Antarctic terrestrial ecosystems: Are they a factor? *Soil Biol. Biochem.* **2006**, *38*, 3035–3040.
6. Wait, B.; Nokes, R.; Webster-Brown, J. Freeze-thaw dynamics and the implications for stratification and brine geochemistry in meltwater ponds on the McMurdo Ice Shelf, Antarctica. *Antarct. Sci.* **2009**, *21*, 243–254.
7. De Mora, S.; Whitehead, R.F.; Gregory, M. The chemical composition of glacial melt water ponds and streams on the McMurdo Ice Shelf, Antarctica. *Antarct. Sci.* **1994**, *6*, 17–27.
8. Matsumoto, G.I.; Nakaya, S.; Murayama, H.; Masuda, N.; Kawano, T.; Watanuki, K.; Torii, T. Geochemical characteristics of Antarctic lakes and ponds. *Proc. NIPR Symp. Polar Biol.* **1992**, *5*, 125 – 145.
9. Wait, B.; Webster-Brown, J.; Brown, K.; Healy, M.; Hawes, I. PChemistry and stratification of Antarctic meltwater ponds I: Coastal ponds near Bratina Island, McMurdo Ice Shelf. *Antarct. Sci.* **2006**, *18*, 515–524.
10. Jackson, E.E.; Hawes, I.; Jungblut, A.D. 16S rRNA gene and 18S rRNA gene diversity in microbial mat communities in meltwater ponds on the McMurdo Ice Shelf, Antarctica. *Polar Biol.* **2021**, *44*, 823–836. https://doi.org/10.1007/s00300-021-02843-2.
11. Archer, S.D.; McDonald, I.R.; Herbold, C.W.; Lee, C.K.; Cary, C.S. Benthic microbial communities of coastal terrestrial and ice shelf Antarctic meltwater ponds. *Front. Microbiol.* **2015**, *6*, 485.
12. Archer, S.D.J.; McDonald, I.R.; Herbold, C.W.; Lee, C.K.; Niederberger, T.S.; Cary, C. Temporal, regional and geochemical drivers of microbial community variation in the melt ponds of the Ross Sea region, Antarctica. *Polar Biol.* **2016**, *39*, 267–282. https://doi.org/10.1007/s00300-015-1780-2.
13. Archer, S.D.J.; McDonald, I.R.; Herbold, C.W.; Cary, S.C. Characterisation of bacterioplankton communities in the meltwater ponds of Bratina Island, Victoria Land, Antarctica. *FEMS Microbiol. Ecol.* **2014**, *89*, 451–464. https://doi.org/10.1111/1574-6941.12358.
14. Smirnova, M.; Miamin, U.; Kohler, A.; Valentovich, L.; Akhremchuk, A.; Sidarenka, A.; Dolgikh, A.; Shapaval, V. Isolation and characterization of fast growing green snow bacteria from coastal East Antarctica. *MicrobiologyOpen* **2021**, *10*, e1152. https://doi.org/10.1002/mbo3.1152.

15. Kudinova, A.; Lysak, L.; Soina, V.; Mergelov, N.; Dolgikh, A.; Shorkunov, I. Bacterial communities in the soils of cryptogamic barrens of East Antarctica (the Larsemann Hills and Thala Hills oases). *Eurasian Soil Sci.* **2015**, *48*, 276–287.
16. Lukashanets, D.A.; Convey, P.; Borodin, O.I.; Miamin, V.Y.; Hihiniak, Y.H.; Gaydashov, A.A.; Yatsyna, A.P.; Vezhnavets, V.V.; Maysak, N.N.; Shendrik, T.V. Eukarya biodiversity in the Thala Hills, East Antarctica. *Antarct. Sci.* **2021**, *33*, 605–623.
17. Dolgikh, A.V.; Mergelov, N.S.; Abramov, A.A.; Lupachev, A.V.; Goryachkin, S.V. Soils of Enderby Land. In *The Soils of Antarctica*; Springer: Berlin/Heidelberg, Germany, 2015; pp. 45–63.
18. Gribanova, E.; Miamin, V. Physiological and biochemical traits of yeasts from soils of various ecosystems of East Antarctica. *Ukr. Antarct. J.* **2021**, *2*, 106 – 116. https://doi.org/10.33275/1727-7485.2.2021.681.
19. Ferrés, I.; Amarelle, V.; Noya, F.; Fabiano, E. Identification of Antarctic culturable bacteria able to produce diverse enzymes of potential biotechnological interest. *Adv. Polar Sci.* **2015**, *26*, 71–79. https://doi.org/10.13679/j.advps.2015.1.00071.
20. Morozova, O.V.; Andreeva, I.S.; Zhirakovskiy, V.Y.; Pechurkina, N.I.; Puchkova, L.I.; Saranina, I.V.; Emelyanova, E.K.; Kamynina, T.P. Antibiotic resistance and cold-adaptive enzymes of antarctic culturable bacteria from King George Island. *Polar Sci.* **2022**, *31*, 100756.
21. Piegza, M.; Łaba, W.; Kačániová, M. New Arctic Bacterial Isolates with Relevant Enzymatic Potential. *Molecules* **2020**, *25*, 3930. https://doi.org/10.3390/molecules25173930.
22. Ray, M.K.; Kumar, G.S.; Janiyani, K.; Kannan, K.; Jagtap, P.; Basu, M.K.; Shivaji, S. Adaptation to low temperature and regulation of gene expression in antarctic psychrotrophic bacteria. *J. Biosci.* **1998**, *23*, 423–435. https://doi.org/10.1007/bf02936136.
23. Rizzo, C.; Conte, A.; Azzaro, M.; Papale, M.; Rappazzo, A.C.; Battistel, D.; Roman, M.; Lo Giudice, A.; Guglielmin, M. Cultivable Bacterial Communities in Brines from Perennially Ice-Covered and Pristine Antarctic Lakes: Ecological and Biotechnological Implications. *Microorganisms* **2020**, *8*, 819. https://doi.org/10.3390/microorganisms8060819.
24. Shawkey, M.D.; Mills, K.L.; Dale, C.; Hill, G.E. Microbial Diversity of Wild Bird Feathers Revealed throughCulture-Based and Culture-Independent Techniques. *Microb. Ecol.* **2005**, *50*, 40–47. https://doi.org/10.1007/s00248-004-0089-4.
25. Yadav, A.N.; Sachan, S.G.; Verma, P.; Tyagi, S.P.; Kaushik, R.; Saxena, A.K. Culturable diversity and functional annotation of psychrotrophic bacteria from cold desert of Leh Ladakh (India). *World J. Microbiol. Biotechnol.* **2015**, *31*, 95–108. https://doi.org/10.1007/s11274-014-1768-z.
26. Dieser, M.; Greenwood, M.; Foreman, C.M. Carotenoid Pigmentation in Antarctic Heterotrophic Bacteria as a Strategy to Withstand Environmental Stresses. *Arct. Antarct. Alp. Res.* **2010**, *42*, 396–405. https://doi.org/10.1657/1938-4246-42.4.396.
27. Fong, N.J.C.; Burgess, M.L.; Barrow, K.D.; Glenn, D.R. Carotenoid accumulation in the psychrotrophic bacterium Arthrobacter agilis in response to thermal and salt stress. *Appl. Microbiol. Biotechnol.* **2001**, *56*, 750–756. https://doi.org/10.1007/s002530100739.
28. Jagannadham, M.V.; Chattopadhyay, M.K.; Subbalakshmi, C.; Vairamani, M.; Narayanan, K.; Mohan Rao, C.; Shivaji, S. Carotenoids of an Antarctic psychrotolerant bacterium, Sphingobacterium antarcticus, and a mesophilic bacterium, Sphingobacterium multivorum. *Arch. Microbiol.* **2000**, *173*, 418–424. https://doi.org/10.1007/s002030000163.
29. Moyer, C.L.; Morita, R.Y. Psychrophiles and psychrotrophs. *Encycl. Life Sci.* **2007**, *1*.
30. Sajjad, W.; Din, G.; Rafiq, M.; Iqbal, A.; Khan, S.; Zada, S.; Ali, B.; Kang, S. Pigment production by cold-adapted bacteria and fungi: Colorful tale of cryosphere with wide range applications. *Extremophiles* **2020**, *24*, 447–473. https://doi.org/10.1007/s00792-020-01180-2.
31. Silva, T.R.E.; Silva, L.C.F.J.; de Queiroz, A.C.; Alexandre Moreira, M.S.; de Carvalho Fraga, C.A.; de Menezes, G.C.A.; Rosa, L.H.; Bicas, J.; de Oliveira, V.M.; Duarte, A.W.F. Pigments from Antarctic bacteria and their biotechnological applications. *Crit. Rev. Biotechnol.* **2021**, *41*, 809–826. https://doi.org/10.1080/07388551.2021.1888068.
32. Gupta, V.K.; Treichel, H.; Shapaval, V.O.; de Oliveira, L.A.; Tuohy, M.G. *Microbial Functional Foods and Nutraceuticals*; John Wiley & Sons: Hoboken, NJ, USA, 2017.
33. Martínez, J.L. Natural antibiotic resistance and contamination by antibiotic resistance determinants: The two ages in the evolution of resistance to antimicrobials. *Front. Microbiol.* **2012**, *3*, 1.
34. Van Goethem, M.W.; Pierneef, R.; Bezuidt, O.K.I.; Van De Peer, Y.; Cowan, D.A.; Makhalanyane, T.P. A reservoir of 'historical' antibiotic resistance genes in remote pristine Antarctic soils. *Microbiome* **2018**, *6*, 40. https://doi.org/10.1186/s40168-018-0424-5.
35. Jara, D.; Bello-Toledo, H.; Domínguez, M.; Cigarroa, C.; Fernández, P.; Vergara, L.; Quezada-Aguiluz, M.; Opazo-Capurro, A.; Lima, C.A.; González-Rocha, G. Antibiotic resistance in bacterial isolates from freshwater samples in Fildes Peninsula, King George Island, Antarctica. *Sci. Rep.* **2020**, *10*, 3145. https://doi.org/10.1038/s41598-020-60035-0.
36. Hobbie, J.E.; Daley, R.J.; Jasper, S. Use of nuclepore filters for counting bacteria by fluorescence microscopy. *Appl. Environ. Microbiol.* **1977**, *33*, 1225–1228.
37. Lane, D. 16S/23S rRNA sequencing. *Nucleic Acid Tech. Bact. Syst.* **1991**, 115–175.
38. Sanger, F.; Nicklen, S.; Coulson, A.R. DNA sequencing with chain-terminating inhibitors. *Proc. Natl. Acad. Sci. USA* **1977**, *74*, 5463–5467.
39. Yoon, S.-H.; Ha, S.-M.; Kwon, S.; Lim, J.; Kim, Y.; Seo, H.; Chun, J. Introducing EzBioCloud: A taxonomically united database of 16S rRNA gene sequences and whole-genome assemblies. *Int. J. Syst. Evol. Microbiol.* **2017**, *67*, 1613–1617. https://doi.org/10.1099/ijsem.0.001755.
40. Kumar, S.; Stecher, G.; Li, M.; Knyaz, C.; Tamura, K. MEGA X: Molecular Evolutionary Genetics Analysis across Computing Platforms. *Mol. Biol. Evol.* **2018**, *35*, 1547–1549. https://doi.org/10.1093/molbev/msy096.
41. Tamura, K.; Nei, M. Estimation of the number of nucleotide substitutions in the control region of mitochondrial DNA in humans and chimpanzees. *Mol. Biol. Evol.* **1993**, *10*, 512–526. https://doi.org/10.1093/oxfordjournals.molbev.a040023.

42. Hillis, D.M.; Bull, J.J. An Empirical Test of Bootstrapping as a Method for Assessing Confidence in Phylogenetic Analysis. *Syst. Biol.* **1993**, *42*, 182–192. https://doi.org/10.1093/sysbio/42.2.182.
43. Bauer, A.W.; Kirby, W.M.; Sherris, J.C.; Turck, M. Antibiotic susceptibility testing by a standardized single disk method. *Am. J. Clin. Pathol.* **1966**, *45*, 493–496.
44. The European Committee on Antimicrobial Susceptibility Testing. Breakpoint Tables for Interpretation of MICs and Zone Diameters, Version 12.0. 2022. Available online: http://www.eucast.org (accessed on 01 April 2022).
45. CLSI: Clinical and Laboratory Standards Institute. 2020 CLSI document M100. In *Performance Standards for Antimicrobial. Susceptibility Tests*, 30th ed.; Pa, W., Ed.; CLSI: Wayne,PA, USA, 2020.
46. Kato, S.; Yamagishi, A.; Daimon, S.; Kawasaki, K.; Tamaki, H.; Kitagawa, W.; Abe, A.; Tanaka, M.; Sone, T.; Asano, K. Isolation of previously uncultured slow-growing bacteria by using a simple modification in the preparation of agar media. *Appl. Environ. Microbiol.* **2018**, *84*, e00807–e00818.
47. Smirnova, M.; Tafintseva, V.; Kohler, A.; Miamin, U.; Shapaval, V. Temperature- and Nutrients-Induced Phenotypic Changes of Antarctic Green Snow Bacteria Probed by High-Throughput FTIR Spectroscopy. *Biology* **2022**, *11*, 890. https://doi.org/10.3390/biology11060890.
48. López-Archilla, A.I.; Moreira, D.; López-García, P.; Guerrero, C. Phytoplankton diversity and cyanobacterial dominance in a hypereutrophic shallow lake with biologically produced alkaline pH. *Extremophiles* **2004**, *8*, 109–115. https://doi.org/10.1007/s00792-003-0369-9.
49. Lecomte, K.L.; Vignoni, P.A.; Córdoba, F.E.; Chaparro, M.A.E.; Kopalová, K.; Gargiulo, J.D.; Lirio, J.M.; Irurzun, M.A.; Böhnel, H.N. Hydrological systems from the Antarctic Peninsula under climate change: James Ross archipelago as study case. *Environ. Earth Sci.* **2016**, *75*, 623 . https://doi.org/10.1007/s12665-016-5406-y.
50. George, S.F.; Fierer, N.; Levy, J.S.; Adams, B. Antarctic Water Tracks: Microbial Community Responses to Variation in Soil Moisture, pH, and Salinity. *Front. Microbiol.* **2021**, *12*, 616730. https://doi.org/10.3389/fmicb.2021.616730.
51. Antony, R.; Sanyal, A.; Kapse, N.; Dhakephalkar, P.K.; Thamban, M.; Nair, S. Microbial communities associated with Antarctic snow pack and their biogeochemical implications. *Microbiol. Res.* **2016**, *192*, 192–202.
52. Núñez-Montero, K.; Barrientos, L. Advances in Antarctic Research for Antimicrobial Discovery: A Comprehensive Narrative Review of Bacteria from Antarctic Environments as Potential Sources of Novel Antibiotic Compounds Against Human Pathogens and Microorganisms of Industrial Importance. *Antibiotics* **2018**, *7*, 90. https://doi.org/10.3390/antibiotics7040090.
53. Joint, I.; Mühling, M.; Querellou, J. Culturing marine bacteria—An essential prerequisite for biodiscovery. *Microb. Biotechnol.* **2010**, *3*, 564–575. https://doi.org/10.1111/j.1751-7915.2010.00188.x.
54. Leiva, S.; Alvarado, P.; Huang, Y.; Wang, J.; Garrido, I. Diversity of pigmented Gram-positive bacteria associated with marine macroalgae from Antarctica. *FEMS Microbiol. Lett.* **2015**, *362*, fnv206. https://doi.org/10.1093/femsle/fnv206.
55. Rego, A.; Raio, F.; Martins, T.P.; Ribeiro, H.; Sousa, A.G.G.; Séneca, J.; Baptista, M.S.; Lee, C.K.; Cary, S.C.; Ramos, V.; et al. Actinobacteria and Cyanobacteria Diversity in Terrestrial Antarctic Microenvironments Evaluated by Culture-Dependent and Independent Methods. *Front. Microbiol.* **2019**, *10*, 1018. https://doi.org/10.3389/fmicb.2019.01018.
56. Jiang, H.; Huang, Q.; Deng, S.; Dong, H.; Yu, B. Planktonic actinobacterial diversity along a salinity gradient of a river and five lakes on the Tibetan Plateau. *Extremophiles* **2010**, *14*, 367–376. https://doi.org/10.1007/s00792-010-0316-5.
57. Antibus, D.E.; Leff, L.G.; Hall, B.L.; Baeseman, J.L.; Blackwood, C.B. Cultivable bacteria from ancient algal mats from the McMurdo Dry Valleys, Antarctica. *Extremophiles* **2012**, *16*, 105–114. https://doi.org/10.1007/s00792-011-0410-3.
58. Zeng, Y.; Zheng, T.; Yu, Y.; Chen, B.; He, J. Relationships between Arctic and Antarctic Shewanella strains evaluated by a polyphasic taxonomic approach. *Polar Biol.* **2010**, *33*, 531–541. https://doi.org/10.1007/s00300-009-0730-2.
59. Ravi, K.; Falkowski, N.R.; Scales, B.S.; Akulava, V.D.; Valentovich, L.N.; Huffnagle, G.B. The Psychrotrophic Pseudomonas lundensis, a Non-aeruginosa Pseudomonad, Has a Type III Secretion System of the Ysc Family, Which Is Transcriptionally Active at 37° C. *Mbio* **2022**, *13*, e03869–e03821.
60. Molin, G.; Ternstrom, A.; Ursing, J. Notes: Pseudomonas lundensis, a New Bacterial Species Isolated from Meat. *Int. J. Syst. Bacteriol.* **1986**, *36*, 339–342. https://doi.org/10.1099/00207713-36-2-339.
61. Nováková, D.; Švec, P.; Zeman, M.; Busse, H.-J.; Mašlaňová, I.; Pantůček, R.; Králová, S.; Krištofová, L.; Sedláček, I. Pseudomonas leptonychotis sp. nov., isolated from Weddell seals in Antarctica. *Int. J. Syst. Evol. Microbiol.* **2020**, *70*, 302–308. https://doi.org/10.1099/ijsem.0.003753.
62. Franzmann, P.D.; Höpfl, P.; Weiss, N.; Tindall, B.J. Psychrotrophic, lactic acid-producing bacteria from anoxic waters in Ace Lake, Antarctica; Carnobacterium funditum sp. nov. and Carnobacterium alterfunditum sp. nov. *Arch. Microbiol.* **1991**, *156*, 255–262. https://doi.org/10.1007/bf00262994.
63. Van Trappen, S.; Vandecandelaere, I.; Mergaert, J.; Swings, J. Flavobacterium degerlachei sp. nov., Flavobacterium frigoris sp. nov. and Flavobacterium micromati sp. nov., novel psychrophilic bacteria isolated from microbial mats in Antarctic lakes. *Int. J. Syst. Evol. Microbiol.* **2004**, *54*, 85–92. https://doi.org/10.1099/ijs.0.02857-0.
64. Bej, A.K.; Aislabie, J.; Atlas, R.M. *Polar Microbiology: The Ecology, Biodiversity and Bioremediation Potential of Microorganisms in Extremely Cold Environments*; CRC Press: Boca Raton, FL, USA, 2009.
65. Reddy, G.S.N.; Prakash, J.S.S.; Srinivas, R.; Matsumoto, G.I.; Shivaji, S. Leifsonia rubra sp. nov. and Leifsonia aurea sp. nov., psychrophiles from a pond in Antarctica. *Int. J. Syst. Evol. Microbiol.* **2003**, *53*, 977–984. https://doi.org/10.1099/ijs.0.02396-0.

66. Mindlin, S.; Petrenko, A.; Kurakov, A.; Beletsky, A.; Mardanov, A.; Petrova, M. Resistance of Permafrost and Modern Acinetobacter lwoffii Strains to Heavy Metals and Arsenic Revealed by Genome Analysis. *BioMed Res. Int.* **2016**, *2016*, 1–9. https://doi.org/10.1155/2016/3970831.
67. Wang, J.-P.; Liu, B.; Liu, G.-H.; Xiao, R.-F.; Zheng, X.-F.; Shi, H.; Ge, C.-B. Draft genome sequence of Sporosarcina globispora W 25T (DSM 4), a psychrophilic bacterium isolated from soil and river water. *Genome Announc.* **2015**, *3*, e01230–e15.
68. Nicholson, W.L.; Zhalnina, K.; De Oliveira, R.R.; Triplett, E.W. Proposal to rename Carnobacterium inhibens as Carnobacterium inhibens subsp. inhibens subsp. nov. and description of Carnobacterium inhibens subsp. gilichinskyi subsp. nov., a psychrotolerant bacterium isolated from Siberian permafrost. *Int. J. Syst. Evol. Microbiol.* **2015**, *65*, 556–561. https://doi.org/10.1099/ijs.0.067983-0.
69. Kumar, R.; Singh, D.; Swarnkar, M.K.; Singh, A.K.; Kumar, S. Complete genome sequence of Arthrobacter alpinus ERGS4: 06, a yellow pigmented bacterium tolerant to cold and radiations isolated from Sikkim Himalaya. *J. Biotechnol.* **2016**, *220*, 86–87.
70. Zhang, D.-C.; Schumann, P.; Liu, H.-C.; Xin, Y.-H.; Zhou, Y.-G.; Schinner, F.; Margesin, R. Arthrobacter alpinus sp. nov., a psychrophilic bacterium isolated from alpine soil. *Int. J. Syst. Evol. Microbiol.* **2010**, *60*, 2149–2153. https://doi.org/10.1099/ijs.0.017178-0.
71. Morita, R.Y. Psychrophilic bacteria. *Bacteriol. Rev.* **1975**, *39*, 144–167.
72. De Souza, M.-J.; Nair, S.; Loka Bharathi, P.A.; Chandramohan, D. Metal and antibiotic-resistance in psychrotrophic bacteria from Antarctic Marine waters. *Ecotoxicology* **2006**, *15*, 379–384. https://doi.org/10.1007/s10646-006-0068-2.
73. Helmke, E.; Weyland, H. Psychrophilic versus psychrotolerant bacteria--occurrence and significance in polar and temperate marine habitats. *Cell. Mol. Biol.* **2004**, *50*, 553–561.
74. Bowman, J.P.; McCammon, S.A.; Brown, M.V.; Nichols, D.S.; McMeekin, T.A. Diversity and association of psychrophilic bacteria in Antarctic sea ice. *Appl. Environ. Microbiol.* **1997**, *63*, 3068–3078. https://doi.org/10.1128/aem.63.8.3068-3078.1997.
75. Lo Giudice, A.; Michaud, L.; De Pascale, D.; De Domenico, M.; Di Prisco, G.; Fani, R.; Bruni, V. Lipolytic activity of Antarctic cold-adapted marine bacteria (Terra Nova Bay, Ross Sea). *J. Appl. Microbiol.* **2006**, *101*, 1039–1048. https://doi.org/10.1111/j.1365-2672.2006.03006.x.
76. Salwoom, L.; Raja Abd Rahman, R.; Salleh, A.; Mohd. Shariff, F.; Convey, P.; Pearce, D.; Mohamad Ali, M. Isolation, Characterisation, and Lipase Production of a Cold-Adapted Bacterial Strain Pseudomonas sp. LSK25 Isolated from Signy Island, Antarctica. *Molecules* **2019**, *24*, 715. https://doi.org/10.3390/molecules24040715.
77. Henderson, R.J.; Olsen, R.E.; Eilertsen, H.C. Lipid composition of phytoplankton from the Barents Sea and environmental influences on the distribution pattern of carbon among photosynthetic end products. *Polar Res.* **1991**, *10*, 229–238. https://doi.org/10.3402/polar.v10i1.6741.
78. Connelly, T.L.; Baer, S.E.; Cooper, J.T.; Bronk, D.A.; Wawrik, B. Urea Uptake and Carbon Fixation by Marine Pelagic Bacteria and Archaea during the Arctic Summer and Winter Seasons. *Appl. Environ. Microbiol.* **2014**, *80*, 6013–6022. https://doi.org/10.1128/aem.01431-14.
79. Williams, T.J.; Allen, M.A.; Demaere, M.Z.; Kyrpides, N.C.; Tringe, S.G.; Woyke, T.; Cavicchioli, R. Microbial ecology of an Antarctic hypersaline lake: Genomic assessment of ecophysiology among dominant haloarchaea. *ISME J.* **2014**, *8*, 1645–1658. https://doi.org/10.1038/ismej.2014.18.
80. Pinchuk, G.E.; Ammons, C.; Culley, D.E.; Li, S.-M.W.; McLean, J.S.; Romine, M.F.; Nealson, K.H.; Fredrickson, J.K.; Beliaev, A.S. Utilization of DNA as a Sole Source of Phosphorus, Carbon, and Energy by Shewanella spp.: Ecological and Physiological Implications for Dissimilatory Metal Reduction. *Appl. Environ. Microbiol.* **2008**, *74*, 1198–1208. https://doi.org/10.1128/aem.02026-07.
81. Gushterova, A.; Vasileva-Tonkova, E.; Dimova, E.; Nedkov, P.; Haertlé, T. Keratinase Production by Newly Isolated Antarctic Actinomycete Strains. *World J. Microbiol. Biotechnol.* **2005**, *21*, 831–834. https://doi.org/10.1007/s11274-004-2241-1.
82. Papale, M.; Lo Giudice, A.; Conte, A.; Rizzo, C.; Rappazzo, A.C.; Maimone, G.; Caruso, G.; La Ferla, R.; Azzaro, M.; Gugliandolo, C.; et al. Microbial Assemblages in Pressurized Antarctic Brine Pockets (Tarn Flat, Northern Victoria Land): A Hotspot of Biodiversity and Activity. *Microorganisms* **2019**, *7*, 333. https://doi.org/10.3390/microorganisms7090333.
83. Zhang, X.-Y.; Han, X.-X.; Chen, X.-L.; Dang, H.-Y.; Xie, B.-B.; Qin, Q.-L.; Shi, M.; Zhou, B.-C.; Zhang, Y.-Z. Diversity of cultivable protease-producing bacteria in sediments of Jiaozhou Bay, China. *Front. Microbiol.* **2015**, *6*, 1021. https://doi.org/10.3389/fmicb.2015.01021.
84. Lo Giudice, A.; Casella, P.; Bruni, V.; Michaud, L. Response of bacterial isolates from Antarctic shallow sediments towards heavy metals, antibiotics and polychlorinated biphenyls. *Ecotoxicology* **2013**, *22*, 240–250. https://doi.org/10.1007/s10646-012-1020-2.
85. Tam, H.K.; Wong, C.M.V.L.; Yong, S.T.; Blamey, J.; González, M. Multiple-antibiotic-resistant bacteria from the maritime Antarctic. *Polar Biol.* **2015**, *38*, 1129–1141. https://doi.org/10.1007/s00300-015-1671-6.

Paper II

Explorative characterization and taxonomy-aligned comparison of alterations in lipids and other biomolecules in Antarctic bacteria grown at different temperatures

Volha Akulava[1*], Margarita Smirnova[1], Dana Byrtusova[1], Boris Zimmermann[1], Dag Ekeberg[2], Achim Kohler[1], Uladzislau Blazhko[1], Uladzislau Miamin[3], Leonid Valentovich[4], Volha Shapaval[1]

[1]Faculty of Science and Technology, Norwegian University of Life Sciences, Ås, Norway

[2]Faculty of Chemistry, Biotechnology and Food Science, Norwegian University of Life Sciences, Ås, Norway

[3]Faculty of Biology, Belarussian State University, Minsk, Belarus

[4]Institute of Microbiology, National Academy of Sciences of Belarus, 220084 Minsk, Belarus

***Correspondence:** Corresponding Author volha.akulava@nmbu.no

Keywords: fatty acids[1], temperature effect[2], lipid extraction[3], gas chromatography[4], FTIR spectroscopy[5], bioprospecting[6]

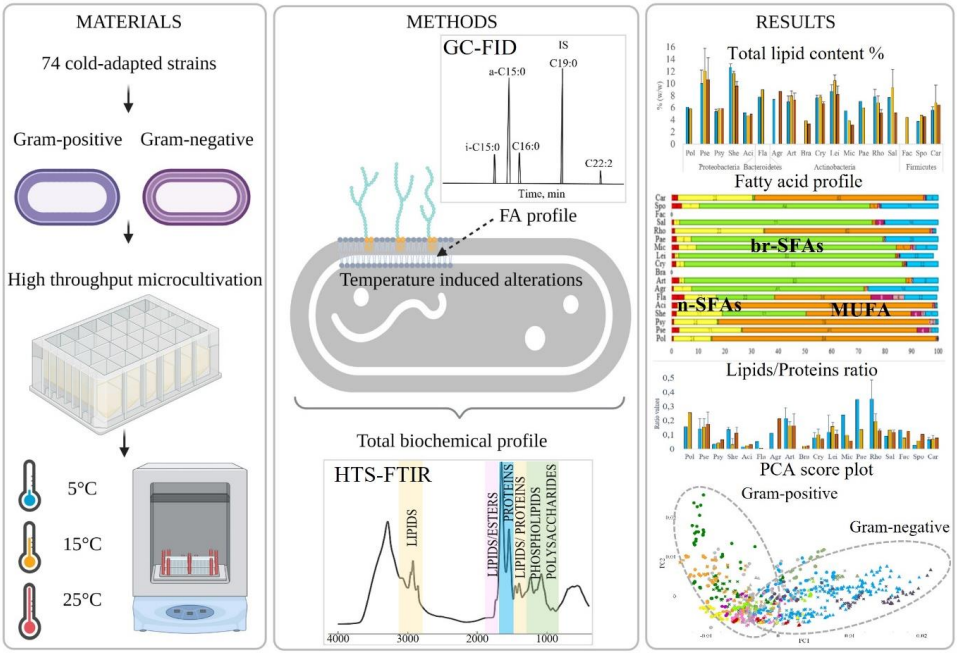

Graphical abstract was partially created with BioRender.com

Abstract

Temperature significantly impacts bacterial physiology, metabolism, and cell chemistry. In this study, we analyzed lipids and total cellular biochemical profile of seventy-four fast-growing Antarctic bacteria grown at different temperatures. Fatty acid diversity and temperature-induced alterations aligned with bacterial classification - Gram-groups, phylum, genus, and species. Total lipid content, varied from 4% to 19% of cell dry weight, was genus- and species-specific. Most bacteria increased lipid content at lower temperatures. The effect of temperature on the profile was complex and more specie-specific, while some common for all bacteria responses were recorded. Gram-negative bacteria adjusted unsaturation and acyl chain length. Gram-positive bacteria adjusted methyl branching (anteiso-/iso-), chain length, and unsaturation. Fourier transform infrared spectroscopy analysis revealed Gram-, genus-, and specie-specific changes in the total cellular biochemical profile triggered by temperature fluctuations. The most significant temperature related alterations detected on all taxonomy levels were recorded for mixed region 1500-900 cm^{-1}, specifically the band at 1083 cm^{-1} related to phosphodiester groups mainly from phospholipids (for Gram-negative bacteria) and teichoic /lipoteichoic acids (for Gram-positive bacteria). Some changes in protein region were detected for few genera, while lipid region remained relatively stable despite the temperature fluctuations.

Introduction

Psychrotrophic and psychrophilic bacteria have garnered attention due to biomolecules they can produce which have application potential in biotechnology and medicine. Their ability to survive and thrive in frigid environments, such as polar regions, often rely on alterations in cellular lipids and production of specific compounds, such as antifreeze proteins (De Maayer et al., 2014), cold-active enzymes, cryoprotection-targeted exopolysaccharides, compatible solutes (Collins and Margesin, 2019), storage compounds and pigments (Sajjad et al., 2020). Some bacterial fatty acids (FAs) and monoglycerides are promising antibacterial agents due to that they destabilize bacterial cell membranes, resulting in a variety of direct and indirect inhibitory effects (Desbois and Smith, 2010; Yoon et al., 2018). Finally, accumulation of storage compounds such as acyl glycerides and polyhydroxyalkanoates (PHAs) has been reported as an adaptation to the low temperatures and nutrient-poor conditions (Goh and Tan, 2012; Tribelli and López, 2018).

Lipids are one of the main temperature sensitive biomolecules in bacterial cells which accounts approximately 10– 15 % (w/w) of cell dry weight (Naumann, 2000). They are localized mainly in the form of phospholipids in the cell membrane or can be accumulated in the form of acyl glycerides and/or free FAs in lipid droplets. Lipids play multiple roles in bacterial cells such as membrane flexibility and its selective permeability, establishment of the environment for many enzyme and proteins transport (Chattopadhyay and Jagannadham, 2001). Fatty acid profile is considered as chemotaxonomy biomarker used for bacterial identification on genus and species level (Sasser, 1990).

For cold-adapted bacteria, temperature associated alterations in amount of lipids, ratio between different types of lipids, and fatty acid profiles have been reported previously (Hassan et al., 2020). Modification of fatty acid composition and ratios of different FAs impact the fluidity, flexibility, and permeability of cell membranes resulting in the elevated survival rate at low and high temperatures. Thus, increased production of saturated fatty acids (SFAs) and cyclopropane fatty acids (cyclic-FA) can increase rigidity and lower permeability of membrane bilayer, while high presence of cis-unsaturated fatty acids (cis-UFAs) can lead to a higher permeability of membrane (Mező et al., 2022). Changes in branched-chain fatty acids can affect membrane fluidity, where increase in anteiso-fatty acids (anteiso-FA) can result in a more fluid membrane structure than for iso-fatty acids (iso-FA) (Mező et al., 2022). The ratio between long- and short-chain fatty acids can also regulate membrane fluidity under unfavorable temperature conditions the same as change of

saturation. Moreover, temperature fluctuations can lead to the conversion of cis-UFAs into their corresponding trans configurations, leading to a quick rigidification of the cell membrane (Mező et al., 2022).

Proteins and carbohydrates are among the primary biomolecules found in bacterial cells that exhibit temperature sensitivity. Proteins are the main components of bacterial cells accounting of approximately 40–60 % (w/w) of cell dry weight (Naumann, 2000). Temperature fluctuations can impact protein structures and activity. Antarctic bacteria thrive in lower temperatures, producing cold-adapted proteins that maintain stability, flexibility, and enhanced catalytic activity. These bacteria also produce antifreeze proteins that bind to ice surfaces, preventing ice crystal formation and enabling survival in freezing conditions (De Maayer et al., 2014). Polysaccharides accounting of approximately 10– 20 % (w/w) of cell dry weight (Naumann, 2000) can significantly be affected by temperature and alter production, composition, and structure. Lower temperatures commonly lead to increased production of exopolysaccharides and induce modifications that contribute to bacterial survival and adaptation to the extreme cold conditions (De Maayer et al., 2014; Tribelli and López, 2018).

The primary objective of this study was to perform explorative characterization and taxonomy-aligned comparison of the temperature-induced alterations of the main biomolecules such as lipids, proteins and polysaccharides in Antarctic cold-adapted bacteria newly isolated from green snow and temporary meltwater ponds and belonging to four phyla and eighteen genera. Total lipid content and fatty acid profiles were analysed by gas chromatography (GC), while Fourier transform infrared (FTIR) spectroscopy was used to evaluate changes of the total cellular biochemical profile. FTIR spectroscopy was chosen due to its advantages and wide application in microbiology and biotechnology for the overall biochemical characterization of microbial cells and their metabolites (Kohler et al., 2015; Forfang et al., 2017; Kosa et al., 2017b; Shapaval et al., 2017; Carnovale et al., 2021; Olsen et al., 2023; Shapaval et al., 2023). One of the main advantages of FTIR analysis are that it can be performed on non-destructed or little processed microbial biomass and combined with the automated sample preparation to increase throughput (Li et al., 2016; Xiong et al., 2019).

Materials and methods

Bacterial strains

Seventy-four fast-growing Antarctic bacteria from the Belarussian Collection of Non-pathogenic Microorganisms (Institute of Microbiology of the National Academy of Science of Belarus) were used in the study. These are Gram-positive and Gram-negative, psychrotrophic and psychrophilic bacteria belongs to four phyla: Proteobacteria, Actinobacteria, Firmicutes, and Bacteroidetes and represented by eighteen genera: *Arthrobacter, Cryobacterium, Leifsonia, Salinibacterium, Paeniglutamicibacter, Rhodococcus, Polaromonas, Pseudomonas, Psychrobacter, Shewanella, Acinetobacter, Sporosarcina, Facklamia, Carnobacterium, Brachybacterium, Micrococcus, Agrococcus* and *Flavobacterium* (Table 1 and Table S1 in SM). Identification and physiological characterization of these bacteria have been reported previously (Smirnova et al., 2021; Akulava et al., 2022; Smirnova et al., 2022).

Microscopy evaluation of Gram-stained bacteria

For Gram staining and microscopy evaluation, the isolated bacteria were cultivated on BHI-agar at 18 °C for 1 to 4 days, depending on the isolate, until the single colony appeared. Gram staining was done following the protocol of the three-step Gram stain procedure kit (Merck KGaA, Germany). The morphology of Gram-stained cells was studied by the direct examination with the light microscope Leica DM4 B (Leica Microsystems, Germany) under a 100× immersion lens.

Cultivation of Antarctic bacteria

Bacteria were recovered from cryo-preserved cultures by culturing on brain heart infusion (BHI) agar (Sigma Aldrich, USA) plates for 7 days at 18°C. A single colonies of each strain were transferred into 7 mL BHI broth (Sigma-Aldrich, India) in the Duetz microtiter plate system (Duetz-MTPS, Enzyscreen, Netherlands) consisting of 24-square extra high polypropylene deep well microtiter plates (MTPs) with low-evaporation sandwich covers and extra high cover clamps (Duetz et al., 2000; Kosa et al., 2017a; Dzurendova et al., 2020a; Dzurendova et al., 2020b). To obtain enough amount of biomass for analysis, each strain was inoculated into four wells of a microtiter plate. Inoculated MTPs were mounted on the shaking platform of the MAXQ 4000 incubator (Thermo Fisher Scientific, Waltham, MA, USA), incubated at 5°C, 15°C and 25°C, and 400 rpm agitation speed (1.9 cm circular orbit) for 7 days. One well in each plate was filled with sterile medium for cross-contamination control. All cultivations were done in two independently performed biological replicates.

Preparation of bacterial biomass for FTIR measurements

Bacterial biomass was separated from the growth medium by centrifugation (Heraeus Multifuge X1R, Thermo Scientific, Waltham, MA, USA) at 2490 g 4°C for 10 min and washed with distilled water three times. Further, at the last washing step, 100 – 500 µL of distilled water was added to the cell pellet and re-suspended. 10 µL of the homogenized bacterial suspension was pipetted onto the IR-light-transparent silicon 384-well silica microplates (Bruker Optics GmbH, Ettlingen, Germany) in three technical replicates, and dried at room temperature for at least 2 hours before the analysis (Smirnova et al., 2021; Smirnova et al., 2022). The remaining bacterial biomass was freeze-dried (Labconco, USA) for 72 h until constant weight, and stored at -20°C. Freeze dried biomass was used for lipids extraction.

Lipid extraction from bacterial biomass

Lipid extraction was done by using the previously described method (El RazakWard and Glassey, 2014), with some modifications. Briefly, 20 mg of freeze-dried bacterial biomass was mixed with 2 mL of 8% methanolic HCl (Ichihara and Fukubayashi, 2010) in reaction glass tubes. Further, 50 µL of 19:0 1,2-dinonadecanoyl-sn-glycero-3-phosphocholine (PC) internal standard solution in chloroform (10 mg/mL) (Avanti, USA) was added to each sample (Quideau et al., 2016). Samples were heated at 70°C for 2 hours and cooled down at room temperature for 30 min. 1 mL of distilled water was added to the samples and vortexed. Phase separation was performed twice: 2 mL of hexane was added to the samples, vortexed for 1 min and centrifuged at 1968 g for 5 min. The upper hexane phase was transferred into clean glass tubes and evaporated under nitrogen at 30°C (SBH130D/3 N2 evaporator, ColePalmer™ Stuart™). Fatty acid methyl esters (FAMEs) were transferred into GC vial by washing the glass tube with 1500 µL hexane containing 0.01% butylated hydroxytoluene (BHT, Sigma-Aldrich, USA), followed by 5 s vortex mixing at low speed.

Gas chromatography analysis of total lipid content and fatty acid profile

Lipid contents and fatty acid profiles were analyzed using GC 820A System (Agilent Technologies, Santa Clara, CA, USA) equipped with Agilent J&W 121-2323 DB-23 column, 20 m x 180 µm x 0.20 µm and a flame ionization detector (FID). Helium as a carrier gas was used. Setup for sample analysis was used as described previously (Langseter et al., 2021). For the identification and quantification of fatty acids, the C4–C24 FAME mixture (Supelco, St. Louis, MO, USA) and bacterial acid methyl esters CP (BAME) mixture (Matreya LLC, High Tech Road, State College, PA 16803 USA) were used as an external standard, in addition to C19:0 PC internal standard. Gas chromatography mass spectrometry (GC-MS) analysis of the fatty acid profile was used to identify

fatty acids which were not present in the external standards used for GC-FID, and this was done as described previously (Kosa et al., 2018b).

FTIR spectroscopy analysis

FTIR transmittance spectra were measured using a high-throughput screening extension unit (HTS-XT) coupled to the Vertex 70 FTIR spectrometer (both Bruker Optik, Germany). The FTIR system was equipped with a globar mid-IR source and a deuterated L-alanine doped triglycine sulfate (DLaTGS) detector. The HTS-FTIR spectra were recorded with a total of 64 scans, using Blackman-Harris 3-Term apodization, spectral resolution of 6 cm^{-1}, and digital spacing of 1.928 cm^{-1}, over the range of 4000–400 cm^{-1}, and an aperture of 6 mm. The ratio of a sample spectrum to a spectrum of the empty IR transparent microplate was used to calculate a final spectrum. Background spectra of the Si microplate were collected prior to each sample measurement to account for variations in water vapor and CO_2. Generated transmittance spectra were exported for further analysis. Each biomass sample was analysed in three technical replicates. For data acquisition and instrument control, the OPUS software (Bruker Optik GmbH, Germany) was used.

Preprocessing and data analysis

GC data

The weight of individual fatty acids (FAs) was calculated based on peak areas, relative response factors (RRF) and C19:0 internal standard. Total lipid content of bacterial biomass was estimated as a sum of FAMEs (the weight of C19:0 was subtracted) divided by the weight of dry biomass. Total lipid content of the biomass was calculated in a percentage (%) by summing up all detected FAs for the whole set of studied strains individually. Detected FAs were grouped according to their structural characteristics: PUFAs (summed polyunsaturated fatty acids), n-SFAs (summed non-branched saturated fatty acids), br-SFAs (summed branched saturated fatty acids), n-MUFAs (summed non-branched monounsaturated fatty acids), hydroxy-FAs (summed hydroxy fatty acids) , cyclic-FAs (summed cyclic fatty acids), summed cis-FAs/trans-FAs and iso-FAs /anteiso-FAs (Mező et al., 2022). Prior to principal component analysis (PCA), GC fatty acid profile data were normalized by using autoscaling with mean-centering, followed by the division of each column (variable) by the standard deviation. PCA analysis was performed without any prior knowledge about the experimental structure to uncover structural relationships between the variables and identify potential clusters in the data.

FTIR data

For PCA analysis, HTS-FTIR spectra of the bacterial biomass were preprocessed in the following way: (1) applying the Savitzky−Golay algorithm using a polynomial order of degree 2 and window size 11 (Savitzky and Golay, 1964) , (2) cutting uninformative regions (4000 – 3100 cm^{-1}, 2800 – 1800 cm^{-1} and 900 – 400 cm^{-1}), (3) the extended multiplicative signal correction (EMSC) was applied to the second-derivative spectra to separate informative signals from spectral artifacts and minimize variability due to the light scattering or sample thickness (Kohler et al., 2020; Tafintseva et al., 2020). For ratio analysis, FTIR-HTS spectra were preprocessed in the following way: (1) applying the Savitzky−Golay algorithm using a polynomial order of degree 2 and window size 11(Savitzky and Golay, 1964), selecting an informative region (1900 – 900 cm^{-1}). The spectral data analysis involved categorizing the spectra into specific regions: lipids (3050–2800 cm−1), esters (1800–1700 cm−1), proteins (1700–1500 cm−1), and a mixed region (1500–900 cm−1).

After preprocessing, the infrared spectra were subjected to multivariate analysis using PCA. For the PCA, whole spectral region was used. The scatter plot of scores was generated for the entire

FTIR dataset, including biological and technical replicates, which was then projected onto a PCA plot. Univariate analysis of the infrared spectra was used to estimate a relative content of lipids, phosphorus containing compounds (i.e. phospholipids) and changes in protein structure, where the amide I peak at 1656 cm^{-1} related to α-helical structure of proteins was selected as a relatively stable reference band. An ester C=O stretching peak at 1742 cm^{-1} was used for the estimation of the relative lipid content (lipid to protein ratio, L/P, 1742 cm^{-1}/1656 cm^{-1}), while P-O-C symmetric stretching peak at 1083 cm^{-1} was used for the estimation of phosphorus containing compounds (phosphorus to protein ratio, P/P, 1083/1656 cm^{-1}) (Naumann, 2000; Maquelin et al., 2002; GaripGozen and Severcan, 2009). Orange data mining toolbox version 3.31.1 (University of Ljubljana, Ljubljana, Slovenia) was used for the preprocessing and spectral analysis (Demšar et al., 2013; Toplak et al., 2017).

Results

The bacteria isolated from Antarctic meltwater ponds were Gram stained and cell morphologies were studied by microscopy. Gram staining showed that among twenty-nine isolates from meltwater ponds eighteen isolates were Gram-negative, and eleven isolates were Gram-positive. The microscopy images for the twelve isolates representing all genera are shown on Figure S1 in SM. Microscopic examination of the Gram stained bacteria revealed a predominance of the cocci-shaped cells such us for *Acinetobacter lwoffii* BIM B-1558 and *Facklamia tabacinasalis* BIM B-1577 or short bacilli-shaped cells as for *Shewanella baltica* BIM B-1563, *Pseudomonas peli* BIM B-1560, *Sporosarcina* sp. BIM B-1539, *Arthrobacter* sp. BIM B-1549 and *Leifsonia rubra* BIM B -1567, while for *Flavobacterium degerlachei* BIM B-1562 and *Carnobacterium funditum* BIM B -1541 peculiar cell morphology in the form of threads was more characteristic (Figure S1 in SM). The result of Gram staining for the green snow bacteria were previously reported (Smirnova et al., 2021) and indicated that among forty-five isolates, thirty-three isolates were Gram-positive, and twelve isolates were Gram-negative. Thus, in total, in this study forty-four were Gram-positive, and thirty isolates were Gram-negative.

To perform explorative characterization of temperature-triggered alterations of cellular biomolecules, bacteria were grown in BHI nutrient-rich broth medium. Notably, the growth performance of some bacteria under disparate temperature conditions in broth media differed from previous observations made on agar media. Among the studied bacteria, fifty-five showed good growth at all three temperatures used, while eight isolates did not exhibit growth at temperatures 5°C or/and 15°C. Additionally, fifteen isolates were only able to grow at 25°C (Table 1). Proteobacteria demonstrated robust growth across a range of tested temperatures, with the exception of psychrophilic strains from genera *Polaromonas* and *Psychrobacter*, which were unable to grow at 25°C. In contrast some Actinobacteria (*Salinibacterium* and *Paeniglutamicibacter*) and Firmicutes (*Carnobacterium*) exhibited greater temperature sensitivity. Psychrophilic bacteria were defined by their ability to thrive at a maximum growth temperature 18°C and didn't grow at 25°C based on previous definition done by (Morita, 1975).

It can be seen that growth ability at different temperatures was more genera and specie-specific. For example, Actinobacteria from genus *Salinibacterium* were not able to grow in liquid culture at 5 and 25°C but grew well on agar media (Smirnova et al., 2022). Strains from genus *Salinibacterium* and some species such as *Leifsonia rubra* and *Facklamia tabacinasalis* exhibited heightened susceptibility to both high (25°C) and low (5°C) temperatures, with better growth occurring exclusively at 15°C. Strains within genera *Polaromonas, Psychrobacter, Flavobacterium, Carnobacterium, Rhodococcus, Salinibacterium, Paeniglutamicibacter* were identified as psychrophiles (didn't grow at 25°C), according to their growth in broth media. On the other hand, some psychrophilic strains within genera *Psychrobacter*, *Arthrobacter, Cryobacterium*

and *Leifsonia* did not appear to be psychrophilic when grown in broth media and displayed an ability to withstand 25°C (Table 1).

Changes in total lipid content

The BHI broth is rich and complex medium that may contain some lipidic compounds which may affect lipid profile of bacteria. In order to exclude this, we analysed the overall biochemical composition of BHI broth by FTIR spectroscopy and we did not observe any lipid-related peaks on FTIR spectra, especially the peak at 1745 cm^{-1} related to C=O vibrations in lipids and used for estimating relative total lipid content, was not detected (Figure S9 in SM).

Total lipid content for two Gram groups differed, where Gram-negative bacteria exhibited in average a higher total lipid content compared to Gram-positive bacteria (Figure S14 in SM).Further, Proteobacteria displayed the highest total lipid content compared to other phyla. However, main variability in total lipid content was observed among genera within a single phylum and among species within a single genus. (Figure S2 in SM). Bacterial isolates from genera *Pseudomonas, Shewanella*, *Leifsonia* and *Salinibacterium* showed relatively high total lipid content from 10 to 19 $\%_{w/w}$ (% of cell dry weight) (Figure 1 and Figure S2 in SM). The highest total lipid content was recorded for *Pseudomona*s isolates grown at 15°C, where *Pseudomonas peli* strains showed the highest values (Figure 1 and Figure S2 in SM). Bacteria from genera *Polaromonas, Psychrobacter, Acinetobacter, Brachybacterium, Micrococcus, Facklamia* and *Sporosarcina* had relatively low total lipid content, below 6 $\%_{w/w}$, and for all other bacteria it was between 6 and 10 $\%_{w/w}$ (Figure 1). It was observed that total lipid content was more genera-specific with an exception of genus *Pseudomonas*, where it considerably varied from 6 to 19 $\%_{w/w}$ between different species (Figure 1 and Figure S2 in SM).

Average total lipid content was higher at 15°C compared to growth at 5/25°C but big variation between the genera were observed (Figure S14 in SM). The effect of temperature on the total lipid content was found to be genus and species specific, with no common effect observed at phylum or Gram-group level. Additionally, genus- and species-specific changes can be seen, where bacterial strains of the same genus or species showed similar temperature-induced changes. For example, total lipid content increased for all isolates *Shewanella*, *Micrococcus* and *Rhodococcus* when grown at 5°C/15°C, and for *Pseudomonas*, *Arthrobacter, Cryobacterium, Leifsonia, Salinibacteriu* and *Carnobacterium* at 15°C (Figure 1 and Figure S2 in SM). Species-specific temperature-triggered changes were observed for *Shewanella baltica, Pseudomonas lundensis, Leifsonia antarctica, Cryobacterium soli* (Figure S2 in SM).

Psychrophilic Proteobacteria related to *Polaromonas, Psychrobacter* genera exhibited the lowest total lipid content, as depicted on Figure S2 in the supplementary material. Within the phylum Actinobacteria, the majority of psychrophilic strains showed total lipid content similar to psychrotrophic bacteria. In contrast, psychrophilic bacteria from phylum Firmicutes displayed lower total lipid content at 15°C. Our comparative analysis of psychrophiles and psychrotrophs revealed that for most of the tested strains alterations in the total lipid content were similar as for psychrotrophic bacteria. Generally, little effect of temperature on the total lipid content was observed for the studied Antarctic psychrophilic strains, that is an indication of remarkable stability of the total lipid content across the range of temperatures tested for these bacteria.

Interestingly, lipid content of Proteobacteria from genera *Polaromonas, Psychrobacter* and *Acinetobacter* was consistent regardless of cultivation temperature, and only few strains showed a slight increase at 25°C (Figure 1 and Figure S2 in SM). *Pseudomonas* sp. strain BIM B-1635 was unique, with a relatively high increase of total lipid production at high temperatures (16 $\%_{w/w}$ at 25°C, compared to 10 $\%_{w/w}$ at 5°C) (Figure S2 in SM).

Temperature effect on taxonomic diversity of fatty acid profile

PCA of the GC data showed a clear distribution of the samples in the first principal component (PC1) mainly according to Gram groups and it was associated with the content of br-SFAs/n-SFAS/n-MUFAs (Figure 2A). Majority of Gram-positive bacteria clustered together mainly due to the presence of br-SFAs and unknown FAs. Genus *Rhodococcus* from phylum Actinobacteria, and genera *Facklamia* and *Carnobacterium* from phylum Firmicutes were grouped with Gram-negative bacteria since they had n-MUFAs as a major group of FAs (Figure 2A). The loading plot showed that the dissimilarities in the production of cyclic and hydroxy FAs in some *Pseudomonas* strains were responsible for the differences observed along the second principal component (PC2) axis (Figure 2B). Moreover, the PC1 axis shows differences caused by the temperature (Figure 2A), which were more apparent for Actinobacteria than for Firmicutes and Proteobacteria. For example, among Actinobacteria genera, *Cryobacterium* strains grown at different temperatures were clustered separately from each other, and *Arthrobacter* and *Leifsonia* strains cultivated at 5°C clustered separately from overlapping strains grown at 15°C and 25°C (Figure 2A). Temperature-based clustering was also observed for some Proteobacteria genera, for example, *Shewanella* and *Pseudomonas,* but it was more specie-specific, and overlapping between different species can be seen. Also, it could be seen from the loading plot that PUFAs did not play a significant role in the clustering along PC1 (Figure 2B).

In order to deeply assess the main taxonomy-aligned similarities and differences in overall fatty acid profile as well as temperature-induced changes, fatty acid GC data were categorized into several groups according to (1) fatty acid chain length, including short-chain fatty acids (SCFAs) containing less than 6 carbon atoms, medium-chain fatty acids (MCLFAs) containing 7-12 carbon atoms, long-chain fatty acids (LCFAs) containing 13-21 carbon atoms and very long-chain fatty acids (VLCFAs) containing 22-24 carbon atoms, (2) fatty acid structural characteristics, including PUFAs (polyunsaturated fatty acids), n-SFAs (non-branched saturated fatty acids), br-SFAs (branched saturated fatty acids), n-MUFAs (non-branched monounsaturated fatty acids), hydroxy-FAs (hydroxy fatty acids), and cyclic-FAs (cyclic fatty acids), (3) geometric isomerism (cis-/trans-FA) and (4) type of branching (iso-/anteiso- FA). Only FAs with the content higher than 1% we included in the analysis.

The analysis of the fatty acids' chain length profile revealed that LCFAs containing 13-21 carbon atoms are the most common type of FAs (60-98%) present in the studied Antarctic bacteria (Table 2). MCLFAs containing 7-12 carbon atoms were present in a relatively small amount (3-11%) in Proteobacteria from genera *Pseudomonas, Acinetobacter, Shewanella* and in Bacteroidetes from genus *Flavobacterium*, where the highest amount was observed for *Pseudomonas* and *Flavobacterium* strains and it increased with increase of the growth temperature. VLCFAs containing 22-24 carbon atoms were present in a small amount as well (up to 7%) in Actinobacteria from genera *Rhodococcus, Micrococcus, Brachybacterium,* all Firmicutes bacteria and Proteobacteria from genus *Acinetobacter*. The amount of VLCFAs increased at elevated cultivation temperatures (15 or 25°C) for *Rhodococcus* and decreased for other genera (Table 2). SCFAs containing less than 6 carbon atoms were not detected in noteworthy amounts in the studied bacteria.

The analysis of fatty acid profile based on the structural characteristics, showed that all Gram-positive bacteria, except *Rhodococcus* from phylum Actinobacteria as well as *Facklamia* and *Carnobacterium* from phylum Firmicutes had branched fatty acids (br-SFAs) as predominant ones (Figure 3 and 6 and Figure S3 – S5 in SM). Interestingly, all Gram-positive bacteria were grouped into two groups according to their temperature-induced changes of br-SFAs: Actinobacteria from genera *Agrococcus*, *Arthrobacter, Brachybacterium, Cryobacterium, Leifsonia* and

Paeniglutamibacter showed a continuous increase in br-SFAs with elevating growth temperature, while *Salinibacterium* and *Sporosarcina* from phylum Firmicutes exhibited the opposite response (Figure 3 and 6 and Figure S3 – S5 in SM).

All Proteobacteria, except *Shewanella,* had straight-chain monounsaturated fatty acids (n-MUFAs) and non-branched saturated fatty acids (n-SFAs) as a major group of FAs at all studied temperatures (Figure 3 and 6 and Figure S3 – S5 in SM). Bacteria from genera *Shewanella* and *Flavobacterium* from phyla Proteobacteria and Bacteroidetes, respectively, had br-SFAs present in their profile, which were not detected for other Gram-negative bacteria. For all Gram-negative bacteria the quantity of n-MUFAs was increasing with the temperature decrease, and the highest quantity was detected at 5°C. The quantity of n-SFAs in Gram-negative bacteria increased with temperature and reached maxima at 25°C (Figure 3 and 6 and Figure S3 – S5 in SM). *Shewanella* strains had n-MUFAs as major FAs when grown at 5°C, and br-SFAs when grown at 15 and 25°C, respectively. No effect of temperature was detected for *Polaromonas* genus. Interestingly, similar fatty acid profile and temperature responses were observed between Proteobacteria and Actinobacteria from genus *Rhodococcus* and Firmicutes from genera *Facklami*a and *Carnobacterium* (Figure 3 and 6 and Figure S3 – S5 in SM).

Small amount of hydroxy-FA was recorded in Antarctic bacteria and mostly for some Gram-negative bacteria from Proteobacteria and Bacteroidetes phyla. For example, Proteobacteria from genus *Pseudomonas* and Bacteroidetes from genus *Flavobacterium* were characterized by higher OH-FA production at higher growth temperatures (15 and 25°C), up to 17% and 19 %, respectively (Figure 3 and 6 and Figure S3 – S5 in SM). Some Proteobacteria strains produced PUFAs, for example *Pseudomonas* sp. BIM B-1674 produced up to 18 % of PUFAs of the total fatty acid content, and *Pseudomonas lundensis* BIM B-1554 produced up to 10 % of PUFAs when grown at 15 and 25°C, respectively (Figure 3 and 6 and Figure S3 – S5 in SM). Interestingly, for genus *Cryobacterium* it was detected an increase in the amount of PUFAs with the increase of growth temperature (Figure 3 and 6, and Figure S3 – S5 in SM). Small amounts of cyclic-FAs produced by Proteobacteria from the genus *Pseudomonas* increased with the increase of temperature. For example, *Pseudomonas* sp. BIM B-1674 produced up to 8 % of cyclic-FAs (Figure 3 and 6, and Figure S3 – S5 in SM).

Distinct patterns in fatty acid profiles and temperature impact were observed for psychrophiles and psychrotrophs. Thus, fatty acid profiles of *Polaromonas*, *Carnobacterium*, and *Rhodococcus* psychrophilic strains remained unchanged at 5 and 15°C of cultivation. In contrast, fatty acid profile of the psychrophilic *Flavobacterium* and *Psychrobacter* strains was influenced by temperature, leading to an increase in n-SFAs and a decrease in n-MUFAs at 15°C compared to 5°C. For psychrotrophic strains from *Paeniglutamibacter* genera the proportion between br-SFAs and unknown FAs decreased at 5°C compare to 15°C (Figure S3 – S4 in SM).

All Gram-negative bacteria were characterized by the production of cis-fatty acids (cis-FAs). *Shewanella* and *Flavobacterium* characterized by the lowest amount of cis-FAs among all studied bacteria. Among Gram-positive bacteria the production of cis-FAs was detected in both phyla, in phyla Actinobacteria for genus *Rhodococcus* and in phyla Firmicutes for *Carnobacterium* and *Facklamia* (Figure 5 and Figure S6-S8 in SM). The presence of trans- fatty acids (trans-FAs) was detected in small quantities (data not shown). A noticeable increase in the synthesis of cis-FAs along with the growth temperature decrease was noted for some Proteobacteria, especially for species of *Pseudomonas, Shewanella, Acinetobacter*, as well as for *Flavobacterium* from phylum Bacteroidetes (Figure 5 and Figure S6-S8 in SM). In contrast, the profile of *Polaromonas* remained unchanged regarding cis-isomerization (Figure 5 and Figure S6-S8 in SM). Among Gram-positive

bacteria, an increase in the production of cis-FAs was detected in *Rhodococcus* and *Carnobacterium* from phyla Actinobacteria and Firmicutes, respectively.

Anteiso-FAs were more characteristic for Actinobacteria and for *Sporosarcina* from phylum Firmicutes. Iso-FAs were detected in small amount in all Actinobacteria, Firmicutes, and Bacteroidetes phyla and in Proteobacteria only genus *Shewanell*a was characterized by the production of this type of FA. Mainly genus-specific temperature induced changes were observed, for example, for the genera *Sporosarcina, Micrococcus*, *Arthrobacter* it decreased with the temperature decrease. For the genera *Paeniglutamicibacter, Leifsonia, Cryobacterium*, and *Agrococcus* the opposite effect was observed. A clear increase in amount of iso-FAs was detected for the genera *Shewanella*, *Agrococcus, Arthrobacter, Brachybacterium, Micrococcus, Paeniglutamicibacter* with an increase in growth temperature, while *Salinibacterium* showed an opposite response (Figure 5 and Figure S6-S8 in SM).

When comparing the ratios of cis-/trans- and iso-/anteiso- FAs in psychrophilic and psychrotrophic bacteria, it can be seen that psychrophilic Gram-negative Proteobacteria genus *Polaromonas* possess little change in the cis-/trans- FAs ratio, with cis-FAs being the predominant type. However, for bacteria from genus *Psychrobacter* the production of trans-FAs was detected at 15°C and not at 5°C (Figure S6 and S7 in SM). Gram-positive Actinobacteria showed genus-specific changes similar to psychrotrophic bacteria. Thus *Leifsonia* strains had an increase in iso-FAs and a decrease in anteiso-FAs with temperature downshift. Interestingly, trans-FAs were not detected at 15°C in psychrophilic *Rhodococcus erythropolis* BIM B -1661 similarly as for psychrotrophic *Rhodoccocus* strains (Figure S6-S7 in SM).

Using GC fatty acid profile, we tried to identify the most predominant fatty acids for different taxonomic groups, and we observed genera-specific differences. Thus, for Proteobacteria from genera *Polaromonas* and *Pseudomonas* a similar fatty acid profile with C16:1, C18:1n7c, and C16:0 as predominant FAs was observed. Other genera from this phylum, such as *Psychrobacter* and *Acinetobacter* share similar profiles, with C16:1 and C18:1n9c as predominant fatty acids, and *Psychrobacter* also having C17:0 as a third dominant fatty acid, while *Acinetobacter* has C16:0 as a third dominant fatty acid. *Shewanella* stands out with the most distinct profile compared to other genera from phylum Proteobacteria and it was characterized by i-C15:0, C16:1, and i-C13:0 as predominant fatty acids. Bacteroidetes phylum was represented by one genus *Flavobacterium* which showed a distinct fatty acid profile sharing some similarities with Gram-positive and Gram-negative, and additionally, we observed other FAs in significant amounts, such as C15:0 and 2OH-C14:0 (Figure 4). Among Gram-positive bacteria the majority of Actinobacteria, except for *Rhodococcus*, *Paeniglutamicibacter*, and *Micrococcus*, exhibit similar fatty acid profile with predominant FAs a-C15:0 and a-C17:0 (Figure 4). However, *Paeniglutamicibacter* and *Micrococcus* have a lower quantity of a-C17:0. On the other hand, *Rhodococcus* displays a completely different profile, resembling profile of Proteobacteria from genera *Pseudomonas*, *Polaromonas*, and *Acinetobacter*. Among Firmicutes, *Carnobacterium* and *Facklamia* have similar profile, with C16:1cis7 and C18:1n9c being as predominant FAs that also differs from *Sporosarcina*, which has predominant FAs a-C15:0 and C17:1 (Figure 4).

For Gram-positive bacteria, some FAs were not identified with the use of external standards and the GC-MS library. The amount of these FAs was increasing with the decrease of growth temperature, so it can be assumed that these unknown FAs belong to a group of unsaturated unbranched FAs or unsaturated branched FAs (Figure 3 and 6 and Figure S3 – S5 in SM).

Strain *Leifsonia antarctica* BIM B-1671 showed a fatty acid profile distinctly different from all other *Leifsonia* strains (Figure S3 – S5 in SM). This and other previously reported considerable similarities of the total cellular biochemical profile of this strain with *Pseudomonas* (Smirnova et

al., 2021; Smirnova et al., 2022) can be an indication of misidentification by 16S rRNA gene sequencing.

Impact of temperature on the total cell chemistry

Intact bacterial biomass obtained from the cultivation at different temperatures was analysed by the HTS-FTIR spectroscopy for evaluating changes in main cellular biomolecules, such as lipids, proteins and polysaccharides. Figure 7 shows the representative FTIR spectra of two Antarctic bacteria with low and high lipid content. On Figure 7, the primary spectral regions associated with lipids are 3100 – 2800 cm^{-1} (C-H), which indicates the presence of fatty acid chains in lipids, and 1800 – 1700 cm^{-1} (C=O), which indicates the presence of triacyl glycerides, free fatty acids, or polyesters. The observed changes in these peaks exhibit a strong correlation with the changes in the total lipid content that was measured using GC-FID.

Preprocessed FTIR spectra were analysed by PCA, and score and loading plots are displayed in the Figure 8. Along the PC1 axis, a clear separation resembling Gram-groups and less clear for phylum- and genera-based classification, and temperature effect could be seen (Figure 8A). Specifically, Gram-negative Proteobacteria predominantly had positive PC1 scores, while Gram-positive Actinobacteria predominantly had negative PC1 scores, bacteria from phyla Bacteroidetes and Firmicutes overlap with each other and other phyla (Figure S10 in SM). Furthermore, a clear separation along the PC1 axis was observed between *Shewanella, Pseudomonas* and *Acinetobacter* cultivated at different temperatures (Figure 8A). Both PC1 and PC2 appeared to be responsible for the dissimilarities between Gram-positive bacteria cultivated at different temperatures. Thus, a clear separation between bacteria grown at 5 and 25°C was observed for *Arthrobacter, Psychrobacter, Carnobacterium, Cryobacterium* and *Leifsonia* genera. The scores for bacteria cultivated at 15°C usually overlapped with scores for those cultivated at 5 or 25°C (Figure 8A). The loading plots on Figure 8B illustrate the weight of each original variable (wavenumbers) on the PCs and the contribution of each spectral feature. The separation along the PC1 axis was due to changes in the C=O stretching peak (amide I) in proteins at 1627 cm^{-1}, P-O-C symmetric stretching peak probably related to phospholipids at 1083 cm^{-1}, and C=O stretching in esters and aldehydes at 1709 cm^{-1} and 1725 cm^{-1}. The separation along the PC2 axis can be explained by the changes in the C-H (CH_2) stretching in saturated lipids at 2924 and 2853 cm^{-1}, C=O stretching of esters and aldehydes at 1742 cm^{-1}, CH_2 bending in lipids with little contributions from protein (membrane lipids) at 1400 cm^{-1}, and P-O-C symmetric stretching peak probably related to phospholipids at 1083 cm^{-1} (Figure 8B).

The effect of temperature on C=O stretching region (1800-1700 cm^{-1}) was evaluated and the increase in absorbance for the ester peak at 1743 cm^{-1} along with the temperature decrease was observed for Gram-positive Actinobacteria from genera *Micrococcus* and *Rhodococcus* (Figure 9). There was no temperature effect on ester peak detected for Firmicutes and all Gram-negative bacteria. An increase in the peak at 1712 cm^{-1} associated with C=O stretching in free FAs along with the decrease of cultivation temperature was detected for all studied bacteria except bacteria Firmicutes (Figure 9, S12 in SM). Some genus-specific changes were observed for Gram-negative bacteria, where *Shewanella* showed significant changes associated with the absorbance decrease for the ester peak at 1745 cm^{-1} and appearance of an additional peak at 1728 cm^{-1} was at 15°C (Figure 9).

In the protein region (1700-1500 cm^{-1}) the biggest effect of temperature was detected for amide I peak at 1640 cm^{-1} related to β-sheet structures of proteins, where an increase in absorbance was observed for majority of the studied Antarctic bacteria grown at higher temperatures. Further, genus-specific effect in the form of a shift to lower wavenumbers was recorded for Proteobacteria genera *Shewanella* and *Pseudomonas* and Firmicutes genus *Carnobacterium* at higher growth temperature (Figure 9). Bacteria from genus *Rhodococcus* showed equal amount of α-helical (peak

at 1656 cm^{-1}) and β-pleated sheet (peak at 1640 cm^{-1}) structures, whereas α-helical structures seem to dominate in all other bacteria (Figure 9). There was no effect of temperature detected for amide II peak associated with the vibrations of N-H plane amide groups at 1548 cm^{-1}.

The most significant temperature-triggered alterations were recorded in the mixed spectral region 1500-900 cm^{-1}, where signals related to carbohydrates, nucleic acids and phosphates are present. Effect of temperature on this region was considerable for all taxonomic levels (Figure 9 and Figure S11, Figure S12 in SM). Thus, an increase in intensity for several peaks in the mixed region (1400 cm^{-1}, 1240 cm^{-1} and 1083 cm^{-1}) along with temperature decrease was recorded for majority of Proteobacteria, Bacteroidetes and Actinobacteria, while changes for Firmicutes were less intense. The most significant changes were detected for genera *Pseudomonas, Psychrobacter, Shewanella, Acinetobacter, Leifsonia, Rhodococcus* and *Salinibacterium.* Nearly all bacteria had changes in symmetric stretching peak at 1083 cm^{-1} which was significantly higher with temperature decrease (Figure 9).

An increase in absorbance for the peak at 1400 cm^{-1}, related to -CH_2 bending vibrations in lipids at lower cultivation temperatures was observed for Bacteroidetes and several genera of Actinobacteria such us *Arthrobacter, Leifsonia Micrococcus* and *Carnobacterium* (Figure 9).

Compositional analysis based on the estimation of ratios using FTIR spectra

To evaluate the effect of growth temperature and estimate the relative content of the main cellular components in bacterial biomass, several ratio-based parameters were effectively estimated. Protein peak at 1654 cm^{-1} (amide I) could be considered as a relatively stable component as it can be seen on Figure 9 and it was used to estimate the relative content of lipids and phosphorus containing components in the same way as it was previously done for microalgae (Dean et al., 2010) and fungi (Dzurendova et al., 2021). The following ratio parameters were calculated: (1) lipid to protein ratio (L/P), allowing to estimate relative total lipid content, was estimated by using ester bond C=O stretching peak at 1743 cm^{-1} and protein amide I peak at 1654 cm^{-1}; (2) ratio of phosphorus containing components over proteins (P/P), determining the total content of phospholipids and to less extent nucleotides, was estimated using P-O-C symmetric stretching peak at 1083 cm^{-1}, probably related to phospholipids and amid I peak at 1654 cm^{-1}.

Overall, the highest L/P ratio was observed for Gram-positive bacteria from Actinobacteria from genera *Rhodococcus* and *Paeniglutamicibacter*, and among Gram-negative Proteobacteria from genera *Polaromonas* and *Pseudomonas*, while the lowest L/P ratio was detected for *Acinetobacter, Flavobacterium* and *Brachybacterium* from phyla Proteobacteria, Bacteroidetes and Actinobacteria, respectively (Figure 10). The L/P ratio for Actinobacteria genera *Rhodococcus, Paeniglutamicibacter, Micrococcus* and *Arthrobacter* and Bacteroidetes genus *Flavobacterium* was significantly increasing along with temperature decrease. An opposite effect was observed for all Proteobacteria except genus *Shewanella,* Firmicutes genera *Sporosarcina* and *Carnobacterium* and Actinobacteria genera *Agrococcus* and *Salinibacterium,* where L/P ratio was rising with temperature increase (Figure 10). Interestingly, L/P ratio for *Shewanella* was lower at 15°C than at 5°C and 25°C (Figure 10). A significant effect of temperature on phospholipids and other phosphorus containing compounds was detected. Thus, for all Gram-negative bacteria and majority of Gram-positive bacteria except *Agrococcus* and *Carnobacterium* a significant increase in P/P ratio with temperature downshift was observed.

Pearson correlation coefficient (r) was calculated to examine the relationship between the L/P ratio and total lipid content (Figure S13 in SM). The correlation coefficient for the entire dataset was found to be 0.36. When comparing Gram-negative and Gram-positive bacteria, a higher correlation coefficient was observed for Gram-negative bacteria (r = 0.63) compared to Gram-positive bacteria

(r = 0.26) (Figure S13A in SM). When comparing correlation for different phyla, Bacteroidetes had the highest correlation (1), then Proteobacteria (0.59) and then Firmicutes (0.56) and the lowest was for Actinobacteria (0.15). When comparing different genera within the Gram-negative group, the highest correlation coefficients were found for *Psychrobacter* (0.59) and *Pseudomonas* (0.57). Among the Gram-positive, the highest correlation coefficients were found for *Rhodococcus* (0.89), *Carnobacterium* (0.88), *Salinibacterium* (0.80), and *Leifsonia* (0.65), whereas the lowest coefficient was observed for *Cryobacterium* (0.13) (Figure S13C in SM). Some genera showed weak positive or negative linear relationships: *Arthrobacter* (-0.05), *Cryobacterium* (0.13), *Shewanella* (0.10). Further analysis revealed that the correlation coefficient decreased along with temperature decrease, where at 25°C, the coefficient was 0.71, at 15°C it was 0.44, and at 5°C it dropped to 0.09 (Figure S13B in SM). The correlation within each genus varies for cultivation at different temperatures. However, for the majority of genera, there is an increase in correlation at higher temperatures (Figure S13D-G in SM).

Discussion

Microorganisms respond to changing environmental conditions by activating their adaptation mechanisms. Polar regions are extreme environments and characterized by the presence of several stress factors, such as nutrient limitation, salinity, water availability, fluctuations in temperature and UV radiation (Rothschild and Mancinelli, 2001; Thomas and Dieckmann, 2002). Due to that, bacteria inhabiting polar regions may have unique adaptation mechanisms allowing them to survive and develop in these conditions (BarriaMalecki and Arraiano, 2013; De Maayer et al., 2014; Mocali et al., 2017; Tribelli and López, 2018; Singh, 2022). Cold-adapted bacteria has been extensively studied for decades, while most of the reported studies focus on very targeted biomolecules. The explorative characterization covering several biomolecules allowing to obtain more comprehensive knowledge have not been previously performed for cold-adapted bacteria. This study reports, for the first time, comprehensive taxonomy-aligned characterization of the total cellular biomolecules profile (lipids, proteins, and polysaccharides) for seventy-four Antarctic bacteria isolated from green snow and meltwater ponds. In addition, we show what changes occur for different cellular biomolecules when these bacteria grow at different temperatures and how these alterations vary for different taxonomic groups. Important to highlight that set of bacteria used in the study is not balanced according to different taxonomic units. For example, nine genera were represented by only one specie, phylum Bacteroidetes was represented by one and Firmicutes by five species. Therefore, comparison of the achieved results on phylum and genus level is limited by this set of bacteria and could not be used to draw any general conclusions. While in the case of Gram-groups we had quite balanced distribution where forty-four strains were Gram-positive, and thirty strains were Gram-negative, therefore, comparison according to Gram can be used to draw general hypothesis.

Research on bacteria from the Antarctic snow and meltwater pounds is important for the prediction of future climate-associated changes in this region. Extensive formation of meltwater pounds in Antarctica results in a higher absorption of solar energy due to the dark color of the meltwater ponds that may lead to a quicker heat transfer to soil (PerovichTucker III and Ligett, 2002; Stokes et al., 2019). Soil in Antarctica and other polar and alpine regions exhibit notable heterogeneity of bacterial communities which play a significant role in these environments (WiebeSheldon Jr and Pomeroy, 1992). Increase in appearance of the meltwater ponds and their long-term existence due to the climate change and longer summers may lead to a change in soil microbiota.

Previously it has been shown that majority of Antarctic bacteria are psychrotrophic (Ray et al., 1998) that was also observed in this study. Psychrotrophic bacteria are well adapted to cold environments but can also survive and function at moderate temperatures (Ilicic et al., 2023). A

previous study proposed that key factors influencing microbial distribution in Antarctic ecosystems are temperature and nutrient availability where increasing temperature potentially stimulating bacterial growth (WiebeSheldon Jr and Pomeroy, 1992). However, opposite results have also been reported (Hodson et al., 1981). In our study, we demonstrate that majority of isolated Antarctic bacteria can thrive across a wide range of temperatures, from 4°C to 30°C and even 37°C, showing their extraordinary high metabolic plasticity.

To perform biomolecular characterization of the studied Antarctic bacteria grown at different temperatures we have selected BHI broth medium. Despite the differences in growth characteristics between BHI agar and BHI broth, BHI broth nutrient-rich medium was selected due to its ability to provide a well-mixed and uniform environment for bacterial growth and to mitigate the impact of nutrient limitations (Bonnet et al., 2020). This medium was effective in supporting growth of all studied bacteria as well as evaluating the overall temperature's effect on total lipid content, fatty acid profile and total cellular biochemical profile as it was previously reported (Smirnova et al., 2021; Smirnova et al., 2022), while to identify potentially oleaginous bacteria, high C/N media are necessary to use. This medium was also chosen due to the lack of lipids since they could potentially affect the fatty acid profile of bacteria, as many bacteria have an ability to incorporate lipids into their cell membranes (Yao and Rock, 2017). Studied Antarctic bacteria are fast-growing as it was previously reported (Smirnova et al., 2021; Akulava et al., 2022), therefore we cultivated them for 7 days until they reach stationary phase. According to the literature the biggest differences in cell chemistry is happening between lag, log and stationary phases and stationary phase considered as the most chemically stable (Kochan et al., 2020). It was also shown in previous works on filamentous fungi that after 3 days of fermentation the fatty acid composition stabilizes (Kosa et al., 2017a).

It has been previously reported that alterations in total lipid content of bacterial cells, as well as their fatty acid composition, are one of the main adaptation mechanisms to continuously changing temperature conditions. Due to the fact that fatty acid composition is used as an important biomarker for identifying, classifying and differentiating closely related bacterial species (Sasser, 1990), the alterations in lipids are often taxonomy-specific, and differ from genus to genus and specie to specie. Determining temperature-associated changes of lipids in bacteria is particularly important for gaining insights into their physiology, diversity (De Carvalho and Caramujo, 2014), resistance mechanisms (Dunnick and O'Leary, 1970) and taxonomic relationships.

In this study we observed that total lipid content and its alterations triggered by temperature changes are mainly species-specific, and it can vary considerably. For example, total lipid content in *Pseudomonas* species varied from 6 to 19 $\%_{w/w}$. Further, a clear difference in the total lipid content between genera of the same phylum was recorded, where genera *Pseudomonas* and *Shewanella* from phylum Proteobacteria were characterized by the highest lipid production. For example *Pseudomonas peli* strains had lipids from 12 to 19 $\%_{w/w}$, depending on the strain and growth temperature. Such a high lipid content in *Pseudomonas peli* was not reported previously, according to the authors' knowledge, and it can be also explained by the possible production of polyesters (Röttig and Steinbüchel, 2016). For *Pseudomonas leptonychotis*, total lipid content ranged from 12 to 14 $\%_{w/w}$, and for *Shewanella baltica* from 10 to 12 $\%_{w/w}$, that was consistent with other *Shewanella* strains described in the literature (Zhang and Burgess, 2017). In overall, the obtained results are in accordance with the previously reported, and can be explained by the fact that Gram-positive bacteria have naturally higher peptidoglycan content, whereas Gram-negative bacteria have higher lipid content (Feijó Delgado et al., 2013; Tripathi and Sapra, 2020). Gram-negative bacteria have an outer membrane, in addition to their inner membrane, which composed of lipopolysaccharides (LPS) and phospholipids that can contribute to the higher lipid content. Interestingly, in our study we observed that certain Gram-negative bacteria possess low lipid

amounts comparable or even lower to those found in Gram-positive bacteria, as for example it was for *Polaromonas, Psychrobacter* and *Acinetobacter.* An increase in total lipid content with temperature decrease was detected for the majority off bacteria tested except for some *Arthrobacter* and *Pseudomonas* species. This adaptation mechanism was previously shown by other researchers (HunterOlawoye and Saynor, 1981).

Fatty acid profiling by GC-FID and GC-MS indicated Gram- and taxon-related differences in the fatty acid composition for the studied Antarctic bacteria. Overall, the obtained results correlated well with the previously reported (Zhang and Rock, 2008; BajerskiWagner and Mangelsdorf, 2017; Hassan et al., 2020; Mező et al., 2022). Thus, most of the Gram-positive bacteria were characterized by the high content of br-SFAs, with exception of *Rhodococcus, Facklamia* and *Carnobacterium*, while Gram-negative bacteria were characterized by the high content of n-MUFAs, with exception of *Shewanella*, these observations are in accordance with previously reported results (Garba et al., 2016).

Chain length in phospholipid tails impacts membrane fluidity. Shortening the average acyl chain length lowers the temperature limit at which the transition from a liquid-crystalline to a gel phase occurs. This adaptation helps to maintain membrane fluidity, which is essential for the survival and growth of bacteria (Russell, 2002). In this study, we observed that long-chain fatty acids (LCFAs) are the predominant type of FAs for all the studied bacteria as it was previously shown (Řezanka and Sigler, 2009; Mező et al., 2022). Earlier it was reported that the production of MCFAs can naturally occur in both Gram-negative and Gram-positive bacteria (Ahn et al., 2023) and we detected production of medium-chain fatty acids (MCFAs) in trace amounts in mainly Gram-negative bacteria from genera *Pseudomonas, Shewanella, Acinetobacter*, and *Flavobacterium*. Furthermore, we found that the production of MCFAs increased along with temperature increase for genera *Pseudomonas, Acinetobacter*, and *Flavobacterium*. It is known that both saturated and monounsaturated VLCFAs are present in almost all organisms but predominantly found in very small quantities (KyselováVítová and Řezanka, 2022). We detected presence of VLFAs in all bacteria and few Gram-positive bacteria, specifically those from the genera *Micrococcus* and all Firmicutes exhibited relatively high production of very long-chain fatty acids (VLCFAs). In the case of *Rhodococcus* it could originate from the mycolic acids layer present in the cell wall and similar results were previously reported for this genus (NishiuchiBaba and Yano, 2000). Overall, increase in the production of VLCFAs with temperature decrease was observed for majority of the studied bacteria. For some bacteria the amount of VLCFAs increased from 5°C to 15°C and decreased from 15°C to 25°C.

Further, higher cultivation temperatures led to an increase in the amount of br-SFAs in Gram-positive bacteria and n-SFAs in Gram-negative bacteria, while lower temperatures led to an increase in the amount of n-MUFAs in all Gram-negative bacteria, and Gram-positive *Rhodococcus* and *Carnobacterium*. In some cases, different genera from the same phylum showed distinct fatty acid profiles varying from the common Gram-specific pattern. Thus, *Shewanella* strains contained br-SFAs that were not detected for bacteria from other Proteobacteria genera but was previously shown in the literature (SkerrattBowman and Nichols, 2002). Furthermore, a significant effect of temperature on the fatty acid (FA) profile of *Shewanella* was detected, indicating a high adaptability of this bacteria to environmental changes what was also pointed out by other researchers (SkerrattBowman and Nichols, 2002; Wang et al., 2009; Kloska et al., 2020). While n-MUFAs were major FAs when *Shewanella* strains were grown at 5°C, br-SFAs where predominant when the strains were grown at 15 and 25°C. The presence of br-SFAs was also detected in *Flavobacterium* from Bacteroidetes phylum. We also observed that Gram-positive Actinobacteria from genus *Rhodococcus* and Firmicutes from genera *Facklamia* and *Carnobacterium* had fatty

acid profile similar to Proteobacteria and were characterized by the predominance of n-MUFA and n-SFAs.

Besides the temperature-triggered changes in the main fatty acids, we also observed temperature-dependent production of some minor fatty acids. For example, hydroxy fatty acids (OH-FA) detected in *Pseudomonas* and *Flavobacterium* and previously reported for these genera (Yano et al., 1976; Mező et al., 2022) showed an increase with the temperature decrease, which was in agreements with the previously reported results (LaliLingfa et al.; KumarJagannadham and Ray, 2002; Mező et al., 2022). The hydroxyl groups of these FAs are likely to serve a similar function as the branched fatty acids in phospholipid membranes, helping to maintain the membrane's viscous state at lower temperatures (LaliLingfa et al.; KumarJagannadham and Ray, 2002; Mező et al., 2022). Small amount of cyclic fatty acids (cyclic-FA) produced in *Pseudomonas* increased with the increase of cultivation temperature that could be due to that cyclic fatty acids stabilize the membranes of bacteria by reducing the fluidity improving its resistance to environmental stress. Production of cyclic fatty acids in small amounts has been found previously in Gram-negative bacteria (Caligiani and Lolli, 2018). Some strains produced PUFAs, for example *Pseudomonas* sp. BIM B-1674 produced up to 18 % of PUFAs of the total fatty acid content, *Pseudomonas lundensis* BIM B-1554 produced up to 10 % of PUFAs when grown at 15 and 25°C. Production of PUFA by Antarctic bacteria was previously reported (NicholsNichols and McMeekin, 1993; Jadhav et al., 2010). Interestingly, we did not observe increase in PUFA production at low temperature as its often reported. And even for some Gram-positive bacteria we observed an opposite pattern of PUFA increase along with temperature increase. In this study, the production of PUFAs in *Shewanella baltica,* a specie previously positioned for PUFA production (Gentile et al., 2003) was not observed, that could be attributed to the preference of alternative mechanisms for maintaining membrane fluidity. The ratio between branched saturated fatty acids (br-SFAs) and non-methylene interrupted n-MUFAs significantly decreased with decreasing temperature, indicating a different adaptation strategy for membrane stability as it was mentioned above.

In addition to traditional GC techniques, we utilized FTIR spectroscopy for expanding knowledge on changes in lipids and other cellular components triggered by temperature. FTIR can provide information on the relative total lipid content, chain length and unsaturation of lipids, presence of different lipid classes, such as acyl glycerides, free fatty acids, polyesters, and it has been widely used for lipid analysis (Dean et al., 2010; Derenne et al., 2013; Shapaval et al., 2014; Forfang et al., 2017; Kosa et al., 2017a; Kosa et al., 2017b; Kosa et al., 2018a; Kosa et al., 2018b; Shapaval et al., 2019). In addition, FTIR spectroscopy is an ideal tool for mapping the total cellular biochemical profile as it provides information on all main biomolecules: lipids, proteins, polyester, polysaccharides, phosphorus-based compounds such as phospholipids, polyphosphates etc. (Kamnev, 2008; Alvarez-Ordóñez et al., 2011).

FTIR analysis of the bacterial biomass obtained after cultivation at different temperatures showed some genera-specific differences. For example, *Rhodococcus* bacteria had the highest intensity of peaks related to -C-H (CH_2) stretching and presence of peak =C-H stretching of cis-alkene HC=CH group found in polyunsaturated lipids that could be connected to the possible production of mycolic acids (Liu et al., 1996) or triacylglycerols (TAGs) (Alvarez et al., 2021) what was also detected by gas chromatography. Spectra of *Flavobacteria, Shewanella* and *Acinetobacter* showed an additional peak at 1728 cm^{-1} often associated with the presence of polyesters (Kamnev et al., 2021) and could indicate about production of PHAs (Christensen et al., 2023), and exploring these bacteria further would be important as bacterial polyesters are important source of bioplastic.

FTIR analysis has shown that temperature fluctuations may induce considerable genera-specific changes in protein structure for some bacteria, as for example, *Shewanella, Pseudomonas* and

Carnobacterium, where a shift to lower wavenumbers was detected for amide I peak at 1640 cm^{-1} related to β-sheet structures of proteins. This might be associated with the decrease in the strength of the hydrogen bond of proteins due to the changes in protein conformation under temperature stress. For example, a decrease in hydrogen bond strength can be observed for the amide I band when proteins are denatured. However, it is important to note that shifts in the protein region can also be influenced by other factors, such as changes in protein-protein or protein-ligand interactions (Barth and Zscherp, 2002).

The most significant temperature related alterations were recorded for the mixed region 1200-900 cm^{-1}, where signals related to carbohydrates, nucleic acids and phosphates are expected. Changes in this region were detected for all bacteria. The spectral region between 1200 and 900 cm^{-1} is rich in signals originating from various components, such as DNA, phospholipids, and complex sugar modes. Within this range, there are distinct and strong absorbance bands that have been observed in different bacteria and attributed to specific components of the cell wall (Kochan et al., 2018). As it was previously shown by (Kochan et al., 2018) phosphodiester groups (found in DNA, phospholipids, and teichoic acids/ lipoteichoic acid) create bands at around 1080 cm^{-1} and 1220 cm^{-1} for symmetric and asymmetric $PO2^{-}$ stretching vibrations. Cell wall in Gram-positive bacteria contain teichoic acids/ lipoteichoic acid as an additional phosphate compound compared to Gram-negative cell walls. Phospholipids in the inner membrane of Gram-positive bacteria may also contribute, but to a lesser extent. Gram-negative bacteria have more phospholipids in their additional outer membrane. Overall, Gram-positive bacteria have higher phosphodiester content, while Gram-negative bacteria have more phospholipids.

Estimation of various ratio parameters using FTIR spectra showed that alterations in the L/P ratio were strictly genus-specific and correlated well with the GC-FID results of the total lipid content that is an additional proof of high sensitivity of FTIR spectroscopy for lipid analysis. These results indicate that temperature adaptation involves not only alterations in lipids but also modifications in proteins structure, with minimal impact on protein concentration in cells. A significant effect of temperature on phospholipids and other phosphorus containing compounds was detected by calculating the 1083/1654 ratio. For all studied bacteria except *Salinibacterium* and *Carnobacterium* a significant increase in the ratio between phosphorus-based compounds and proteins with temperature downshift was observed. The increased production of phosphorus containing compounds at low temperatures may have connection to the increased synthesis of phospholipids, as it was shown by Gao et al. (Gao et al., 2019). In that study, they observed an increase of total lipids and phospholipids in *Shewanella putrefaciens* along with temperature decrease. On the other hand, they noticed a decrease of glycerolipids, sphingolipids, and saccharolipids at lower temperatures. This suggests a possible shift in lipid composition towards an increased proportion of phospholipids in response to lower temperatures. Also, an increase in absorbance for the peak responsible for phosphorus containing compounds at 1083 cm^{-1} for some bacteria at lower temperature could have a connection to an increase in total content of nucleic acids in bacterial cells that could be related to fluctuations in growth rate (Bates et al., 1985; Kochan et al., 2020).

A dataset obtained from measurements using a single technique can only provide insights from a single perspective. In this study, we employed a combination of analytical techniques – HTS-FTIR, a rapid non-destructive technique, and GC, a traditional analytical technique, to examine alterations in lipids and other biomolecules of Antarctic bacteria grown at different temperatures. The results from the correlation analysis show that for majority of the studied bacteria, correlation between the L/P ratio measured by FTIR spectroscopy and total lipid content measured by GC had moderate (r around 0.6) or strong (r around 0.8) linear relationships. The correlation within each genus varied

after cultivation at different temperatures. However, for majority of the genera, there is a higher correlation at moderate temperature (25°C) compared to 5 and 15°C.

This study shows both environmental and biotechnological importance of Antarctic bacteria. It has been observed that some Antarctic bacteria can accumulate lipids up to 20% at low temperatures that might interesting to explore further and investigate whether it is possible to establish lipid production by these bacteria. In addition, some bacteria were able to produce fatty acids of special industrial interest such as mycolic acid and branched unsaturated fatty acids.

Conclusion

This study is one of the few previously published reporting comprehensive data on lipid and overall cellular biochemical profile and its temperature-triggered changes for cold-adapted bacteria. We showed that bacteria isolated from cold environment possess taxonomy-aligned fatty acid profile as it was earlier reported for bacteria from other environments. Our findings indicate that variations in temperature may induce some modifications in cellular lipids. These alterations encompass changes in the total lipid content, fatty acid composition, and lipid classes. Additionally, we observed notable transformations in other cellular components such as proteins and phosphorus containing compounds. These changes are taxonomy specific, meaning that despite of principle similarity in cell structure bacteria do not have a single common adaptation mechanism to temperature fluctuations and often show different chemical responses.

Data Availability Statement

All datasets generated for this study available in Zenodo repository (10.5281/zenodo.10051608).

Author Contributions

VA, MS, VS, UM, LV designed the research work. UM collected the samples from green snow and temporary meltwater pounds and isolated bacteria. VA and MS characterized bacterial isolates and performed cultivations at different temperatures. VA, MS and DB performed extractions and GC measurements. DE performed GC/MS measurements. VA and BZ performed data analysis and revised the manuscript. UB performed optimization of computational processes. AK contributed to data analysis and revised the manuscript. VA, MS and VS wrote and revised the manuscript, UM and LV revised the manuscript. All authors read and approved the final manuscript.

Funding

This research was supported by the project “Belanoda—Multidisciplinary graduate and post-graduate education in big data analysis for life sciences” (CPEA-LT-2016/10126), funded by the Eurasia program, Norwegian Agency for International Cooperation and Quality Enhancement in Higher Education (Diku), and the Belanoda Digital learning platform for boosting multidisciplinary education in data analysis for life sciences in the Eurasia region (CPEA-STA-2019/10025).

Conflict of Interest

The authors declare that the research was conducted in the absence of any commercial or financial relationships that could be construed as a potential conflict of interest.

References

Ahn, J.H., Jung, K.H., Lim, E.S., Kim, S.M., Han, S.O., and Um, Y. (2023). Recent advances in microbial production of medium chain fatty acid from renewable carbon resources: a comprehensive review. *Bioresource Technology*, 129147.

Akulava, V., Miamin, U., Akhremchuk, K., Valentovich, L., Dolgikh, A., and Shapaval, V. (2022). Isolation, Physiological Characterization, and Antibiotic Susceptibility Testing of Fast-Growing Bacteria from the Sea-Affected Temporary Meltwater Ponds in the Thala Hills Oasis (Enderby Land, East Antarctica). *Biology* 11(8), 1143. doi: 10.3390/biology11081143.

Alvarez-Ordóñez, A., Mouwen, D., López, M., and Prieto, M. (2011). Fourier transform infrared spectroscopy as a tool to characterize molecular composition and stress response in foodborne pathogenic bacteria. *Journal of microbiological methods* 84(3), 369-378.

Alvarez, H.M., Hernández, M.A., Lanfranconi, M.P., Silva, R.A., and Villalba, M.S. (2021). *Rhodococcus* as biofactories for microbial oil production. *Molecules* 26(16), 4871.

Bajerski, F., Wagner, D., and Mangelsdorf, K. (2017). Cell membrane fatty acid composition of *Chryseobacterium frigidisoli* PB4T, isolated from Antarctic glacier forefield soils, in response to changing temperature and pH conditions. *Frontiers in Microbiology* 8, 677.

Barria, C., Malecki, M., and Arraiano, C.M. (2013). Bacterial adaptation to cold. *Microbiology* 159(Pt_12), 2437-2443. doi: 10.1099/mic.0.052209-0.

Barth, A., and Zscherp, C. (2002). What vibrations tell about proteins. *Quarterly reviews of biophysics* 35(4), 369-430.

Bates, D.B., Gillett, J.A., Barao, S.A., and Bergen, W.G. (1985). The effect of specific growth rate and stage of growth on nucleic acid-protein values of pure cultures and mixed ruminal bacteria. *Journal of Animal Science* 61(3), 713-724.

Bonnet, M., Lagier, J.C., Raoult, D., and Khelaifia, S. (2020). Bacterial culture through selective and non-selective conditions: the evolution of culture media in clinical microbiology. *New microbes and new infections* 34, 100622.

Caligiani, A., and Lolli, V. (2018). Cyclic fatty acids in food: An under investigated class of fatty acids. *Biochemistry and Health Benefits of Fatty Acids* 2018.

Chattopadhyay, M., and Jagannadham, M. (2001). Maintenance of membrane fluidity in Antarctic bacteria. *Polar Biology* 24(5), 386-388. doi: 10.1007/s003000100232.

Christensen, M., Chiciudean, I., Jablonski, P., Tanase, A.-M., Shapaval, V., and Hansen, H. (2023). Towards high-throughput screening (HTS) of polyhydroxyalkanoate (PHA) production via Fourier transform infrared (FTIR) spectroscopy of *Halomonas* sp. R5-57 and *Pseudomonas* sp. MR4-99. *Plos one* 18(3), e0282623.

Collins, T., and Margesin, R. (2019). Psychrophilic lifestyles: mechanisms of adaptation and biotechnological tools. *Applied microbiology and biotechnology* 103, 2857-2871.

De Carvalho, C., and Caramujo, M.-J. (2014). Fatty Acids as a Tool to Understand Microbial Diversity and Their Role in Food Webs of Mediterranean Temporary Ponds. *Molecules* 19(5), 5570-5598. doi: 10.3390/molecules19055570.

De Maayer, P., Anderson, D., Cary, C., and Cowan, D.A. (2014). Some like it cold: understanding the survival strategies of psychrophiles. *EMBO reports* 15(5), 508-517. doi: 10.1002/embr.201338170.

838 Dean, A.P., Sigee, D.C., Estrada, B., and Pittman, J.K. (2010). Using FTIR spectroscopy for rapid
839 determination of lipid accumulation in response to nitrogen limitation in freshwater
840 microalgae. *Bioresource technology* 101(12)**,** 4499-4507.

841 Demšar, J., Curk, T., Erjavec, A., Gorup, Č., Hočevar, T., Milutinovič, M., et al. (2013). Orange:
842 data mining toolbox in Python. *the Journal of machine Learning research* 14(1)**,** 2349-
843 2353.

844 Derenne, A., Claessens, T., Conus, C., and Goormaghtigh, E. (2013). "Infrared Spectroscopy of
845 Membrane Lipids." Springer Berlin Heidelberg), 1074-1081.

846 Desbois, A.P., and Smith, V.J. (2010). Antibacterial free fatty acids: activities, mechanisms of
847 action and biotechnological potential. *Applied microbiology and biotechnology* 85**,** 1629-
848 1642.

849 Duetz, W.A., RüEdi, L., Hermann, R., O'Connor, K., BüChs, J., and Witholt, B. (2000). Methods
850 for Intense Aeration, Growth, Storage, and Replication of Bacterial Strains in Microtiter
851 Plates. *Applied and Environmental Microbiology* 66(6)**,** 2641-2646. doi:
852 10.1128/aem.66.6.2641-2646.2000.

853 Dunnick, J.K., and O'Leary, W.M. (1970). Correlation of bacterial lipid composition with
854 antibiotic resistance. *Journal of Bacteriology* 101(3)**,** 892-900.

855 Dzurendova, S., Zimmermann, B., Kohler, A., Reitzel, K., Nielsen, U.G., Dupuy--Galet, B.X., et
856 al. (2021). Calcium affects polyphosphate and lipid accumulation in mucoromycota fungi.
857 *Journal of Fungi* 7(4)**,** 300.

858 Dzurendova, S., Zimmermann, B., Kohler, A., Tafintseva, V., Slany, O., Certik, M., and
859 Shapaval, V. (2020a). Microcultivation and FTIR spectroscopy-based screening revealed a
860 nutrient-induced co-production of high-value metabolites in oleaginous *Mucoromycota*
861 fungi. *PLOS ONE* 15(6)**,** e0234870. doi: 10.1371/journal.pone.0234870.

862 Dzurendova, S., Zimmermann, B., Tafintseva, V., Kohler, A., Ekeberg, D., and Shapaval, V.
863 (2020b). The influence of phosphorus source and the nature of nitrogen substrate on the
864 biomass production and lipid accumulation in oleaginous *Mucoromycota* fungi. *Applied*
865 *Microbiology and Biotechnology* 104(18)**,** 8065-8076. doi: 10.1007/s00253-020-10821-7.

866 El Razak, A.A., Ward, A.C., and Glassey, J. (2014). Screening of Marine Bacterial Producers of
867 Polyunsaturated Fatty Acids and Optimisation of Production. *Microbial Ecology* 67(2)**,**
868 454-464. doi: 10.1007/s00248-013-0332-y.

869 Feijó Delgado, F., Cermak, N., Hecht, V.C., Son, S., Li, Y., Knudsen, S.M., et al. (2013).
870 Intracellular water exchange for measuring the dry mass, water mass and changes in
871 chemical composition of living cells. *PloS one* 8(7)**,** e67590.

872 Forfang, K., Zimmermann, B., Kosa, G., Kohler, A., and Shapaval, V. (2017). FTIR Spectroscopy
873 for Evaluation and Monitoring of Lipid Extraction Efficiency for Oleaginous Fungi. *PLOS*
874 *ONE* 12(1)**,** e0170611. doi: 10.1371/journal.pone.0170611.

875 Gao, X., Liu, W., Mei, J., and Xie, J. (2019). Quantitative analysis of cold stress inducing
876 lipidomic changes in *Shewanella putrefaciens* using UHPLC-ESI-MS/MS. *Molecules*
877 24(24)**,** 4609.

878 Garba, L., Latip, W., Mohamad Ali, M., Oslan, S., and Zaliha, R. (2016). Unsaturated fatty acids
879 in Antarctic Bacteria. *Research Journal of Microbiology* 11(146152.18).

880 Garip, S., Gozen, A.C., and Severcan, F. (2009). Use of Fourier transform infrared spectroscopy
881 for rapid comparative analysis of *Bacillus* and *Micrococcus* isolates. *Food Chemistry*
882 113(4)**,** 1301-1307.

Gentile, G., Bonasera, V., Amico, C., Giuliano, L., and Yakimov, M. (2003). *Shewanella* sp. GA-22, a psychrophilic hydrocarbonoclastic antarctic bacterium producing polyunsaturated fatty acids. *Journal of applied microbiology* 95(5)**,** 1124-1133.

Goh, Y.S., and Tan, I.K.P. (2012). Polyhydroxyalkanoate production by antarctic soil bacteria isolated from Casey Station and Signy Island. *Microbiological research* 167(4)**,** 211-219.

Hassan, N., Anesio, A.M., Rafiq, M., Holtvoeth, J., Bull, I., Haleem, A., et al. (2020). Temperature driven membrane lipid adaptation in glacial psychrophilic bacteria. *Frontiers in Microbiology* 11**,** 824.

Hodson, R., Azam, F., Carlucci, A., Fuhrman, J., Karl, D., and Holm-Hansen, O. (1981). Microbial uptake of dissolved organic matter in McMurdo Sound, Antarctica. *Marine Biology* 61**,** 89-94.

Hunter, M., Olawoye, T., and Saynor, D. (1981). The effect of temperature on the growth and lipid composition of the extremely halophilic coccus, *Sarcina marina*. *Antonie van Leeuwenhoek* 47**,** 25-40.

Ichihara, K.I., and Fukubayashi, Y. (2010). Preparation of fatty acid methyl esters for gas-liquid chromatography. *Journal of Lipid Research* 51(3)**,** 635-640. doi: 10.1194/jlr.d001065.

Ilicic, D., Ionescu, D., Woodhouse, J., and Grossart, H.-P. (2023). Temperature-Related Short-Term Succession Events of Bacterial Phylotypes in Potter Cove, Antarctica. *Genes* 14(5)**,** 1051.

Jadhav, V.V., Jamle, M.M., Pawar, P.D., Devare, M.N., and Bhadekar, R.K. (2010). Fatty acid profiles of PUFA producing Antarctic bacteria: correlation with RAPD analysis. *Annals of Microbiology* 60(4)**,** 693-699. doi: 10.1007/s13213-010-0114-4.

Kamnev, A.A. (2008). FTIR spectroscopic studies of bacterial cellular responses to environmental factors, plant-bacterial interactions and signalling. *Spectroscopy* 22(2-3)**,** 83-95.

Kamnev, A.A., Dyatlova, Y.A., Kenzhegulov, O.A., Vladimirova, A.A., Mamchenkova, P.V., and Tugarova, A.V. (2021). Fourier Transform Infrared (FTIR) Spectroscopic Analyses of Microbiological Samples and Biogenic Selenium Nanoparticles of Microbial Origin: Sample Preparation Effects. *Molecules* 26(4)**,** 1146. doi: 10.3390/molecules26041146.

Kloska, A., Cech, G.M., Sadowska, M., Krause, K., Szalewska-Pałasz, A., and Olszewski, P. (2020). Adaptation of the marine bacterium *Shewanella baltica* to low temperature stress. *International Journal of Molecular Sciences* 21(12)**,** 4338.

Kochan, K., Lai, E., Richardson, Z., Nethercott, C., Peleg, A.Y., Heraud, P., and Wood, B.R. (2020). Vibrational spectroscopy as a sensitive probe for the chemistry of intra-phase bacterial growth. *Sensors* 20(12)**,** 3452.

Kochan, K., Perez-Guaita, D., Pissang, J., Jiang, J.-H., Peleg, A.Y., McNaughton, D., et al. (2018). In vivo atomic force microscopy–infrared spectroscopy of bacteria. *Journal of The Royal Society Interface* 15(140)**,** 20180115.

Kohler, A., Solheim, J.H., Tafintseva, V., Zimmermann, B., and Shapaval, V. (2020). Model-based pre-processing in vibrational spectroscopy.

Kosa, G., Kohler, A., Tafintseva, V., Zimmermann, B., Forfang, K., Afseth, N.K., et al. (2017a). Microtiter plate cultivation of oleaginous fungi and monitoring of lipogenesis by high-throughput FTIR spectroscopy. *Microbial Cell Factories* 16(1). doi: 10.1186/s12934-017-0716-7.

Kosa, G., Shapaval, V., Kohler, A., and Zimmermann, B. (2017b). FTIR spectroscopy as a unified method for simultaneous analysis of intra-and extracellular metabolites in high-throughput screening of microbial bioprocesses. *Microbial cell factories* 16**,** 1-11.

Kosa, G., Vuoristo, K.S., Horn, S.J., Zimmermann, B., Afseth, N.K., Kohler, A., and Shapaval, V. (2018a). Assessment of the scalability of a microtiter plate system for screening of oleaginous microorganisms. *Applied Microbiology and Biotechnology* 102(11)**,** 4915-4925. doi: 10.1007/s00253-018-8920-x.

Kosa, G., Zimmermann, B., Kohler, A., Ekeberg, D., Afseth, N.K., Mounier, J., and Shapaval, V. (2018b). High-throughput screening of Mucoromycota fungi for production of low- and high-value lipids. *Biotechnology for Biofuels* 11(1). doi: 10.1186/s13068-018-1070-7.

Kumar, G.S., Jagannadham, M., and Ray, M. (2002). Low-temperature-induced changes in composition and fluidity of lipopolysaccharides in the Antarctic psychrotrophic bacterium *Pseudomonas syringae*. *Journal of bacteriology* 184(23)**,** 6746-6749.

Kyselová, L., Vítová, M., and Řezanka, T. (2022). Very long chain fatty acids. *Progress in Lipid Research***,** 101180.

LaliLingfa, N.T., Prudhvi, C., Sharmila, R., Deepa, R., and Rajan, A.P. Study of membrane fatty acids of Gram-negative bacteria and its influence towards the terrestrial ecosystem

Langseter, A.M., Dzurendova, S., Shapaval, V., Kohler, A., Ekeberg, D., and Zimmermann, B. (2021). Evaluation and optimisation of direct transesterification methods for the assessment of lipid accumulation in oleaginous filamentous fungi. *Microbial Cell Factories* 20(1). doi: 10.1186/s12934-021-01542-1.

Liu, J., Barry, C.E., Besra, G.S., and Nikaido, H. (1996). Mycolic acid structure determines the fluidity of the mycobacterial cell wall. *Journal of Biological Chemistry* 271(47)**,** 29545-29551.

Maquelin, K., Kirschner, C., Choo-Smith, L.-P., van den Braak, N., Endtz, H.P., Naumann, D., and Puppels, G. (2002). Identification of medically relevant microorganisms by vibrational spectroscopy. *Journal of microbiological methods* 51(3)**,** 255-271.

Mező, E., Hartmann-Balogh, F., Madarászné Horváth, I., Bufa, A., Marosvölgyi, T., Kocsis, B., and Makszin, L. (2022). Effect of Culture Conditions on Fatty Acid Profiles of Bacteria and Lipopolysaccharides of the Genus *Pseudomonas*—GC-MS Analysis on Ionic Liquid-Based Column. *Molecules* 27(20)**,** 6930. doi: 10.3390/molecules27206930.

Mocali, S., Chiellini, C., Fabiani, A., Decuzzi, S., de Pascale, D., Parrilli, E., et al. (2017). Ecology of cold environments: new insights of bacterial metabolic adaptation through an integrated genomic-phenomic approach. *Scientific Reports* 7(1)**,** 1-13.

Morita, R.Y. (1975). Psychrophilic bacteria. *Bacteriological reviews* 39(2)**,** 144-167.

Naumann, D. (2000). Infrared spectroscopy in microbiology. *Encyclopedia of analytical chemistry* 102**,** 131.

Nichols, D.S., Nichols, P.D., and McMeekin, T.A. (1993). Polyunsaturated fatty acids in Antarctic bacteria. *Antarctic Science* 5(2)**,** 149-160.

Nishiuchi, Y., Baba, T., and Yano, I. (2000). Mycolic acids from *Rhodococcus*, *Gordonia*, and *Dietzia*. *Journal of microbiological methods* 40(1)**,** 1-9.

Perovich, D., Tucker III, W., and Ligett, K. (2002). Aerial observations of the evolution of ice surface conditions during summer. *Journal of Geophysical Research: Oceans* 107(C10)**,** SHE 24-21-SHE 24-14.

970 Quideau, S.A., McIntosh, A.C.S., Norris, C.E., Lloret, E., Swallow, M.J.B., and Hannam, K.
971 (2016). Extraction and Analysis of Microbial Phospholipid Fatty Acids in Soils. *Journal*
972 *of Visualized Experiments* (114). doi: 10.3791/54360.

973 Ray, M.K., Kumar, G.S., Janiyani, K., Kannan, K., Jagtap, P., Basu, M.K., and Shivaji, S. (1998).
974 Adaptation to low temperature and regulation of gene expression in Antarctic
975 psychrotrophic bacteria. *Journal of biosciences* 23**,** 423-435.

976 Řezanka, T., and Sigler, K. (2009). Odd-numbered very-long-chain fatty acids from the microbial,
977 animal and plant kingdoms. *Progress in lipid research* 48(3-4)**,** 206-238.

978 Rothschild, L.J., and Mancinelli, R.L. (2001). Life in extreme environments. *Nature* 409(6823)**,**
979 1092-1101.

980 Röttig, A., and Steinbüchel, A. (2016). "Bacteria as sources of (commercial) lipids".).

981 Sajjad, W., Din, G., Rafiq, M., Iqbal, A., Khan, S., Zada, S., et al. (2020). Pigment production by
982 cold-adapted bacteria and fungi: colorful tale of cryosphere with wide range applications.
983 *Extremophiles* 24(4)**,** 447-473. doi: 10.1007/s00792-020-01180-2.

984 Sasser, M. (1990). "Identification of bacteria by gas chromatography of cellular fatty acids".
985 MIDI technical note 101. Newark, DE: MIDI inc).

986 Savitzky, A., and Golay, M.J. (1964). Smoothing and differentiation of data by simplified least
987 squares procedures. *Analytical chemistry* 36(8)**,** 1627-1639.

988 Shapaval, V., Afseth, N., Vogt, G., and Kohler, A. (2014). Fourier transform infrared
989 spectroscopy for the prediction of fatty acid profiles in *Mucor* fungi grown in media with
990 different carbon sources. *Microbial Cell Factories* 13(1)**,** 86. doi: 10.1186/1475-2859-13-
991 86.

992 Shapaval, V., Brandenburg, J., Blomqvist, J., Tafintseva, V., Passoth, V., Sandgren, M., and
993 Kohler, A. (2019). Biochemical profiling, prediction of total lipid content and fatty acid
994 profile in oleaginous yeasts by FTIR spectroscopy. *Biotechnology for Biofuels* 12(1). doi:
995 10.1186/s13068-019-1481-0.

996 Singh, V. (2022). "Microbial Genes Responsible for Cold Adaptation." Springer Singapore), 153-
997 171.

998 Skerratt, J.H., Bowman, J.P., and Nichols, P.D. (2002). *Shewanella olleyana* sp. nov., a marine
999 species isolated from a temperate estuary which produces high levels of polyunsaturated
1000 fatty acids. *International journal of systematic and evolutionary microbiology* 52(6)**,**
1001 2101-2106.

1002 Smirnova, M., Miamin, U., Kohler, A., Valentovich, L., Akhremchuk, A., Sidarenka, A., et al.
1003 (2021). Isolation and characterization of fast-growing green snow bacteria from coastal
1004 East Antarctica. *MicrobiologyOpen* 10(1). doi: 10.1002/mbo3.1152.

1005 Smirnova, M., Tafintseva, V., Kohler, A., Miamin, U., and Shapaval, V. (2022). Temperature-
1006 and Nutrients-Induced Phenotypic Changes of Antarctic Green Snow Bacteria Probed by
1007 High-Throughput FTIR Spectroscopy. *Biology* 11(6)**,** 890. doi: 10.3390/biology11060890.

1008 Stokes, C.R., Sanderson, J.E., Miles, B.W., Jamieson, S.S., and Leeson, A.A. (2019). Widespread
1009 distribution of supraglacial lakes around the margin of the East Antarctic Ice Sheet.
1010 *Scientific reports* 9(1)**,** 13823.

1011 Tafintseva, V., Shapaval, V., Smirnova, M., and Kohler, A. (2020). Extended multiplicative
1012 signal correction for FTIR spectral quality test and pre-processing of infrared imaging
1013 data. *Journal of Biophotonics* 13(3). doi: 10.1002/jbio.201960112.

Thomas, D., and Dieckmann, G. (2002). Antarctic sea ice--a habitat for extremophiles. *Science* 295(5555)**,** 641-644.

Toplak, M., Birarda, G., Read, S., Sandt, C., Rosendahl, S., Vaccari, L., et al. (2017). Infrared orange: connecting hyperspectral data with machine learning. *Synchrotron Radiation News* 30(4)**,** 40-45.

Tribelli, P., and López, N. (2018). Reporting Key Features in Cold-Adapted Bacteria. *Life* 8(1)**,** 8. doi: 10.3390/life8010008.

Tripathi, N., and Sapra, A. (2020). Gram staining.

Wang, F., Xiao, X., Ou, H.-Y., Gai, Y., and Wang, F. (2009). Role and regulation of fatty acid biosynthesis in the response of *Shewanella piezotolerans* WP3 to different temperatures and pressures. *Journal of bacteriology* 191(8)**,** 2574-2584.

Wiebe, W., Sheldon Jr, W., and Pomeroy, L. (1992). Bacterial growth in the cold: evidence for an enhanced substrate requirement. *Applied and Environmental Microbiology* 58(1)**,** 359-364.

Yano, I., Ohno, Y., Masui, M., Kato, K., Yabuuchi, E., and Ohyama, A. (1976). Occurrence of 2- and 3-hydroxy fatty acids in high concentrations in the extractable and bound lipids of *Flavobacterium meningosepticum* and *Flavobacterium* IIb. *Lipids* 11**,** 685-688.

Yao, J., and Rock, C.O. (2017). Exogenous fatty acid metabolism in bacteria. *Biochimie* 141**,** 30-39.

Yoon, B., Jackman, J., Valle-González, E., and Cho, N.-J. (2018). Antibacterial Free Fatty Acids and Monoglycerides: Biological Activities, Experimental Testing, and Therapeutic Applications. *International Journal of Molecular Sciences* 19(4)**,** 1114. doi: 10.3390/ijms19041114.

Zhang, J., and Burgess, J.G. (2017). Enhanced eicosapentaenoic acid production by a new deep-sea marine bacterium *Shewanella electrodiphila* MAR441T. *PLOS ONE* 12(11)**,** e0188081. doi: 10.1371/journal.pone.0188081.

Zhang, Y.-M., and Rock, C.O. (2008). Membrane lipid homeostasis in bacteria. *Nature Reviews Microbiology* 6(3)**,** 222-233.

Tables

Table 1. List of bacterial strains used in the study. X – no growth, /-not enough biomass for analysis, ** – psychrophilic bacteria based on growth on agar media, [GS]– green snow bacteria, [MP]– temporary meltwater ponds bacteria.

Genus	Strain name and collection №	T°C		
		5	15	25
Gram-negative				
Proteobacteria				
Pol	*Polaromonas* sp. BIM B–1676 GS**			⊠
Pse	*Pseudomonas extremaustralis* BIM B–1672 GS			
	Pseudomonas fluorescens BIM B–1668 GS			
	Pseudomonas leptonychotis BIM B–1559 MP			
	Pseudomonas leptonychotis BIM B–1568 MP			
	Pseudomonas leptonychotis BIM B–1566 MP			
	Pseudomonas lundensis BIM B–1554 MP			
	Pseudomonas lundensis BIM B–1555 MP			
	Pseudomonas lundensis BIM B–1556 MP			
	Pseudomonas peli BIM B–1560 MP			
	Pseudomonas peli BIM B–1569 MP			
	Pseudomonas peli BIM B–1546 MP			
	Pseudomonas peli BIM B–1552 MP			
	Pseudomonas peli BIM B–1542 MP			
	Pseudomonas peli BIM B–1548 MP			
	Pseudomonas sp. BIM B–1635 GS			
	Pseudomonas sp. BIM B–1667 GS			
	Pseudomonas sp. BIM B–1673 GS			
	Pseudomonas sp. BIM B–1674 GS			
Psy	*Psychrobacter glacinicola* BIM B–1629 GS**			⊠
	Psychrobacter urativorans BIM B–1655 GS**			⊠
	Psychrobacter urativorans BIM B–1662 GS			
She	*Shewanella baltica* BIM B–1565 MP			
	Shewanella baltica BIM B–1557 MP			
	Shewanella baltica BIM B–1561 MP			
	Shewanella baltica BIM B–1563 MP			
Aci	*Acinetobacter lwoffii* BIM B–1558 MP			
Bacteroidetes				
Fla	*Flavobacterium degerlachei* BIM B–1562 MP**			⊠
Gram-positive				
Actinobacteria				
Agr	*Agrococcus citreus* BIM B–1547 MP		/	
Art	*Arthrobacter agilis* BIM B–1543 MP			
	Arthrobacter cryoconiti BIM B–1627 GS			
	Arthrobacter oryzae BIM B–1663 GS			
	Arthrobacter sp. BIM B–1624 GS			
	Arthrobacter sp. BIM B–1625 GS			

Genus	Strain name and collection №	T°C		
		5	15	25
Gram-positive				
	Arthrobacter sp. BIM B–1626 GS			
	Arthrobacter sp. BIM B–1628 GS			
	Arthrobacter sp. BIM B–1664 GS			
	Arthrobacter sp. BIM B–1666 GS**			⊠
	Arthrobacter sp. BIM B–1656 GS			
	Arthrobacter sp. BIM B–1549 MP			
Bra	*Brachybacterium paraconglomeratum* BIM B–1571 MP	⊠		
Cry	*Cryobacterium arcticum* BIM B–1619 GS			
	Cryobacterium soli BIM B–1620 GS			
	Cryobacterium soli BIM B–1658 GS			
	Cryobacterium soli BIM B–1659 GS			
	Cryobacterium soli BIM B–1677 GS			
	Cryobacterium soli BIM B–1675 GS			
Lei	*Leifsonia antarctica* BIM B–1631 GS	⊠		
	Leifsonia antarctica BIM B–1632 GS			
	Leifsonia antarctica BIM B–1637 GS			
	Leifsonia antarctica BIM B–1638 GS			
	Leifsonia antarctica BIM B–1639 GS			
	Leifsonia antarctica BIM B–1669 GS			
	Leifsonia antarctica. BIM B–1671 GS			
	Leifsonia kafniensis BIM B–1633 GS		/	
	Leifsonia rubra BIM B–1622 GS			
	Leifsonia rubra BIM B–1623 GS**	⊠		⊠
	Leifsonia rubra BIM B–1634 GS	⊠		/
	Leifsonia rubra BIM B–1567 MP			
Mic	*Micrococcus luteus* BIM B–1545 MP			
Pae	*Paeniglutamicibacter antarcticus* BIM B–1657 GS**			⊠
Rho	*Rhodococcus erythropolis* BIM B–1660 GS			
	Rhodococcus erythropolis BIM B–1661 GS			
	Rhodococcus yunnanensis BIM B–1621 GS**			⊠
	Rhodococcus yunnanensis BIM B–1670 GS			
Sal	*Salinibacterium* sp. BIM B–1630 GS**	⊠		⊠
	Salinibacterium sp. BIM B–1636 GS	⊠	⊠	/
	Salinibacterium sp. BIM B–1654 GS**	⊠		⊠
	Salinibacterium sp. BIM B–1665 GS**			⊠
Firmicutes				
Fac	*Facklamia tabacinasalis* BIM B–1577 MP	⊠		⊠
Spo	*Sporosarcina* sp. BIM B–1539 MP			
Car	*Carnobacterium funditum* BIM B–1541 MP**			⊠
	Carnobacterium iners BIM B–1544 MP**			⊠
	Carnobacterium inhibens BIM B–1540 MP			

Table 2. The profile of different groups of FAs with varying chain lengths in Antarctic bacteria grown at different temperatures. The standard deviation was calculated for genera that were represented by two or more strains. '-' – no growth, /not enough biomass for analysis

Gram	Genus	SCFAs			MCFAs			LCFAs			VLCFAs		
		5°C	15°C	25°C	5°C	15°C	25°C	5°C	15°C	25°C	5°C	15°C	25°C
Gram-negative	**Proteobacteria**												
	Pol	0	0.03	-	0.39	0.4	-	**98.93**	**96.2**	-	0.43	0.58	-
	Pse	0.02 ±0.01	0.02±0.02	0.06±0.08	8.87±1.02	10.10±1.44	11.31±2.79	**86.83±2.14**	**85.79±2.14**	**85.27±3.77**	1.82±1.34	1.58±1.23	0.92±0.49
	Psy	0.03±0.02	0.03±0.02	0.07	0.40±0.07	0.48±0.19	0.39	**97.87±0.25**	**97.80±0.73**	**97.59**	0.72±0.29	1.10±0.97	1.14
	She	0.01±0.01	0.01±0.00	0.21±0.09	3.28±0.12	3.32±0.09	2.85±0.10	**62.18±0.95**	**54.72±1.34**	**43.34±1.34**	1.69±1.22	1.17±0.82	0.76±0.07
	Aci	0.05	0.11	0.44	5.76	5.28	7.9	**89.31**	**89.52**	**88.29**	4.29	3.35	1.25
	Bacteroidetes												
	Fla	0.02	0	-	3.26	10.56	-	**73.62**	**72.22**	-	0.92	1.63	-
Gram-positive	**Actinobacteria**												
	Agr	0.08	-	0.02	0.27	-	0.29	**63.19**	-	**88.41**	1.93	-	1.29
	Art	0.03±0.02	0.02±0.01	0.02±0.02	0.36±0.07	0.34±0.13	0.35±0.11	**86.89±4.02**	**90.97±3.56**	**90.12±3.01**	0.80±0.36	0.73±0.48	0.76±0.41
	Bra	-	0.32	0.02	-	0.64	2.45	-	**78.25**	**76.26**	-	7.93	1.33
	Cry	0.05±0.02	0.02±0.02	0.04±0.02	0.46±0.12	0.43±0.23	0.33±0.07	**78.63±1.56**	**90.32±2.58**	**96.35±0.61**	0.56±0.15	0.51±0.30	0.97±0.35
	Lei	0.05±0.02	0.04±0.02	0.03±0.02	1.35±0.12	2.05±0.23	0.88±1.78	**77.60±1.56**	**84.65±2.58**	**94.65±2.86**	1.17±0.15	0.73±0.30	0.77±0.33
	Mic	0.04	0.05	0.03	0.71	0.56	0.52	**84.98**	**80.47**	**69.78**	4.84	1.63	3.08
	Pae	0.01	0.03	-	0.26	0.43	-	**77.77**	**86.76**	-	0.36	0.35	-
	Rho	0.03±0.04	0.03±0.02	0.03±0.00	1.44±0.41	1.17±0.18	0.89±0.14	**94.20±2.65**	**92.30±5.11**	**90.86±3.86**	3.38±2.70	5.08±4.93	7.51±3.56
	Sal	0.05	0.02±0.02	0.08	3.13	3.15±2.52	0.63	**63.66**	**83.35±6.04**	**85.39**	0.44	0.93±0.92	2.22
	Firmicutes												
	Fac	-	0.08	-	-	0.72	-	-	**87.89**	-	-	7.16	-
	Spo	0.12	0.03	0.05	0.69	0.48	0.39	**89.42**	**88.37**	**64.61**	5.31	3.02	2.77
	Car	0.03±0.00	0.13±0.17	0.38	0.62±0.04	1.10±0.76	0.5	**92.13±1.76**	**87.69±11.21**	**97.12**	3.07±1.31	1.54±0.56	0.84

Figures

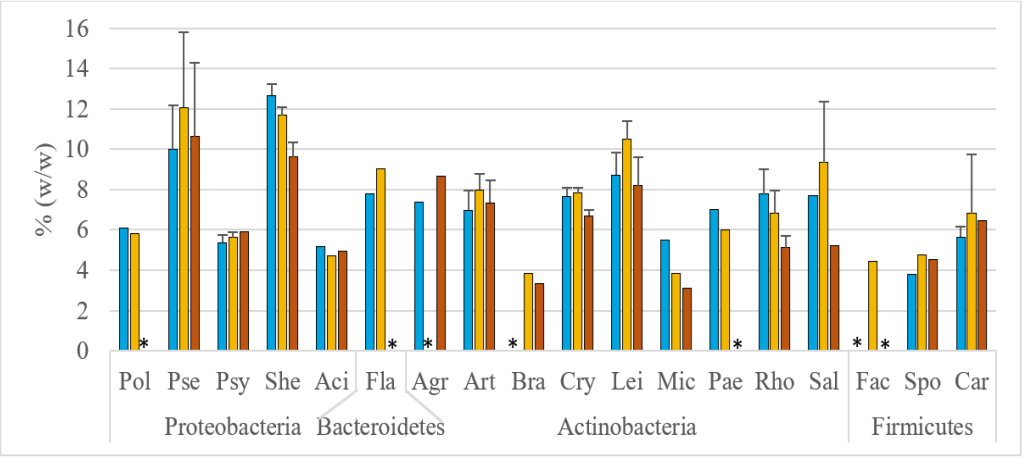

Figure 1. Total lipid content (%, w/w) of bacterial biomass of different genera grown at different temperatures (blue – 5°C, yellow – 15°C and orange – 25°C), * – no growth or not enough biomass to perform the analysis. The standard deviation was calculated for genera that were represented by two or more strains; Genera: Pse-*Pseudomonas*, Psy-*Psychrobacter*, She-*Shewanella*, Aci-*Acinetobacter*, Art-*Arthrobacter*, Cry-*Cryobacterium*, Lei-*Leifsonia*, Mic-*Micrococcus*, Rho-*Rhodococcus*, Sal-*Salinibacterium*, Spo-*Sporosarcina*, Car-*Carnobacterium*

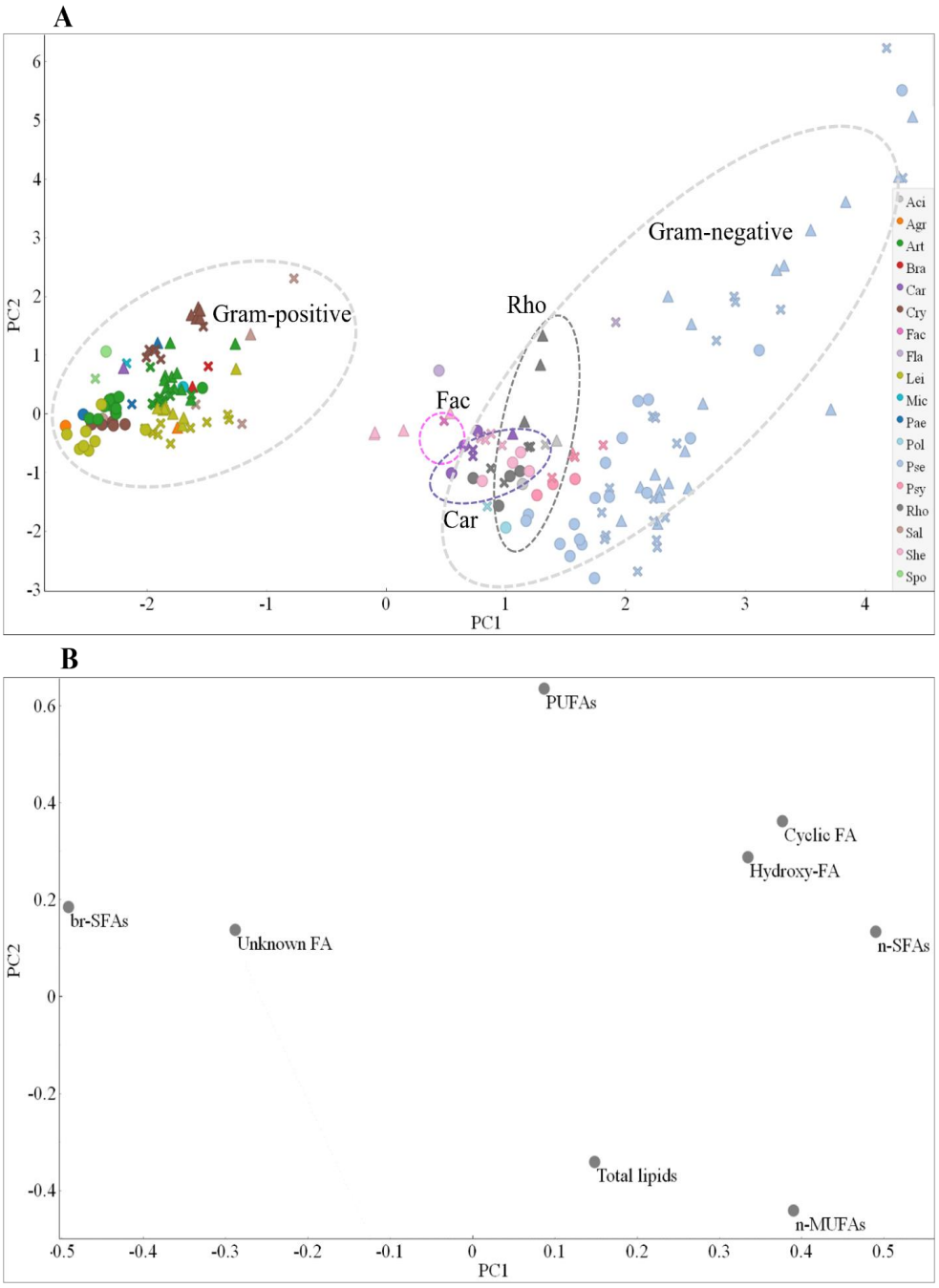

Figure 2. PCA of the GC fatty acid profile data for Antarctic bacteria grown at different temperatures. A – Score plot of PC1 and PC2, colors represent genera, '●' – 5°C, '✖' – 15°C and '▲' – 25°C, different colors represent genera (Pol-*Polaromonas*, Pse-*Pseudomonas*, Psy-*Psychrobacter*, She-*Shewanella*, Aci-*Acinetobacter*, Fla-*Flavobacterium*, Agr-*Agrococcus*, Art-*Arthrobacter*, Bra-*Brachybacterium*, Cry-*Cryobacterium*, Lei-*Leifsonia*, Mic-*Micrococcus*, Pae-*Paeniglutamicibacter*,

Rho-*Rhodococcus*, Sal-*Salinibacterium*, Fac-*Facklamia*, Spo-*Sporosarcina*, Car-*Carnobacterium*), B – Loading plot of GC fatty acid data. PC1 – 44% explained variance, PC2 – 23% explained variance. Fatty acid data were autoscaled before PCA. PUFAs (summed polyunsaturated fatty acids), n-SFAs (summed non-branched saturated fatty acids), br-SFAs (summed branched saturated fatty acids), n-MUFAs (summed non-branched monounsaturated fatty acids), hydroxy-FAs (summed hydroxy fatty acids), Cyclic-FAs (summed cyclic fatty acids).

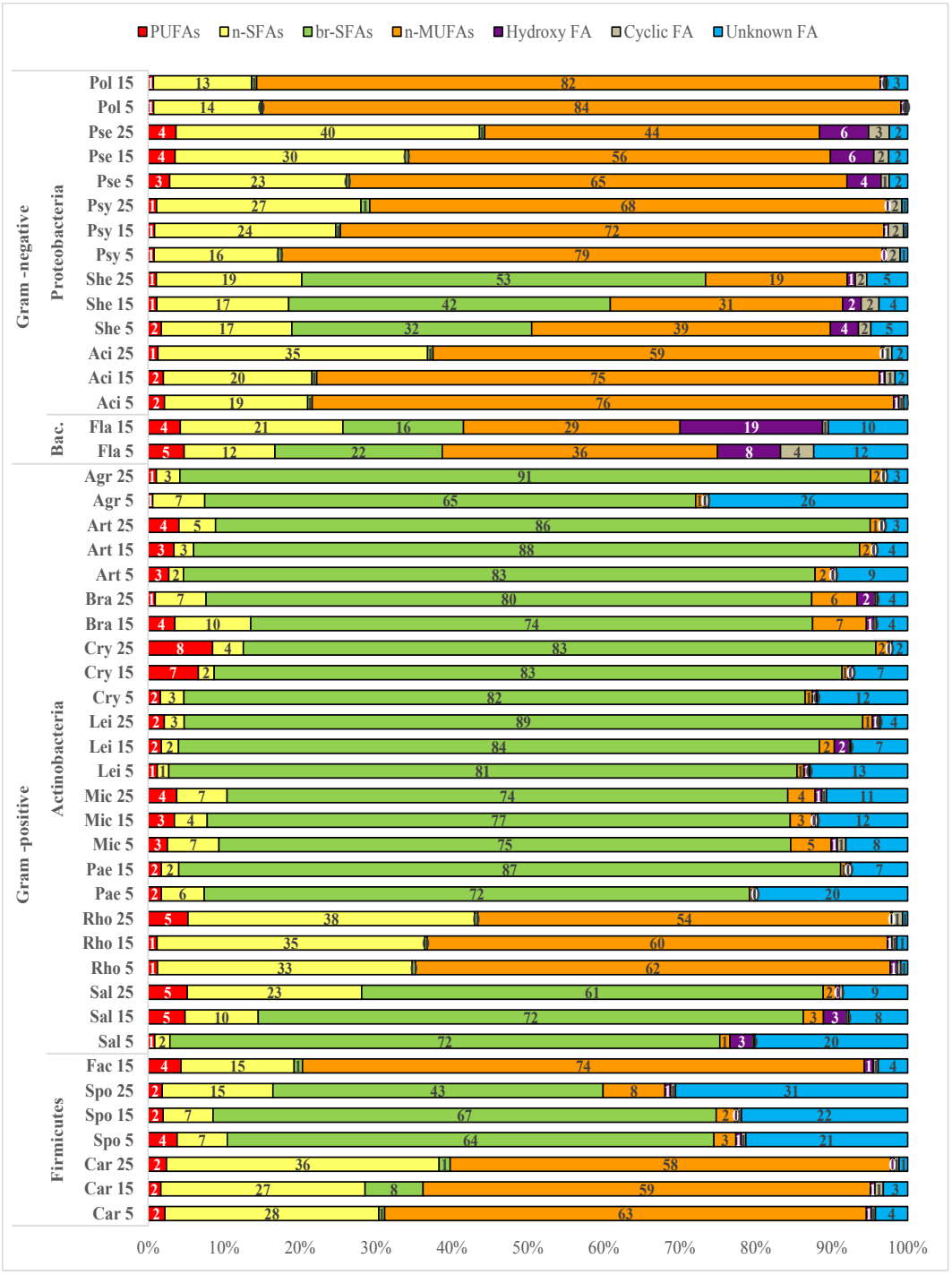

Figure 3. Fatty acid profile of bacteria grown at different temperatures (%, w/w), *- no growth/ not enough biomass to perform analysis. Group of Fas: PUFAs (summed polyunsaturated fatty acids), n-

SFAs (summed non-branched saturated fatty acids), br-SFAs (summed branched saturated fatty acids), n-MUFAs (summed non-branched monounsaturated fatty acids), hydroxy-FAs (summed hydroxy fatty acids), Cyclic-FAs (summed cyclic fatty acids).

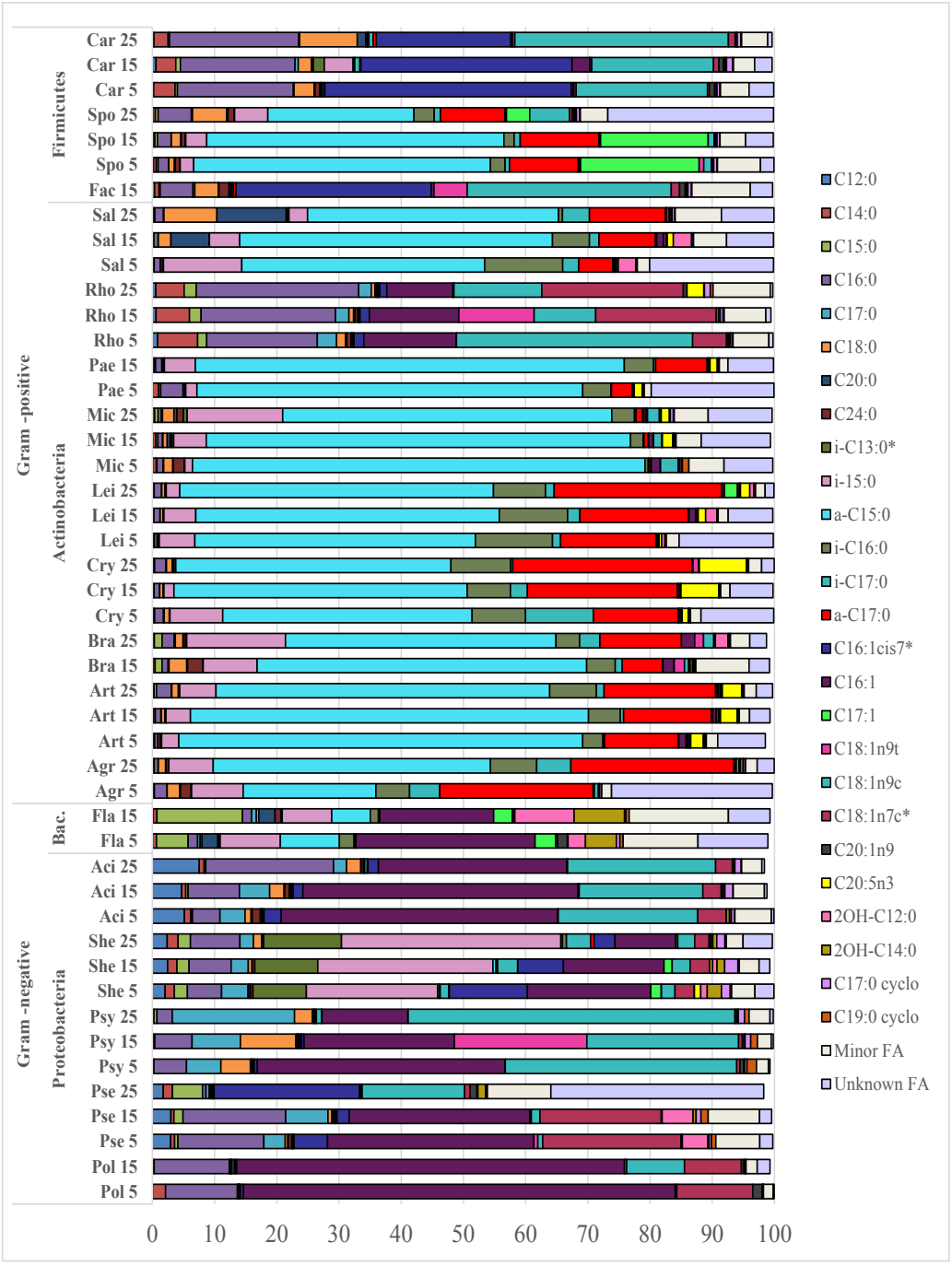

Figure 4. Fatty acid profile of Antarctic bacteria grown at varying growth temperatures. FAs with the content lower than 1 % were summed in "Minor FA",* – FAs identified by GC-MS.

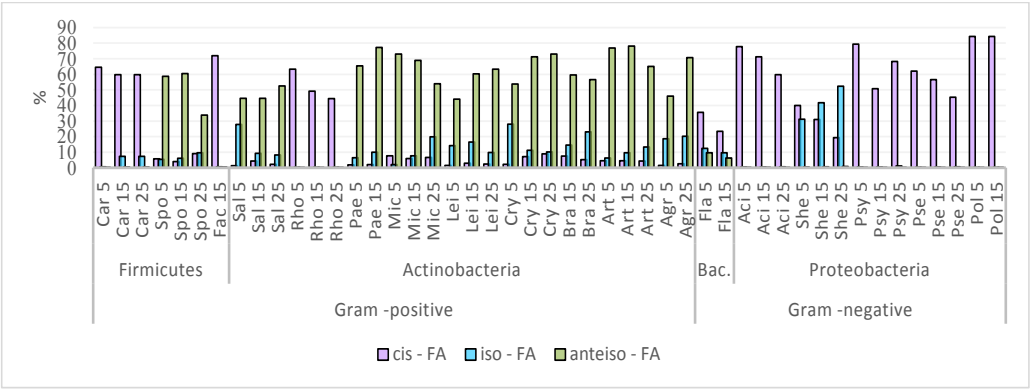

Figure 5. The amount of cis-, iso- and anteiso- FAs of Antarctic bacteria grown at varying growth temperatures.

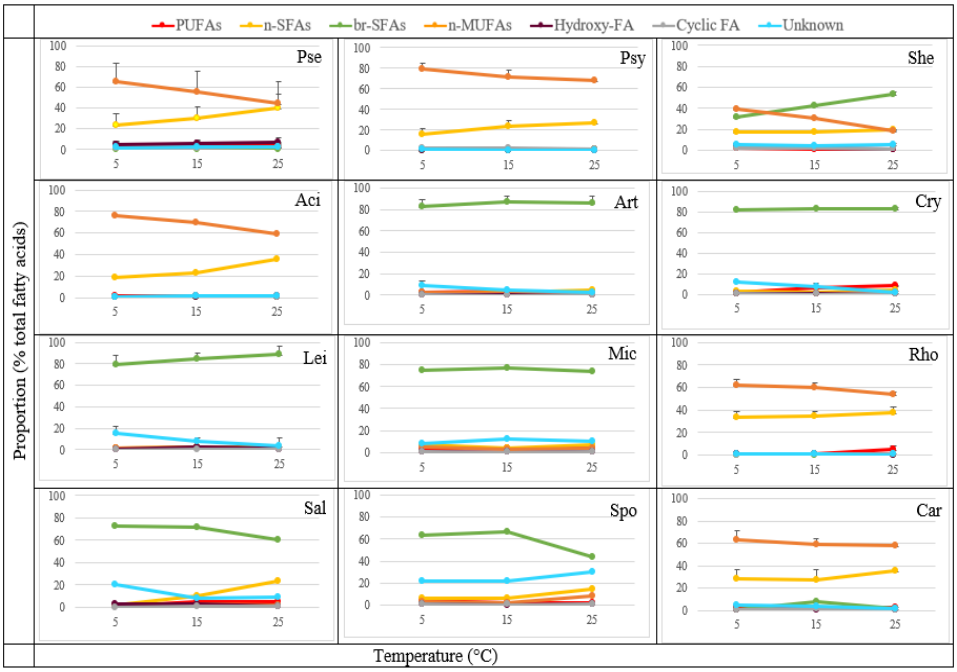

Figure 6. The effect of temperature on fatty acid classes in bacteria cultivated at 5°C, 15°C and 25°C (mean ±SD). The standard deviation was calculated for genera that were represented by two or more strains. Group of FAs: PUFAs (summed polyunsaturated fatty acids), n-SFAs (summed non-branched saturated fatty acids), br-SFAs (summed branched saturated fatty acids), n-MUFAs (summed non-branched monounsaturated fatty acids), hydroxy-FAs (summed hydroxy fatty acids), Cyclic-FAs (summed cyclic fatty acids); Genera: Pse-*Pseudomonas*, Psy-*Psychrobacter*, She-*Shewanella*, Aci-*Acinetobacter*, Art-*Arthrobacter*, Cry-*Cryobacterium*, Lei-*Leifsonia*, Mic-*Micrococcus*, Rho-*Rhodococcus*, Sal-*Salinibacterium*, Spo-*Sporosarcina*, Car-*Carnobacterium*

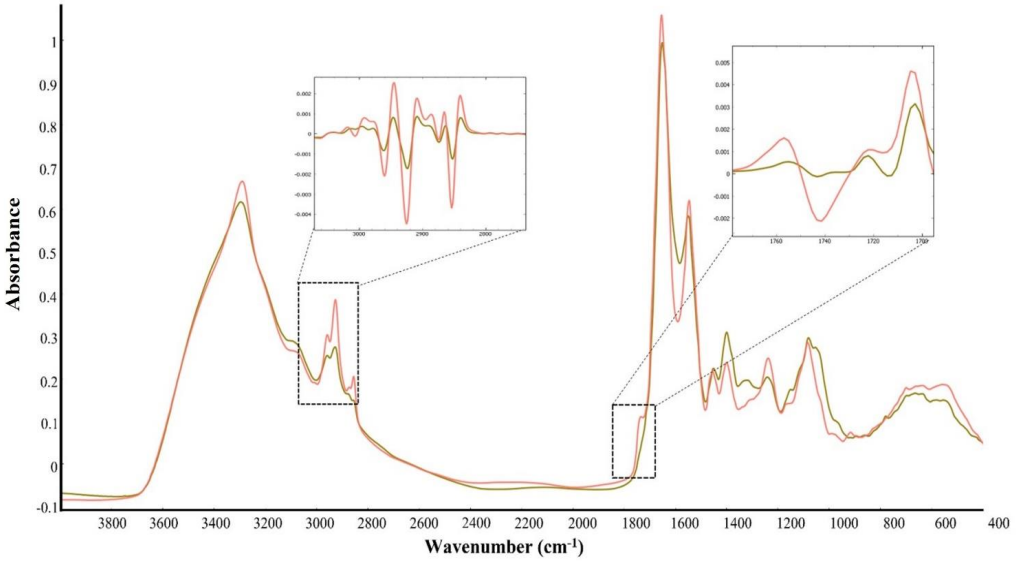

Figure 7. EMSC corrected FTIR spectra of two bacteria grown at 15°C with different total lipid content (%): olive – *Brachybacterium paraconglomeratum* BIM B – 1571 (4%), orange – *Pseudomonas peli* BIM B – 1546 (18%).

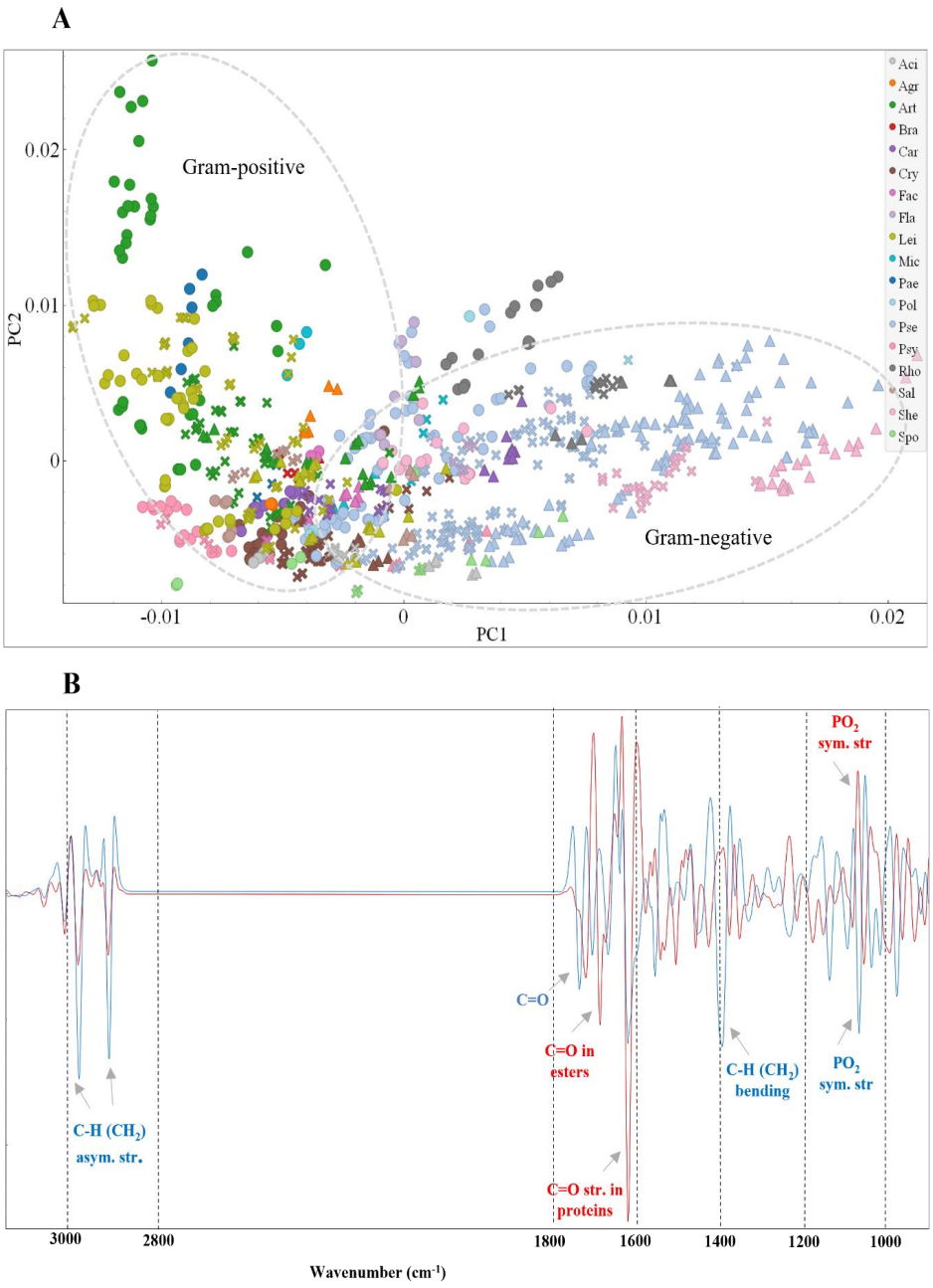

Figure 8. PCA of the preprocessed FTIR spectra of Antarctic bacteria grown at different temperatures ('●' – 5°C, '✖' – 15°C and '▲' – 25°C). A – Score plot of PC1 and PC2 components, colors represent genera, shapes represent cultivation temperatures, different colors represent genera (Pol-*Polaromonas*, Pse-*Pseudomonas*, Psy-*Psychrobacter*, She-*Shewanella*, Aci-*Acinetobacter*, Fla-*Flavobacterium*, Agr-*Agrococcus*, Art-*Arthrobacter*, Bra-*Brachybacterium*, Cry-*Cryobacterium*, Lei-*Leifsonia*, Mic-*Micrococcus*, Pae-*Paeniglutamicibacter*, Rho-*Rhodococcus*, Sal-*Salinibacterium*, Fac-*Facklamia*,

Spo-*Sporosarcina*, Car-*Carnobacterium*), B – Loading plot of FTIR data with the main contributing peaks, PC1 (red) and PC2 (blue). PC1 provided 35% of explained variance and PC2 provided 17% of explained variance.

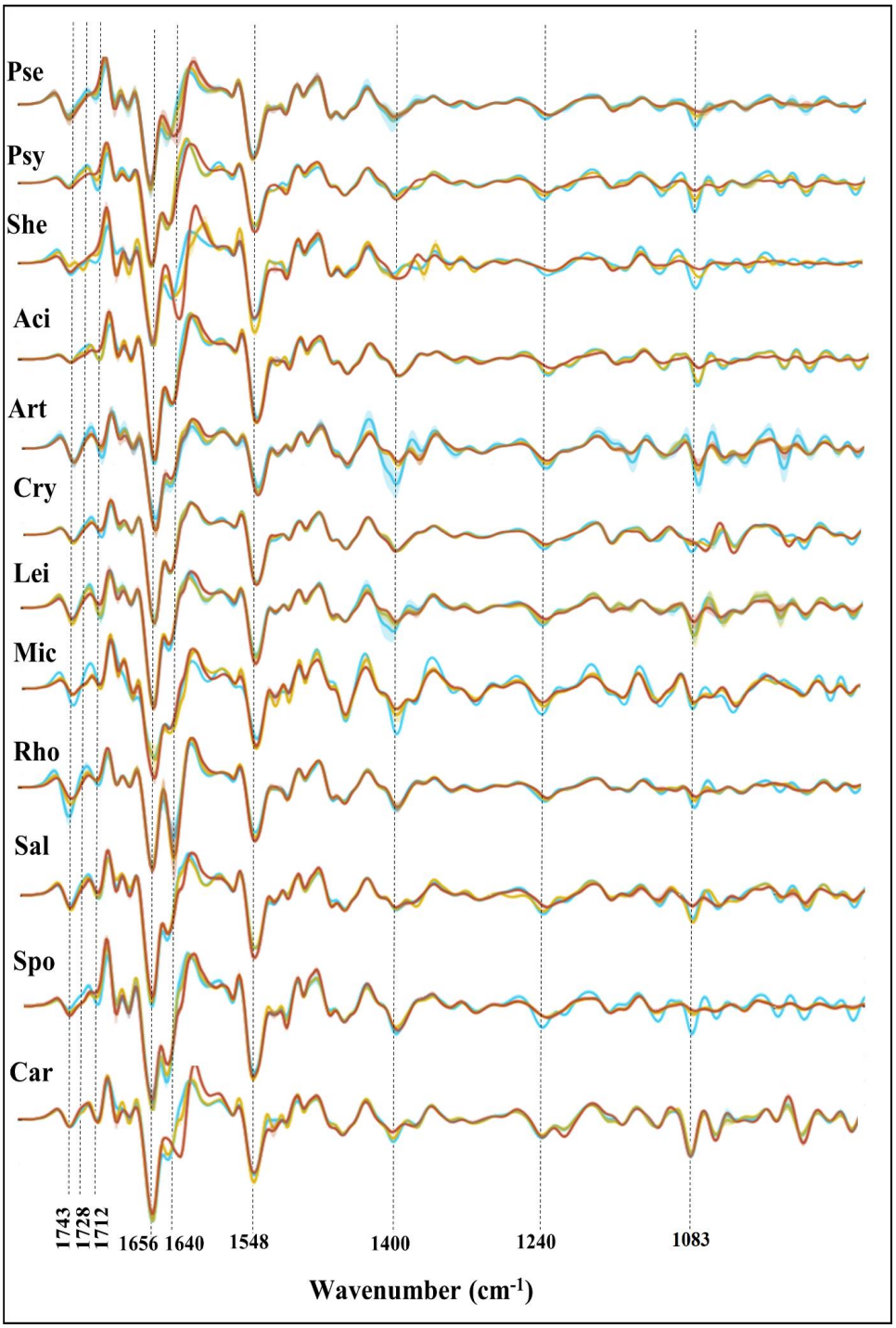

Figure 9. Second derivative FTIR spectra of bacterial biomass of different genera grown at different temperatures (blue – 5°C, yellow – 15°C and orange – 25°C). Genera: Pse-*Pseudomonas*, Psy-*Psychrobacter*, She-*Shewanella*, Aci-*Acinetobacter*, Art-*Arthrobacter*, Cry-*Cryobacterium*, Lei-

1119 *Leifsonia*, Mic-*Micrococcus*, Rho-*Rhodococcus*, Sal-*Salinibacterium*, Spo-*Sporosarcina*, Car-
1120 *Carnobacterium.*

Figure 10. Relative content of the cellular components in bacterial biomass grown at different temperatures (blue – 5°C, yellow – 15°C and orange – 25°C) estimated by ratio-based analysis using FTIR spectra, where: A – lipid/protein ratio (1734/1656 cm^{-1}) and B – phosphorus-based compounds/protein ratio (1083/1656 cm^{-1}). The standard deviation was calculated for genera that were represented by two or more strains. Genera: Pol-*Polaromonas*, Pse-*Pseudomonas*, Psy-*Psychrobacter*, She-*Shewanella*, Aci-*Acinetobacter*, Fla-*Flavobacterium*, Agr-*Agrococcus*, Art-*Arthrobacter*, Bra-*Brachybacterium*, Cry-*Cryobacterium*, Lei-*Leifsonia*, Mic-*Micrococcus*, Pae-*Paeniglutamicibacter*, Rho-*Rhodococcus*, Sal-*Salinibacterium*, Fac-*Facklamia*, Spo-*Sporosarcina*, Car-*Carnobacterium*

Supplementary materials

• Alterations in lipids and other biochemical components of Antarctic bacteria grown at different temperatures

Volha Akulava[1*], Margarita Smirnova[1], Dana Byrtusova[1], Boris Zimmermann[1], Dag Ekeberg[2], Achim Kohler[1], Uladzislau Blazhko[1], Uladzislau Miamin[3], Leonid Valentovich[4], Volha Shapaval[1]

[1]Faculty of Science and Technology, Norwegian University of Life Sciences, Ås, Norway

[2]Faculty of Chemistry, Biotechnology and Food Science, Norwegian University of Life Sciences, Ås, Norway

[3]Faculty of Biology, Belarussian State University, Minsk, Belarus

[4]Institute of Microbiology, National Academy of Sciences of Belarus, 220084 Minsk, Belarus

***Correspondence:** Corresponding Author volha.akulava@nmbu.no

1141 Table S1. Gen Bank accession numbers of bacteria used in this study

Phylum	Genus	Strain name and collection №	Gen Bank Accession Number
	Polaromonas	*Polaromonas sp.* BIM B–1676 GS**	MT890199
		Pseudomonas extremaustralis BIM B–1672 GS	MT890192
		Pseudomonas fluorescens BIM B–1668 GS	MT89019
		Pseudomonas leptonychotis BIM B–1559MP	ON248066
		Pseudomonas leptonychotis BIM B–1568MP	ON248076
		Pseudomonas leptonychotis BIM B–1566MP	ON248077
		Pseudomonas lundensis BIM B–1554MP	ON248061
		Pseudomonas lundensis BIM B–1555MP	ON248062
		Pseudomonas lundensis BIM B–1556MP	ON248063
		Pseudomonas peli BIM B–1560MP	ON248067
		Pseudomonas peli BIM B–1569MP	ON248075
		Pseudomonas peli BIM B–1546 MP	ON248078
		Pseudomonas peli BIM B–1552MP	ON248080
		Pseudomonas peli BIM B–1542MP	ON248083
		Pseudomonas peli BIM B–1548MP	ON248084
		Pseudomonas sp. BIM B–1635GS	MT890174
		Pseudomonas sp. BIM B–1667GS	MT890189
		Pseudomonas sp. BIM B–1673GS	MT890191
	Pseudomonas	*Pseudomonas sp.* BIM B–1674GS	MT890193
		Psychrobacter glacinicola BIM B–1629GS**	MT890168
		Psychrobacter urativorans BIM B–1655 GS**	MT890181
	Psychrobacter	*Psychrobacter urativorans* BIM B–1662GS**	MT890182
		Shewanella baltica BIM B–1565MP	ON248060
		Shewanella baltica BIM B–1557MP	ON248064
		Shewanella baltica BIM B–1561MP	ON248069
	Shewanella	*Shewanella baltica* BIM B–1563MP	ON248072
Proteobacteria	*Acinetobacter*	*Acinetobacter lwoffii* BIM B–1558MP	ON248065
Bacteroidetes	*Flavobacterium*	*Flavobacterium degerlachei* BIM B–1562MP	ON248071
	Agrococcus	*Agrococcus citreus* BIM B–1547MP	ON248081
		Arthrobacter agilis BIM B–1543 MP	ON248082
		Arthrobacter cryoconiti BIM B–1627GS**	MT890166
		Arthrobacter oryzae BIM B–1663GS	MT890183
		Arthrobacter sp. BIM B–1624GS**	MT890163
		Arthrobacter sp. BIM B–1625 GS	MT890164
		Arthrobacter sp. BIM B–1626GS**	MT890165
		Arthrobacter sp. BIM B–1628GS**	MT890167
		Arthrobacter sp. BIM B–1664GS	MT890186
		Arthrobacter sp. BIM B–1666GS**	MT890188
Actinobacteria	*Arthrobacter*	*Arthrobacter sp.* BIM B–1656GS	MT890194

		Arthrobacter sp. BIM B–1549[MP]	ON248073
	Brachybacterium	*Brachybacterium paraconglomeratum* BIM B–1571 [MP]	ON248074
	Cryobacterium	*Cryobacterium arcticum* BIM B–1619 [GS]**	MT890158
		Cryobacterium soli BIM B–1620 [GS]**	MT890159
		Cryobacterium soli BIM B–1658[GS]	MT890196
		Cryobacterium soli BIM B–1659[GS]	MT890197
		Cryobacterium soli BIM B–1677[GS]	MT890198
		Cryobacterium soli BIM B–1675[GS]	MT890200
	Leifsonia	*Leifsonia antarctica* BIM B–1631[GS]**	MT890170
		Leifsonia antarctica BIM B–1632[GS]	MT890171
		Leifsonia antarctica BIM B–1637 [GS]	MT890176
		Leifsonia antarctica BIM B–1638 [GS]	MT890177
		Leifsonia antarctica BIM B–1639 [GS]	MT890178
		Leifsonia antarctica BIM B–1669 [GS]	MT890179
		Leifsonia antarctica. BIM B–1671[GS]	MT890184
		Leifsonia kafniensis BIM B–1633[GS]	MT890172
		Leifsonia rubra BIM B–1622 [GS]**	MT890161
		Leifsonia rubra BIM B–1623 [GS]	MT890162
		Leifsonia rubra BIM B–1634 [GS]**	MT890173
		Leifsonia rubra BIM B–1567[MP]	ON248088
	Micrococcus	*Micrococcus luteus* BIM B–1545[MP]	ON248079
	Paeniglutamicibacter	*Paeniglutamicibacter antarcticus* BIM B–1657[GS]**	MT890195
	Rhodococcus	*Rhodococcus erythropolis* BIM B–1660[GS]	MT890201
		Rhodococcus erythropolis BIM B–1661[GS]	MT890202
		Rhodococcus yunnanensis BIM B–1621[GS]**	MT890160
		Rhodococcus yunnanensis BIM B–1670[GS]	MT890185
	Salinibacterium	*Salinibacterium sp*. BIM B–1630 [GS]	MT890169
		Salinibacterium sp. BIM B–1636[GS]	MT890175
		Salinibacterium sp. BIM B–1654[GS]	MT890180
		Salinibacterium sp. BIM B–1665[GS]	MT890187
Firmicutes	*Facklamia*	*Facklamia tabacinasalis* BIM B–1577[MP]	ON248087
	Sporosarcina	*Sporosarcina sp*. BIM B–1539 [MP]	ON248068
	Carnobacterium	*Carnobacterium funditum* BIM B–1541[MP]**	ON248085
		Carnobacterium iners BIM B–1544[MP]**	ON248086
		Carnobacterium inhibens BIM B–1540[MP]	ON248070

1142

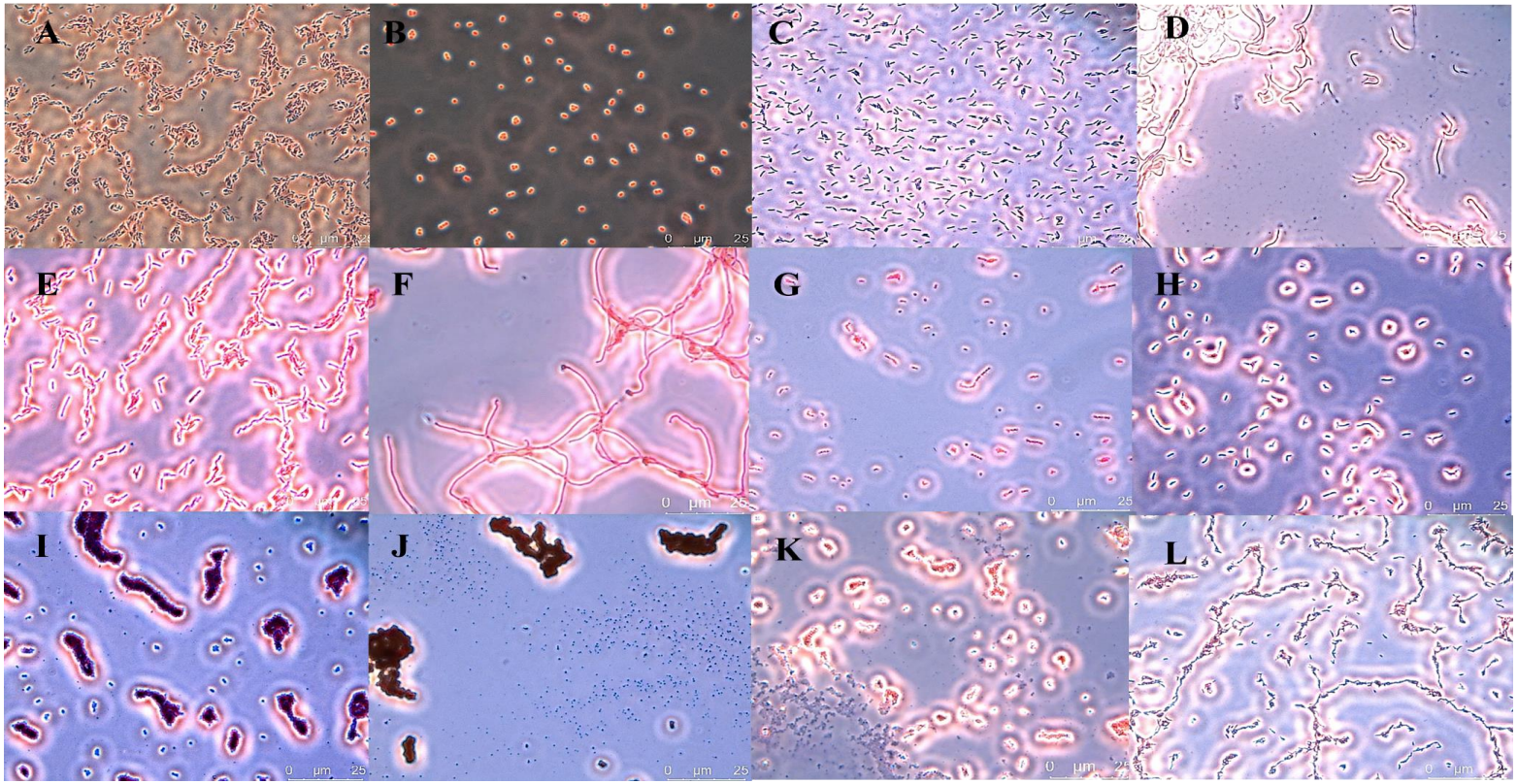

Figure S1– Gram-stained fast-growing bacteria isolated from the temporary meltwater ponds of the coastal area of East Antarctica: A - *Shewanella baltica* BIM B – 1563; B - *Acinetobacter lwoffii* BIM B – 1558; C - *Pseudomonas peli* BIM B – 1560; D - *Flavobacterium degerlachei* BIM B – 1562; E - *Sporosarcina* sp. BIM B – 1539; F - *Carnobacterium funditum* BIM B – 1541; G - *Facklamia tabacinasalis* BIM B – 1577; H - *Arthrobacter* sp. BIM B – 1549; I - *Brachybacterium paraconglomeratum* BIM B – 1571; J - *Micrococcus luteus* BIM B – 1545; K - *Agrococcus citreus* BIM B – 1547; L - *Leifsonia rubra* BIM B – 1567.

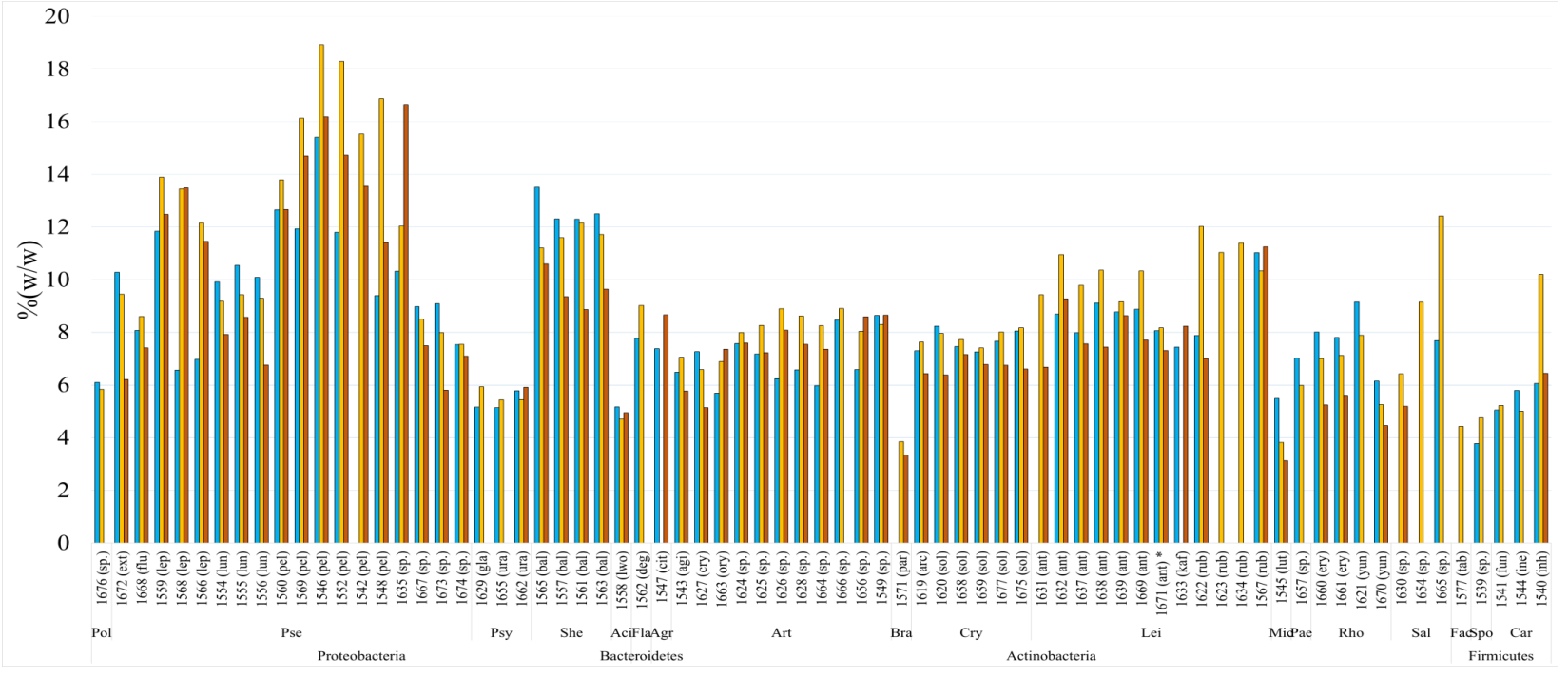

Figure S2. Total lipid content (%, w/w) of bacterial biomass grown at different temperatures (blue – 5°C, yellow – 15°C and orange – 25°C).

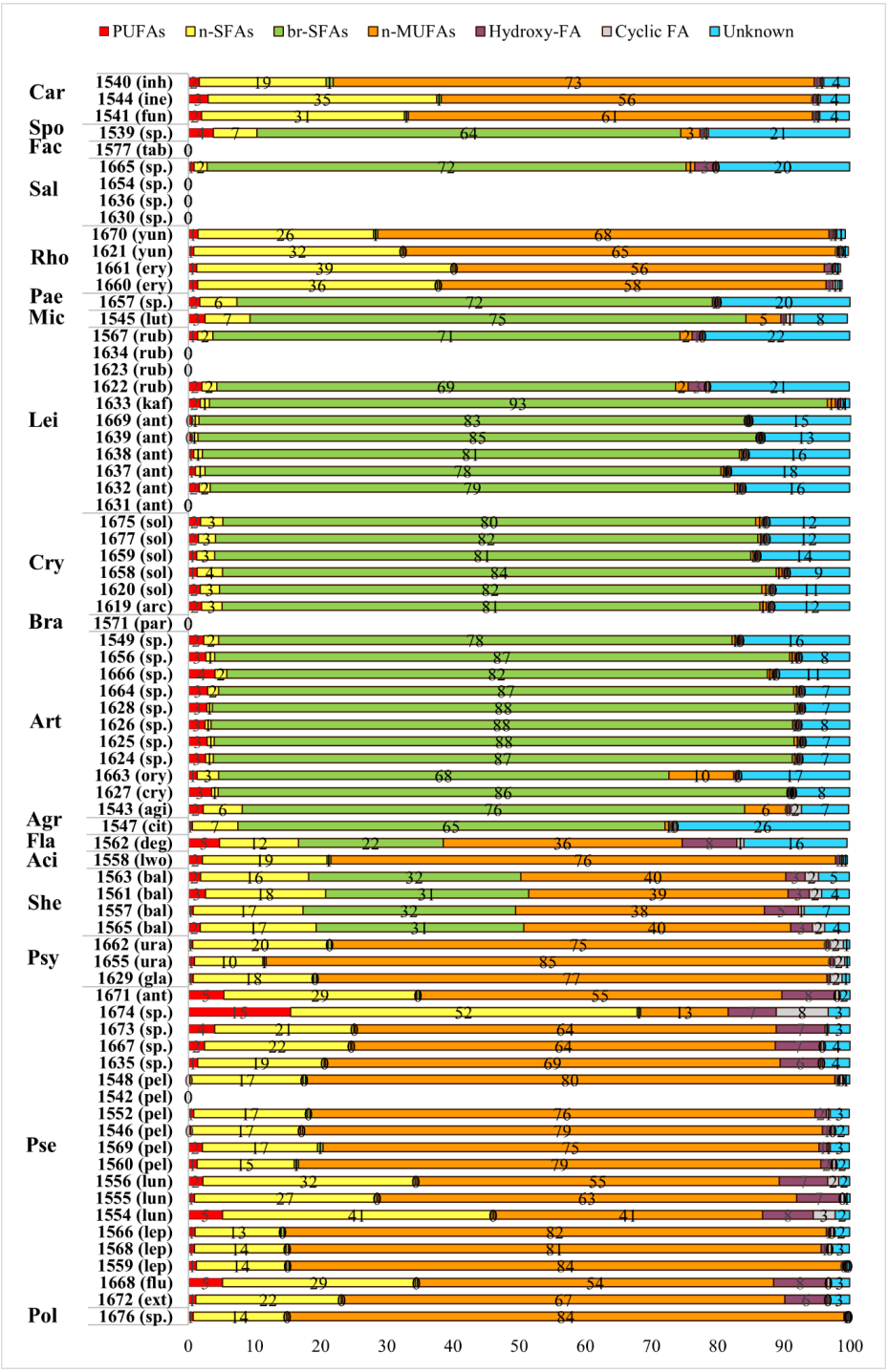

Figure S3. Fatty acid profile of Antarctic bacteria grown at 5°C (%, w/w).

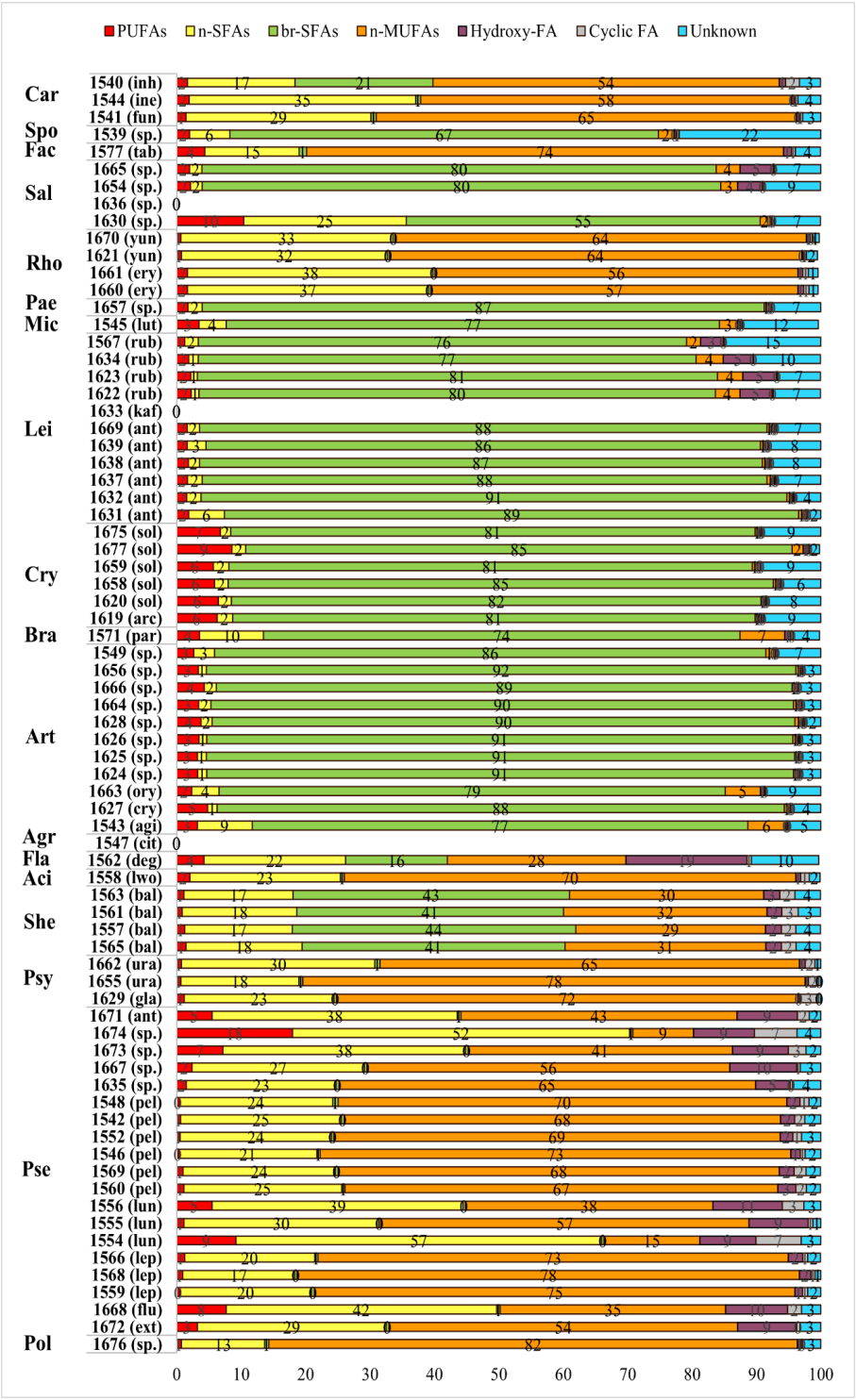

Figure S4. Fatty acid profile of Antarctic bacteria grown at 15°C (%, w/w).

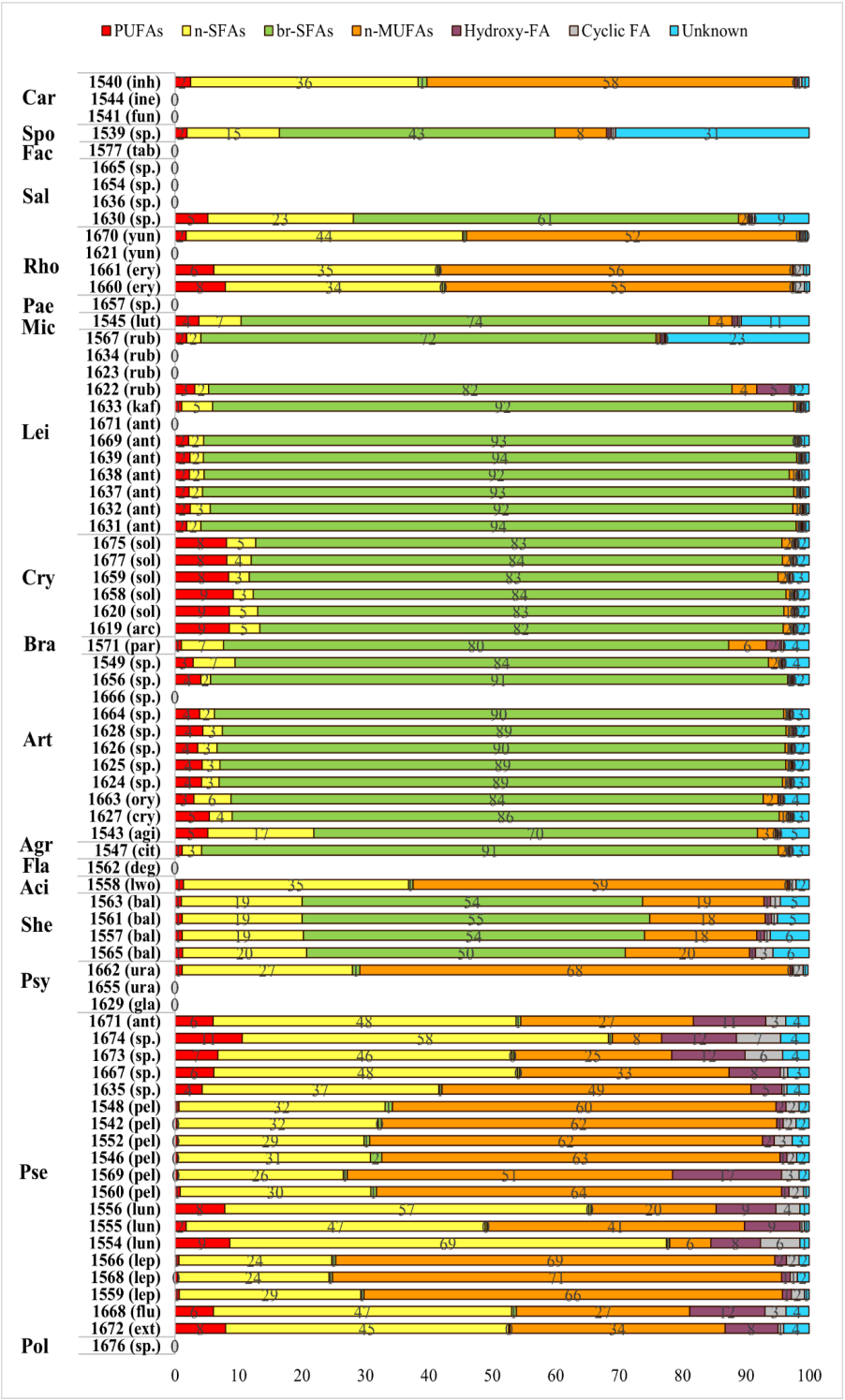

Figure S5. Fatty acid profile of Antarctic bacteria grown at 25°C (%, w/w).

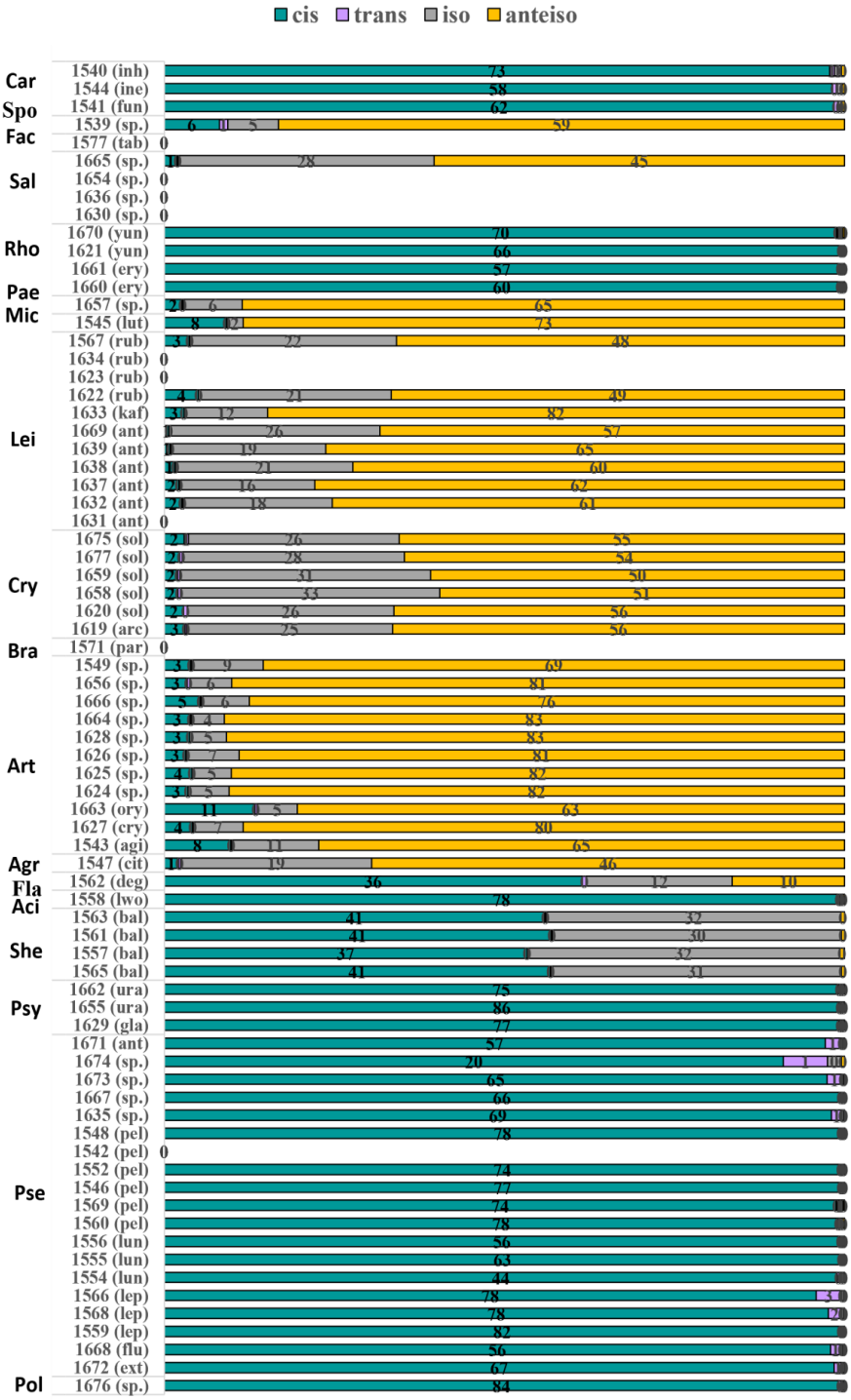

7

8 Figure S6. Fatty acid profile of Antarctic bacteria grown at 5°C (%, w/w).

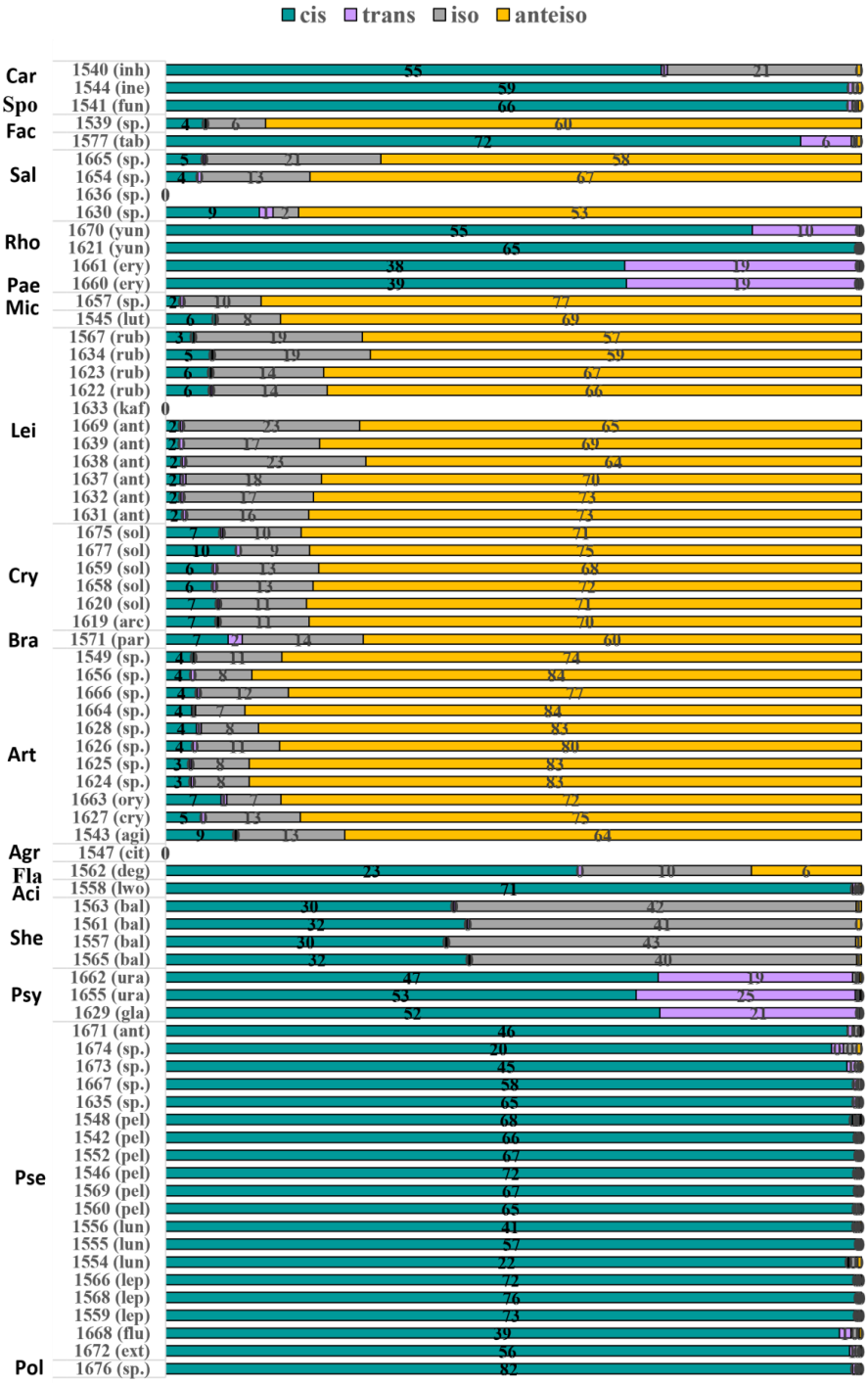

Figure S7. Fatty acid profile of Antarctic bacteria grown at 15°C (%, w/w).

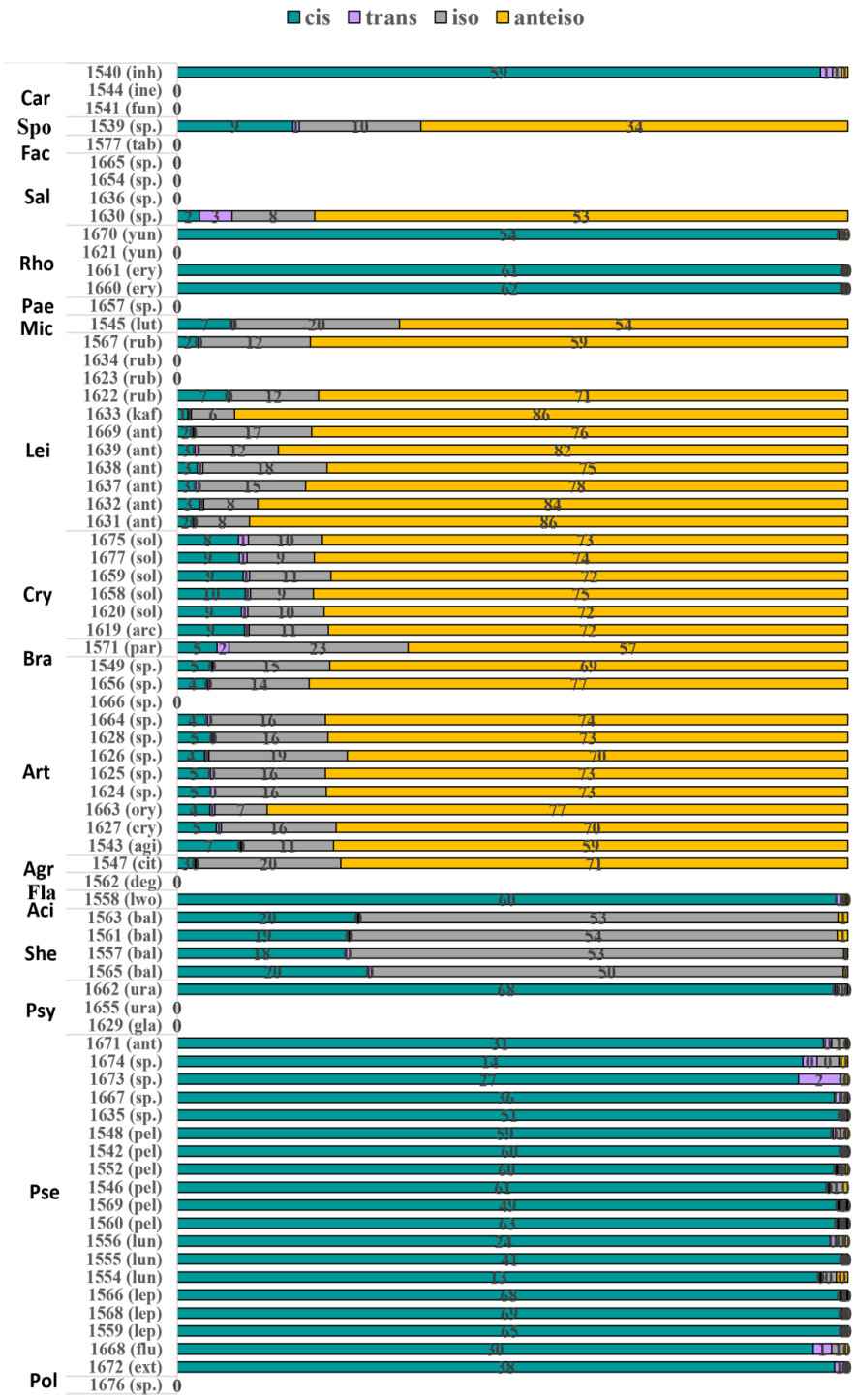

11

12 Figure S8. Fatty acid profile of Antarctic bacteria grown at 15°C (%, w/w).

13

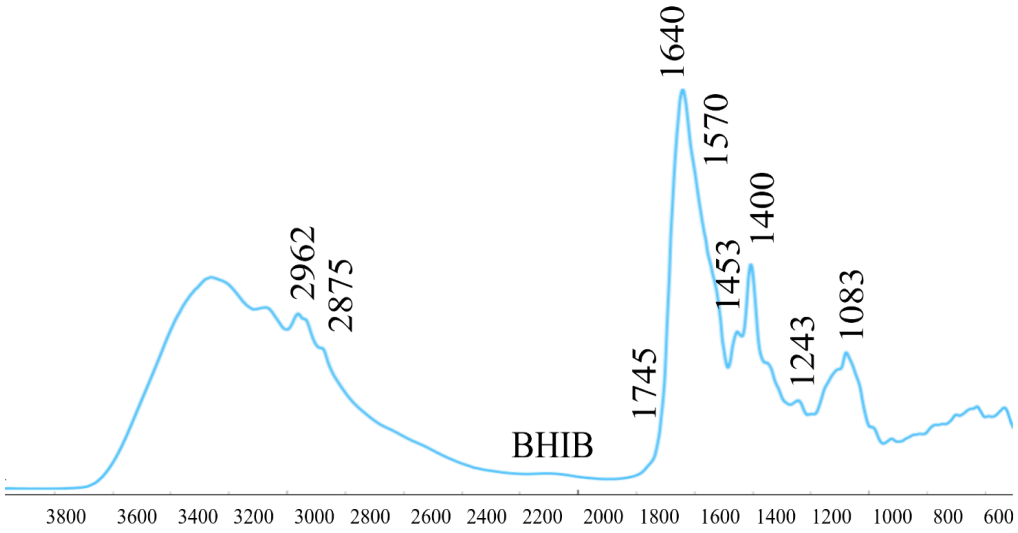

14

15 Figure S9. FTIR-HTS spectra of BHIB media.

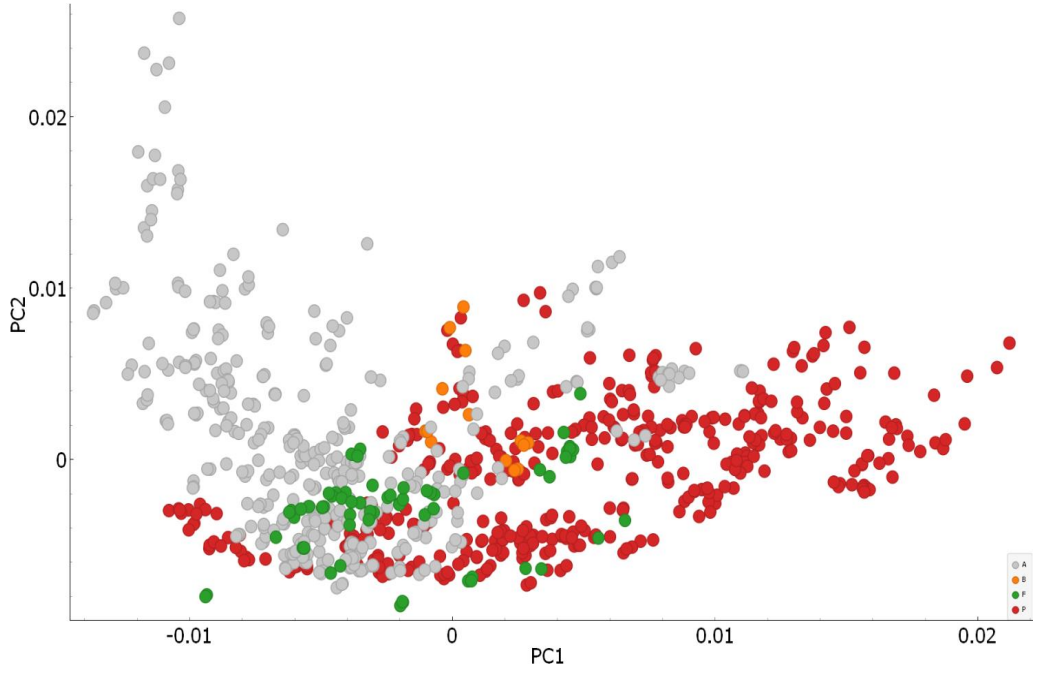

16

17 Figure S10. PCA plot on phyla level for the whole spectral region. P-Proteobacteria, A-
18 Actinobacteria, F-Firmicutes, and B-Bacteroidetes.

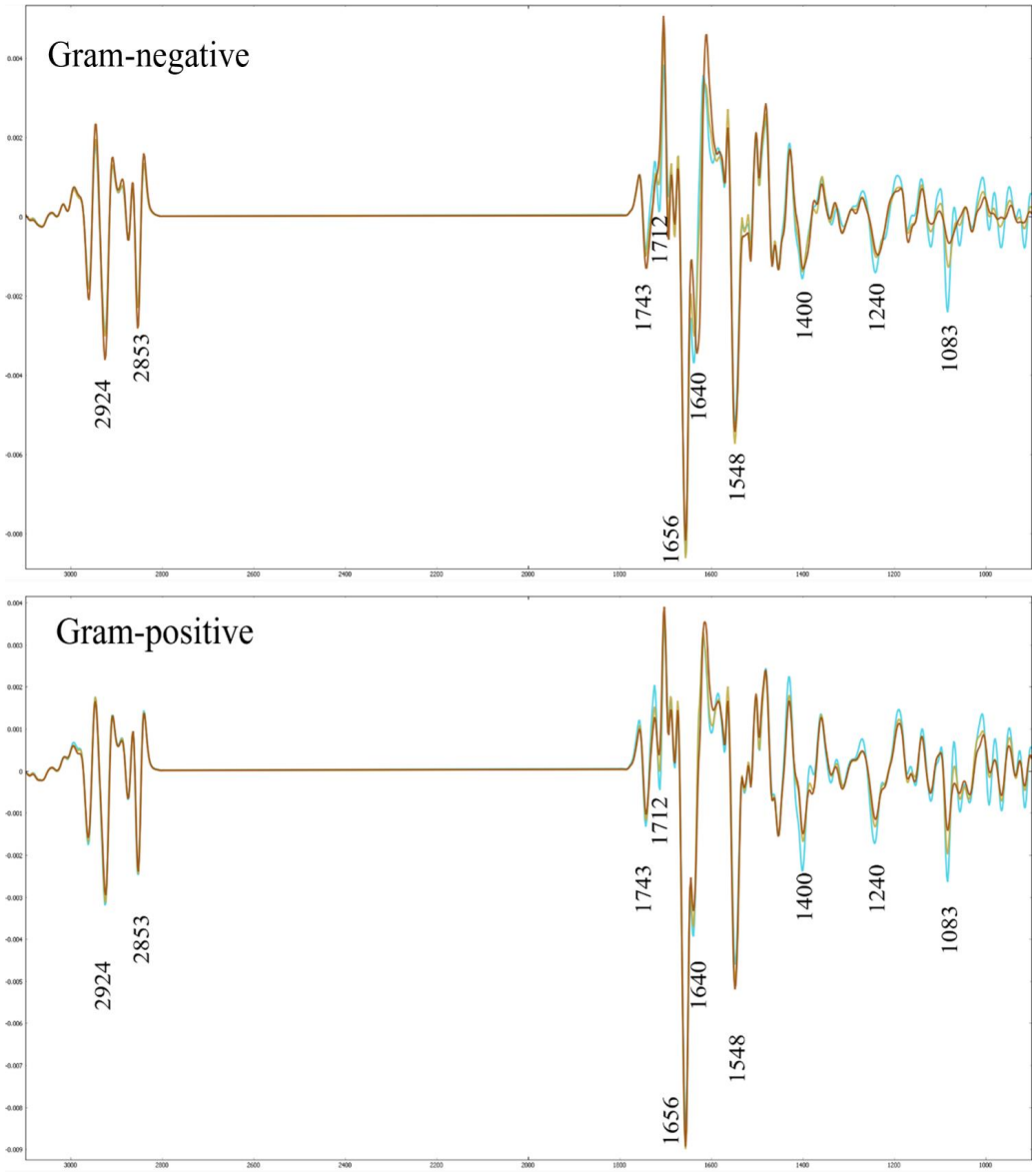

Figure S11. Second derivative FTIR spectra of bacterial biomass of different Gram groups averaged for different temperatures (blue – 5°C, yellow – 15°C and orange – 25°C).

26

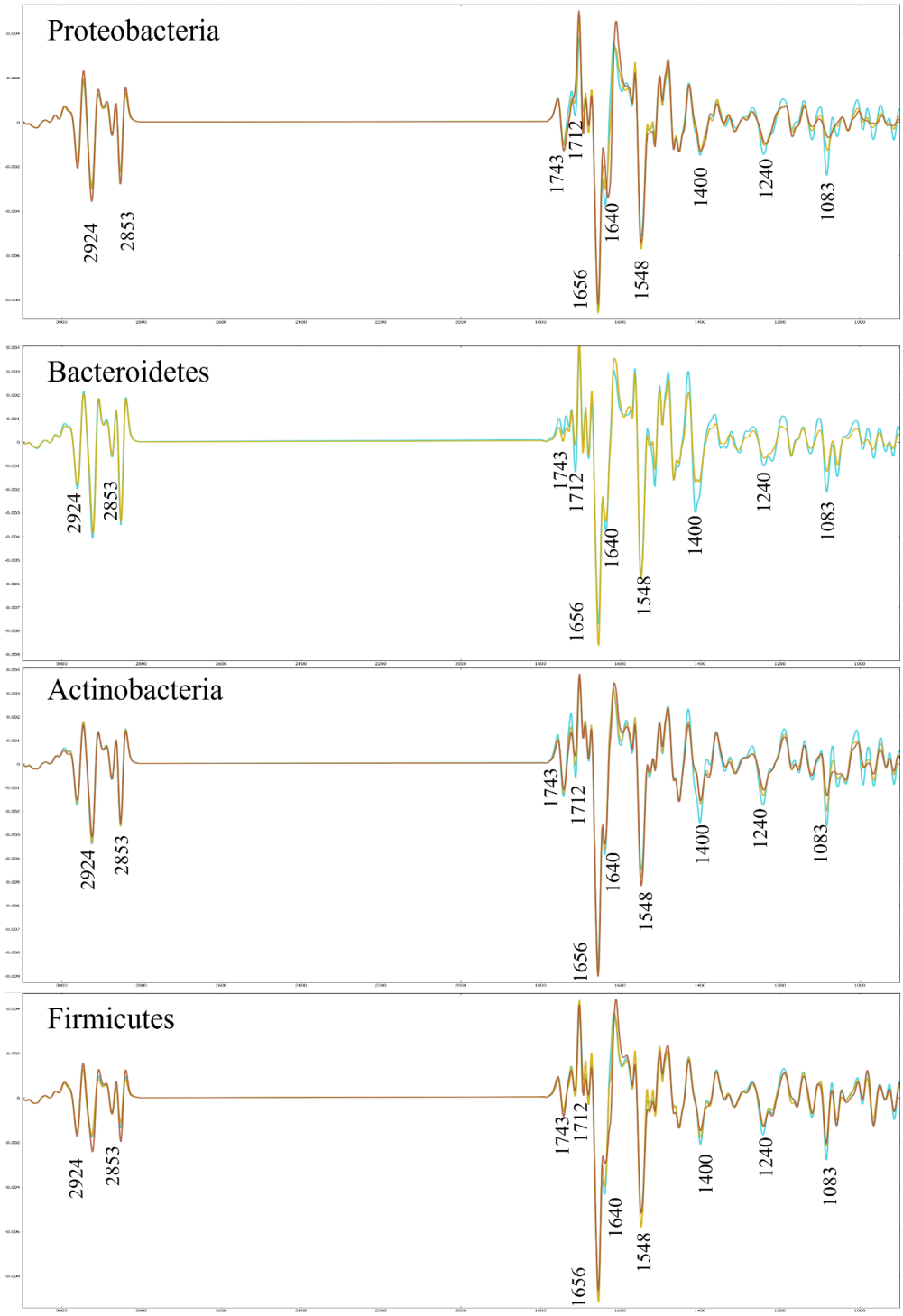
Proteobacteria
2924
2853
1743
1712
1656
1640
1548
1400
1240
1083
Bacteroidetes
2924
2853
1743
1712
1656
1640
1548
1400
1240
1083
Actinobacteria
2924
2853
1743
1712
1656
1640
1548
1400
1240
1083
Firmicutes
2924
2853
1743
1712
1656
1640
1548
1400
1240
1083

27

Figure S12. Second derivative FTIR spectra of bacterial biomass of different phyla averaged for different temperatures (blue – 5°C, yellow – 15°C and orange – 25°C).

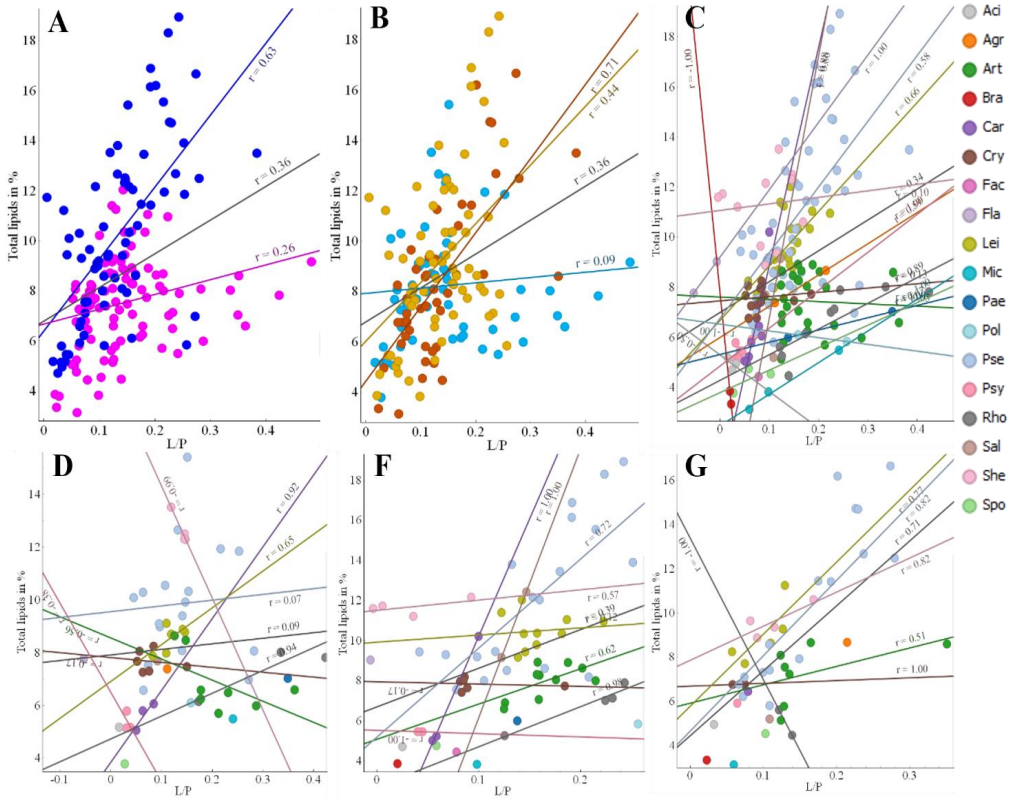

Figure S13. Pearson's correlation coefficients between total lipids in % measured by GC and lipid to protein ratio calculated based on FTIR spectra: A – Gram negative (blue) and gram-positive (pink) bacteria, B – different temperatures (blue – 5°C, yellow – 15°C and orange – 25°C), C – different genera, D – different genera cultivated at 5°C, F – different genera cultivated at 15°C, G – different genera cultivated at 25°C.

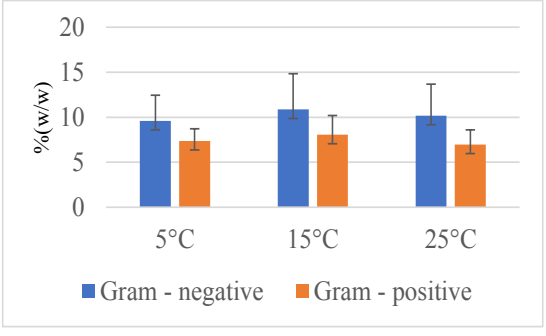

Figure S14. Averaged total lipid content (%, w/w) of bacterial biomass grown at different temperatures for Gram-negative and Gram-positive bacteria.

Paper III

Global biochemical profiling of fast-growing Antarctic bacteria isolated from meltwater ponds by high-throughput FTIR spectroscopy

Volha Akulava[1] (volha.akulava@nmbu.no), Valeria Tafintseva[1] (valeria.tafintseva@nmbu.no), Uladzislau Blazhko[1] (uladzislau.blazhko@nmbu.no), Achim Kohler[1] (achim.kohler@nmbu.no), Uladzislau Miamin[2] (vladmiamin@mail.ru), Leonid Valentovich[3] (valentovich@mbio.bas-net.by), Volha Shapaval[1] (volha.shapaval@nmbu.no)

(1) Faculty of Science and Technology, Norwegian University of Life Sciences, 1432 Ås, Norway

(2) Faculty of Biology, Belarusian State University, 220030 Minsk, Belarus

(3) Institute of Microbiology, National Academy of Sciences of Belarus, 220141 Minsk, Belarus

Keywords: Antarctic bacteria, Fourier-Transform Infrared Spectroscopy (FTIR), biochemical phenotyping, variability, multivariate analysis, principal component analysis (PCA)

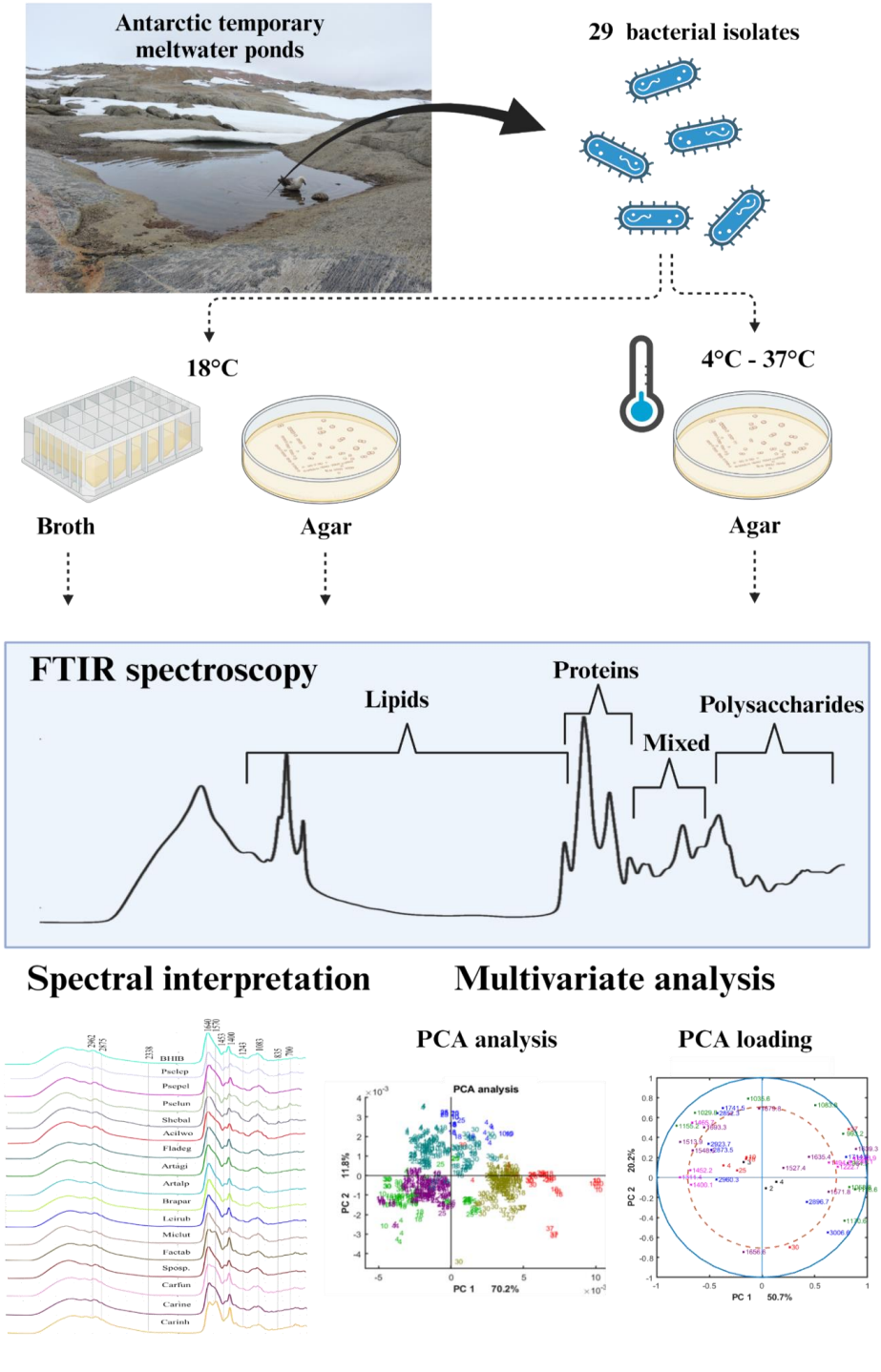

14

15 Graphical abstract was partially created with BioRender.com

Abstract

Fourier transform infrared (FTIR) spectroscopy is a biophysical technique used for non-destructive biochemical profiling of biological samples. It can provide comprehensive information about the total cellular biochemical profile of microbial cells. In this study FTIR spectroscopy was used to perform biochemical characterization of twenty-nine bacterial strains isolated from the Antarctic meltwater ponds. The bacteria were grown on two forms of brain heart infusion (BHI) medium (agar and broth) and at different temperatures (4, 10, 15, 18, 25, 30, and 37°C). Multivariate data analysis approaches such as principal component analysis (PCA) and correlation analysis were used to study the biochemical profiles and their changes triggered by the cultivation conditions. The observed results showed that FTIR resembled well phylogenetic relationships of the studied bacteria where the best phylogeny-aligned clustering was obtained for bacteria cultivated on agar. Cultivation on two forms of BHI medium provided biochemically different bacterial biomass. The impact of temperature on the total cellular biochemical profile of the studied bacteria was specie-specific and for all bacteria lipid spectral region was the least affected while polysaccharide region was the most affected by temperature. The biggest temperature-triggered changes of the cell chemistry were detected for bacteria with a wide temperature tolerance such us *Pseudomonas lundensis* strains and *Acinetobacter lwoffii* BIM B – 1558. While the least biochemical changes were observed for the biomass of *Micrococcus luteus* BIM B – 1545 and *Leifsonia* sp. BIM B – 1567.

Introduction

During the last decade, Fourier transform infrared (FTIR) spectroscopy became as a standard analytical technique for comprehensive biochemical profiling of microorganisms (1-6). FTIR spectroscopy allows to identify all main biomolecules present in microbial biomass, including proteins, lipids, carbohydrates, and nucleic acids (6, 7). Each biomolecule has specific functional groups which possess vibrational modes with unique spectral signatures when assessed by FTIR (8). Therefore, FTIR spectroscopy has been suggested as a powerful tool for compositional and structural analysis of microbial biomass. For example, by examining protein spectral region 1700 – 1500 cm^{-1} details on protein's secondary structure such as presence of α-helices or β-sheets can be obtained (9). It has been

shown that FTIR spectra can be used for the estimation of a relative total lipid content and its changes in oleaginous microorganisms (10-12). Further, numerous studies reported successful application of FTIR spectroscopy for the identification of microorganisms, where it has been shown that FTIR biochemical signatures of different bacteria often reflect their phylogenetic relationships (13, 14). FTIR spectroscopy can contribute to understanding of molecular underpinnings of phenomena like adaptive tolerance responses of bacteria when they are subjected to various environmental stress conditions (15, 16).

FTIR analysis is little destructive allowing to chemically profile cells in their natural intact form. The typical protocol to prepare microbial cells for FTIR analysis includes: (i) cultivation step to obtain enough amount of microbial biomass, (ii) washing of microbial cells to remove medium components which may interfere with biomass signals on the FTIR spectra, (iii) depositing a small amount of cell culture (8-10 µl) on the FTIR silica plate with subsequent drying at room temperature before measurements (17). One of the main advantageous of FTIR spectroscopy is that it can be performed in a high throughput setting where cultivation of microorganisms is done in microtiter plates and biomass preparation is automated (18-20). Therefore, FTIR spectroscopy has been positioned as a next generation phenotyping technique for building chemotaxonomic maps of existing microbes and identification of newly isolated (21, 22).

FTIR spectroscopy for the characterization and identification of bacteria has been employed since 90s. (23-30). Numerous studies have been done on characterization of bacterial metabolites such as lipidic compounds (31, 32) exopolysaccharides (33), biosurfactants (34), enzymes (35) as well as bacterial processes such fermentation (36, 37) , bioremediation (38), degradation of feathers (35), degradation of plastics (39) and petroleum materials (40). Recently, we successfully applied FTIR spectroscopy for biochemical characterization and bioprospecting of green snow Antarctic bacteria (35, 41, 42). In one of the studies, we have shown that green-snow Antarctic bacteria cultivated in two forms of culture medium – semi-solid agar and broth and at different temperatures possessed considerable differences in cell chemistry (41). These biochemical cellular differences were associated with the changes across all spectral regions of the FTIR spectrum (6): (i) lipid region 3050 – 2800 cm^{-1} and 1700 – 1800 cm^{-1}

indicating changes in membrane lipids and some storage compounds such as polyhydroxyalkanoates (PHAs), (ii) protein region 1700 – 1500 cm^{-1} providing information on the protein structure, (iii) mixed region 1500 – 1200 cm^{-1} where the information about some proteins, lipids and phosphorus compounds structure is reflected, (iv) polysaccharide region 1200 – 700 cm^{-1} reflecting information about cell wall and storage polysaccharides and (v) so called fingerprint region at 900 – 700 cm^{-1} consisting of mainly peaks without any special assignment but very characteristic for different microbial strains (6).

The main aim of the present study was to perform global biochemical characterization of newly isolated bacteria from Antarctic meltwater temporary ponds and evaluate cellular biochemical changes in bacterial cells when grown in different culture forms and temperatures by high-throughput FTIR spectroscopy.

Materials and Methods

Bacterial strains

Twenty-nine fast-growing Antarctic bacteria from the Belarussian Collection of Non-pathogenic Microorganisms (Institute of Microbiology of the National Academy of Science of Belarus) were used in the study. The bacteria are Gram-positive and Gram-negative, psychrotrophic and belong to seventeen species. The bacteria were isolated from water samples collected during the 5th Belarusian Antarctic Expedition in the austral summer season (January 2013) from the middle part of the water column of nine non-flowing temporary meltwater ponds (TMPs) located in rock baths of the Vecherny region of the Thala Hills oasis in the central part of Enderby Land (East Antarctica). Identification by 16S rRNA gene sequencing and comprehensive physiological characterization (enzymatic activity, optimal growth temperature and antibiotic resistance) of the isolates were previously reported (43).

Experiment design and cultivation conditions

For the biochemical profiling by FTIR spectroscopy, bacteria were cultivated on brain heart infusion agar (BHIA) and broth (BHIB) (Sigma Aldrich, USA) at 18 °C. Cultivation on BHIA was performed for 3 – 5 days, depending on the isolate, to obtain enough biomass for FTIR measurements. Cultivation in BHIB was performed at 18 °C for 3 days for all isolates in the Duetz Microtiter Plate System – Duetz-

MTPS (Enzyscreen, Heemstede, Netherlands), consisting of 24-square low polypropylene deepwell plates, low-evaporation sandwich covers and extra high cover clamp system as was previously described (18-20, 44-46). Cultivation media and Duetz-MTPS were sterilized by autoclaving at 121 °C for 15 min before inoculation. The autoclaved MTPs were filled with 3 mL of sterile broth medium per well, and each well was inoculated with a single colony of fresh cultures prepared on BHIA. For the sterility control, one well in each microtiter plate was filled with the medium without inoculation. Duetz-MTPS were mounted on the shaking platform of MAXQ 4000 shaking incubator (Thermo Fisher Scientific, Waltham, MA, USA) and incubated for 3 days at 18 °C with 370 rpm agitation speed (1.9 cm circular orbit). For each bacterial isolate and media, cultivations were done in three biological replicates which were prepared from separate Petri dishes and MTPs and performed as independent experiments.

In order to evaluate effect of temperature on the total cellular biochemical profile, bacterial isolates were cultivated at 4, 10, 15, 25, 30 and 37°C on BHIA. The cultivation time was for 1 – 12 days depending on the cultivation temperature and strain growth ability (Table 1S in SM). The cultivations were performed in two independent biological replicates for each bacterial isolate and temperature.

Preparation of bacterial biomass for FTIR measurements

Bacterial biomass was separated from the supernatant by centrifugation (Heraeus Multifuge X1R, Thermo Scientific, Waltham, MA, USA) at 25.200 g at 4°C for 30 min and washed with distilled water three times. Further, at the last washing step, 100 – 500 µL of distilled water was added to the cell pellet and re-suspended. 10 µL of both the homogenized bacterial suspension and supernatant samples diluted ten times with water were pipetted onto the IR-light-transparent silicon 384-well silica microplates (Bruker Optics GmbH, Ettlingen, Germany) in three technical replicates, and dried at room temperature for at least 1 hours before the analysis.

FTIR spectroscopy analysis

FTIR transmittance spectra were measured using a high-throughput screening extension unit (HTS-XT) coupled to the Vertex 70 FTIR spectrometer (both Bruker Optik, Germany). The FTIR system was

equipped with a globar mid-IR source and a deuterated L-alanine doped triglycine sulfate (DLaTGS) detector. The HTS-FTIR spectra were recorded with a total of 64 scans, using Blackman-Harris 3-Term apodization, spectral resolution of 6 cm^{-1}, and digital spacing of 1.928 cm^{-1}, over the range of 4000–400 cm^{-1}, and an aperture of 6 mm. The ratio of a sample spectrum to a spectrum of the empty IR transparent microplate was used to calculate a final spectrum. Background spectra of the silica microplate were collected prior to each sample measurement to account for variations in water vapor and CO2. Generated transmittance spectra were exported for further analysis. Each sample was analysed in three technical replicates. For data acquisition and instrument control, the OPUS software (Bruker Optik GmbH, Germany) was used.

Estimation of chemical variability

In order to evaluate chemical variability of bacterial biomass produced at different conditions, FTIR data were used to estimate Pearson's correlation coefficient (PCC) which was expressed as $(1–PCC)\times10^3$ for the whole spectrum and the following spectral regions: lipid region at 3050 – 2800 cm^{-1} combined with ester region 1800 – 1700 cm^{-1}, protein region at 1700 – 1500 cm^{-1}, mixed region at 1500 – 1200 cm^{-1}, and polysaccharide region at 1200 – 700 cm^{-1}. Variability was estimated for (1) technical and biological replicates, (2) cultivation conditions such as time, temperatures, and media and (3) phylogenetic units such as strain, specie and genus. Variability was calculated for all data together and separately for data acquired from agar and broth cultivations. Chemical variability of spectra within a group was estimated by median distance from a sample to the center of the group. The center of the group was calculated as a mean of all spectra within the group and the distance was calculated as 1 - Pearson correlation coefficient. The closer this value is to 0, the more similar the individual spectrum is to the mean spectrum, indicating lower variability. As some categories may include several groups (e.g. 17 species), the variability were calculated first for each group and then averaged.

Spectral preprocessing and multivariate data analysis

Prior to data analysis, the spectra were quality checked to select good quality spectra using quality test developed by Tafintseva et al. (22, 47, 48). The selected spectra were preprocessed in the following

way: (1) averaging of technical replicates for each sample by calculating arithmetic mean; (2) applying Savitzky−Golay algorithm with second polynomial degree and different window sizes depending on the spectral region were used – 9 points for lipids region, 19 points for protein region and 13 for carbohydrate region, 11 points when the whole spectral region was used (Savitzky and Golay 1964); (3) splitting the data into three informative regions based on the type of macromolecules: 3050–2800 cm^{-1} and 1800–1700 cm^{-1} for lipids, 1700–1500 cm^{-1} for proteins, mixed region at 1500–1200 cm^{-1} and 1200–700 cm^{-1} for polysaccharides or the whole spectral region 4000-400 cm^{-1}; (4) extended multiplicative signal correction (EMSC) in order to separate informative signals from spectral artefacts and minimize variability due to light scattering or sample thickness (48-53).

After preprocessing, multivariate data analysis techniques such as principal component analysis (PCA) was applied to analyze total cellular biochemical profile of bacteria reveal underlying patterns and to visually represent the positions of data points in fewer dimensions, preserving maximum information, and investigating relationships among dependent variables (54). For PCA whole spectral region as well as single spectral regions of lipids, proteins, mixed and polysaccharides were used as previously described in (42). Further, correlation analysis was performed to investigate the effect of temperature. Due to that variability between different genera was higher than variability between temperatures, correlation analysis was done for each specie separately using second derivative preprocessed spectra, second order polynomial, and 13, 17, 21, and 13 windows sizes for the lipid, mixed, protein, and polysaccharide regions, respectively. For the correlation analysis all peaks listed in Table 2 were used. The Unscrambler, V10.01 (CAMO PROCESS AS, Oslo, Norway) and algorithms in Matlab, V12.a (The Mathworks, Inc., Natick, MA) were used to perform the analysis. Orange data mining toolbox version 3.31.1 (University of Ljubljana, Ljubljana, Slovenia) was used for the preprocessing spectral analysis, ratiometric analysis, PCA analysis (55, 56).

Results

Variability of the total cellular biochemical profile

Due to that bacterial biomass used for FTIR analysis was obtained from different cultivations using various media and cultivation conditions that may influence chemical composition of the biomass, therefore, variability of the biochemical profile was estimated by calculating PCC from the FTIR spectra and the results are presented in Table 2. The estimates PCC showed that agar cultivations resulted in less chemical variability of bacterial biomass than liquid culture cultivations (Table 2). The highest chemical variability was observed between different genera followed by species and strains, while the lowest variability was for biological and technical replicates. Variability between strains of the same specie was much higher than the variability in biological and technical replicates (Table 2). Carbohydrate spectral region showed the highest variability for all tested levels, while the lowest variability was observed for lipid region for biomass obtained from agar and proteins for biomass from broth. Temperature affected chemical variability of the bacterial biomass, for example increase in temperature resulted in the higher variability for carbohydrate, lipid and mixed regions, while protein region showed increase in variability when both low and high temperatures were used (Table 2). Variability between cultivation days was lower than variability between cultivation temperatures.

Biochemical profile of Antarctic meltwater bacteria grown on agar and broth

Total cellular biochemical profile of the studied Antarctic meltwater bacteria using FTIR spectroscopy was first evaluated when bacteria were grown on agar and in liquid BHI media at 18°C. Overall FTIR biochemical profiles of the studied bacteria grown on agar and in broth are presented on Figure 1 and Table 1, which shows averaged spectra and the assignment of the main characteristic peaks and their difference for Gram-positive and Gram-negative bacteria, respectively.

A visual comparison of FTIR biochemical spectral profiles revealed distinct chemical differences which are related to phylogeny of the studied bacteria and/or growth medium. Several shifts for characteristic peaks were observed for the spectra of bacteria from different Gram groups. Thus, all Gram-negative bacteria grown on agar and in broth media showed higher absorbance values of all lipid peaks compared to Gram-positive bacteria, that is an indication of a higher total lipid content in their cells, possibly due to the presence of the cell wall, which is rich in lipopolysaccharides and phospholipids (Figure 1 A and B). The averaged spectrum of Gram-negative bacteria had elevated lipid peaks at 3006 cm^{-1}, 2925 cm^{-1}, 2853 cm^{-1} and 1741 cm^{-1} indicating a higher content of unsaturated, saturated lipids and polyesters,

202 respectively (Figure 1 A and B). A slight peak shift was detected for -CH_3 group from 2960 cm^{-1} for
203 Gram-negative bacteria to 2962 cm^{-1} for Gram-positive bacteria (Figure A and B, Table 1). Also, another
204 peak shift was detected for the ester peak, where it was at 1743 cm^{-1} for Gram-positive bacteria and at
205 1741 cm^{-1} for Gram-negative (Figure and Table 1). Further, a peak at 1466 cm^{-1} related to C-H
206 deformation/scissoring of -CH_2 group mainly in lipids with a little contribution from proteins was
207 detected on the averaged spectrum of Gram-negative bacteria and it was absent for the Gram-positive
208 bacteria cultivated on agar and broth (Figure A and B). While averaged spectrum of Gram-positive
209 bacteria showed a higher absorbance for the peak at 1452 cm^{-1} related to -CH_3 deformation in lipids.
210 (Figure 1, Table 1 A and B).
211 Proteins are the major biochemical components of bacterial cells, therefore, typically they are
212 represented by the peaks with the highest absorbance in the region 1700 – 1500 cm^{-1}. This was also
213 observed for the studied Antarctic bacteria grown on agar and broth media, where the most characteristic
214 protein peaks were C=O stretching vibrations in amino acids (Amide I) at 1656 cm^{-1} associated with α-
215 helical structures, peak at 1636/1640 cm^{-1} associated with β-pleated sheet structures, peak at 1548 cm^{-1}
216 related to N-H deformation vibrations (Amide II) and the peak at 1311 cm^{-1} associated with C-N
217 vibrations of Amide III bond. The main differences in the protein region for the bacteria grown on agar
218 and in broth were related to the lower absorbance of protein peaks in Gram-negative bacteria and
219 appearance of a shift for the C=O stretching Amide I peak at 1636 cm^{-1} for Gram-negative to 1640 cm^{-1}
220 for Gram-positive (Figure 1 A and B, Table 1).
221 Further, some differences between Gram-positive and Gram-negative bacteria grown on agar and in
222 broth were observed in mixed spectral region 1500-1200 and polysaccharide spectral region 1200–700
223 cm^{-1}, were peaks associated with phosphodiester group present in various molecules, such as DNA,
224 phospholipids and teichoic acids and lipoteichoic acid at 1400 cm^{-1}, 1240 cm^{-1} had higher absorbance
225 values for Gram-positive bacteria and peak at 1170 cm^{-1} had a higher absorbance values for the spectra
226 of Gram-negative bacteria. For the spectra of Gram-positive bacteria, the peak at 1156 cm^{-1} associated
227 with C-O, C-C str., C-O-H, C-O-C def. in carbohydrates had higher absorbance had higher absorbance
228 (Figure 1, Table 1 A and B). Interestingly, the difference between Gram-groups in carbohydrate region
229 is significantly bigger when bacteria were cultivated in broth medium then on agar.

After visual comparison reported above, preprocessed FTIR spectra of bacterial biomass were analysed by PCA to investigate biochemical relationships between biochemical profiles of the studied bacteria grown on different forms of BHI medium. PCA score and loading plots for the whole spectral region are displayed on the Figure 2 A and B, respectively. It can be seen that samples of Gram-negative bacteria except *Acinetobacter lwoffii* BIM B – 1558 and *Pseudomonas lundensis* isolates are located in the area of positive PC1 score that indicates a higher lipid content in the cells of these bacteria, while most of the samples of Gram-positive bacteria are located in the area of negative PC1 scores, meaning higher protein content in the cells (Figure 2 A). The most significant peaks, identified on the loading plot, to be responsible for the distribution of samples along the PC1 axis are lipid peaks associated with (i) chain length (-CH_2 stretching at 2924 cm^{-1} and 2853 cm^{-1} and -CH_2 bending at 1466 cm^{-1}), (ii) relative total content of lipidic compounds (C=O stretching at 1738 cm^{-1}) and protein peaks associated with proteins' structure (-C=O stretching at 1627 cm^{-1} and 1646 cm^{-1}) (Figure 2B). A separation along the PC2 axis is mainly due to the proteins and the following peaks were registered on the loading plot as significant: peaks associated with the -C=O stretching in proteins at 1627 cm^{-1}, 1513 cm^{-1} and 1400 cm^{-1}. Both PC1 and PC2 appears to be responsible for the dissimilarities between different bacterial species cultivated on different media forms (agar and broth) (Figure 2A).

When evaluating clustering on genus level, it should be noted that some genera were represented only by one specie and/or strain, therefore the reported results cannot be used to draw conclusions on biochemical relationships of these genera. Genera represented by two and more species were discussed. The total cellular biochemical profile of bacteria from genera *Carnobacterium* showed to be little affected by the cultivation media. It can be seen from the PCA score plot that specie-specific variability inside of genera *Pseudomonas* and *Arthrobacter* is high, and each specie forms a separate cluster for cultivation on agar and in broth media. Interestingly, bacteria from genus *Carnobacterium* did not show a big variation of biochemical profile for different species cultivated on different media. Interestingly, *Pseudomonas peli* BIM B – 1542 grown on agar and in broth clustered outside of other *Pseudomonas* strains and can be characterized by a higher lipid content.

To uncover specie-specific differences in biochemical profile of the studied bacteria, visual comparison of the preprocessed FTIR spectra was performed for each specie separately and it presented on Figure

1S. It could be seen that the most pronounced effect of cultivation media on the total cellular biochemical profile was detected for Gram-positive bacteria from phylum Actinobacteria, especially it was visible for *Micrococcus luteus* BIM B-1545. Further, it can be seen that lipid region is little affected by the cultivation media and visible changes were observed only for all strains *Pseudomonas peli* in the peaks related to CH_2 stretching in lipids at 2935 cm^{-1} and 2853 cm^{-1} and esters at 1741 cm^{-1} and *Micrococcus luteus* BIM B-1545 in the peaks related to CH_3 stretching in lipids at 2960 cm^{-1} and 2875 cm^{-1} and esters at 1743 cm^{-1}. In protein region, changes in intensity of Amid I band at 1565 cm^{-1}, 1636 cm^{-1} and Amid II at 1548 cm^{-1} was slightly higher after bacteria were cultivated on agar for Gram-positive bacteria and lower for Gram-negative. Additionally, slight shift to lower wavenumbers was detected for amide I peak at 1640 cm^{-1} related to β-sheet structures of proteins on broth media compare to agar media for Gram-negative bacteria. In mixed region highest effect was observed for *Micrococcus luteus* BIM B-1545 and bacteria related to *Arthrobacter* genus in peaks related to CH_2 bending in lipids with little contributions from protein (membrane lipids) at 1400 cm^{-1} and in vibrational modes of the phosphate groups at 1240 cm^{-1} .The polysaccharide region showed to be the most affected by cultivation media and numerous changes in polysaccharides were recorded for *Micrococcus luteus* BIM B-1545, *Leifsonia* sp. BIM B – 1567 and *Arthrobacter agilis* BIM B – 1543 (Figure 1S).

In order to gain a deeper understanding on what biomolecules are the main biomarkers for differentiating the studied bacteria and what biomolecules are more affected by the cultivation media, we conducted PCA of lipid, protein, mixed, and carbohydrate regions. The analysis revealed that lipid region is the most discriminative and provide clustering well aligned with phylogeny of the studied bacteria. This was observed for majority of the bacteria cultivated on both forms of BHI medium, and spectra from agar-cultivated bacteria in most of the cases provided better phylogeny-aligned clustering than broth (Figure 4 A and E). For example, bacteria from genera *Carnobacterium* and *Micrococcus* clustered distinctly from each other after cultivation on agar, while showed overlapping clustering after broth cultivation. Some bacteria showed more discriminative clustering after being grown in broth than on agar, for example, *Flavobacterium degerlachei* BIM B – 1562, *Acinetobacter lwoffii* BIM B – 1558, *Brachybacterium paraconglomeratum* BIM B – 1571 showed FTIR profile overlapping with other strains when grown on agar and formed individual clusters after cultivation in broth (Figure 4E). The

clustering on the PCA score plot of the lipid region is defined by the same lipid peaks as in PCA of the whole spectral region with addition of peak at 1714 cm^{-1} indicating a presence of free fatty acids (Figure 5 A and E).

The PCA of protein region showed a high level of similarity between many bacteria from different genera and species, while Gram groups clustered separately (Figure 4B). The following bacteria cultivated on agar exhibited relatively distinct clustering according to proteins: (i) *Sporosarcina* sp BIM B – 1539, *Micrococcus luteus* BIM B – 1545, (ii) all strains related to *Pseudomonas leptonychotis* and *Shewanella baltica* (Figure 4B). Cultivation in broth resulted in a relatively high variation of protein profile between different bacteria and even biological replicates (Figure 4F). The observed distribution of strains on the PCA score plot when using protein spectral region was based on the contribution from peaks at 1636 cm^{-1} and 1656 cm^{-1} related to β-pleated sheet and a-helical structures, respectively, and -C=O stretching Amide I peak at 1680 cm^{-1} related to antiparallel pleated sheets (Figure 5 B and F).

The PCA analysis of the mixed spectral region showed a clear clustering according to Gram, genus and specie phylogeny for bacteria grown on agar and in broth. The loading plot of PC1 indicates that clustering according to Gram groups is defined by the lipid related peaks associated with $-CH_2$ stretching at 1463 cm^{-1} and C= O symmetric stretching in amino acids and fatty acyl chains (peptidoglycan) at 1400 cm^{-1} (Figure 5 C and G).

PCA analysis of polysaccharide spectral region showed distinctive clustering of several agar-cultivated bacterial species, for example, *Pseudomonas leptonychotis* strains and *Acinetobacter lwoffii* BIM B – 1558, *Arthrobacter agilis* BIM B – 1543, *Brachybacterium paraconglomeratum* BIM B – 1571 and *Micrococcus luteus* BIM B – 1545 (Figure 4 D and H). From the PCA loading plots it can be seen that clustering using polysaccharide region was defined by the peaks related to νC-O, νC-C, C-O-C, νP-O-C, νP-O-P group vibrations in polysaccharide sugar rings of the cell wall polysaccharides and peptidoglycan (Figure 5 D and H).

In addition to biomass, FTIR analysis of supernatants obtained after centrifugation of bacterial cultures grown in BHI broth was performed. FTIR spectra of pure BHI broth show that the main characteristic peaks are C=O stretching of the proteins at 1645 cm^{-1} and 1570 cm^{-1}, C= O symmetric stretching of COO- group in amino acids at 1400 cm^{-1} and peaks associated with phosphorus containing compounds

at 1083 cm^{-1} (Figure 2S). Analysis of supernatant spectra showed that bacteria from genus *Carnobacterium* and *Facklamia tabacinasalis* BIM B – 1577 strain were characterized by additional peak at 1570 cm^{-1} (Figure 2S). Similarly, additional peaks at 2338 cm^{-1}, 835 cm^{-1} and 700 cm^{-1} occurred for *Shewanella baltica, Pseudomonas lundensis* and *Pseudomonas leptonychotis* species (Figure 2S in SM). The PCA analysis of supernatant revealed a clear separation along PC1 for *Shewanella baltica* species from all other strains and another clear cluster was represented by *Pseudomonas lundensis* and *Pseudomonas leptonychotis* species (Figure 3A). The loading plot shows that the main changes occurred in protein region (Figure 3B).

Impact of cultivation temperature on the cellular biochemical profile of meltwater bacteria

To investigate the impact of temperature on the total cellular biochemical profile of the Antarctic meltwater bacteria, we conducted cultivation experiments at various temperatures using BHIA medium. BHIA medium was chosen due to that it provided better clustering according to the phylogeny. The PCA analysis of the whole spectral region of the entire dataset of bacteria grown at different temperatures showed similar clustering as it was reported on the Figure 6, where Gram-negative bacteria with the exception of *Acinetobacter* and *Pseudomonas lundensis* strains, exhibited predominantly positive PC1 scores, suggesting higher lipid content, while Gram-positive bacteria predominantly displayed negative PC1 scores, indicating a higher protein content (Figure 6 A). In addition, a clear separation along the PC2 axis was observed between strains *Pseudomonas leptonychotis* (BIM B – 1559, BIM B – 1568, BIM B – 1566), *Pseudomonas peli* (BIM B – 1560, BIM B – 1569, BIM B – 1546, BIM B – 1552, BIM B – 1542, BIM B – 1548), *Flavobacterium degerlachei* BIM B – 1562 and *Shewanella baltica* (BIM B – 1565, BIM B – 1557, BIM B – 1561 and BIM B – 1563), which according to the loading plot could be associated with the differences in proteins, phosphorus-containing molecules, and carbohydrates.

Both, PC1 and PC2 were found to contribute to the dissimilarities observed between different species of bacteria cultivated at different temperatures (Figure 6A). Several bacterial species and strains showed a noteworthy specie-specific differences in clustering when grown at different temperatures (Figure 6 A):

i. *Pseudomonas lundensis* BIM B – 1554, BIM B – 1555 and BIM B – 1556 grown at 37°C

ii. *Flavobacterium degerlachei* BIM B – 1562 grown at 4°C/10°C and 18°C/25°C

iii. *Micrococcus luteus* BIM B – 1545 grown at 37°C, 25°C and 18°C

iv. Strains of *Pseudomonas leptonychotis* and *Pseudomonas peli* grown at 25°C

v. Strains of *Shewanella baltica* grown at 4°C and 30°C

vi. *Acinetobacter lwoffii* BIM B – 1558 grown at 18°C/25°C, 4°C/30°C and 10°C

vii. *Brachybacterium paraconglomeratum* and *Facklamia tabacinasalis* grown at 10°C

viii. *Shewanella baltica* cultivated at all temperatures was the only specie grouped separately from all other species with almost no overlapping.

A visual comparison of different spectral regions for the studied bacterial species indicated that lipid/ester region 1800-1700 cm^{-1} is relatively consistent and little affected by the temperature (Figure 3S in SM). A change in the lipid region was observed for *Pseudomonas leptonychotis* strains and it was related to an increase in absorbance for the ester peak at 1742 cm^{-1} at low and extremely high temperatures. Further, an increase of intensity for the peak at 1713 cm^{-1} associated with C=O stretching in free fatty acids was observed for many bacteria grown at lower temperatures. For *Pseudomonas lundensis* strains and *Acinetobacter lwoffii* BIM B – 1558 strains peak at 1713 cm^{-1} disappeared when bacteria were grown at 37°C (Figure 3S). This is an indication of increased production and possibly accumulation of free fatty acids with a temperature change. For the protein region 1700-1500 cm^{-1} the biggest effect of temperature in the form of shifts and change in intensity was detected for amide I peak at 1640 cm^{-1} and 1656 cm^{-1} related to β-sheet and α-helix structures of proteins, respectively. A shift to lower wavenumbers for the peak at 1640 cm^{-1} was detected for *Pseudomonas lundensis* strains *and Acinetobacter lwoffii* BIM B – 1558 when grown at 37°C (Figure 3S), and an increase of protein-related peaks was detected for *Carnobacterium funditum* BIM B – 1541 and *Carnobacterium iners* BIM B – 1544 (Figure 3S).

The most significant temperature-triggered alterations were recorded in the mixed and polysaccharide spectral regions 1500-900 cm^{-1}, where signals related to carbohydrates, nucleic acids and phosphates are present. Thus, an increase of intensity for the phosphodiester-related bands at 1240 cm^{-1} in mixed region and at 1083 cm^{-1} in polysaccharide region along with temperature decrease was recorded for

majority of Gram-negative bacteria while changes for Gram-positive bacteria were less intense with exception of *Arthrobacter agilis* BIM B – 1543 (Figure 3S).

The PCA correlation analysis was performed individually for each species to uncover temperature effect individually for each specie. The resulting correlation loading plots presented on the Figure 7 illustrate the correlations between spectral variables (characteristic peaks) and design variables (temperature). As a result, correlation loading plots showing a subset of the most relevant spectral variables (peaks) and temperature were obtained. Red and blue circles indicate the limit for 50% explained variance (red) and 100% explained variance (blue) and the variable close to the center of the correlation plot are less important. The variables located outside of the red circle exhibit a high degree of correlation, while variables located closer to the center are considered less important. By examining the correlation loading plots, the correlation between temperature and selected infrared peaks was assessed that was used as an indication of changes of cellular biochemical profile. In a correlation loading plot, the following types of correlation can be found: (i) Positive correlation refers to a relationship where two variables change in the same direction, meaning that if one variable increases, another variable also tends to increase. The positive correlation is indicated by the variables being positioned in the same quadrant or direction away from the center on the correlation loading plot. (ii) Negative correlation, indicates a relationship where two variables change in opposite directions, meaning that if one variable increases, another variable tends to decrease. Negative correlation is represented by variables positioned in different quadrants or directions from the center on the correlation loading plot.

The most consistent FTIR biochemical profile for all studied species was at 18°C while the growth at 25°C triggered changes in *Pseudomonas leptonychotis* strains (Figure 7A), *Pseudomonas peli* strains (Figure 7B) , *Flavobacterium degerlachei* BIM B – 1562 (Figure 7F) , *Arthrobacter alpinus* BIM B – 1549 (Figure 7H), *Arthrobacter agilis* BIM B – 1543 (Figure 7G) , where each specie had specific responses. The growth at higher temperatures 30°C and 37°C was affecting only *Shewanella baltica* strains and *Pseudomonas lundensis, Acinetobacter lwoffii* BIM B – 1558 strains, respectively, where the main changes were associated with proteins and polysaccharides (Figure 7D and 7C). Low temperatures (4°C and 10°C) showed to have the highest effect on majority of the studied species, except all *Pseudomonas* species, *Arthrobacter alpinus* BIM B – 1549, *Leifsonia* sp. BIM B – 1567 and

Carnobacterium iners BIM B – 1544 where each specie showed specific responses (Figure 7). Correlation analysis showed that *Micrococcus luteus* BIM B – 1545 (Figure 7J) and *Leifsonia* sp. BIM B – 1567 (Figure 7K) have consistent biochemical profile not affected by the temperature.

Discussion

Characterization of the Antarctic meltwater bacteria by FTIR spectroscopy showed biochemical differences of these bacteria on various phylogenetic levels and the most obvious differences were observed for different Gram groups, which showed considerable variation in lipid region. These results are in accordance with the previously reported and can be explained by the fact that Gram-positive bacteria have naturally higher peptidoglycan content, whereas Gram-negative bacteria have higher lipid content (57-59). Gram-negative bacteria have an outer membrane, in addition to their inner membrane, which composed of lipopolysaccharides (LPS) and phospholipids that can contribute to the higher total lipid content. Second noticeable differences between two Gram groups were related to peaks associated with phosphodiester group present in various molecules, such as DNA, phospholipids and teichoic acids and lipoteichoic acid (58). In Gram-positive bacteria these peaks seem to be associated with mainly teichoic acids and lipoteichoic acid due to a low amount of phospholipids (58). In addition, FTIR analysis revealed differences in protein structure between two Gram groups. The studied bacteria are psychrotrophic but according to the literature the same differences between Gram-negative and Gram-positive bacteria characterized as mesophilic can be expected (8, 58).

In addition to Gram classification, FTIR profiling provided clear clustering on genus and specie level that was well aligned with phylogeny. Cultivation on agar provided better phylogeny-aligned clustering than cultivation on broth. Also, chemical variability was much lower for bacterial biomass obtained from agar cultivation than from broth cultivation. This can be due to that agar-based cultivation are static and characterized by the consistency of conditions such as oxygen availability and temperature, while cultivation in broth can vary in oxygen accessibility and overall gas transfer. Further, the total cellular biochemical profile of bacteria grown on agar and broth differed considerably especially for some spectral regions such as polysaccharide region. Interestingly, lipid spectral region was little affected by different forms of cultivation medium and provided clear phylogeny-aligned clustering on genus and specie levels. This might be an indication that lipids are the most steady component of

425 bacterial cells. As its well known, fatty acid profile of lipids is also used as classification biomarkers
426 for chemotaxonomy of bacteria (60).
427 In polar regions, temperature is a factor considerably affecting microbiota (61) and it plays a crucial
428 role in developing adaptation mechanisms in microbes inhabiting these regions (62). Therefore, in this
429 study we investigated the impact of temperature on the total cellular biochemical profile of the Antarctic
430 meltwater bacteria. Temperature experiments were performed using agar BHI medium since it provided
431 clustering well aligned with the phylogeny of the studied bacteria. The observed results indicate that
432 temperature impact is specie-specific and variation of biochemical profile for different strains within a
433 single species is less than variations caused by temperature as it was also shown previously (42). For
434 majority of the tested bacteria, the highest impact on cell chemistry was from low and high temperature
435 and lipids were less affected in comparison to proteins and polysaccharides. However, some bacteria,
436 as for example, *Pseudomonas leptonychotis* had an increase of absorbance for ester peak at 1743 cm^{-1}
437 when grown at low and high temperatures that could be due to the accumulation of PHAs to increase
438 the survival capabilities. The same results were previously reported for other strains of genus
439 *Pseudomonas* (63). Further, for many studied strains, proteins and especially polysaccharides were
440 considerably affected by temperature meaning that these cell components might play a key role in
441 temperature adaptation and survival. For example, an increase in intensity of protein peaks with
442 temperature change was observed for psychrophiles *Carnobacterium funditum* BIM B – 1541 and
443 *Carnobacterium iners* BIM B – 1544 that could be due to about possible production of cold-shock
444 proteins as was previously described (64). Overall, correlation analysis showed that the biggest
445 temperature impact was for the bacteria with the wide growth temperature range and able to grow at 4
446 to 37°C such as *Pseudomonas lundensis* strains and *Acinetobacter lwoffii* BIM B – 1558. Correlation
447 analysis showed that *Micrococcus luteus* BIM B – 1545 and *Leifsonia* sp. BIM B – 1567 have consistent
448 biochemical profile not affected by the temperature. To the authors knowledge, this study is, for the
449 first time, reporting a complexity of temperature-triggered cellular biochemical responses where
450 proteins and polysaccharides stay as the most affected cell components.
451
452 **Conclusion**

This study, for the first time, reports the total cellular biochemical profile of the Antarctic meltwater bacteria as well as its variation under different cultivation conditions. The results suggest that agar is the best form of BHI medium for understanding biochemical nature of phylogenetic relations and studying effect of abiotic factors on cell chemistry. Temperature-induced changes in the cellular biochemical profile were specie-specific, with the most significant effects observed in bacteria having a broad growth temperature range. Furthermore, the study found that alterations in lipids and proteins due to temperature were less pronounced and detected only in few species while changes in polysaccharides were more common for all bacteria. Interesting observation was made for *Micrococcus luteus* BIM B – 1545 remaining stable biochemical profile in a big range of temperatures but extensively affected by form of cultivation media what need to be further explored. Overall, FTIR spectroscopy for bacterial profiling offers a promising approach for efficiently screening the impact of cultivation conditions in high-throughput settings.

Author Contributions

Conceptualization: Volha Akulava, Volha Shapaval, Achim Kohler**, Data curation:** Volha Akulava, Valeria Tafintseva, Uladzislau Blazhko, **Formal analysis:** Volha Akulava, **Funding acquisition:** Achim Kohler, Volha Shapaval. **Investigation:** Volha Akulava, **Methodology:** Volha Shapaval, Volha Akulava, **Resources:** Volha Shapaval, Achim Kohler, **Supervision:** Volha Shapaval, Achim Kohler, Leonid Valentovich, Uladzislau Miamin, **Validation:** Volha Akulava, Volha Shapaval, **Visualization:** Volha Akulava, Valeria Tafintseva, **Writing – original draft:** Volha Akulava, **Writing – review & editing:** Volha Akulava, Volha Shapaval, Valeria Tafintseva, Uladzislau Blazhko, Leonid Valentovich, Uladzislau Miamin, Achim Kohler

Funding

This research was supported by the project “Belanoda—Multidisciplinary graduate and post-graduate education in big data analysis for life sciences” (CPEA-LT-2016/10126), funded by the Eurasia program, Norwegian Agency for International Cooperation and Quality Enhancement in Higher Education (Diku), and the Belanoda Digital learning platform for boosting multidisciplinary education

in data analysis for life sciences in the Eurasia region (CPEA-STA-2019/10025). Additional support was covered by BYPROVALUE (NFR-MATFONDAVTALE- 301834/E50), SAFE (NFR-BIONÆR 327114), SFI-IB (NFR-SFI 309558) and OIL4FEED (NFR-HAVBRUK2, 302543/E40) projects.

Conflict of Interest

The authors declare that the research was conducted in the absence of any commercial or financial relationships that could be construed as a potential conflict of interest.

Tables

Table 1. Peaks assignment for the FTIR-HTS spectra of Antarctic bacteria. Peak frequencies have been obtained from second derivative spectra. Abbreviations: asym, antisymmetric; sym, symmetric; str, stretching; def, deformation (23, 24, 27, 31, 58, 65-69).

Wavenumber (cm^{-1})		**Molecular vibration**	**Cell component**
Gram -	**Gram+**		
Lipid region 3050-2800 cm^{-1} + 1800-1700 cm^{-1}			
3006		=C-H stretching	Polyunsaturated lipids
2960	2962	-C-H (CH_3) stretching	Mainly unsaturated lipids, little contribution from proteins, carbohydrates, nucleic acids
2925		-C-H (CH_2) stretching	
2875		-C-H (CH_3) stretching	
2853		-C-H (CH_2) stretching	
1742		>C= O stretching	Acyl glycerides, esters, lipids
1714		νC=O stretching	Esters, carboxylic acids
Protein region 1700-1500 cm^{-1}			
1693, 1680	1693,1680	-C=O stretching	Antiparallel pleated sheets of amide I band
1656		-C=O stretching	amide I of a-helical structures
1636	1640	-C=O stretching	amide I of β-pleated sheet structures
1570		νCOO asym	Asparatate, glutamate
1548		CONH bending	Amid II
1513		Benzene ring stretch	Aromatic amino acids (Phe, Tyr, Trp)
Mixed region/ 1500-1200 cm^{-1}			
1466	-	CH2 deformation	mainly lipids with little contributions from protein (membrane lipids)
-	1453	CH3 deformation	
1376		C-O	
1400		C= O symmetric stretching of COO^-	Amino acids, fatty acyl chains (peptidoglycan)
1311		C-N	Amide III band
1240	1243		

1222	1220	P=O asymmetric stretching of >PO2	Phosphodiesters, phospholipids (membrane), teichoic acids, lipoteichoic acids (cell wall), nucleic acids (nucleoid) mainly nucleic acids with the little contribution from phospholipids
Carbohydrate region 1200-700 cm^{-1}			
1082		C–O stretching of glycogen PO−2 symmetric stretching	Phosphodiesters, phospholipids (membrane), nucleic acids (nucleoid), teichoic acids (peptidoglycan), glycogen
1059	1058	PO2 str. and C-O-H str.	Phosphate ester. and oligosaccharides
1170		C-O, C-C str., C-O-H, C-O-C def.	Carbohydrates
1155			
1119			
1037	1030		
965			
1045–1025		O stretching of glycogen	
993		νC-O ribose, νC-C	Ribose skelet (ARN) ribosomes, sugars
‘‘fingerprint region’’ 900-400 cm^{-1}			

489

490 **Table 2.** Variability and reproducibility of FTIR data

Variability estimated as 1-PCC' 10^{-4}					
Type of variability	**Spectral region**				
	whole	**lipids**	**proteins**	**mixed**	**carbs**
	4000-700 cm^{-1}	**3050–2800 cm^{-1} 1800–1700 cm^{-1}**	**1700–1500 cm^{-1}**	**1500–1200 cm^{-1}**	**1200–700 cm^{-1}**
Cultivation in BHIB at 18 °C					
Technical replicates	0,4	0,1	0,4	0,2	0,5
Biological replicates	8,2	6,2	5,6	5,2	24,8
Strain	17,1	8,0	7,9	9,7	48,9
Specie	16,6	11,4	7,1	11,6	47,5
Genus	40,0	23,6	17,2	25,1	111,7
Cultivation in BHIA at 18 °C					
Technical replicates	0,7	0,2	0,6	0,5	1,0
Biological replicates	3,6	1,6	2,7	2,9	5,1
Strain	7,4	2,9	2,2	6,4	25,3
Specie	10,3	5,0	4,9	12,0	40,8
Genus	32,8	27,5	10,3	26,6	58,6
Cultivation at different temperatures on BHIA					
Technical replicates	0,7	0,4	0,5	0,5	1,2
Biological replicates	3,1	1,6	2,0	2,3	5,3
Cultivation time (days)	7,9	4,2	3,8	6,7	17,3
Strain	10,0	4,9	4,0	8,9	32,5
Specie	17,8	7,9	5,6	17,2	56,6
Genus	34,2	28,5	11,3	27,8	75,3

4 °C	33,0	32,7	8,7	27,9	46,1
10 °C	41,2	32,3	8,3	25,9	57,8
18 °C	32,8	27,5	10,3	26,6	58,6
25 °C	32,1	23,1	12,6	24,2	88,0
30 °C	22,2	16,1	12,4	16,7	91,2
37 °C	10,6	6,6	8,4	7,7	84,1

491

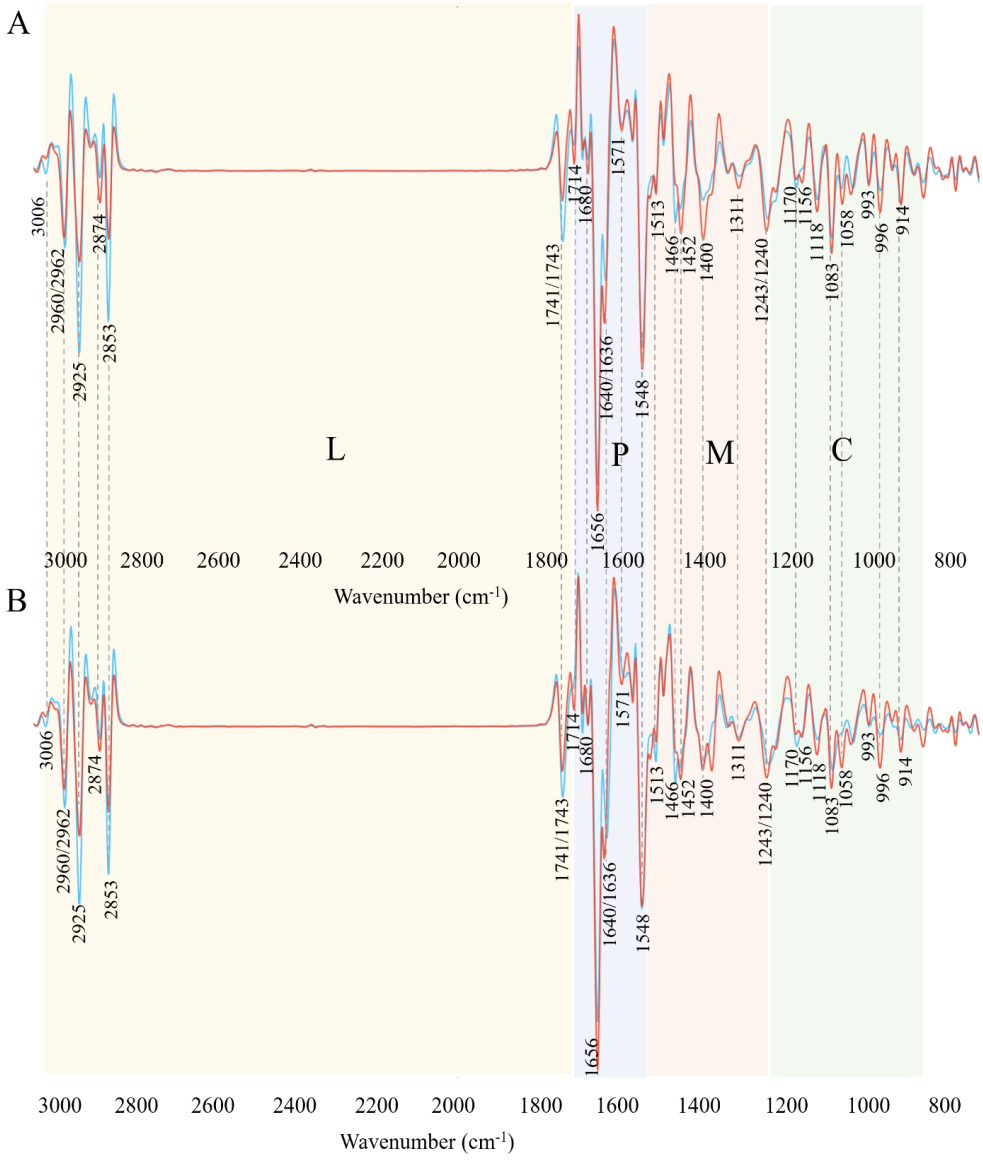

Figure 1. Second derivative spectra of Gram-positive (red) and Gram-negative (blue) Antarctic bacteria grown on (A) BHIA, (B)- BHIB. Colors and letters represent regions: L-lipid/ester region, P-protein region, M-mixed region, C-carbohydrate region. Peak assignment given in Table 1.

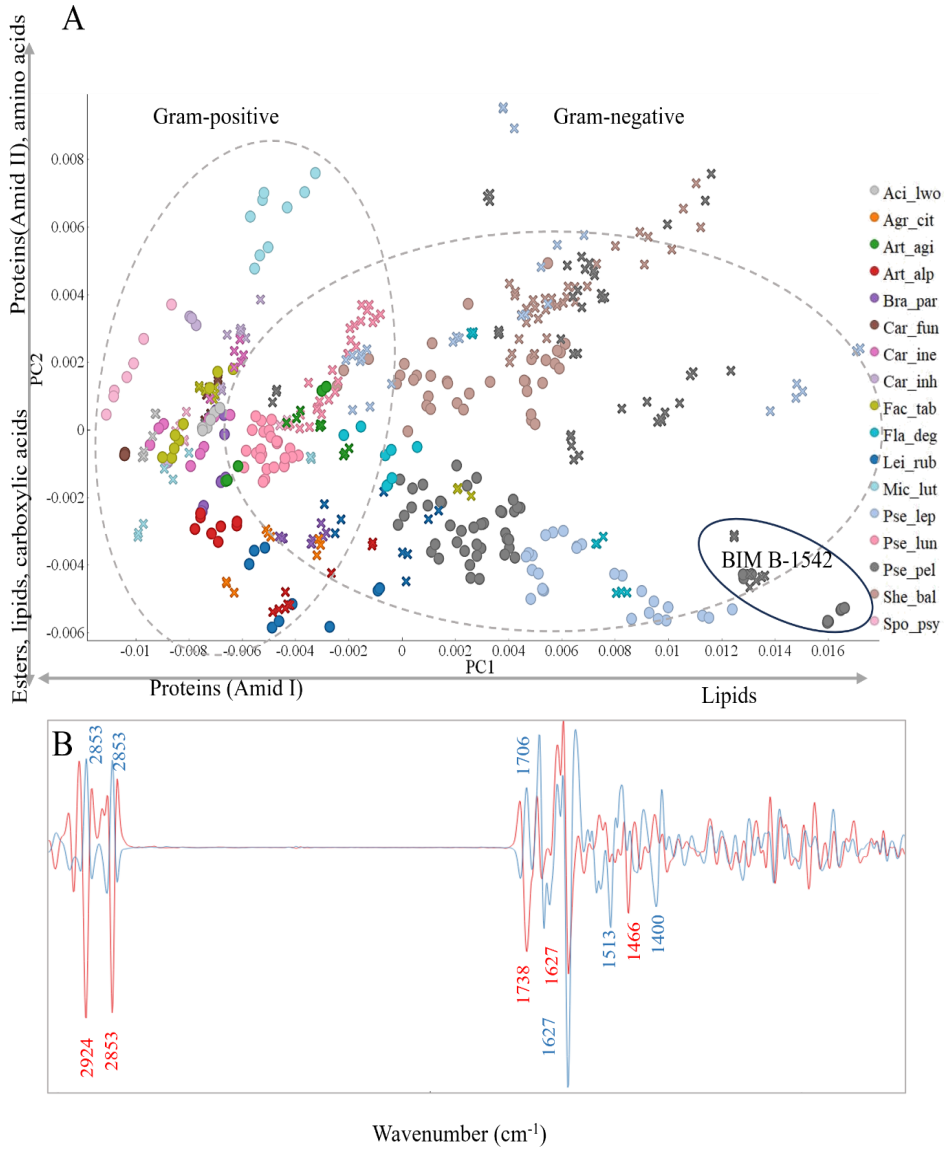

496

497 **Figure 2.** Principal component analysis (PCA) of the preprocessed FTIR spectra of Antarctic bacteria
498 grown in different media ('●' – Agar, '✕' – Broth) at 18°C. A – Score plot of PC1 and PC2 components,
499 colors represent genera, shapes represent cultivation temperatures. B – Loading plot of FTIR data with
500 main contributing peaks, PC1 (red) and PC2 (blue). PC1 provided 53% of explained variance and PC2
501 provided 12% of explained variance
502

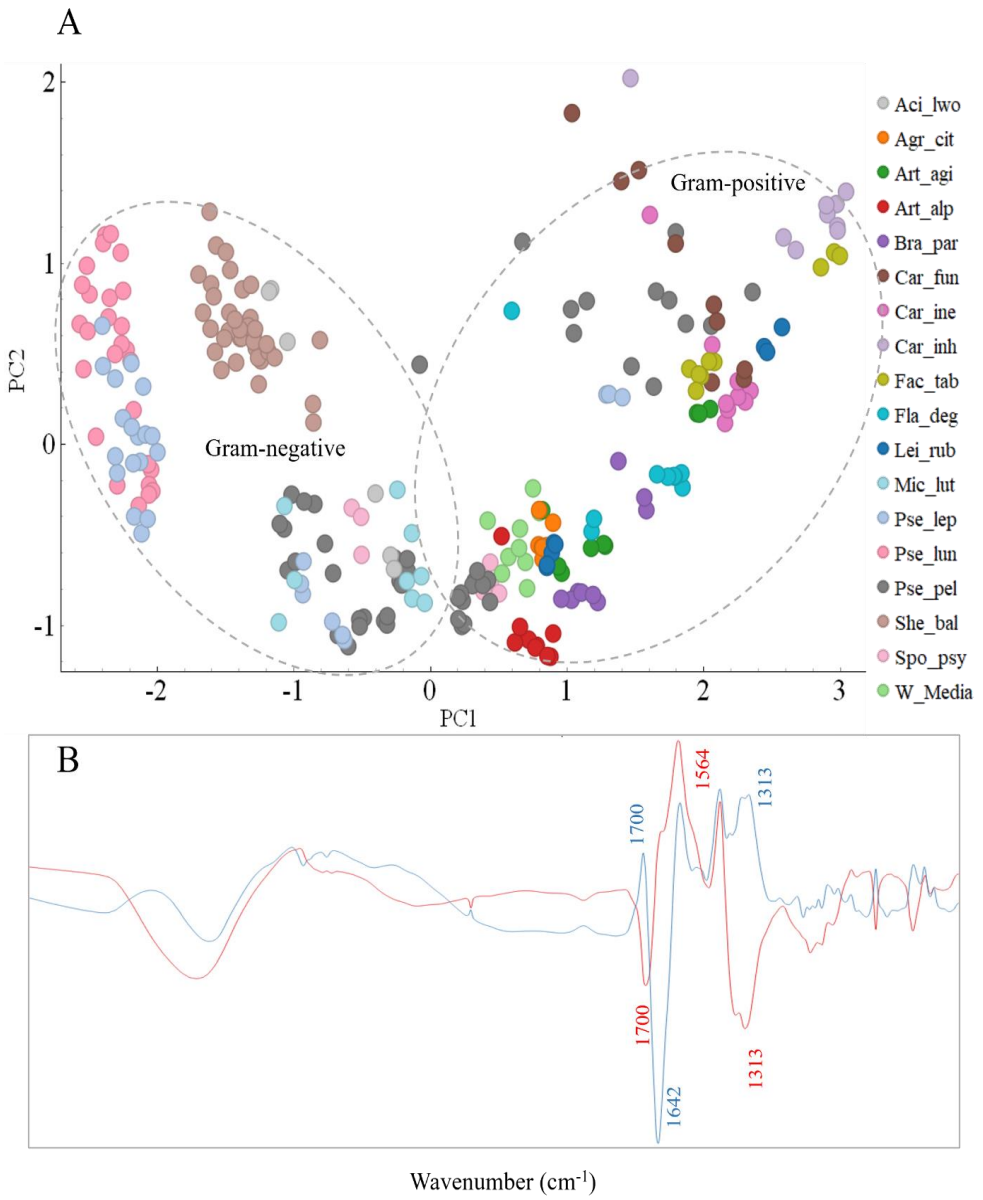

503

504 **Figure 3.** Principal component analysis (PCA) of the preprocessed FTIR spectra of supernatants
505 obtained after cultivation of Antarctic bacteria in BHIB at 18°C. A – Score plot of PC1 and PC2
506 components, colors represent genera, shapes represent cultivation temperatures. B – Loading plot of
507 FTIR data with main contributing peaks, PC1 (red) and PC2 (blue). PC1 provided 66% of explained
508 variance and PC2 provided 15% of explained variance.

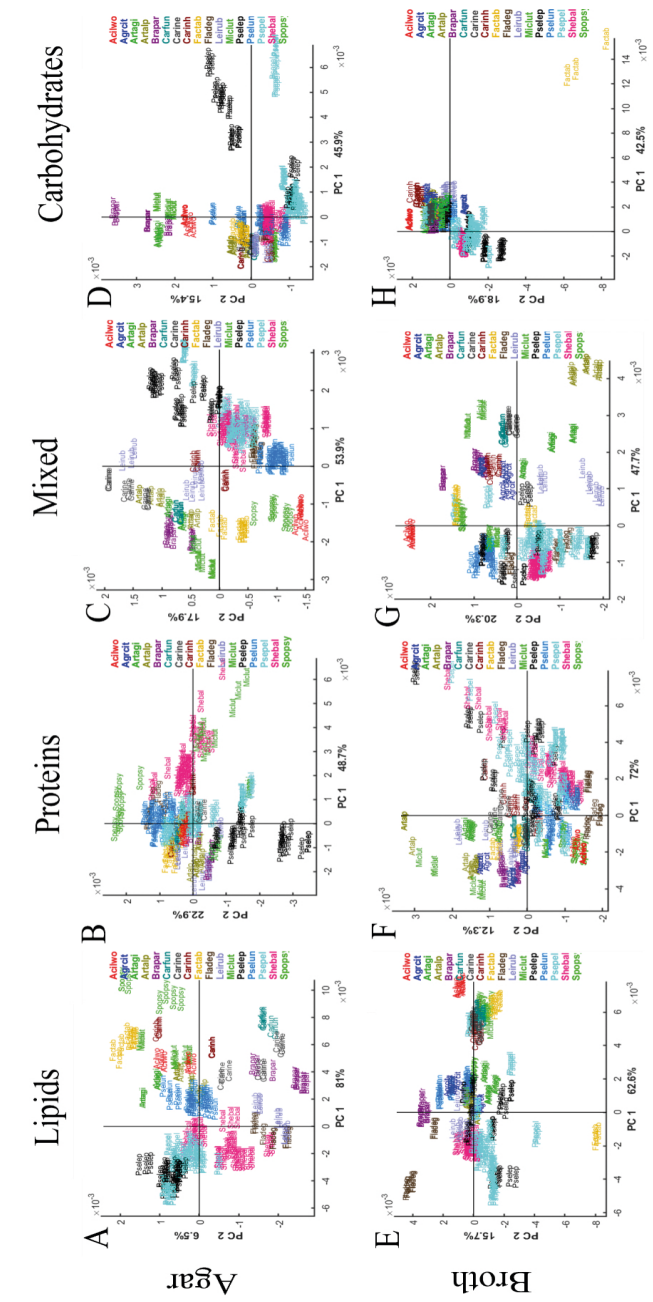

Figure 4. PCA score plots of normalized spectra of lipid (A, E), protein (B, F), mixed (C, G) and polysaccharide (D, H) spectral regions of the Antarctic meltwater bacteria cultivated on BHIA (A-D) and BHIB (E-H). Different colors correspond to different genera and short abbreviations given in Table 1S SM.

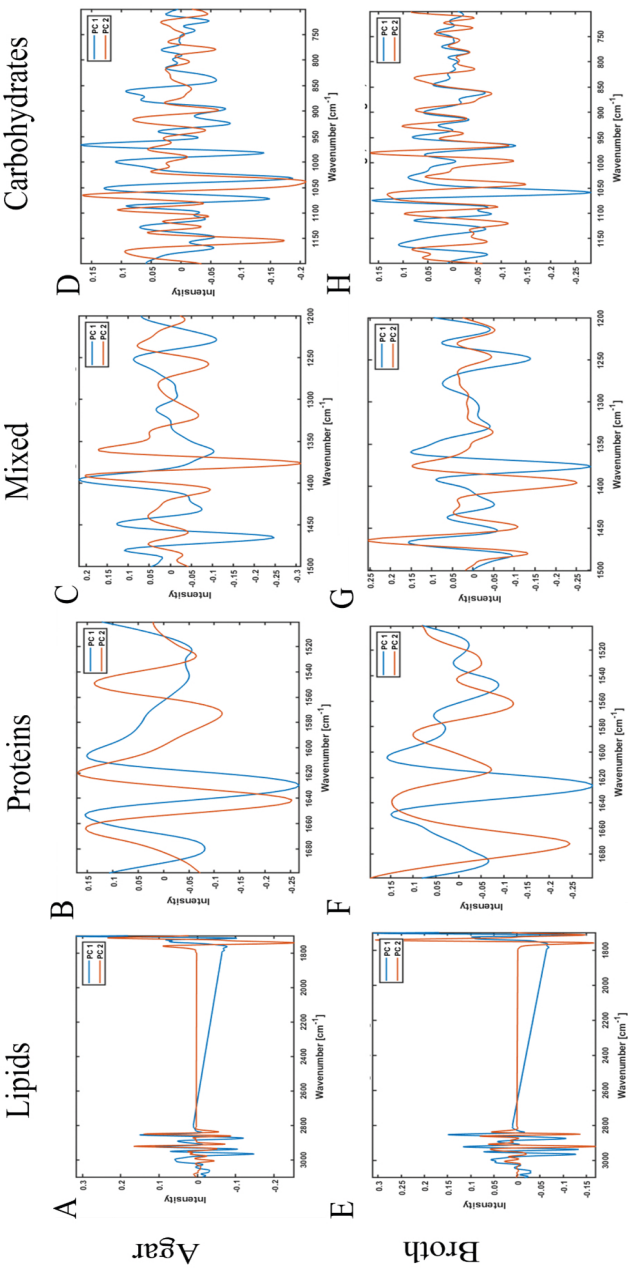

Figure 5. PCA loading plots of PC1 and PC2 components of normalized spectra of lipid (A, E), protein (B, F), mixed (C, G) and polysaccharide (D, H) spectral regions of Antarctic meltwater bacteria cultivated on BHIA (A-D) and BHIB (E-H) .

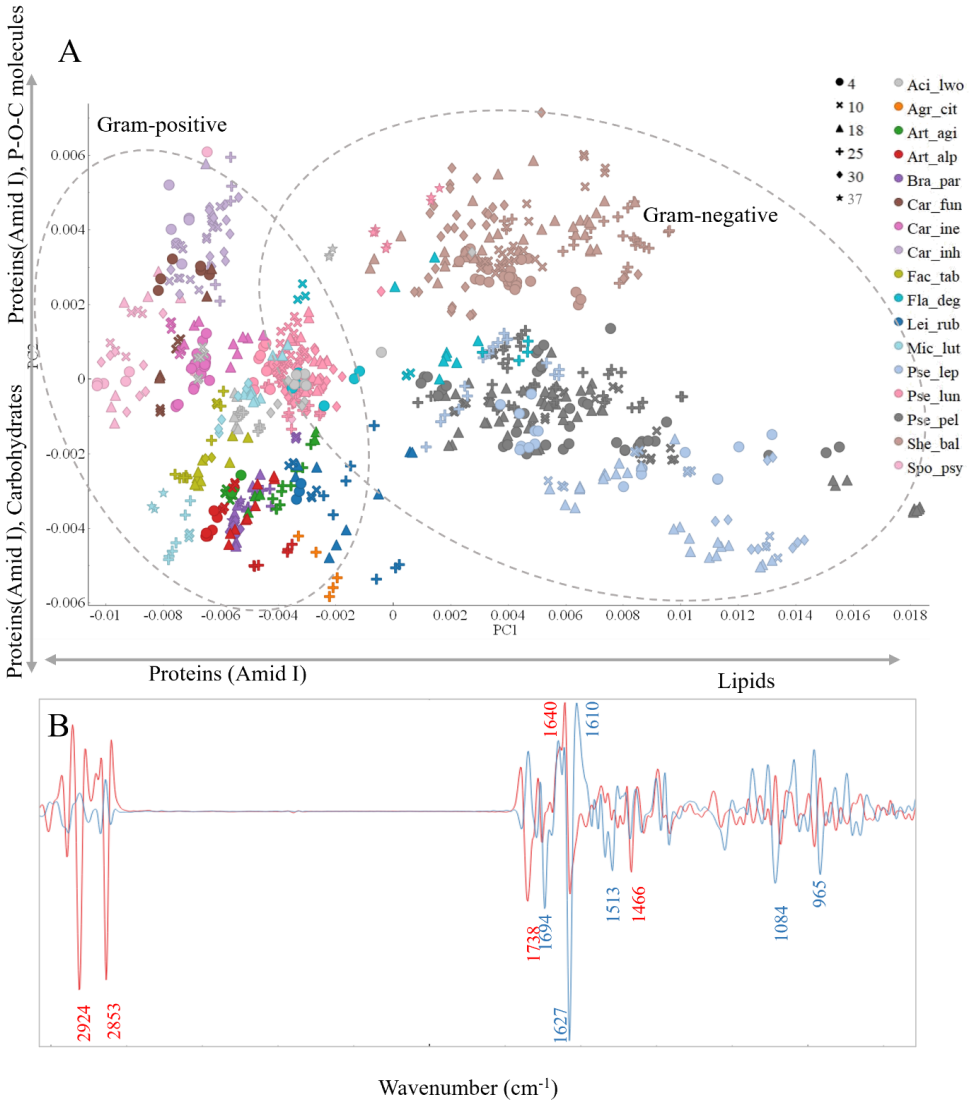

519

520 **Figure 6**. PCA of the preprocessed second derivative FTIR spectra of the Antarctic meltwater bacteria
521 grown at different temperatures ('●' – 4°C, '✕' – 10°C, '▲' – 18°C, '✚' – 25°C, '◆' – 30°C, '★' –
522 37°C). A – Score plot of PC1 and PC2 components, colors represent genera, shapes represent cultivation
523 temperatures. B – Loading plot of the FTIR data with the main contributing peaks, PC1 (red) and PC2
524 (blue). PC1 provided 53% of explained variance and PC2 provided 12% of explained variance.

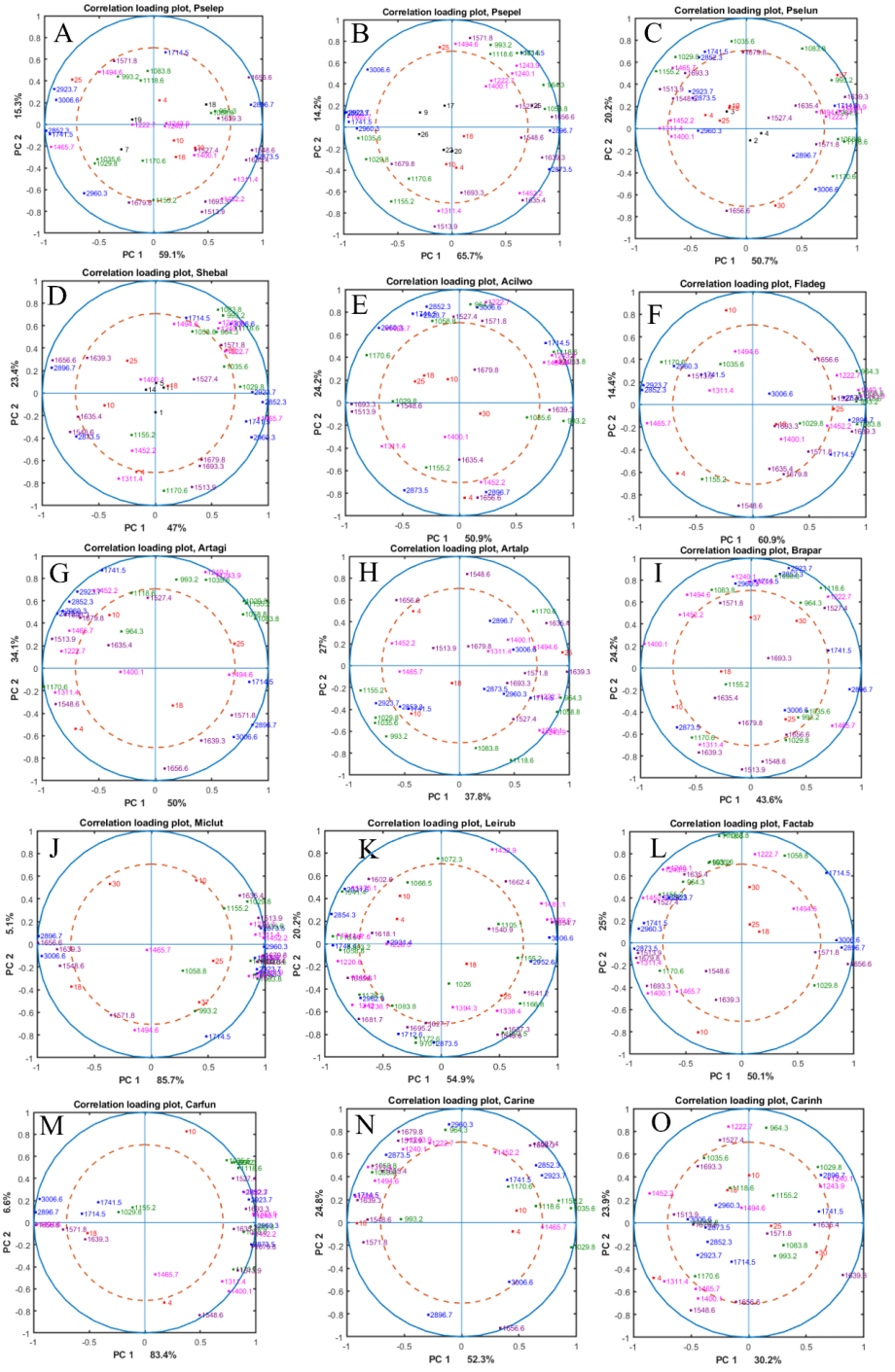

Figure 7. Correlation loading plots for PC1/PC2 for each specie. Black—isolate number; red temperature; blue—lipid/ester region; pink—mixed region; violet—protein region, green—polysaccharide region

Supplementary material

Table 1S. Overview over cultivation time (days), temperatures and growth of the Antarctic meltwater bacteria cultivated on BHIB and BHIA. Gray color indicates the absence or very little growth, *moderate psychrophiles

Genus	Specie	Short abbreviation	Strain	Collection number	BHIB	BHIA				
					18°C	4	10	18	25	30	37
Gram-negative											
Shewanella	*Shewanella baltica*	Shebal	TMP1	BIM B – 1565	3	4	4	2	1	1	
			TMP5	BIM B – 1557	3	4	4	2	1	2	
			TMP11	BIM B – 1561	3	4	4	2	1	2	
			TMP14	BIM B – 1563	3	4	4	2	1	1	
Acinetobacter	*Acinetobacter lwoffii*	Acilwo	TMP6	BIM B – 1558	3	16	4	2	1	2	3
Pseudomonas	*Pseudomonas lundensis*	Pselun	TMP2	BIM B – 1554	3	4	4	2	1	1	3
			TMP3	BIM B – 1555	3	4	4	2	1	1	3
			TMP4	BIM B – 1556	3	4	4	2	1	1	3
	Pseudomonas leptonychotis	Pselep	TMP7	BIM B – 1559	3	6	4	3	3	4	
			TMP18	BIM B – 1568	3	6	3	3	3	2	
			TMP19	BIM B – 1566	3	6	3	3	3	4	
	Pseudomonas peli	Psepel	TMP9	BIM B – 1560	3	9	4	3	3		
			TMP17	BIM B – 1569	3	6	5	3	3		
			TMP20	BIM B – 1546	3	9	4	3	3		
			TMP22	BIM B – 1552	3	6	4	4	3		
			TMP25	BIM B – 1542	3	6	5	5	3		
			TMP26	BIM B – 1548	3	6	4	3	3		
Flavobacterium	*Flavobacterium degerlachei*	Fladeg	TMP13	BIM B – 1562	3	6	5	5	3		
Gram-positive											
Sporosarcina	*Sporosarcina* sp.	Sposp	TMP10	BIM B – 1539	3	6	4	3	3	2	
Carnobacterium	*Carnobacterium funditum*	Carfun*	TMP27	BIM B – 1541	3	6	5	5			
	Carnobacterium iners	Carine*	TMP28	BIM B – 1544	3	9	4	5			
	Carnobacterium inhibens	Carinh	TMP12	BIM B – 1540	3	6	7	4	2	2	
Facklamia	*Facklamia tabacinasalis*	Factab	TMP29	BIM B – 1577	3		5	5	4	4	
Arthrobacter	*Arthrobacter alpinus.*	Artalp	TMP15	BIM B – 1549	3	4	4	3	3		
	Arthrobacter agilis	Artagi	TMP24	BIM B – 1543	3	9	6	3	4		
Brachybacterium	*Brachybacterium paraconglomeratum*	Brapar	TMP16	BIM B – 1571	3		5	4	3	2	3
Micrococcus	*Micrococcus luteus*	Miclut	TMP21	BIM B – 1545	3		6	3	3	1	3
Agrococcus	*Agrococcus citreus*	Agrcit	TMP23	BIM B – 1547	3				4		
Leifsonia	*Leifsonia* sp.	Leisp	TMP30	BIM B – 1567	3	8	5	4	4		

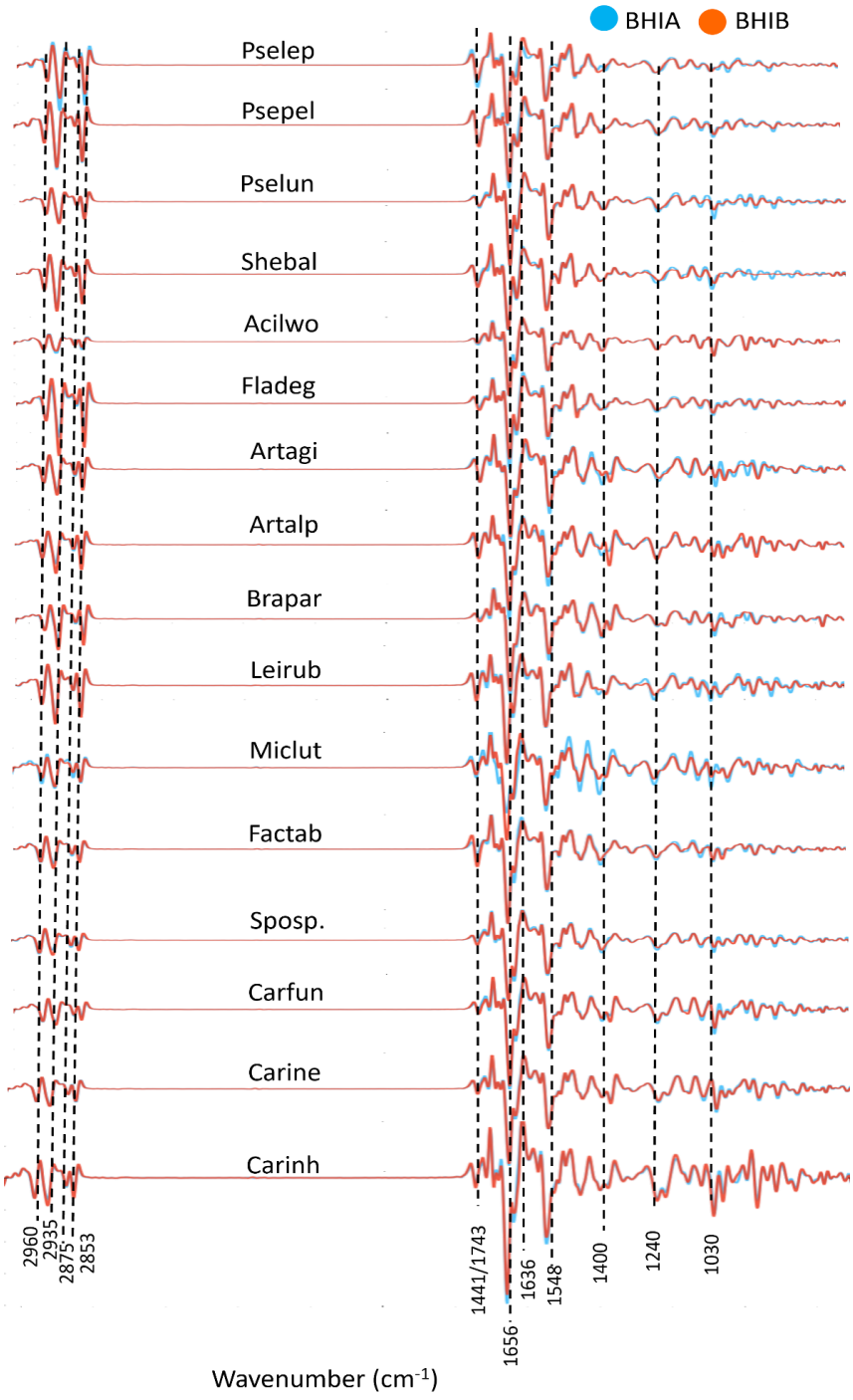

534

535 **Figure 1S.** Preprocessed second derivative FTIR-HTS spectra averaged for agar and broth media of
536 each specie.

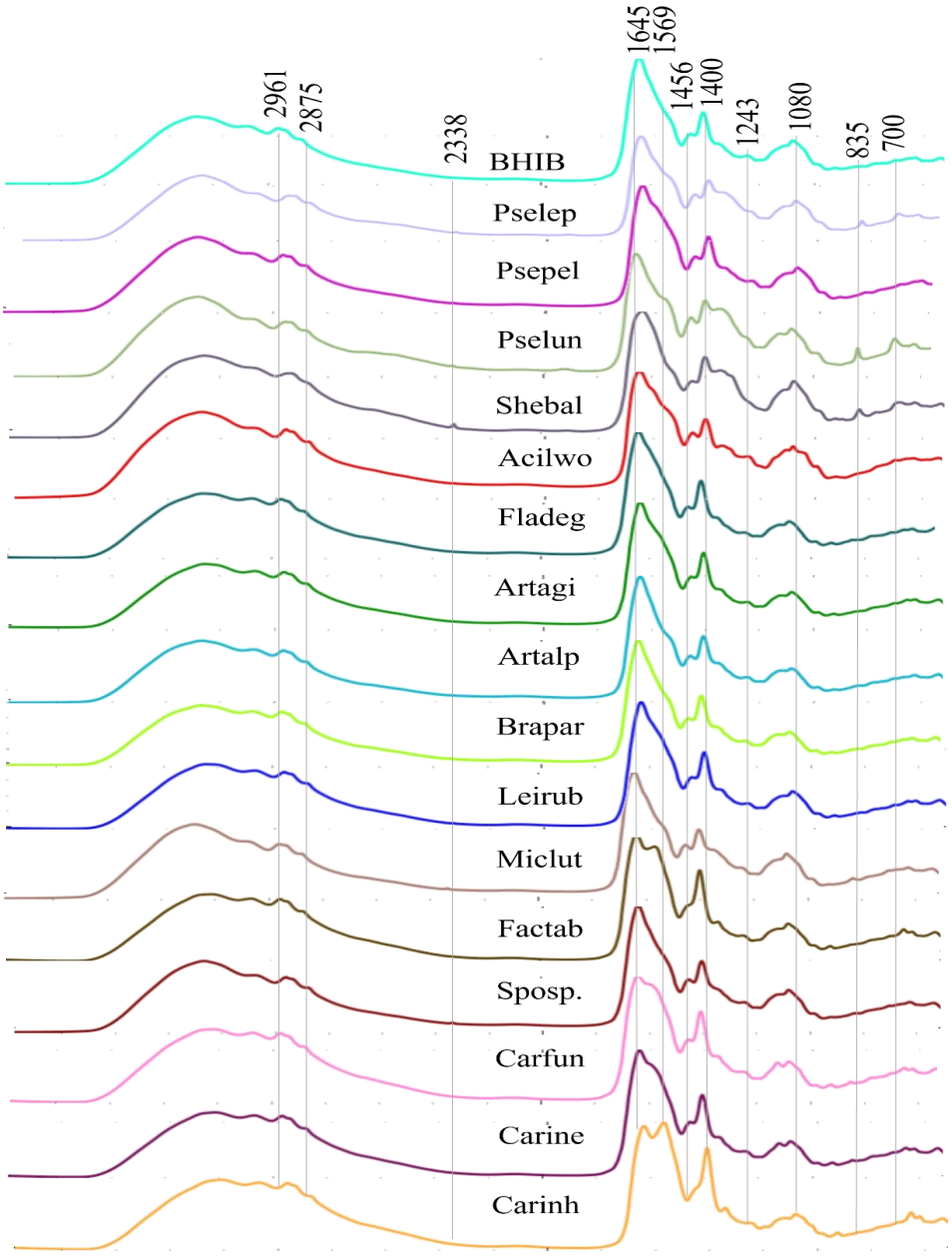

537

538 **Figure 2S.** Preprocessed FTIR-HTS spectra of BHIB media and spectra of supernatant for each specie

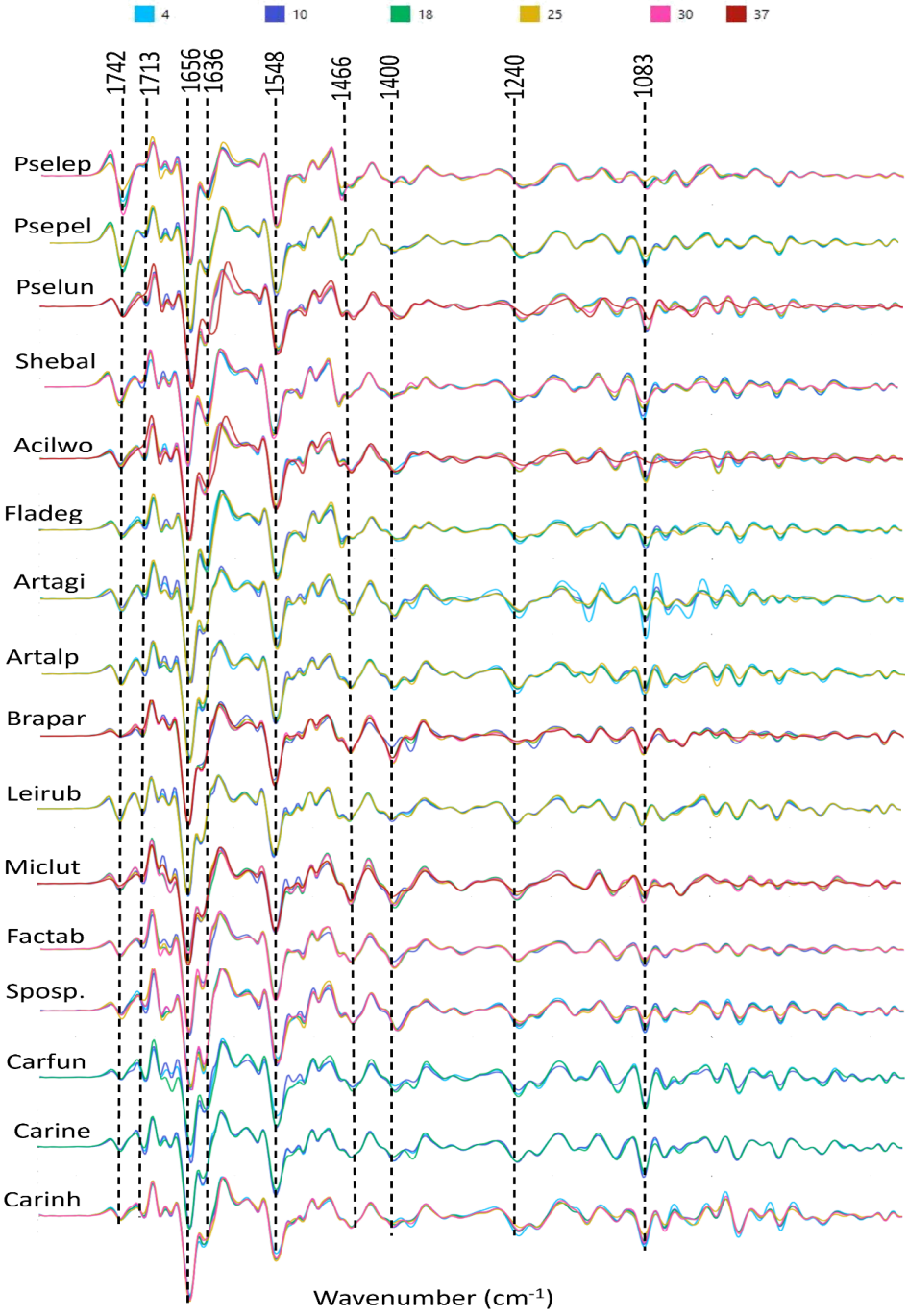

539

540 **Figure 3S.** Second derivative FTIR spectra of bacterial biomass of different bacterial species grown
541 at different temperatures (blue – 5°C, dark blue– 10°C, green – 18°C, orange – 25°C, pink – 25°C
542 and red – 25°C).

References

1. Mariey L, Signolle J, Amiel C, Travert J. Discrimination, classification, identification of microorganisms using FTIR spectroscopy and chemometrics. Vibrational spectroscopy. 2001;26(2):151-9.
2. Del Bove M, Lattanzi M, Rellini P, Pelliccia C, Fatichenti F, Cardinali G. Comparison of molecular and metabolomic methods as characterization tools of Debaryomyces hansenii cheese isolates. Food microbiology. 2009;26(5):453-9.
3. Oust A, Møretrø T, Naterstad K, Sockalingum GD, Adt I, Manfait M, Kohler A. Fourier transform infrared and Raman spectroscopy for characterization of Listeria monocytogenes strains. Applied and Environmental Microbiology. 2006;72(1):228-32.
4. Kirschner C, Maquelin K, Pina P, Ngo Thi N, Choo-Smith L-P, Sockalingum G, et al. Classification and identification of enterococci: a comparative phenotypic, genotypic, and vibrational spectroscopic study. Journal of clinical microbiology. 2001;39(5):1763-70.
5. Sockalingum G, Bouhedja W, Pina P, Allouch P, Bloy C, Manfait M. FT-IR spectroscopy as an emerging method for rapid characterization of microorganisms. Cellular and Molecular Biology (Noisy-le-Grand, France). 1998;44(1):261-9.
6. Naumann D, Helm D, Labischinski H. Microbiological characterizations by FT-IR spectroscopy. Nature. 1991;351(6321):81-2.
7. Ojeda JJ, Dittrich M. Fourier transform infrared spectroscopy for molecular analysis of microbial cells. Microbial Systems Biology: Methods and Protocols. 2012:187-211.
8. Jiang W, Saxena A, Song B, Ward BB, Beveridge TJ, Myneni SC. Elucidation of functional groups on gram-positive and gram-negative bacterial surfaces using infrared spectroscopy. Langmuir. 2004;20(26):11433-42.
9. Litvinov RI, Faizullin DA, Zuev YF, Weisel JW. The α-helix to β-sheet transition in stretched and compressed hydrated fibrin clots. Biophysical journal. 2012;103(5):1020-7.
10. Shapaval V, Brandenburg J, Blomqvist J, Tafintseva V, Passoth V, Sandgren M, Kohler A. Biochemical profiling, prediction of total lipid content and fatty acid profile in oleaginous yeasts by FTIR spectroscopy. Biotechnology for biofuels. 2019;12(1):1-12.
11. Ami D, Posteri R, Mereghetti P, Porro D, Doglia SM, Branduardi P. Fourier transform infrared spectroscopy as a method to study lipid accumulation in oleaginous yeasts. Biotechnology for biofuels. 2014;7(1):1-14.
12. Dean AP, Sigee DC, Estrada B, Pittman JK. Using FTIR spectroscopy for rapid determination of lipid accumulation in response to nitrogen limitation in freshwater microalgae. Bioresource technology. 2010;101(12):4499-507.
13. Helm D, Labischinski H, Schallehn G, Naumann D. Classification and identification of bacteria by Fourier-transform infrared spectroscopy. Microbiology. 1991;137(1):69-79.
14. Lin M, Al-Holy M, Al-Qadiri H, Chang S-S, Kang D-H, Rodgers BD, Rasco BA. Phylogenetic and spectroscopic analysis of Alicyclobacillus isolates by 16S rDNA sequencing and mid-infrared spectroscopy. Sensing and Instrumentation for Food Quality and Safety. 2007;1:11-7.
15. Alvarez-Ordóñez A, Mouwen D, López M, Prieto M. Fourier transform infrared spectroscopy as a tool to characterize molecular composition and stress response in foodborne pathogenic bacteria. Journal of microbiological methods. 2011;84(3):369-78.
16. Corte L, Rellini P, Roscini L, Fatichenti F, Cardinali G. Development of a novel, FTIR (Fourier transform infrared spectroscopy) based, yeast bioassay for toxicity testing and stress response study. Analytica chimica acta. 2010;659(1-2):258-65.
17. Yang H, Shi H, Feng B, Wang L, Chen L, Alvarez-Ordóñez A, et al. Protocol for bacterial typing using Fourier transform infrared spectroscopy. STAR protocols. 2023;4(2):102223.
18. Kosa G, Kohler A, Tafintseva V, Zimmermann B, Forfang K, Afseth NK, et al. Microtiter plate cultivation of oleaginous fungi and monitoring of lipogenesis by high-throughput FTIR spectroscopy. Microbial cell factories. 2017;16:1-12.
19. Kosa G, Shapaval V, Kohler A, Zimmermann B. FTIR spectroscopy as a unified method for simultaneous analysis of intra-and extracellular metabolites in high-throughput screening of microbial bioprocesses. Microbial cell factories. 2017;16:1-11.

20. Kosa G, Vuoristo KS, Horn SJ, Zimmermann B, Afseth NK, Kohler A, Shapaval V. Assessment of the scalability of a microtiter plate system for screening of oleaginous microorganisms. Applied Microbiology and Biotechnology. 2018;102(11):4915-25.
21. Colabella C, Corte L, Roscini L, Shapaval V, Kohler A, Tafintseva V, et al. Merging FT-IR and NGS for simultaneous phenotypic and genotypic identification of pathogenic Candida species. PloS one. 2017;12(12):e0188104.
22. Tafintseva V, Vigneau E, Shapaval V, Cariou V, Qannari EM, Kohler A. Hierarchical classification of microorganisms based on high-dimensional phenotypic data. Journal of Biophotonics. 2018;11(3):e201700047.
23. Garip S, Gozen AC, Severcan F. Use of Fourier transform infrared spectroscopy for rapid comparative analysis of Bacillus and Micrococcus isolates. Food Chemistry. 2009;113(4):1301-7.
24. Girardeau A, Passot S, Meneghel J, Cenard S, Lieben P, Trelea I-C, Fonseca F. Insights into lactic acid bacteria cryoresistance using FTIR microspectroscopy. Analytical and Bioanalytical Chemistry. 2022;414(3):1425-43.
25. Harz M, Rösch P, Popp J. Vibrational spectroscopy—A powerful tool for the rapid identification of microbial cells at the single-cell level. Cytometry Part A: The Journal of the International Society for Analytical Cytology. 2009;75(2):104-13.
26. Jehlička J, Edwards HG, Osterrothová K, Novotná J, Nedbalová L, Kopecký J, et al. Potential and limits of Raman spectroscopy for carotenoid detection in microorganisms: implications for astrobiology. Philosophical Transactions of the Royal Society A: Mathematical, Physical and Engineering Sciences. 2014;372(2030):20140199.
27. Kochan K, Lai E, Richardson Z, Nethercott C, Peleg AY, Heraud P, Wood BR. Vibrational spectroscopy as a sensitive probe for the chemistry of intra-phase bacterial growth. Sensors. 2020;20(12):3452.
28. Naumann D. Infrared spectroscopy in microbiology. Encyclopedia of analytical chemistry. 2000;102:131.
29. Siebert F, Hildebrandt P. Vibrational spectroscopy in life science: John Wiley & Sons; 2008.
30. Zarnowiec P, Lechowicz L, Czerwonka G, Kaca W. Fourier transform infrared spectroscopy (FTIR) as a tool for the identification and differentiation of pathogenic bacteria. Current medicinal chemistry. 2015;22(14):1710-8.
31. Garip S, Bozoglu F, Severcan F. Differentiation of mesophilic and thermophilic bacteria with Fourier transform infrared spectroscopy. Applied spectroscopy. 2007;61(2):186-92.
32. Millan-Oropeza A, Rebois R, David M, Moussa F, Dazzi A, Bleton J, et al. Attenuated total reflection Fourier transform infrared (ATR FT-IR) for rapid determination of microbial cell lipid content: correlation with gas chromatography-mass spectrometry (GC-MS). Applied Spectroscopy. 2017;71(10):2344-52.
33. Mancuso Nichols C, Garon S, Bowman J, Raguénès G, Guezennec J. Production of exopolysaccharides by Antarctic marine bacterial isolates. Journal of Applied Microbiology. 2004;96(5):1057-66.
34. Jadhav VV, Yadav A, Shouche YS, Aphale S, Moghe A, Pillai S, et al. Studies on biosurfactant from Oceanobacillus sp. BRI 10 isolated from Antarctic sea water. Desalination. 2013;318:64-71.
35. Smirnova M, Losada CB, Akulava V, Zimmermann B, Kohler A, Miamin U, et al. New cold-adapted bacteria for efficient hydrolysis of feather waste at low temperature. Bioresource Technology Reports. 2023:101530.
36. Fayolle P, Picque D, Corrieu G. Monitoring of fermentation processes producing lactic acid bacteria by mid-infrared spectroscopy. Vibrational Spectroscopy. 1997;14(2):247-52.
37. Schuster KC, Mertens F, Gapes J. FTIR spectroscopy applied to bacterial cells as a novel method for monitoring complex biotechnological processes. Vibrational Spectroscopy. 1999;19(2):467-77.
38. Chakraborty J, Das S. Application of spectroscopic techniques for monitoring microbial diversity and bioremediation. Applied Spectroscopy Reviews. 2017;52(1):1-38.
39. Kale SK, Deshmukh AG, Dudhare MS, Patil VB. Microbial degradation of plastic: a review. Journal of Biochemical Technology. 2015;6(2):952-61.

40. Yi-bin W, Fang-ming L, Qiang L, Bi-juan H, Jin-lai M. Low-temperature degradation mechanism analysis of petroleum hydrocarbon-degrading Antarctic psychrophilic strains. J Pure Appl Microbiol. 2014;8(1):47-53.
41. Smirnova M, Miamin U, Kohler A, Valentovich L, Akhremchuk A, Sidarenka A, et al. Isolation and characterization of fast-growing green snow bacteria from coastal East Antarctica. MicrobiologyOpen. 2021;10(1).
42. Smirnova M, Tafintseva V, Kohler A, Miamin U, Shapaval V. Temperature- and Nutrients-Induced Phenotypic Changes of Antarctic Green Snow Bacteria Probed by High-Throughput FTIR Spectroscopy. Biology. 2022;11(6):890.
43. Akulava V, Miamin U, Akhremchuk K, Valentovich L, Dolgikh A, Shapaval V. Isolation, Physiological Characterization, and Antibiotic Susceptibility Testing of Fast-Growing Bacteria from the Sea-Affected Temporary Meltwater Ponds in the Thala Hills Oasis (Enderby Land, East Antarctica). Biology. 2022;11(8):1143.
44. Byrtusová D, Shapaval V, Holub J, Šimanský S, Rapta M, Szotkowski M, et al. Revealing the Potential of Lipid and β-Glucans Coproduction in Basidiomycetes Yeast. Microorganisms. 2020;8(7):1034.
45. Dzurendova S, Zimmermann B, Kohler A, Tafintseva V, Slany O, Certik M, Shapaval V. Microcultivation and FTIR spectroscopy-based screening revealed a nutrient-induced co-production of high-value metabolites in oleaginous Mucoromycota fungi. PLOS ONE. 2020;15(6):e0234870.
46. Dzurendova S, Zimmermann B, Tafintseva V, Kohler A, Ekeberg D, Shapaval V. The influence of phosphorus source and the nature of nitrogen substrate on the biomass production and lipid accumulation in oleaginous Mucoromycota fungi. Applied Microbiology and Biotechnology. 2020;104(18):8065-76.
47. Tafintseva V, Shapaval V, Blazhko U, Kohler A. Correcting replicate variation in spectroscopic data by machine learning and model-based pre-processing. Chemometrics and Intelligent Laboratory Systems. 2021;215:104350.
48. Tafintseva V, Shapaval V, Smirnova M, Kohler A. Extended multiplicative signal correction for FTIR spectral quality test and pre-processing of infrared imaging data. Journal of Biophotonics. 2020;13(3):e201960112.
49. Kohler A, Böcker U, Shapaval V, Forsmark A, Andersson M, Warringer J, et al. High-throughput biochemical fingerprinting of Saccharomyces cerevisiae by Fourier transform infrared spectroscopy. PLoS One. 2015;10(2):e0118052.
50. Kohler A, Solheim JH, Tafintseva V, Zimmermann B, Shapaval V. Model-based pre-processing in vibrational spectroscopy. 2020.
51. Martens H, Stark E. Extended multiplicative signal correction and spectral interference subtraction: new preprocessing methods for near infrared spectroscopy. Journal of pharmaceutical and biomedical analysis. 1991;9(8):625-35.
52. Kohler A, Kirschner C, Oust A, Martens H. Extended multiplicative signal correction as a tool for separation and characterization of physical and chemical information in Fourier transform infrared microscopy images of cryo-sections of beef loin. Applied spectroscopy. 2005;59(6):707-16.
53. Kohler A, Sule-Suso J, Sockalingum G, Tobin M, Bahrami F, Yang Y, et al. Estimating and correcting Mie scattering in synchrotron-based microscopic Fourier transform infrared spectra by extended multiplicative signal correction. Applied spectroscopy. 2008;62(3):259-66.
54. Syms C. Principal components analysis. Elsevier; 2008.
55. Demšar J, Curk T, Erjavec A, Gorup Č, Hočevar T, Milutinovič M, et al. Orange: data mining toolbox in Python. the Journal of machine Learning research. 2013;14(1):2349-53.
56. Toplak M, Birarda G, Read S, Sandt C, Rosendahl S, Vaccari L, et al. Infrared orange: connecting hyperspectral data with machine learning. Synchrotron Radiation News. 2017;30(4):40-5.
57. Feijó Delgado F, Cermak N, Hecht VC, Son S, Li Y, Knudsen SM, et al. Intracellular water exchange for measuring the dry mass, water mass and changes in chemical composition of living cells. PloS one. 2013;8(7):e67590.
58. Kochan K, Perez-Guaita D, Pissang J, Jiang J-H, Peleg AY, McNaughton D, et al. In vivo atomic force microscopy–infrared spectroscopy of bacteria. Journal of The Royal Society Interface. 2018;15(140):20180115.
59. Tripathi N, Sapra A. Gram staining. 2020.

60. Sasser M. Identification of bacteria by gas chromatography of cellular fatty acids. MIDI technical note 101. Newark, DE: MIDI inc; 1990.
61. Lauritano C, Rizzo C, Lo Giudice A, Saggiomo M. Physiological and molecular responses to main environmental stressors of microalgae and bacteria in polar marine environments. Microorganisms. 2020;8(12):1957.
62. Moon S, Ham S, Jeong J, Ku H, Kim H, Lee C. Temperature matters: Bacterial response to temperature change. Journal of Microbiology. 2023;61(3):343-57.
63. Goh YS, Tan IKP. Polyhydroxyalkanoate production by antarctic soil bacteria isolated from Casey Station and Signy Island. Microbiological research. 2012;167(4):211-9.
64. Jin S, Wang Y, Zhao X. Cold-adaptive mechanism of psychrophilic bacteria in food and its application. Microbial pathogenesis. 2022;169:105652.
65. de Magalhães CR, Carrilho R, Schrama D, Cerqueira M, Rosa da Costa AM, Rodrigues PM. Mid-infrared spectroscopic screening of metabolic alterations in stress-exposed gilthead seabream (Sparus aurata). Scientific reports. 2020;10(1):1-9.
66. Wang Y, Zhou Q, Li B, Liu B, Wu G, Ibrahim M, et al. Differentiation in MALDI-TOF MS and FTIR spectra between two closely related species Acidovorax oryzae and Acidovorax citrulli. BMC microbiology. 2012;12(1):1-7.
67. Shapaval V, Afseth N, Vogt G, Kohler A. Fourier transform infrared spectroscopy for the prediction of fatty acid profiles in Mucor fungi grown in media with different carbon sources. Microbial Cell Factories. 2014;13(1):86.
68. Maquelin K, Kirschner C, Choo-Smith L-P, van den Braak N, Endtz HP, Naumann D, Puppels G. Identification of medically relevant microorganisms by vibrational spectroscopy. Journal of microbiological methods. 2002;51(3):255-71.
69. Lu X, Liu Q, Wu D, Al-Qadiri HM, Al-Alami NI, Kang D-H, et al. Using of infrared spectroscopy to study the survival and injury of Escherichia coli O157: H7, Campylobacter jejuni and Pseudomonas aeruginosa under cold stress in low nutrient media. Food microbiology. 2011;28(3):537-46.

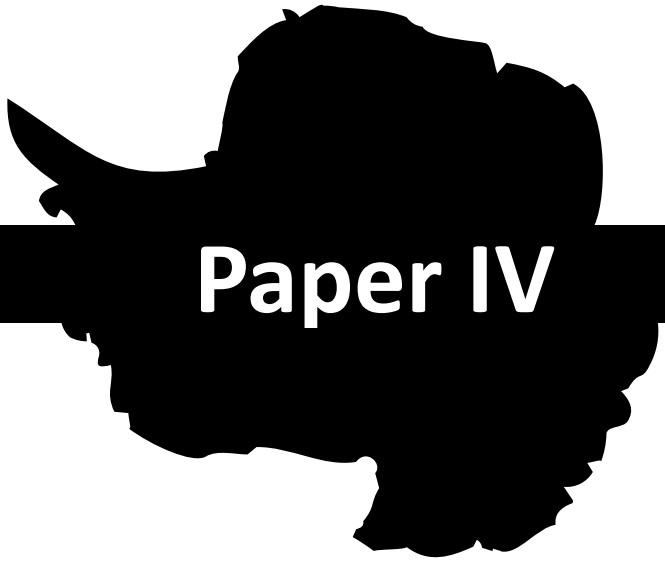

Paper IV

Screening for pigment production and characterization of pigment profile and photostability in cold-adapted Antarctic bacteria using FT-Raman spectroscopy

Volha Akulava[1], Dana Byrtusova[1], Boris Zimmermann[1], Margarita Smirnova[1], Achim Kohler[1], Uladzislau Miamin[2], Leonid Valentovich[3], Volha Shapaval[1]

[1]Faculty of Science and Technology, Norwegian University of Life Sciences, Ås, Norway

[2]Faculty of Biology, Belarussian State University, Minsk, Belarus

[3]Institute of Microbiology, National Academy of Sciences of Belarus, Minsk, Belarus

*** Correspondence:**
Corresponding Author
volha.akulava@nmbu.no

Keywords: pigments, carotenoids, Antarctic bacteria, Fourier-transform Raman spectroscopy, ratiometric analysis, pigment photostability, blue light effect

Highlights

Bacteria from the genera *Leifsonia*, *Cryobacterium*, *Flavobacterium*, and *Rhodococcus* displayed the highest relative pigment content.

Temperature had distinct species-specific effects on pigments production in bacteria.

FT-Raman spectroscopy proved to be a powerful method for library-independent and descriptive assessment of pigment production in bacteria.

Blue light-induced production of carotenoids in bacteria.

Pronounced pigments photodegradation effect was observed in the pigmented bacterial biomass after exposure to light 900 lux for 60 hours.

Abstract

Microbial pigments can replace synthetic organic pigments which often produced in unsustainable way and can be toxic. Therefore, search for new pigment producing microorganisms is of high interest for industry. In this study, a screening and characterization of pigment profile and photostability in seventy-four newly isolated Antarctic bacteria using Fourier-transform (FT) Raman spectroscopy and HPLC-MS was performed. Screening of the bacterial biomass by FT-Raman identified thirty-seven bacterial strains from the genera *Agrococcus, Arthrobacter, Brachybacterium, Cryobacterium, Leifsonia, Micrococcus, Paeniglutamicibacter, Rhodococcus, Salinibacterium* and *Flavobacterium* as having relatively high pigment content. The impact of growth temperature on the pigment production in the studied Antarctic bacteria was species - specific, while blue light exposure triggered pigment production in majority of the studied bacteria. HPLC-MS analysis of a biomass of a set of ten pigmented Antarctic bacteria identified eighteen different carotenoids and precursors. FT-Raman spectroscopy showed to be suitable for both, semi-qualitative library-independent identification of pigment producing bacteria and determination of pigment profile using spectral library of reference pigment standards. This study provides valuable insights into the

pigment production capabilities of Antarctic bacteria and highlighting the potential of FT-Raman spectroscopy for characterizing microbial pigments.

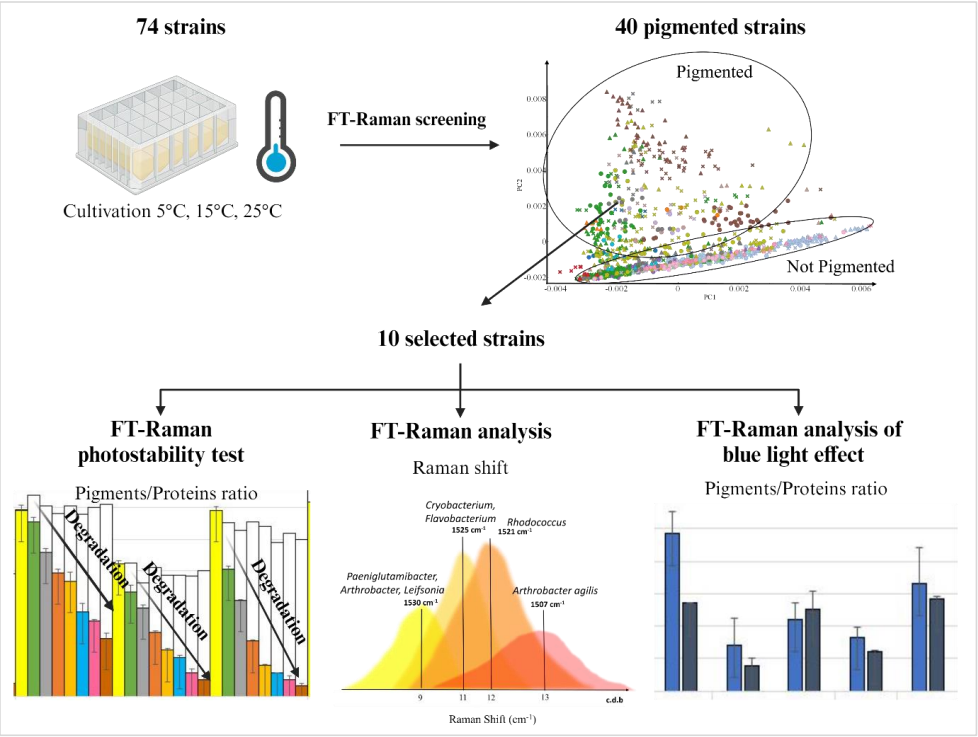

Graphical abstract was created with BioRender.com

Introduction

Pigments have a significant industrial importance and find diverse applications in food, feed, cosmetics, and chemical industry. Majority of pigments used in industry are synthetic (Kumar et al., 2015). Synthetic organic pigments can be obtained with high purity, consistency, and stability and they can be customized for specific properties depending on the final application (Singh et al., 2023). Despite these advantages, there is an increasing trend in the industry to switch from synthetic organic to natural pigments that creates a high demand of naturally sourced pigments (Kumar et al., 2015;Singh et al., 2023). This is mainly due to the reported toxicity, pollution potential and many environmental and sustainability concerns of their production. Many food, feed and cosmetic producers tend to include more natural ingredients in their products (Kumar et al., 2015;Di Salvo et al., 2023). Also, textile and dye industry searches for natural alternatives of pigments. Therefore, exploring new bio-based sources of pigments and establishing their production becomes a crucial step in elevating sustainability of the modern industry (Sajjad et al., 2020).

Naturally sourced pigments usually have plant, insect, mineral ores or microbial origin (bacteria, cyanobacteria, algae, fungi, yeast, archaea) (SenBarrow and Deshmukh, 2019;Singh et al., 2023). Industrial production of plant-based pigments is often restricted by high extraction cost and availability of plant biomass which often comes as a by-product, rest material or waste of

other productions (Lyu et al., 2022). Establishing agricultural production of plants dedicated to pigment production is challenging and hindered by the European Green Deal which aims to make land use more sustainable and environmentally friendly. Therefore, in recent years, considerable attention has been given to microbe-based pigments, production of which is independent on land use or climate and can be performed in accordance with sustainability standards fulfilling all main EU Bioeconomy strategies.

Among pigment-producing microorganisms the most promising are bacteria, cyanobacteria, yeast and microalgae which are unicellular and characterized by a rapid uniform growth and ability to utilize various substrates often considered as wastes, side-streams, or by-products (SenBarrow and Deshmukh, 2019;Pailliè-JiménezStincone and Brandelli, 2020). Microbes produce a wide range of pigments with different structures and biological properties, such as actinorhodin, carotenoids, flexirubin, melanin, phycocyanin, phycoerythrin etc. (Chatragadda and Dufossé, 2021). Today, among all carotenoids, six are regarded as industrially significant: astaxanthin, β-carotene, canthaxanthin, lutein, lycopene, and zeaxanthin (Martínez-Cámara et al., 2021). But similarly to plants, industrial production of microbe-based pigments is represented by very few examples: astaxanthin (Alga Technologies, Israel; BlueBiotech, Germany; Cyanotech, USA), astaxanthin and mixture of β-carotene, zeaxanthin, cryptoxanthin and lutein (Parry Nutraceuticals, India; Plankton Australia Pty Limited, Australia) (Igreja et al., 2021). Bacterial pigments with current or potential use as natural food colourants include astaxanthin (a pink-red pigment) from *Agrobacterium aurantiacum* and *Paracoccus carotinifaciens*, rubrolone (a red pigment) from *Streptomyces echinoruber*, zeaxanthin (a yellow pigment) from *Flavobacterium* sp. and *Paracoccus zeaxanthinifaciens* (Ahmad et al., 2012). Limited availability of industrially produced natural pigments of microbial origin replacing synthetic alternatives is mainly due to the lack of knowledge on the availability of microorganisms capable to synthesize certain pigments. According to the Carotenoid Database Japan, there are 702 microorganisms registered as capable of producing natural carotenoids, but many of them produce the same type of carotenoids or their precursors which have no industrial applications (Yabuzaki, 2017). Thus, there is an increasing need in searching, identifying and characterizing new pigment-producing microbes.

Among pigment-producing microorganisms those isolated from polar regions are of special interest since they often possess an ability to synthesize a wide variety of pigments which function as cell photoprotectors and antioxidants allowing them to survive and adapt to extreme conditions such as low temperature and high UV radiation (Fong et al., 2001;DieserGreenwood and Foreman, 2010;Tuncer et al., 2014;Silva et al., 2019;Seel et al., 2020;Styczynski et al., 2020;Silva et al., 2021). In addition, it has been reported that pigments from polar microorganisms have unique properties such as high photostability and light-absorbing capability, and higher resistance to UV radiation (Silva et al., 2019).

Recently, it has been suggested that microbial pigments or even microbial pigmented biomass can be used in solar cells dyeing or dye-synthesized solar cells (Órdenes-Aenishanslins et al., 2016). Photostability is a critical factor in assessing the feasibility of microbial pigments as photosensitizers for implementation in solar cells (Hernández-Velasco et al., 2020). The average illuminance for direct sunlight exposure ranges from 30.000 to 100.000 lux. In the Antarctic, light intensity ranges from almost nothing during winter (max 500 lux during this period) up to 100 000 lux in summer (Owen and Arendt, 1992).

In this study we performed screening of 74 fast-growing cold-adapted Antarctic bacteria to uncover their capability to produce various pigments. For the screening, we utilized Fourier-transform (FT) Raman spectroscopy which is well-known for sensing pigments and performing

qualitative pigment analysis of the biomass (Dzurendová et al., 2021). HPLC-MS was utilized for characterizing pigments profile of the extracted pigments for the most promising pigment-producing Antarctic bacteria. Furthermore, we evaluated biotechnological potential of the Antarctic bacteria identified as the most promising pigments producers and studied their pigment photostability in an intact biomass.

Materials and methods

Bacterial strains

Seventy-four fast-growing cold-adapted Antarctic bacteria obtained from the Belarussian Collection of Non-pathogenic Microorganisms, Institute of Microbiology of the National Academy of Science of Belarus (Minsk, Belarus) were used in the study for screening experiment, from them ten strains were selected for detail pigment analysis, evaluation of blue light effect on pigments production and photostability testing (Table S1 in SM). The bacteria were isolated from green snow and meltwater ponds in the Vecherniy District of the Tala Hills oasis, located in the Western part of Enderby Land (East Antarctica) during the 5th (2013) and 7th (2014-2015) Belarusian Antarctic Expedition. All bacteria were identified by 16S rRNA gene sequencing and deposited in Belarussian Collection of Non-pathogenic Microorganisms. Detailed biochemical and physiological characterization was performed and reported previously (Akulava et al., 2022;Smirnova et al., 2022;Smirnova et al., 2023).

Cultivation and sample preparation for screening by FT-Raman analysis

Bacteria were recovered from cryo-preserved cultures by culturing on brain heart infusion (BHI) agar (Sigma Aldrich, USA) for 7 days at 18°C. A single colony of each strain was transferred into 7 mL of BHI broth (Sigma-Aldrich, USA) in a Duetz microtiter plate system (Duetz-MTPS, Enzyscreen, Netherlands) consisting of 24-square extra high polypropylene deep well microtiter plates (MTPs) with low-evaporation sandwich covers and extra high cover clamps. To obtain enough biomass for FT-Raman analysis, each strain was inoculated into four wells of a microtiter plate. Inoculated MTPs were mounted on the shaking platform of MAXQ 4000 incubator (Thermo Fisher Scientific, Waltham, MA, USA) and incubated at 5, 15 and 25 °C, with 400 rpm agitation speed (1.9 cm circular orbit) for 7 days. One well in each plate was filled with a sterile medium for cross-contamination control. All cultivations were done in two independently performed biological replicates.

Bacterial biomass was separated from the growth medium by centrifugation (Heraeus Multifuge X1R, Thermo Scientific, Waltham, MA, USA) at 2330 g, 4 °C for 10 min and washed with distilled water three times. After the washing step, bacterial biomass was freeze-dried (Labconco, USA) until constant weight and stored at -80 °C for further FT-Raman measurements.

Cultivation and sample preparation for HPLC-MS analysis

Cultivation of the selected strains for analysis by high-performance liquid chromatography coupled with mass spectrometry (HPLC-MS) and evaluation of pigment stability in bacterial biomass was done in shake flasks using BHI broth. First, overnight inoculum culture was prepared in 10 mL BHI broth at 15 °C. Then, shake flasks with 100 mL of BHI broth medium were inoculated with 10 mL of the overnight inoculum. All cultivations were carried out in the shaker incubator MAXQ 4000 (Thermo Fisher Scientific, Waltham, MA, USA) at 15 °C and

400 rpm agitation (1.9 cm circular orbit). All cultivations were done for 7 days, in two biological replicates which were independent cultivation runs performed on different days.

Bacterial biomass was separated from the growth medium by centrifugation (Heraeus Multifuge X1R, Thermo Scientific) at 11510 g, 4 °C for 10 min and washed with distilled water three times. After the washing step bacterial biomass was freeze-dried (Labconco, USA) until constant weight and stored at -80 °C. Freeze-dried biomass was then used directly for extraction of pigments for HPLC-MS, FT-Raman, and TLC analysis and evaluation of pigments stability. All these steps were carried out under low light conditions to avoid pigment degradation.

Cultivation under blue light exposure

To determine the effect of light on growth and carotenoid accumulation, cultivation of bacteria in 500 mL baffled shake flasks was conducted using blue (455 nm) LED light as it was reported previously (Sumi et al., 2019). The level of illuminance for the experiment was in a range of 470-680 lux. Blue light spectra for each experimental setup are depicted on Figure S1 in SM. The cultivation in blue light was done in ISFX1 Climo-Shaker (Kuhner, Germany) equipped with LED lights using single output LED Driver mix mode (Mean Well, Taiwan) (Benjamin Dupuy--Galet). To ensure light-free conditions for control samples, the flasks were also shaded with aluminum foil, and the glass door of the shaker was covered with aluminum foil. Control samples were collected from cultures incubated in the dark.

Extractions of bacterial pigments for HPLC-MS and TLC analysis

Extraction of pigments for HPLC-MS was done as follows: each sample of 30 mg of bacterial biomass was treated with 1 mL MeOH (Sigma-Aldrich, USA) at 60 °C and followed by 15 min homogenization in an ultrasonic bath (Crest Powersonic P1100 Ultrasonic Cleaner, USA). After that insoluble material was separated by centrifugation (Centrifuge ELMI CM-50) at 18000 g for 10 min and supernatant was filtered using PTFE filter with pore size 0.45 µm into 1.8 mL glass vial. Extraction of pigments for thin layer chromatography (TLC) analysis and FT-Raman measurements was done as described by (Byrtusová et al., 2021).

HPLC-MS analysis

The extracted pigments were separated using the HPLC-DAD-MS system Agilent Q-TOF 6550 (Agilent Technologies, Santa Clara, CA, USA). The samples in a volume of 5 µL were injected into Thermo Fisher Scientific Hypersil GOLD 1.9 µm HPLC analytical column. The stepped linear gradient of buffers A (0.1% formic acid (VWR chemicals, USA) in water) and B (0.1% formic acid and 99.9% acetonitrile (Sigma-Aldrich, Germany) were distributed as follows: 00-05 min – 50% buffer A and 50% buffer B, 05-40 min – gradient from 50-100% buffer B, 40-45 min – 100% buffer B. The separation of components was monitored using a photodiode array detector at the 190-600 nm range and a mass spectrometer tandem quadrupole-time-of-flight at the 50-1700 m/z range. A positive electrospray ionization mode (ESI+) with a time-of-flight TOF detector was used. The peak area (450 nm) representing carotenoids was used for semi-quantitative calculations.

Thin-layer chromatography

TLC was used to separate pigments extracted from the bacteria for the subsequent analysis by FT-Raman spectroscopy. For TLC the following solvent mixtures were used: (1) Acetone: n-heptane (1:1) (SuiLiu and Deng, 2014), 2) Chloroform: methanol (93:7) (Squillaci et al., 2017).

Silica Gel 60 F254 (0.25 mm, Merck, Darmstadt, Germany) was activated in the solvent used for the separation before each analysis. All samples were placed on TLC plates, dried, and measured directly with FT-Raman. The following pigments were used as standards: canthaxantin (No. 0380), phytoene (No. 0044), lycopene (No. 0031), zeaxanthin (No. 0119), echinenone (No. 0283), neurosporene (No. 0034), and beta-carotene (CaroteNature GmbH, Münsingen, Switzerland), astaxanthin (Sigma Aldrich, Country) and bacterioruberin extract (32719-43-0, HALOTEK Biotechnologie GmbH, Leipzig, Germany) (Mandelli et al., 2012).

FT-Raman measurements

Raman spectra were acquired in a backscattering configuration using a MultiRAM FT-Raman spectrometer (Bruker Optik GmbH in Ettlingen, Germany). The instrument was equipped with a neodymium-doped yttrium aluminium garnet (Nd:YAG) laser operating at 1064 nm (9394 cm^{-1}) and a germanium detector cooled with liquid nitrogen.

FT-Raman spectroscopy analysis of the pigments in intact biomass was performed using freeze-dried bacterial biomass. Approximately 5-10 mg of the biomass was transferred to flat-bottom 400 µL glass inserts (Agilent, USA). The glass inserts were then placed in a 96-well multi-well holder, and measurements were conducted using a high-throughput setting stage measurement accessory (Figure S2A in SM).

To measure pure pigment standards using FT-Raman, the pigments were dissolved in chloroform to achieve a final concentration of 1 mg/mL. The pigment solution was then deposited onto a TLC silica plate (Merck, Germany), and the solvent was evaporated. Finally, the plate with the deposited pigments was placed on the Z-motorized stage measurement accessory for subsequent measurements (Figure S2B in SM).

For the analysis of extracted pigments using FT-Raman, the pigments were deposited onto a TLC silica plate (Figure S2A in SM). After solvent was evaporated, the plate was placed on a Z-motorized stage measurement accessory for further measurements. Additionally, thin-layer chromatography (TLC) was performed to separate different pigments in the extract. Each pigment fraction on the TLC plate was then measured by FT-Raman by placing it on the Z-motorized stage measurement accessory (Figure S2C in SM).

For screening experiment, evaluation of blue light effect and photostability testing the acquisition of spectra involved the following parameters: 2048 scans, Blackman–Harris 4-term apodization, a spectral resolution of 8 cm^{-1}, and a digital resolution of 1.928 cm^{-1}, spanning the spectral range from 3785 to 45 cm^{-1}. The laser power used was set at 500 mW. For analysis of pigment extracts and standards on TLC plate the acquisition of spectra involved the following parameters: 128 scans, Blackman–Harris 4-term apodization, a spectral resolution of 4 cm^{-1}, and a digital resolution of 1.928 cm^{-1}, spanning the spectral range from 3785 to 45 cm^{-1}. The laser power used was set at 900 mW. All measurements were performed in two technical replicates for all type of samples (biomass, standards and extracts). The acquisition and control of data were performed using the OPUS software (Bruker Optik GmbH in Ettlingen, Germany).

Evaluation of pigments stability in bacterial biomass with FT-Raman spectroscopy

To measure pigment stability, 5 mg of the freeze-dried biomass was placed onto a weighing boat (VWR, USA) in a monolayer. Solar simulator Sun 2000 (Abet Technologies, USA) was used for light explosion. Light emission in the full spectral range (280-2500 nm) was used with

an AM 1.5G and UVC blocking filters implemented: Atmospheric Edge (AE) filter for terrestrial cells with response below 360 nm and for life sciences, UVC blocking filters for material and life sciences, resulting with the emission in 300-2500 nm spectral range. Light intensity was set at 550W. Calibration of the instrument was performed before each measurement with digital multimeter (Fluke 175, USA) attached to silicon reference cell (Rera solutions, Netherlands) to ensure same energy of light for each exposure equal to 93.7 mV. Illuminance meter T-10A (Konica Minolta, Japan) was used to measure illuminance before each measurement. The level of illuminance for the experiment was 900 lux. Measurements were performed every 5 hours and every 10 hours after the first 10 hours of measurements. Control samples were placed at the same temperature but covered with aluminum foil to prevent exposure to light. All measurements were done in duplicates.

Data analysis

HPLC-MS data

The obtained HPLC-MS data were analyzed by Feature (Table S2 in SM) algorithms in Mass Hunter Qualitative Analysis software (Agilent, USA) and by Find by Formula (Table S3 in SM).

PCA analysis of FT-Raman data

For principal component analysis (PCA), FT-Raman spectra of the bacterial biomass were preprocessed in the different way for different set of data. For screening experiment, 2011 raw spectra were preprocessed in the following way: (1) Truncation of data to spectral range 3200-600 cm^{-1}; (2) Baseline correction with rubber band algorithm; (3) Normalization by applying area normalization (integral from 0); (4) Quality test: The peak maximum values within the biomass region (1430-1470 cm^{-1}) and the non-informative region (1800-2000 cm^{-1}) were identified, and the ratio between these maximum values was calculated. Spectra with a ratio lower than 5 were excluded due to the low signal-to-noise ratio. 1885 spectra have passed the quality check and were used in the PCA. For library-dependent experiment of the samples measured on TLC plate, 118 raw spectra were preprocessed in the following way: (1) Truncation of the region of interest 1570-1460 cm; (2) Baseline correction with rubber band algorithm; (3) Normalization by applying area normalization (integral from 0).

Orange data mining toolbox version 3.31.1 (University of Ljubljana, Ljubljana, Slovenia) was used for the preprocessing and spectral analysis (Demšar et al., 2013; Toplak et al., 2017).

Ratiometric analysis of FT-Raman data

Ratiometric analysis using FT-Raman spectra was used to determine the relative pigment content in bacterial biomass obtained under both optimal and stress growth conditions, while also assessing pigment degradation under exposure to light and temperature (Svechkarev et al., 2018;Kochan et al., 2020). For screening experiment, 1885 spectra (preprocessed in aforementioned way) were analyzed. For blue-light exposition experiment, 318 raw spectra were preprocessed in the following way: (1) Truncation of data to spectral range 3200-600 cm^{-1}; (2) Baseline correction with rubber band algorithm; (3) Quality test: The peak maximum values within the biomass region (1430-1470 cm^{-1}) and the non-informative region (1800-2000 cm^{-1}) were identified, and the ratio between these maximum values was calculated. Spectra with a ratio lower than 2.5 were excluded due to the low signal-to-noise ratio. 290 spectra have passed the quality check. For light stability testing, 243 raw spectra were preprocessed in the

following way (1) Truncation of data to spectral range 3200-600 cm^{-1};(2) Spectral smoothing by applying the Savitzky−Golay algorithm using a polynomial order of degree 2, derivative order 2 and window size 11 (Savitzky and Golay, 1964); (3) Quality test: The peak maximum values within the biomass region (1430-1470 cm^{-1}) and the non-informative region (1800-2000 cm^{-1}) were identified, and the ratio between these maximum values was calculated. Spectra with a ratio lower than 2 were excluded due to the low signal-to-noise ratio. 239 spectra have passed the quality check.

After preprocessing, for estimating the relative content of pigments, carotenoid-to-biomass ratio (C/B) was calculated. Specifically, the ratio between peak maxima in the range of 1500-1540 cm^{-1} (related to C=C stretching in polyene chain of carotenoids) and peak maxima in the range of 1430-1470 cm^{-1} (related to CH_2 and CH_3 deformations of lipids, proteins and carbohydrates, thus serving as proxy signal for total biomass) was calculated (Dzurendová et al., 2021). Orange data mining toolbox version 3.31.1 (University of Ljubljana, Ljubljana, Slovenia) was used for the preprocessing and spectral analysis (Demšar et al., 2013; Toplak et al., 2017).

Results

Semi-qualitative library-independent screening by FT-Raman spectroscopy

The screening of seventy-four fast-growing Antarctic bacteria using FT-Raman spectroscopy was conducted to investigate their pigment production capabilities at different temperatures. The bacteria were cultivated at three different temperatures (5°C, 15°C, and 25°C) the results of the growth ability present in Table S1. The resulting biomass was analyzed using FT-Raman spectroscopy. This screening is semi-qualitative and is based on the library-independent analysis of FT-Raman data.

Carotenoid pigments exhibit strong resonance Raman effect. Specifically, the conjugated nature of π-electrons from the polyene backbone causes electronic states of lower energy, leading to strong resonant enhancement of certain vibrational frequencies by excitation lasers emitting in red and near-infrared part of the spectrum. The Raman spectra of carotenoids are dominated by three characteristic vibrational bands: C=C stretching vibration (ν_1), typically observed as peaks in the Raman spectrum around 1500-1520 cm^{-1}, indicating the presence of carbon-carbon double bonds within the carotenoid molecule. Additionally, the conjugated carbon backbone gives rise to C–C stretching vibration (ν_2), visible as peaks in the range of 1100-1120 cm^{-1}. Carotenoids often exhibit a peak around 1000 cm^{-1} related to the C–CH_3 deformation mode (ν_3), allowing the identification of methyl (CH_3) groups in the carotenoid structure (Jehlička et al., 2014) (Figure 1). Based on the visual inspection of FT-Raman spectra it can be concluded that majority of pigments present in the studied Antarctic bacteria are carotenoids.

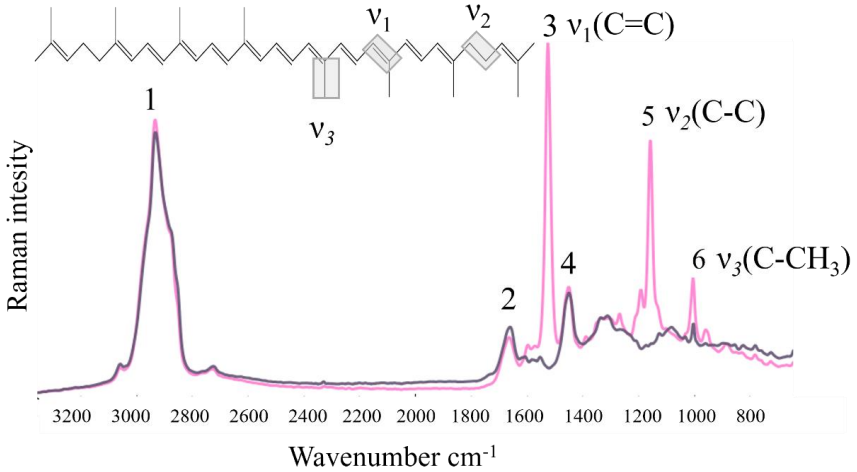

Peak №	Wavenumber cm^{-1}	Molecular vibration
1	2800-3100	C-H str. (CH, CH_2 and CH_3) carb., lipids, proteins
2	1665	C=O str. (Amide I) proteins, C=C str. lipids
3 ν_1	1500-1550	C=C str. carotenoids
4	1452	CH_2 and CH_3 de def. lipids, proteins, carb.
5 ν_2	1100-1120	C-C str. carotenoids
6 ν_3	1000-1010	C-CH_3 str carotenoids

Figure 1. Normalized FT-Raman representative spectra of pigmented bacteria *Cryobacterium soli* BIM B-1658 (pink) and non-pigmented bacteria *Shewanella baltica* BIM B-1557 (grey) with main peak assignments.

As a first step of the screening, we performed qualitative analysis to evaluate capability of the studied bacteria to produce pigments. For this, the obtained FT-Raman data were analysed by performing principal component analysis (PCA) for the whole spectral region (3200 - 600 cm^{-1}) where a distinct distribution of samples along the first principal component (PC1) was observed on the score plot (Figure 2A). The loading plots in Figure 2B illustrate the weight of each original variable (wavenumbers) on the PCs and the contribution of each spectral feature. The separation along both PC axes was due to changes in the C=C at 1525 cm^{-1}, C-C at 1156 cm^{-1} and C-CH_3 at 1005 cm^{-1} related to carotenoids (Figure 2B). PCA analysis of FT-Raman data revealed that all bacteria belonging exclusively to Actinobacteria and Bacteroidetes phyla showed presence of pigments in a considerable amount in their biomass based on appearance of carotenoid-specific peaks at high intensity. Among them, strains related to the genera *Leifsonia*, *Cryobacterium*, *Flavobacterium*, and *Rhodococcus* showed the highest absorption values for all pigment specific peaks. Additionally, the PC1 axis exhibited temperature-induced differences (Figure 2A), particularly noticeable for *Cryobacterium*, where bacteria cultivated at 5°C were clearly separated from those grown at 15°C and 25°C (Figure 2A).

The PCA score plot for the first and second components of FT-Raman spectra of freeze-dried bacterial biomass is presented in Figures S3A, S3B and S3C in SM, while the corresponding loadings can be found in Figures S3D, S3E and S3F in SM. The PCA score plot demonstrates

distinct clustering based on genera. Optimal clustering occurred at 15°C and 25°C. Further 15°C was used for the cultivation of samples for reference analysis and for assessing stability and photostability, as not all bacteria could thrive at 25°C. The loadings depicted in Figures S3D, S3Eand S3F reveal that genera-specific variations in biomass composition are primarily influenced by the ratio of main cellular components, specifically proteins in PC1 (2925 cm^{-1}), lipids in PC2 (2891 and 2854 cm^{-1}) and carotenoids in both PC1 and PC2 (1525, 1156, and 1005 cm^{-1}) (Figure 2). For instance, at 5°C *Arthrobacter* and *Leifsonia* displayed the highest pigment production, while at 15°C, the highest production was observed in *Rhodococcus, Leifsonia*, and at 25°C, in *Cryobacterium* and *Arthrobacter*.

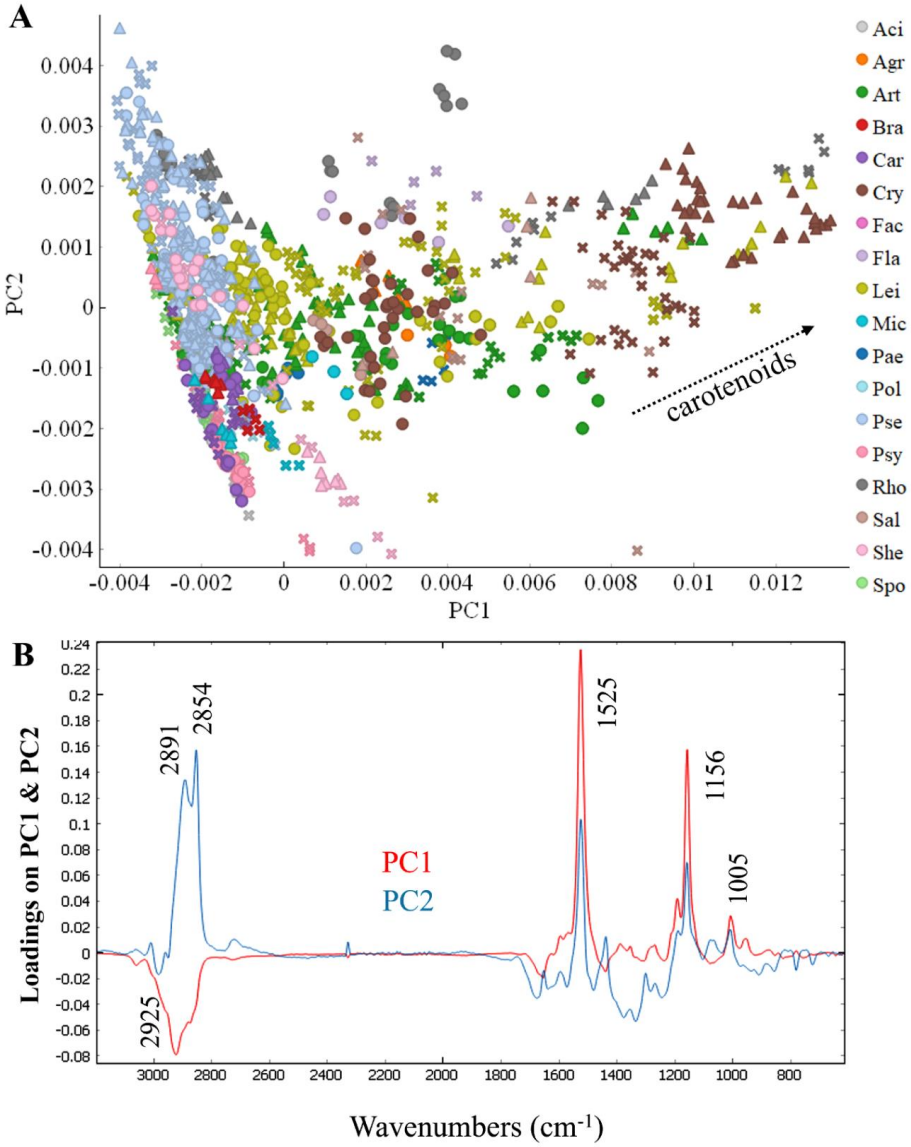

Figure 2. Principal component analysis (PCA) of the preprocessed FT-Raman spectra of Antarctic bacteria grown at different temperatures ('●' – 5°C, '✖' – 15°C and '▲' – 25°C). A – Score plot of PC1 and PC2 components, different colors represent genera (Aci-*Acinetobacter*, Agr-*Agrococcus*, Art-*Arthrobacter*, Bra-*Brachybacterium*, Car-*Carnobacterium*, Cry-*Cryobacterium*, Fac-*Facklamia*, Fla-*Flavobacterium*, Lei-*Leifsonia*, Mic-*Micrococcus*, Pae-*Paeniglutamicibacter*, Pol-*Polaromonas,* Pse-*Pseudomonas,* Psy-*Psychrobacter*, Rho-*Rhodococcus*, Sal-*Salinibacterium*, She-*Shewanella*, Spo-*Sporosarcina*), vector indicates the direction of increasing carotenoid content within the biomass. B – Loading plot of FT-Raman data with the main contributing peaks, PC1 (red) and PC2 (blue). PC1 provided 67% of explained variance and PC2 provided 12% of explained variance.

To assess the impact of temperature on the bacterial pigment profiles, we compared spectra of bacterial biomass obtained after cultivation at different temperatures and examined the presence of shift(s) for pigment related peaks. Overall, the obtained results showed that bacteria share a common spectral fingerprint with similar pigment-specific peaks registered with different intensities (Figure 3A). However, some genera and species exhibited varying pigment profiles detected as a shift of the peak related to the C=C stretching observed as peaks in the Raman spectrum around 1500-1550 cm^{-1} (Figure 3B). Thus, it could be seen that based on the peak maxima of the C=C stretching vibrations in carotenoids all bacteria could be split into groups on genus level: (1) *Agrococcus, Brachybacterium, Micrococcus* and *Paeniglutamicibacter* with peak maxima at 1530 cm^{-1}; (2) *Arthrobacter, Leifsonia, Salinibacterium* with maxima of the peak around 1528 cm^{-1}; (3) *Flavobacterium, Cryobacterium, Salinibacterium* with maxima of the peak around 1525 cm^{-1} ; (4) *Rhodococcus* with peak maxima at 1520 cm^{-1} and (5) unique spectra with peak maxima at 1506 cm^{-1} for *Arthrobacter agilis* BIM B-1543. Peak shifts were observed among different species within a single genus for *Arthrobacter*, *Rhodococcus, Leifsonia*, except of *Cryobacterium* (Figure 3B). Additionally, it was noticed that temperature had a discernible effect on the peak shift for *Rhodococcus* strains (Figure 3B).

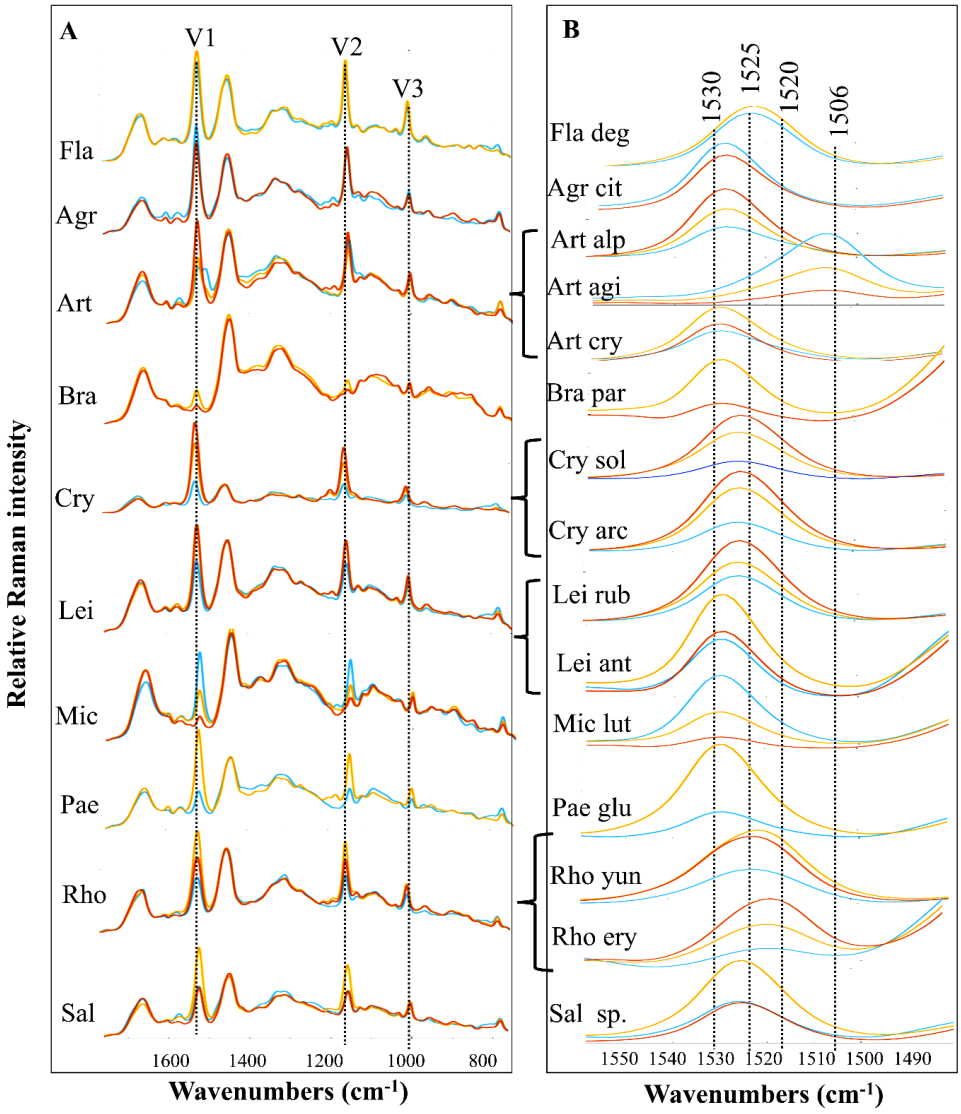

Figure 3. A- Temperature-averaged FT-Raman spectra of bacterial biomass for different genera grown at different temperatures (blue – 5°C, yellow – 15°C and orange – 25°C). B- Position of the peak related to the C=C stretching vibrations in carotenoids observed for different genera grown at different temperatures (blue – 5°C, yellow – 15°C and orange – 25°C). Strains related to *Flavobacterium, Brachybacterium* and *Paeniglutamicibacter* genera did not grow at all three tested temperatures (see Table S1). Agr-*Agrococcus*, Art-*Arthrobacter*, Bra-*Brachybacterium*, Cry-*Cryobacterium*, Fla-*Flavobacterium*, Lei-*Leifsonia*, Mic-*Micrococcus*, Pae-*Paeniglutamicibacter*, Rho-*Rhodococcus*, Sal-*Salinibacterium.* Spectra are vertically off-set for better visualization.

As the next screening step, we estimated relative total content of pigments in the bacterial biomass to identify the most promising pigment-producing strains. The estimation of relative

total pigment content was performed by calculating carotenoids/biomass (C/B) ratio from the FT-Raman data, which previously was proven to be an effective measure (Dzurendová et al., 2021). Among the seventy-four studied bacterial strains, thirty-seven strains from 9 genera of Actinobacteria phylum (*Agrococcus, Arthrobacter, Brachybacterium, Cryobacterium, Leifsonia, Micrococcus, Paeniglutamicibacter, Rhodococcus, Salinibacterium*) and one genus of Bacteroidetes phylum (*Flavobacterium*) showed C/B ratio in the range of 0.5 – 10 (Figure 4, Figure S4 in SM). Other bacteria had C/B ratio in the range of 0- 0.5 (Figure 4, Figure S4 in SM).

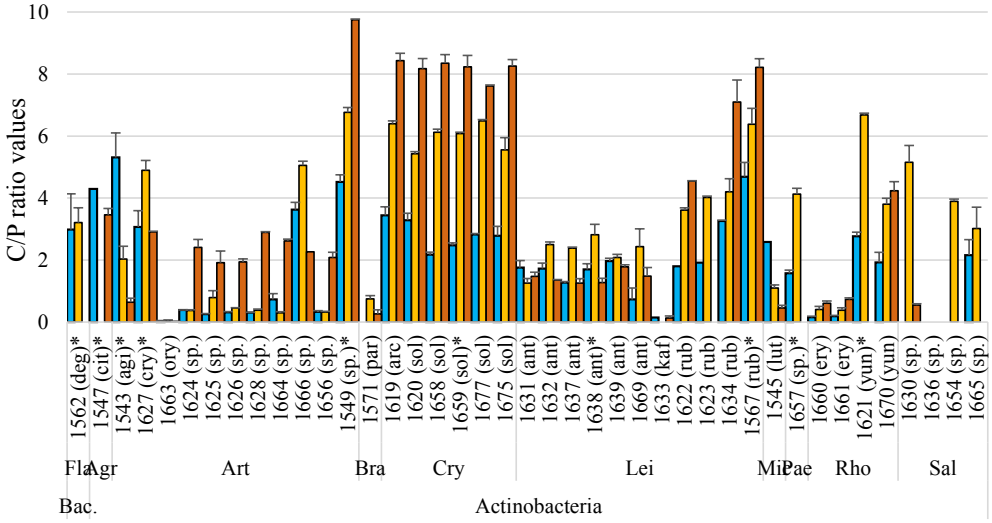

Figure 4. Ratiometric analysis based on FT-Raman spectra of pigmented bacterial biomass obtained after cultivation at different temperatures (blue – 5°C, yellow – 15°C, and orange – 25°C). The standard deviation was calculated for genera that were represented by two or more strains. Genera: Agr-*Agrococcus*, Art-*Arthrobacter*, Bra-*Brachybacterium*, Cry-*Cryobacterium*, Fla-*Flavobacterium*, Lei-*Leifsonia*, Mic-*Micrococcus*, Pae-*Paeniglutamicibacter*, Rho-*Rhodococcus*, Sal-*Salinibacterium*. * - strains selected for future analysis.

The highest C/B ratio was detected for all strains from genus *Cryobacterium*, for strain *Arthrobacter* sp. BIM B-1549, for all strains from *Leifsonia rubra* and *Rhodococcus yunnanensis* species demonstrated on Figure 4. Low C/B ratio was detected for all strains from *Arthrobacter* sp., *Leifsonia antarctica and Rhodococcus erythropolis* species and for strains Micrococcus *luteus* BIM B-1545, and *Brachybacterium paraconglomeratum* BIM B-1571. No pigments were detected for strain *Arthrobacter oryzae* BIM B-1663, *Leifsonia kafniensis* BIM B-1633 and *Salinibacterium* sp. BIM B-1636. Bacteria belonging to Actinobacteria and Bacteroidetes phyla exhibited extraordinarily high C/B ratio indicating high pigment content in the biomass, as depicted in Figure S4 in SM. Interestingly, while certain genera exhibited relatively similar pigment production across all species and strains (e.g., *Cryobacterium*), other genera showed species-specific variations, resulting in significant differences in the relative pigment content within a single genus, as it was observed for *Arthrobacter*, *Leifsonia* and *Rhodococcus* (Figure 4).

Analysis of FT-Raman data of bacteria grown at different temperatures showed three main trends of the temperature influencing pigment content in bacterial biomass: (1) increase of relative pigment content with temperature increase, as it was observed for all strains from *Flavobacterium, Cryobacterium, Paeniglutamicibacter* and *Rhodococcus* genera and for majority of *Arthrobacter* sp. *and Leifsonia rubra* strains ; (2) increase of relative pigment content with temperature decrease, as it was detected for *Agrococcus citreus* BIM B-1547*,* *Arthrobacter agilis* BIM B-1543 *, Brachybacterium paraconglomeratum* BIM B-1571 and *Micrococcus luteus* BIM B-1545 strains; (3) higher relative pigment content at temperature close to optimal, as it was detected for *Arthrobacter cryoconiti* BIM B-1627, *Arthrobacter* sp. BIM B-1666 and *Leifsonia antarctica* strains. Overall, it can be noted that relative pigment content and its alteration triggered by temperature fluctuations were mainly species-specific and varied considerably (Figure 4).

Based on the screening experiment a set of ten bacterial isolates showing relatively high pigment content was selected for detail pigment analysis, evaluation of blue light effect on pigments production and photostability testing. In addition, the selected isolates were chosen based on variations in pigments spectral profile (Figure 3B) and different responses to temperature fluctuations (Figure 4). The selected bacterial isolates belong to genera *Flavobacterium*, *Arthrobacter, Leifsonia*, *Rhodococcus*, *Agrococcus*, *Cryobacterium,* and *Paeniglutamicibacte*r (Figure 4 and 5) and most of them produce yellow pigments, except *Arthrobacter agilis* BIM B-1543 and *Rhodococcus yunnanensis* BIM B-1621 producing red and orange pigments respectively (Figure 5).

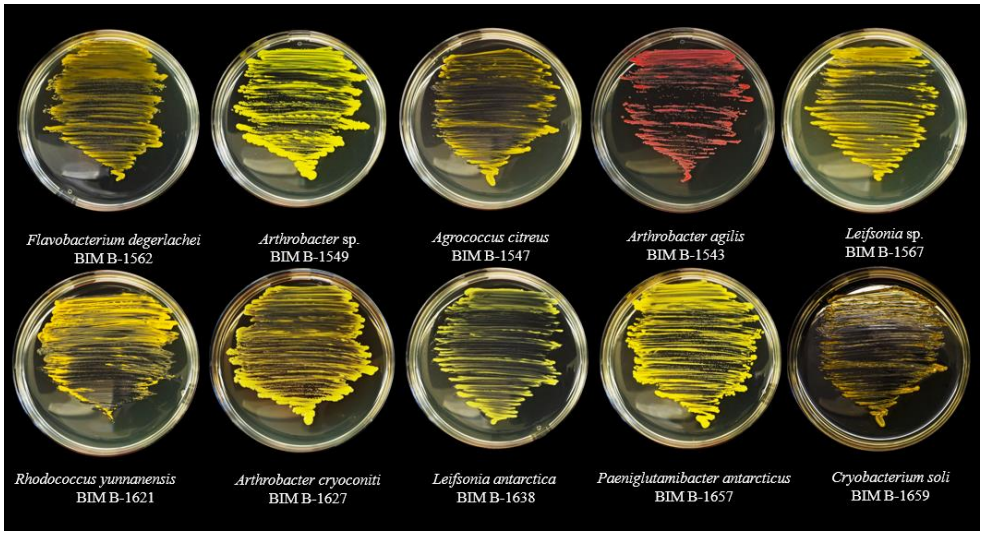

Figure 5. Petri dish images of the strains selected for further study.

Pigments profile by HPLC-MS

To perform detailed study of pigment profile of the selected set of pigmented Antarctic bacteria, HPLC-MS analysis was performed, and the results are presented in Table S5. HPLC-MS analysis of the extracted pigments revealed the presence of eighteen different carotenoids and their precursors in the biomass of the selected bacteria (Table S5). Mixtures of different carotenoids were found in all studied bacteria, thus from five to seven carotenoids were

identified in each strain depending on the strain (Table S5). Also, precursors of carotenoids such as farnesyl diphosphate and geranylgeranyl diphosphate were detected in 5 out of 10 studied bacteria (Table S5). The following pigments were identified by HPLC-MS in the studied Antarctic bacteria: C40 (Lycopene, beta-carotene, neurosporene, zeta-carotene, phytoene, echinenone, canthaxanthin, zeaxanthin), C45 (nonaflavuxanthin, dihydroisopentenyldehydrorhodopin) and C50 carotenoids (flavuxanthin, decaprenoxanthin, and dihydrobisanhydrobacterioruberin, monoanhydrobacterioruberin and bacterioruberin, (5Z)-bacterioruberin, (9Z)-bacterioruberin, (13Z)-bacterioruberin: 5Z.9'Z-bacterioruberin 9Z.9'Z-bacterioruberin) which were also major group of carotenoids found in these bacteria (Figure 6A and Table S5).

Further, HPLC-MS data showed that the studied bacteria have pigments with the following amounts of conjugated double bonds (CDBs) 3, 7, 9, 11, 12, 13 and 16 (Figure 6B, Table S5). The peak area (450 nm) representing carotenoids was used for semi-quantitative calculations based on HPLC-MS data. Thus, phytoene with 3 CDBs was detected only in one strain *Leifsonia rubra* BIM B-1567. Carotenoids with 11 CDBs were the most abundant in bacteria from genera *Arthrobacter, Leifsonia* and *Rhodococcus*. Genera *Arthrobacter* and *Paeniglutamicibacter* were characterized by the presence of carotenoids with 12 CDBs Pigments with 13 and 12 CDBs were detected in *Leifsonia antarctica* BIM B-1638 in small quantities (Figure 6B, Table S5). Overall, pigments with 11 CDBs were the most abundant in the studied bacteria (Figure 6B, Table S5). The unknown pigments were summed and shown (Figure 6B, Table S5).

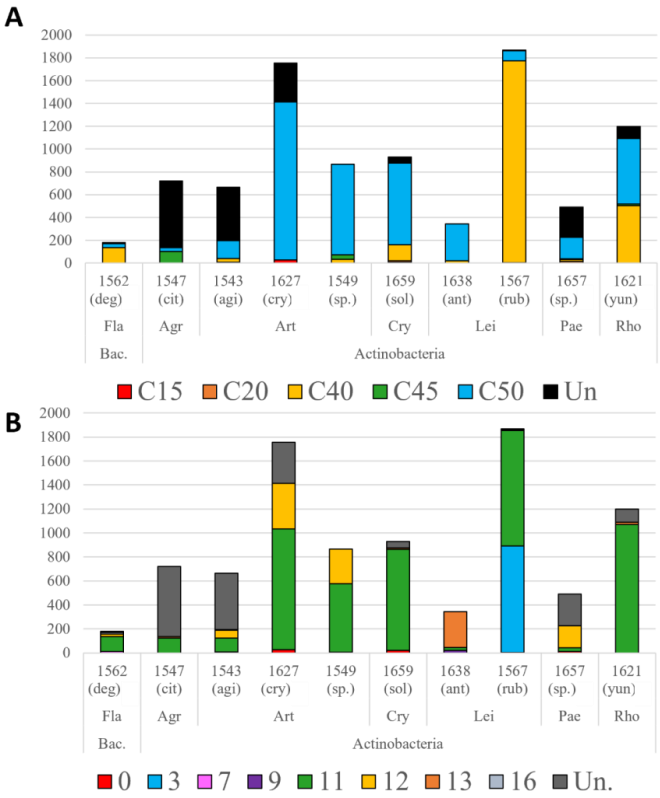

Figure 6. Summed peak area of extracted carotenoids with different number of conjugated double bounds (A) and different chain lengths (B). Genera: Agr-*Agrococcus*, Art-*Arthrobacter*, Bra-*Brachybacterium*, Cry-*Cryobacterium*, Fla-*Flavobacterium*, Lei-*Leifsonia*, Mic-*Micrococcus*, Pae-*Paeniglutamicibacter*, Rho-*Rhodococcus*, Sal-*Salinibacterium*.

HPLC-MS data mapped a diversity of pigment profiles for the studied bacteria. For example, *Flavobacterium degerlachei* BIM B-1562 from Bacteroidetes phylum, showed a distinctive pigment profile characterized by the presence of C40 ehinenone, canthaxanthin, and zeaxanthin as the main carotenoids (Table S5). Controversially, bacteial strains from genus *Arthrobacter* showed C50 flavuxanthin, decaprenoxanthin, and dihydrobisanhydrobacterioruberin as the main pigments. The strain *Rhodococcus erythropolis* BIM B-1661 had C40 carotenoids canthaxanthin and zeaxanthin, accompanied by C50 carotenoids decaprenoxanthin as major carotenoids. For the strain *Cryobacterium soli* BIM B-1659, decaprenoxanthin emerged as a main carotenoid. Interestingly, carotenoid profiles of bacterial strains from genus *Leifsonia* varied significantly. For instance, strain *Leifsonia antarctica* BIM B-1638 displayed bisanhydrobacterioruberin as its primary carotenoid, while strain *Leifsonia rubra* BIM B-1567 exhibited C40 lycopene and phytoene as the main carotenoids. The strain *Agrococcus citreus* BIM B-1547 exhibited relatively low levels of carotenoids, with only C45 and C50 variants being detected. However, for certain bacterial species such as bacteria related to genera *Agrococcus*, *Paeniglutamicibacter* and strains *Arthrobacter agilis* BIM B-1543 and *Arthrobacter cryoconiti* BIM B-1627 numerous carotenoids remained unidentified, underscoring the complexity of their pigment profiles and the need for further analysis (Table S5).

Library-dependent analysis of carotenoids by FT-Raman

FT-Raman spectroscopy can be highly specific in identifying pigment-producing microorganisms and is often used for semi-qualitative screenings. We evaluated the potential of this technology to perform detailed pigment profiling of the extracted and purified pigments using reference spectral library of pigment standards. For this, eight commercially available pigment standards selected based on the HPLC-MS data were measured by FT-Raman to establish a reference spectral library. This reference library was used to analyse composition of the bacterial pigment extracts and single pigments purified by TLC and measured by FT-Raman. The recorded spectral data were analysed by PCA, and the results are presented in Figure 7.

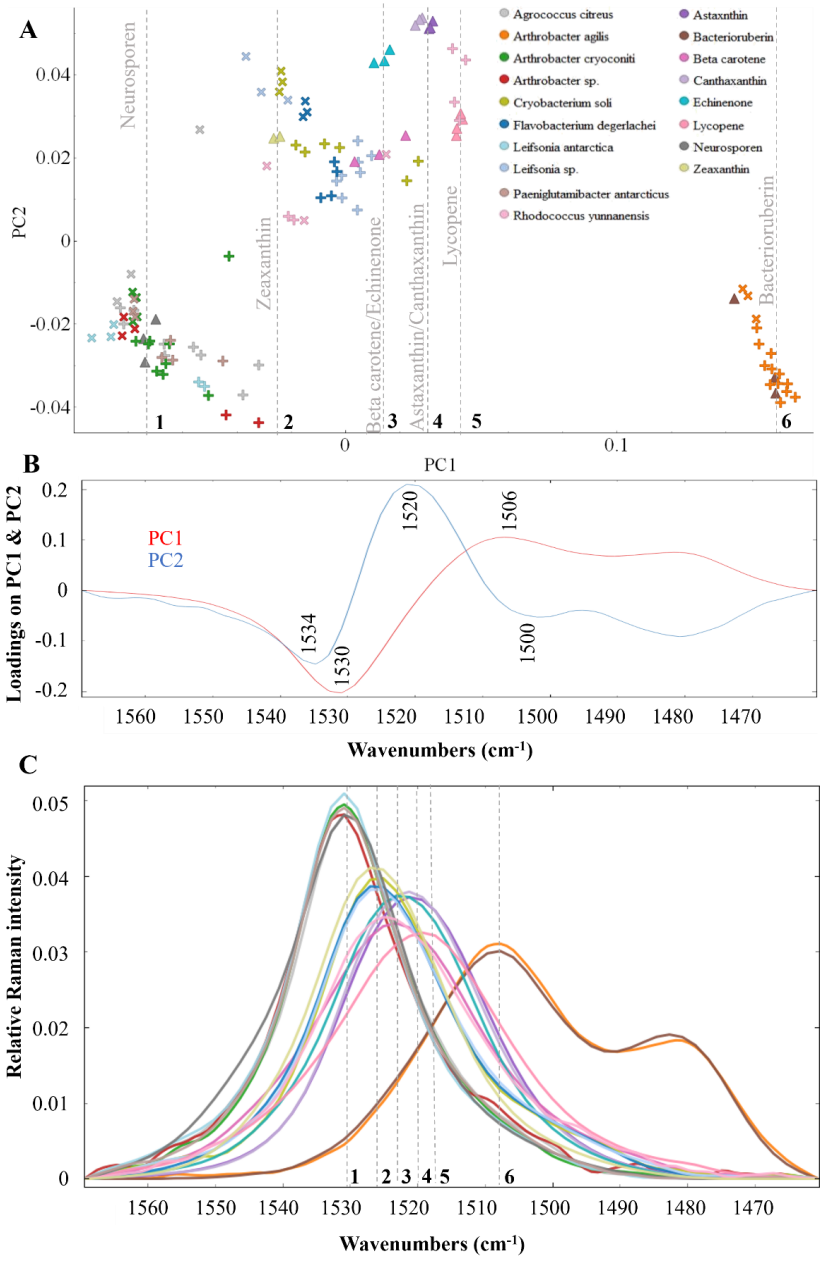

Figure 7. A – Score plot of PC1 and PC2 components where different colors represent genera and standards from the reference spectral library and shapes represent types of the sample: '✕' – bacterial pigment extracts, '▲' – pigment standards; ✚-purified pigments. B – Loading plot of FT-Raman data with the main contributing peaks, PC1 (red) and PC2 (blue). PC1 and PC2 provided 83% and 12% of explained variance, respectively. C – Raman shift between different samples in the peak between 1600-1500 cm^{-1} related to C=C stretching vibrations in carotenoids.

The PCA results revealed clear correlation between pigment standards and some bacterial extracts (Figure 7A), where all bacterial extracts and purified pigments were grouped into several clusters along the first principal component (PC1) axis, which correlated with Raman shifts of the peak at 1500-1550 cm^{-1} related to variations in pigment structures (Figure 7B). These peak shifts are dependent on the pigment's structure and the number of conjugated double bonds in carotenoids. The first component effectively separates all samples based on the peak position and shift between 1530 cm^{-1} and 1506 cm^{-1} (Figure 7B).

The first well-separated cluster comprises of the extracts and purified pigments from the strains *Paeniglutamibacter antarcticus* BIM B-1657, *Agrococcus citreus* BIM B-1547, *Leifsonia antarctica* BIM B-1638, *Arthrobacter cryoconiti* BIM B-1627, and *Arthrobacter* sp. BIM B-1549 (Figure 7A). These extracts are grouped with neurosporene standard (9 c.d.b., no oxygen) and exhibit similar peak maxima around 1530 cm^{-1} (Figure 7A, C). Interestingly, the grouping of the purified pigments from *Arthrobacter cryoconiti* BIM B-1627 (TLC fraction 3 and 5) appear slightly dislocated than neurosporene standard along PC1, suggesting the presence of other pigments with longer chain lengths of conjugated double bonds (Figure S5). The second cluster is represented by the pigment extracts and purified pigments from *Flavobacterium degerlachei* BIM B-1562*, Leifsonia* sp. BIM B-1567, and *Cryobacterium soli* BIM B-1659, which are grouped with zeaxanthin (11 CBDs, oxygen) and show the same peak maxima at 1525 cm^{-1}. Notably, for *Flavobacterium degerlachei* BIM B-1562, spectra of the pigments extract and purified pigment (TLC fraction 2) are separated, indicating that the pure pigment separated by TLC differs from the extract and that the extract likely consists of several pigments with different structures (Figure S5). For *Cryobacterium soli* BIM B-1659, it is obvious that purified pigments (TLC fractions 1 and 2) exhibit closer proximity to the extract, while fraction 3 appears separate from the rest, suggesting the presence of chemically different pigments with longer chain lengths of conjugated double bonds. Fraction 3 of *Cryobacterium soli* BIM B-1659 is located between cluster of beta-carotene/echinenone, and canthaxanthin/astaxanthin. Purified pigments from *Leifsonia* sp. BIM B-1567 are grouped together, suggesting their structural similarity, and closely grouped with beta-carotene and echinenone, which could indicate predominance of this type of carotenoid structure. The extract and TLC fractions from *Rhodococcus yunnanensis* BIM B-1621 shows presence of different pigments. Thus, the extract of all pigments is grouped together with one purified pigment (TLC fraction 3) and have the same peak maxima as zeaxanthin 1525 cm^{-1}, while other purified pigments (TLC fractions 1 and 2) are grouped distinctly and have the same peak maxima as lycopene at 1519 cm^{-1}, indicating the presence of pigments with different structures (Figure S5A, B). The most distinct cluster is represented by the extracts from *Arthrobacter agilis* BIM B-1543, spectra of which are grouped together with spectra of bacterioruberin (16 CDBs) (Figure S5A, C). A significant increase in the number of conjugated double bonds leads to a pronounced shift of bacterioruberin to lower wavenumbers, with maxima at 1506 cm^{-1} and 1482 cm^{-1}, distinctly separating it from all other pigments (Figure 7A, B). PCA analysis reviled that bacterial pigment profiles are complex and contain more than one type of carotenoids. Based on the result of separation of the bacterial extract by TLC it was detected that for bacteria such as *Cryobacterium soli* BIM B-1659, *Rhodococcus yunnanensis* BIM B-1621, and *Arthrobacter cryoconiti* BIM B-1627 the extract contains several different pigments with different structure and different conjugation chain length. For bacteria *Leifsonia antarctica* BIM B-1638, *Flavobacterium degerlachei* BIM B-1562, and *Arthrobacter agilis* BIM B-1543 pigments separated by TLC are grouped together, which indicates their structural similarity.

Evaluating biotechnological potential and testing photostability

To determine biotechnological potential of the selected pigment-producing Antarctic bacteria we evaluated their biomass and pigment production under conditions triggering pigments production (blue light exposure). The experiment was performed at 15 °C since six out of ten selected strains exhibited a poor growth at 25 °C (Figure 3). The highest biomass production was recorded for the strains *Paeniglutamicibacter antarcticus* BIM B-1657 (~5 g/L), followed by *Arthrobacter* strains (from 2 to 3.5 g/L) and *Rhodococcus yunnanensis* BIM B-1621 (up to 2 g/L) (Figure 8). When comparing biomass production at 15 °C between control samples (no light exposure) and samples after light exposure, it was observed that exposure to blue light had a genus and species-specific impact on pigment production. Thus, for *Flavobacterium degerlachei* BIM B-1562, *Arthrobacter cryoconiti* BIM B-1627and *Paeniglutamicibacter antarcticus* BIM B-1657 the biomass production was higher after blue light exposure (Figure 8), while for *Agrococcus citreus* BIM B-1547, *Arthrobacter agilis* BIM B-1543, *Leifsonia rubra* BIM B-1567 and *Rhodococcus yunnanensis* BIM B-1621 the biomass after exposure was lower compared to the control samples, and for the rest of bacterial isolates no light effect was detected (Figure 8).

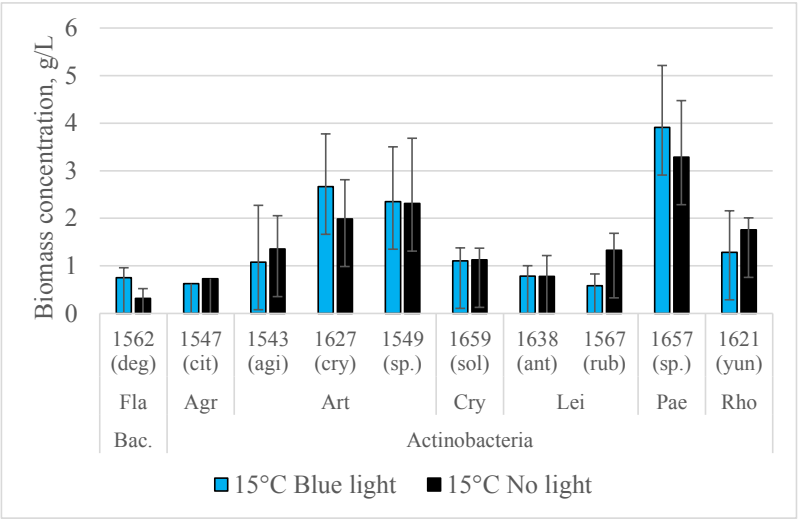

Figure 8. Biomass production at 15 °C under the blue light exposure and no light exposure (control). Genera: Fla-*Flavobacterium*, Agr-*Agrococcus*, Art-*Arthrobacter*, Bra-*Brachybacterium*, Cry-*Cryobacterium*, Lei-*Leifsonia*, Mic-*Micrococcus*, Pae-*Paeniglutamicibacter*, Rho-*Rhodococcus*, Sal-*Salinibacterium*.

In addition to biomass production, the effect of blue light on pigment production at 15 °C was evaluated using FT-Raman spectroscopy, specifically by quantifying the C/B ratio of the biomass spectra (Figure 9). For *Flavobacterium degerlachei* BIM B-1562, *Agrococcus citreus* BIM B-1547, *Arthrobacter agilis* BIM B-1543, *Cryobacterium soli* BIM B-1659, *Leifsonia antarctica* BIM B-1638, *Paeniglutamicibacter antarcticus* BIM B-1657 and *Rhodococcus yunnanensis* BIM B-1621 the C/B ratio was higher when the strains were exposed to blue light, indicating that these strains exhibited light-induced production of carotenoids (Figure 9). The biggest effect of blue light exposure was detected for *Cryobacterium soli* BIM B-1659, *Agrococcus citreus* BIM B-1547 and *Flavobacterium degerlachei* BIM B-1562 (Figure 9).

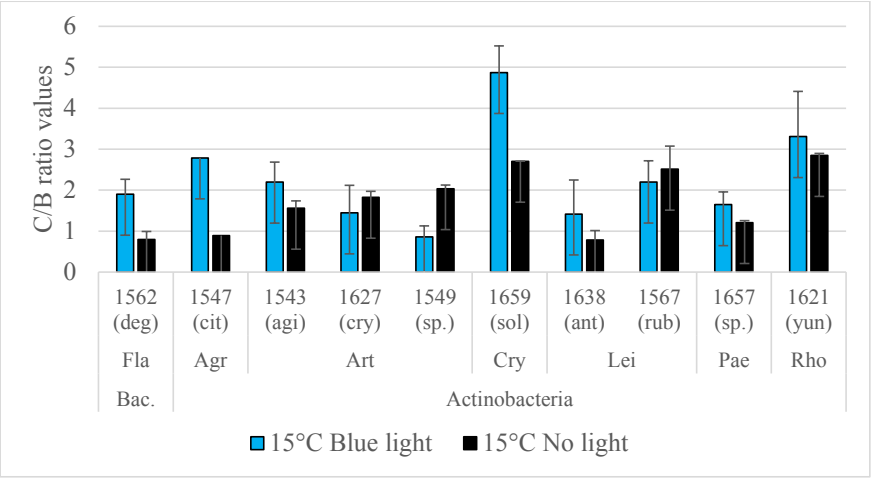

Figure 9. Relative pigment amount at 15 °C under the blue light exposure and no light exposure (control) measured by quantifying the C/B ratio of the freeze-dried biomass. Genera: Fla-*Flavobacterium*, Agr-*Agrococcus*, Art-*Arthrobacter*, Bra-*Brachybacterium*, Cry-*Cryobacterium*, Lei-*Leifsonia*, Mic-*Micrococcus*, Pae-*Paeniglutamicibacter*, Rho-*Rhodococcus*, Sal-*Salinibacterium*

To assess the photostability of selected bacteria, freeze-dried biomass was exposed to light at an illuminance value of 900 lux for 60 hours, covering a spectral range from 300 to 2500 nm. To determine the photostability of the pigments, carotenoids/biomass (C/B) ratio was calculated. The results revealed a pronounced pigments photodegradation effect in the pigmented bacterial biomass after exposure to light leading to a noticeable decrease in the C/B ratio (color bars) compared to the control samples without light exposure (white bars) (Figure 10A). Thus, *Flavobacterium degerlachei* BIM B-1562, *Arthrobacter* sp. BIM B-1549, *Rhodococcus yunnanensis* BIM B-1621 and *Leifsonia rubra* BIM B-1567, demonstrated a notably higher rate and speed of photodegradation after light explosion compared to other bacterial strains, thus the C/B ratio decreases fast especially during first 20 hours of light exposure (Figure 10A, B). Interestingly, these bacteria have short C40 carotenoids as prevalent. The lowest degradation rate of the pigments was observed for *Arthrobacter agilis* BIM B-1543, *Arthrobacter cryoconiti* BIM B-1627, and *Paeniglutamibacter antarcticus* BIM B-1657 which have C50 carotenoids as predominant. The fluctuations in the control samples were insignificant during the first 5 hours of exposure and remained stable thereafter. After 60 hours of light exposure, *Arthrobacter agilis* BIM B-1543 and *Paeniglutamibacter antarcticus* BIM B-1657 exhibited the most promising results in terms of pigment stability. No peak shift or change in the profile was detected with FT-Raman spectroscopy for the samples exposed by light (Figure S6).

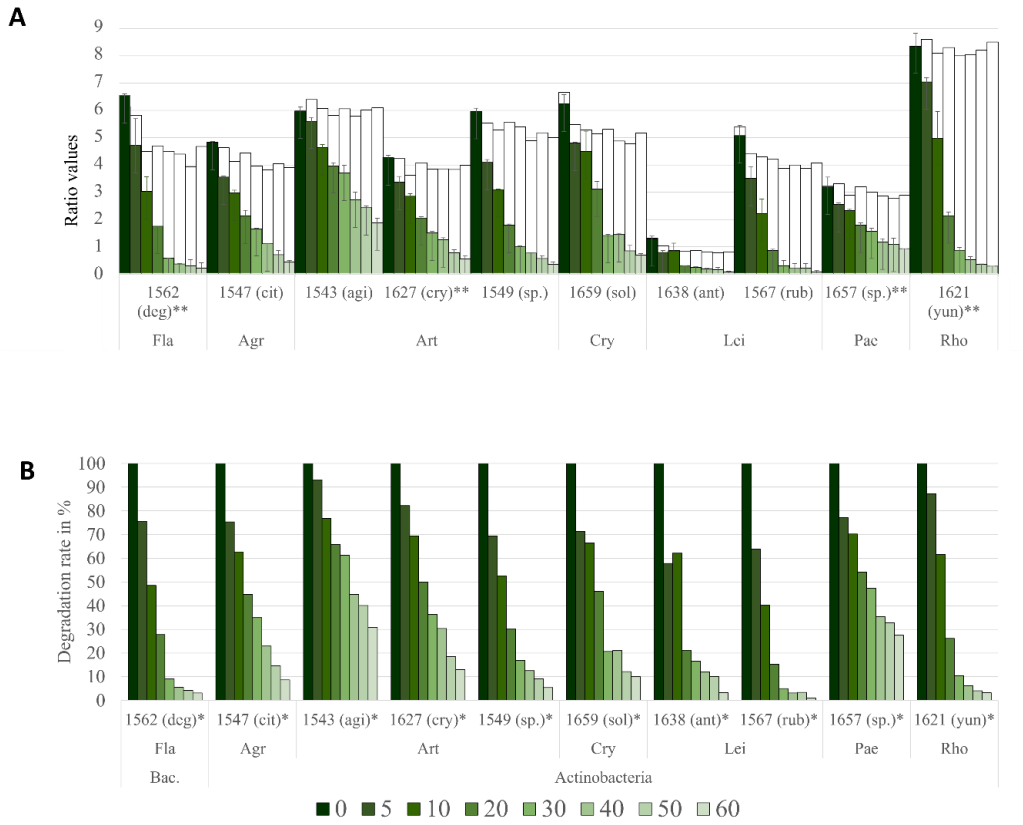

Figure 10. A-Ratiometric analysis and B- Ratiometric analysis normalized by time 0 of FT-Raman spectra of the freeze-dried bacterial biomass exposed to light for 5, 10, 20, 30, 40, 50, 60 hours, Colors represent exposure time, white color represent control samples. Genera: Fla-*Flavobacterium*, Agr-*Agrococcus*, Art-*Arthrobacter*, Bra-*Brachybacterium*, Cry-*Cryobacterium*, Lei-*Leifsonia*, Mic-*Micrococcus*, Pae-*Paeniglutamicibacter*, Rho-*Rhodococcus*, Sal-*Salinibacterium*.

Discussion

In this study we performed a high-throughput screening and comprehensive characterization of the relative pigment content and profile for seventy-four Antarctic bacteria isolated from green snow and temporary meltwater ponds. According to FT-Raman analysis, majority of the studied bacteria identified as pigmented were able to produce carotenoids. Thirty-seven strains from nine genera *Agrococcus, Arthrobacter, Brachybacterium, Cryobacterium, Leifsonia, Micrococcus, Paeniglutamicibacter, Rhodococcus,* and *Salinibacterium* and *Flavobacterium* displayed relatively high total pigment content, as indicated by FT-Raman data analysis. Strains from many of these genera have been previously reported as pigment producing (Leiva et al., 2015;Vila et al., 2019;Sajjad et al., 2020;Silva et al., 2021). Semi-quantitative analysis based on the calculation of ratio of carotenoids versus proteins (C/P) using FT-Raman spectra showed that bacteria from genera *Arthrobacter, Cryobacterium, Leifsonia* and *Rhodococcus* have the highest total pigment content. Important to note, while several studies previously

reported pigment analysis of Antarctic bacteria biomass, many bacterial species characterized in the study have not been previously analysed for pigment production.

Carotenoids protecting bacterial cells against the harmful effects of solar radiation by preventing DNA damage, countering reactive oxygen species formation, and modulating membrane fluidity in cold environments like Antarctica (Styczynski et al., 2020). A strong influence of temperature and UV radiation on bacterial pigment production was reported previously (Rehman and Dixit, 2020). We observed that changes of the relative pigment content (C/B ratio) triggered by temperature are mainly species specific, and it can vary considerably. Temperature triggered changes in pigment profile, estimated by analyzing presence of peak shifts, varied between different genera while it was conserved within single species. This indicates that temperature-triggered metabolic cell responses associated with the pigment profile changes can be conserved within a single genus. This was not reported previously, and more research would be needed involving large and balanced set of bacteria. For most of the strains increase in pigment production with temperature increase was detected as it was shown for *Flavobacterium, Arthrobacter* sp.*, Cryobacterium, Leifsonia rubra, Paeniglutamicibacter* and *Rhodococcus* and for few strains such as *Arthrobacter agilis* BIM B-1543 and *Micrococcus luteus* BIM B-1545 an opposite effect of decrease in pigment production at elevated temperature was detected that possibly connected to the regulation of cellular membrane fluidity at low temperatures (Fong et al., 2001).

The pigment profiles obtained by HPLC-MS for many Antarctic bacteria were consistent with the published results in the literature. Among all carotenoids identified in the Antarctic bacteria, six are regarded as industrially significant - astaxanthin, β-carotene, canthaxanthin, lutein, lycopene, and zeaxanthin (Martínez-Cámara et al., 2021). Thus, a presence of C40 ehinenone, canthaxanthin, and zeaxanthin, beta-carotene in *Flavobacterium degerlachei* BIM B-1562 recorded in our study was in accordance with the previously reported for *Flavobacterium frigidarium* (Humphry et al., 2001) *Flavobacterium* sp. (Vila et al., 2019), while production of flexirubin was not detected in our study (Van Trappen et al., 2004). *Flavobacterium* has been mentioned in the literature as a promising producer of zeaxanthin with productivity 500 mg/L (Ram et al., 2020). For *Arthrobacter* bacteria, similar profile of C50 carotenoids (flavuxanthin, decaprenoxanthin, and dihydrobisanhydrobacterioruberin) was reported earlier (ArpinLiaaen-Jensen and Trouilloud, 1972;Vila et al., 2019). Interestingly, bacterioruberin detected in *Arthrobacter agilis* BIM B-1543 was previously reported for other *Arthrobacter agilis* strains (Fong et al., 2001) was not identified by HPLC-MS but identified by FT-Raman using reference spectral library. For *Cryobacterium soli* BIM B-1659 production of lycopene and decaprenoxanthin were detected similarly as in previous studies (Vila et al., 2019). Our study for the first-time reports production of C40 canthaxanthin and zeaxanthin and C50 decaprenoxanthin for *Rhodococcus erythropolis* BIM B-1661. For some bacterial strains, such as *Paeniglutamicibacter antarcticus* BIM B-1657, *Arthrobacter agilis* BIM B-1543 and *Arthrobacter cryoconiti* BIM B-1627, several pigments were unidentified by HPLC-MS. This can be due to that some carotenoids are highly instable (Styczynski et al., 2020).

Evaluation of biomass productivity under the blue light exposure triggering pigment production showed that *Paeniglutamicibacter antarcticus* BIM B-1657 and *Cryobacterium soli* BIM B-1659 could be promising strains to explore further for the production of lycopene and dihydrobisanhydrobacterioruberin. Lycopene is a widely used food industry pigment with growing interest due to its health benefits, including antioxidant, anti-cancer, and cardioprotective properties (Martínez-Cámara et al., 2021). The biomass production for pigment producing strains reported in the literature is in a range from 3-12 g/L and the

carotenoid content ranged from 0.4 mg/g to 7.4 mg/g or from 0.3 mg/L to 500 mg/L (Khodaiyan et al., 2007;Ram et al., 2020). The primary objective of this study was to conduct a high-throughput screening and characterization of the pigment producing Antarctic bacteria, while the proper quantification of carotenoids content, aside the rough estimate by C/B ratio, was not performed. Also, it is important to note that cultivation conditions used in the study are not optimized for pigments production, and further studies need to be performed for optimizing cultivation parameters and media composition. While BHI broth medium has been used as a production medium in some previous studies for canthaxanthin production by *Gordonia jacobea* MV-26 (Veiga-Crespo et al., 2005).

In this study, blue light exposure triggered pigment production in all studied pigment producing strains. This phenomenon had previously been reported for gram-positive Actinobacteria from genera *Arthrobacter*, *Leifsonia*, *Paeniglutamicibacter* (Sumi et al., 2019), *Rhodococcus* (Engelhart-Straub et al., 2022) and *Flavobacterium* (Liu et al., 2021). It was also shown for *P. aeruginosa NR1* that no light, red, and blue light are optimal conditions for maximizing extracellular pigment production, whereas yellow and green light are favorable for achieving the highest biomass and intracellular pigment production (Rehman and Dixit, 2020). To the authors knowledge, light-inducible pigment production observed for *Agrococcus* and *Cryobacterium* is reported for the first time.

Carotenoids are chemically unstable molecules due to their high degree of unsaturation, causing oxidation as a primary cause of their degradation. Additionally, external factors like temperature, light, or pH can trigger significant qualitative transformations in carotenoids through isomerization reactions (Meléndez-Martínez Vicario and Heredia, 2004). Photostability is a critical factor in determining the suitability of carotenoids as photosensitizers for use in solar cells. The conventional method for assessing the photostability of bacterial pigments involves pigment extraction and measuring absorbance decay at various time intervals during light exposure (Órdenes-Aenishanslins et al., 2016). In our research, we, for the first time, used FT-Raman spectroscopy to directly evaluate the photostability of bacterial pigments in intact freeze-dried biomass, eliminating the need of pigment extraction. The obtained results showed that bacterial biomass containing mainly C40 carotenoids was less photostable than biomass with C50 carotenoids. The highest photostability was observed for *Arthrobacter agilis* BIM B-1543 producing red pigment bacterioruberin, *Arthrobacter cryoconiti* BIM B-1627, and *Paeniglutamibacter antarcticus* BIM B-1657. The higher photostability of the red pigments was previously shown (Órdenes-Aenishanslins et al., 2016). The experimental conditions described in the paper were quite severe, and we anticipated relatively rapid degradation. The Antarctic bacteria were subjected to elevated light stress, which is a common occurrence during the Antarctic summer, marked by intense UVB and UVA radiation.

In this study we demonstrated exceptionally versatile potential of FT-Raman spectroscopy for pigment analysis of microbial biomass. Fourier-transform Raman spectroscopy (FT-Raman) has recently emerged as a promising technology for the characterization of bacterial pigments. FT-Raman spectroscopy offers non-destructive analysis, without extensive sample preparation, making it valuable for rare or limited samples. Additionally, it can be conducted in a high-throughput manner, allowing for the screening of many isolates. Compared to conventional (dispersive) Raman measurements, FT-Raman spectroscopy uses high-wavelength near infrared (NIR) laser excitation, thus diminishing risk of detrimental effects, such as sample heating, photodegradation and strong fluorescence (Kenđel and Zimmermann, 2020). Even notwithstanding detrimental effects, FT-Raman spectra are often superior to the corresponding

spectra obtained by dispersive Raman spectrometers since, in the FT-Raman spectra, carotenoid bands are not completely obscuring signals of proteins, carbohydrates and other compounds (Kenđel and Zimmermann, 2020). Notably, FT-Raman spectroscopy has been used to build databases of Raman spectra for various bacterial pigments, facilitating rapid and reliable characterization of pigmented microorganisms (Jehlička et al., 2014). Carotenoids stand out as remarkable pigments in Raman spectroscopic analysis of microbial communities since resonance Raman effect enables measurement of very low concentration of these pigments (Jehlička et al., 2014). In this study we showed that FT-Raman allows to (i) perform large high-throughput library-independent screenings to identify pigment producing microorganisms, (ii) estimate relative total pigment content, (iii) determine pigment profile when reference spectral libraries are available, (iv) determine temperature and light effect on pigments production, (v) determine photostability of the pigments in intact biomass.

Conclusion

This study showed a high relevance of screening and studying polar bacteria for identifying new potential pigment producers. More than half of the studied Antarctic bacteria were able to produce pigments and many of them of high industrial importance. Some Antarctic bacteria such as *Leifsonia, Cryobacterium, Flavobacterium* and *Rhodococcus* exhibited the high levels of pigment content achieved under non-optimized cultivation conditions. In addition, in this study we demonstrated that FT-Raman spectroscopy is truly powerful analytical tool for both semi-qualitative screenings and descriptive analysis of pigmented microorganisms.

Funding

This research was supported by the project “Belanoda—Multidisciplinary graduate and post-graduate education in big data analysis for life sciences” (CPEA-LT-2016/10126) and the Belanoda Digital learning platform for boosting multidisciplinary education in data analysis for life sciences in the Eurasia region (CPEA-STA-2019/10025) funded by the Eurasia program, Norwegian Agency for International Cooperation and Quality Enhancement in Higher Education (Diku). Additional support was covered by BYPROVALUE (NFR-MATFONDAVTALE- 301834/E50), SAFE (NFR-BIONÆR 327114), SFI-IB (NFR-SFI 309558) and OIL4FEED (NFR-HAVBRUK2, 302543/E40) projects.

Conflict of Interest

The authors declare that the research was conducted in the absence of any commercial or financial relationships that could be construed as a potential conflict of interest.

References

Ahmad, A., Ahmad, W.W., Zakaria, Z., and Yosof, N. (2012). "Applications of bacterial pigments as colorant: the Malaysian perspective". New York: Springer Briefs in Molecular Science).

Arpin, N., Liaaen-Jensen, S., and Trouilloud, M. (1972). Bacterial carotenoids. XXXVIII. C 50-Carotenoids. 9. Isolation of decaprenoxanthin mono-and diglucoside from an Arthrobacter sp. *Acta Chem. Scand* 26.

Benjamin Dupuy--Galet, A.K., Xavier Álvarez Montero, Volha Shapaval Evaluating the suitability of the Duetz-MTPS and FTIR spectroscopy for high-throughput screening of microalgae. *Algal Research*

763 Byrtusová, D., Szotkowski, M., Kurowska, K., Shapaval, V., and Márová, I. (2021).
764 Rhodotorula kratochvilovae CCY 20-2-26—The source of multifunctional metabolites.
765 *Microorganisms* 9**,** 1280.
766 Chatragadda, R., and Dufossé, L. (2021). Ecological and biotechnological aspects of pigmented
767 microbes: A way forward in development of food and pharmaceutical grade pigments.
768 *Microorganisms* 9**,** 637.
769 Di Salvo, E., Lo Vecchio, G., De Pasquale, R., De Maria, L., Tardugno, R., Vadalà, R., and
770 Cicero, N. (2023). Natural Pigments Production and Their Application in Food, Health
771 and Other Industries. *Nutrients* 15**,** 1923.
772 Dieser, M., Greenwood, M., and Foreman, C.M. (2010). Carotenoid Pigmentation in Antarctic
773 Heterotrophic Bacteria as a Strategy to Withstand Environmental Stresses. *Arctic,*
774 *Antarctic, and Alpine Research* 42**,** 396-405.
775 Dzurendová, S., Shapaval, V., Tafintseva, V., Kohler, A., Byrtusová, D., Szotkowski, M.,
776 Márová, I., and Zimmermann, B. (2021). Assessment of biotechnologically important
777 filamentous fungal biomass by Fourier transform Raman spectroscopy. *International*
778 *Journal of Molecular Sciences* 22**,** 6710.
779 Engelhart-Straub, S., Cavelius, P., Hölzl, F., Haack, M., Awad, D., Brueck, T., and Mehlmer,
780 N. (2022). Effects of Light on Growth and Metabolism of Rhodococcus erythropolis.
781 *Microorganisms* 10**,** 1680.
782 Fong, N.J.C., Burgess, M.L., Barrow, K.D., and Glenn, D.R. (2001). Carotenoid accumulation
783 in the psychrotrophic bacterium Arthrobacter agilis in response to thermal and salt
784 stress. *Applied Microbiology and Biotechnology* 56**,** 750-756.
785 Hernández-Velasco, P., Morales-Atilano, I., Rodríguez-Delgado, M., Rodríguez-Delgado,
786 J.M., Luna-Moreno, D., Ávalos-Alanís, F.G., and Villarreal-Chiu, J.F. (2020).
787 Photoelectric evaluation of dye-sensitized solar cells based on prodigiosin pigment
788 derived from Serratia marcescens 11E. *Dyes and Pigments* 177**,** 108278.
789 Humphry, D.R., George, A., Black, G.W., and Cummings, S.P. (2001). Flavobacterium
790 frigidarium sp. nov., an aerobic, psychrophilic, xylanolytic and laminarinolytic
791 bacterium from Antarctica. *International journal of systematic and evolutionary*
792 *microbiology* 51**,** 1235-1243.
793 Igreja, W.S., Maia, F.D.A., Lopes, A.S., and Chisté, R.C. (2021). Biotechnological production
794 of carotenoids using low cost-substrates is influenced by cultivation parameters: A
795 review. *International Journal of Molecular Sciences* 22**,** 8819.
796 Jehlička, J., Edwards, H.G., Osterrothová, K., Novotná, J., Nedbalová, L., Kopecký, J., Němec,
797 I., and Oren, A. (2014). Potential and limits of Raman spectroscopy for carotenoid
798 detection in microorganisms: implications for astrobiology. *Philosophical*
799 *Transactions of the Royal Society A: Mathematical, Physical and Engineering Sciences*
800 372**,** 20140199.
801 Kenđel, A., and Zimmermann, B. (2020). Chemical analysis of pollen by FT-Raman and FTIR
802 spectroscopies. *Frontiers in plant science* 11**,** 352.
803 Khodaiyan, F., Razavi, S.H., Emam-Djomeh, Z., Mousavi, S.M.A., and Hejazi, M.A. (2007).
804 Effect of culture conditions on canthaxanthin production by Dietzia natronolimnaea
805 HS-1. *Journal of microbiology and biotechnology* 17**,** 195.
806 Kochan, K., Lai, E., Richardson, Z., Nethercott, C., Peleg, A.Y., Heraud, P., and Wood, B.R.
807 (2020). Vibrational spectroscopy as a sensitive probe for the chemistry of intra-phase
808 bacterial growth. *Sensors* 20**,** 3452.
809 Kumar, A., Vishwakarma, H.S., Singh, J., Dwivedi, S., and Kumar, M. (2015). Microbial
810 pigments: production and their applications in various industries. *Int. J. Pharm. Chem.*
811 *Biol. Sci* 5**,** 203-212.

Leiva, S., Alvarado, P., Huang, Y., Wang, J., and Garrido, I. (2015). Diversity of pigmented Gram-positive bacteria associated with marine macroalgae from Antarctica. *FEMS Microbiology Letters* 362**,** fnv206.

Liu, Q., Li, W., Liu, D., Li, L., Li, J., Lv, N., Liu, F., Zhu, B., Zhou, Y., and Xin, Y. (2021). Light stimulates anoxic and oligotrophic growth of glacial Flavobacterium strains that produce zeaxanthin. *The ISME Journal* 15**,** 1844-1857.

Lyu, X., Lyu, Y., Yu, H., Chen, W., Ye, L., and Yang, R. (2022). Biotechnological advances for improving natural pigment production: A state-of-the-art review. *Bioresources and Bioprocessing* 9**,** 1-38.

Mandelli, F., Miranda, V.S., Rodrigues, E., and Mercadante, A.Z. (2012). Identification of carotenoids with high antioxidant capacity produced by extremophile microorganisms. *World Journal of Microbiology and Biotechnology* 28**,** 1781-1790.

Martínez-Cámara, S., Ibañez, A., Rubio, S., Barreiro, C., and Barredo, J.-L. (2021). Main carotenoids produced by microorganisms. *Encyclopedia* 1**,** 1223-1245.

Órdenes-Aenishanslins, N., Anziani-Ostuni, G., Vargas-Reyes, M., Alarcón, J., Tello, A., and Pérez-Donoso, J. (2016). Pigments from UV-resistant Antarctic bacteria as photosensitizers in dye sensitized solar cells. *Journal of Photochemistry and Photobiology B: Biology* 162**,** 707-714.

Owen, J., and Arendt, J. (1992). Melatonin suppression in human subjects by bright and dim light in Antarctica: time and season-dependent effects. *Neuroscience letters* 137**,** 181-184.

Pailliè-Jiménez, M.E., Stincone, P., and Brandelli, A. (2020). Natural pigments of microbial origin. *Frontiers in Sustainable Food Systems* 4**,** 590439.

Ram, S., Mitra, M., Shah, F., Tirkey, S.R., and Mishra, S. (2020). Bacteria as an alternate biofactory for carotenoid production: A review of its applications, opportunities and challenges. *Journal of Functional Foods* 67**,** 103867.

Rehman, N.N.M.A., and Dixit, P.P. (2020). Influence of light wavelengths, light intensity, temperature, and pH on biosynthesis of extracellular and intracellular pigment and biomass of Pseudomonasaeruginosa NR1. *Journal of King Saud University-Science* 32**,** 745-752.

Sajjad, W., Din, G., Rafiq, M., Iqbal, A., Khan, S., Zada, S., Ali, B., and Kang, S. (2020). Pigment production by cold-adapted bacteria and fungi: colorful tale of cryosphere with wide range applications. *Extremophiles* 24**,** 447-473.

Savitzky, A., and Golay, M.J. (1964). Smoothing and differentiation of data by simplified least squares procedures. *Analytical chemistry* 36**,** 1627-1639.

Seel, W., Baust, D., Sons, D., Albers, M., Etzbach, L., Fuss, J., and Lipski, A. (2020). Carotenoids are used as regulators for membrane fluidity by Staphylococcus xylosus. *Scientific Reports* 10**,** 330.

Sen, T., Barrow, C.J., and Deshmukh, S.K. (2019). Microbial pigments in the food industry—challenges and the way forward. *Frontiers in nutrition* 6**,** 7.

Silva, T.R., Tavares, R.S., Canela-Garayoa, R., Eras, J., Rodrigues, M.V., Neri-Numa, I.A., Pastore, G.M., Rosa, L.H., Schultz, J.A., and Debonsi, H.M. (2019). Chemical characterization and biotechnological applicability of pigments isolated from Antarctic bacteria. *Marine biotechnology* 21**,** 416-429.

Silva, T.R.E., Silva, L.C.F., De Queiroz, A.C., Alexandre Moreira, M.S., De Carvalho Fraga, C.A., De Menezes, G.C.A., Rosa, L.H., Bicas, J., De Oliveira, V.M., and Duarte, A.W.F. (2021). Pigments from Antarctic bacteria and their biotechnological applications. *Critical Reviews in Biotechnology* 41**,** 809-826.

Singh, T., Pandey, V.K., Dash, K.K., Zanwar, S., and Singh, R. (2023). Natural bio-colorant and pigments: Sources and applications in food processing. *Journal of Agriculture and Food Research*, 100628.

Squillaci, G., Parrella, R., Carbone, V., Minasi, P., La Cara, F., and Morana, A. (2017). Carotenoids from the extreme halophilic archaeon Haloterrigena turkmenica: Identification and antioxidant activity. *Extremophiles* 21, 933-945.

Styczynski, M., Rogowska, A., Gieczewska, K., Garstka, M., Szakiel, A., and Dziewit, L. (2020). Genome-based insights into the production of carotenoids by Antarctic bacteria, Planococcus sp. ANT_H30 and Rhodococcus sp. ANT_H53B. *Molecules* 25, 4357.

Sui, L., Liu, L., and Deng, Y. (2014). Characterization of halophilic C50 carotenoid-producing archaea isolated from solar saltworks in Bohai Bay, China. *Chinese journal of oceanology and limnology* 32, 1280-1287.

Sumi, S., Suzuki, Y., Matsuki, T., Yamamoto, T., Tsuruta, Y., Mise, K., Kawamura, T., Ito, Y., Shimada, Y., and Watanabe, E. (2019). Light-inducible carotenoid production controlled by a MarR-type regulator in Corynebacterium glutamicum. *Scientific Reports* 9, 13136.

Svechkarev, D., Sadykov, M.R., Bayles, K.W., and Mohs, A.M. (2018). Ratiometric fluorescent sensor array as a versatile tool for bacterial pathogen identification and analysis. *ACS sensors* 3, 700-708.

Tuncer, P.B., Büyükleblebici, S., Eken, A., Taşdemir, U., Durmaz, E., Büyükleblebici, O., and Çoşkun, E. (2014). Comparison of cryoprotective effects of lycopene and cysteamine in different cryoprotectants on bull semen and fertility results. *Reproduction in Domestic Animals* 49, 746-752.

Van Trappen, S., Vandecandelaere, I., Mergaert, J., and Swings, J. (2004). Flavobacterium degerlachei sp. nov., Flavobacterium frigoris sp. nov. and Flavobacterium micromati sp. nov., novel psychrophilic bacteria isolated from microbial mats in Antarctic lakes. *International journal of systematic and evolutionary microbiology* 54, 85-92.

Veiga-Crespo, P., Blasco, L., Dos Santos, F.R., Poza, M., and Villa, T.G. (2005). Influence of culture conditions of Gordonia jacobaea MV-26 on canthaxanthin production. *International Microbiology* 8, 55-58.

Vila, E., Hornero-Méndez, D., Azziz, G., Lareo, C., and Saravia, V. (2019). Carotenoids from heterotrophic bacteria isolated from fildes peninsula, king george island, antarctica. *Biotechnology Reports* 21, e00306.

Yabuzaki, J. (2017). Carotenoids Database: Structures, chemical fingerprints and distribution among organisms. *Database* 2017, bax004.

Supplementary materials

Screening for pigment production and characterization of pigment profile and photostability in cold-adapted Antarctic bacteria using FT-Raman spectroscopy

Volha Akulava[1], Dana Byrtusova[1], Boris Zimmermann[1], Margarita Smirnova[1], Achim Kohler[1], Uladzislau Miamin[2], Leonid Valentovich[3], Volha Shapaval[1]

[1]Faculty of Science and Technology, Norwegian University of Life Sciences, Ås, Norway

[2]Faculty of Biology, Belarussian State University, Minsk, Belarus

[3]Institute of Microbiology, National Academy of Sciences of Belarus, Minsk, Belarus

[4]Institute of Microbiology, National Academy of Sciences of Belarus, 220084 Minsk, Belarus*** Correspondence:**
Corresponding Author
volha.akulava@nmbu.no

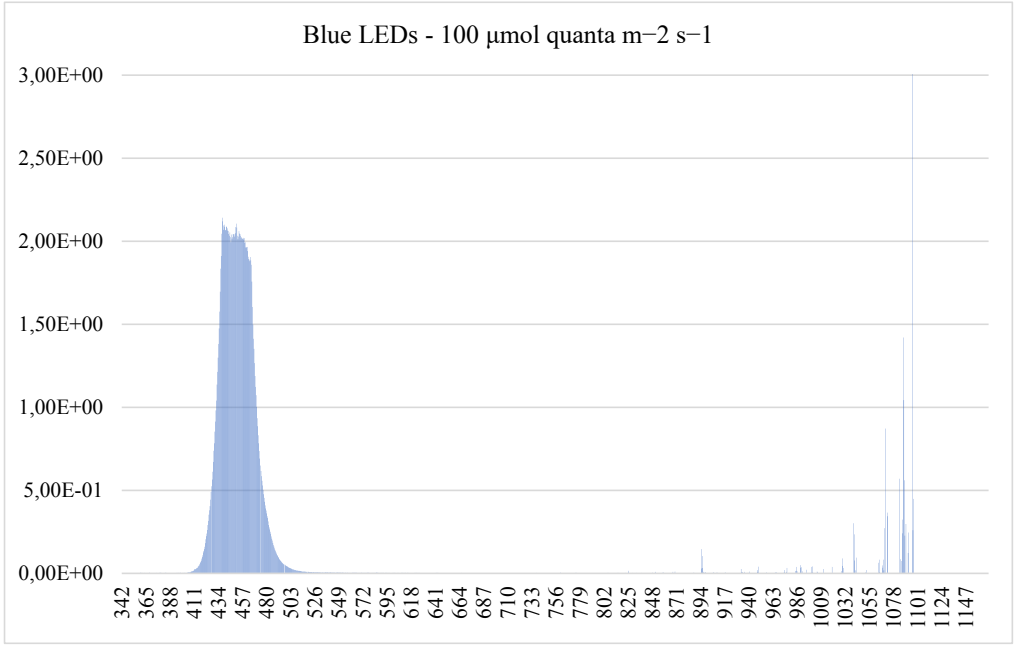

Figure S1. Blue LEDs light spectra.

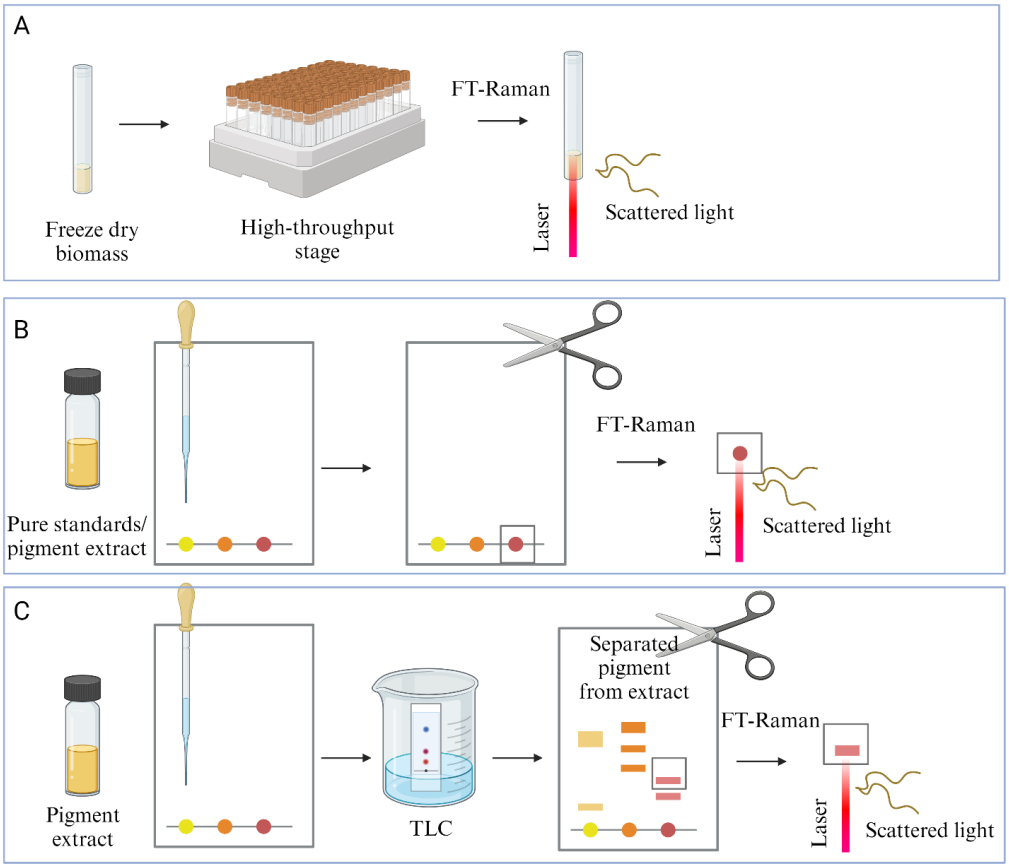

910

911 Figure S2. Sample preparation for TLC coupled with FT-Raman spectroscopy.

912

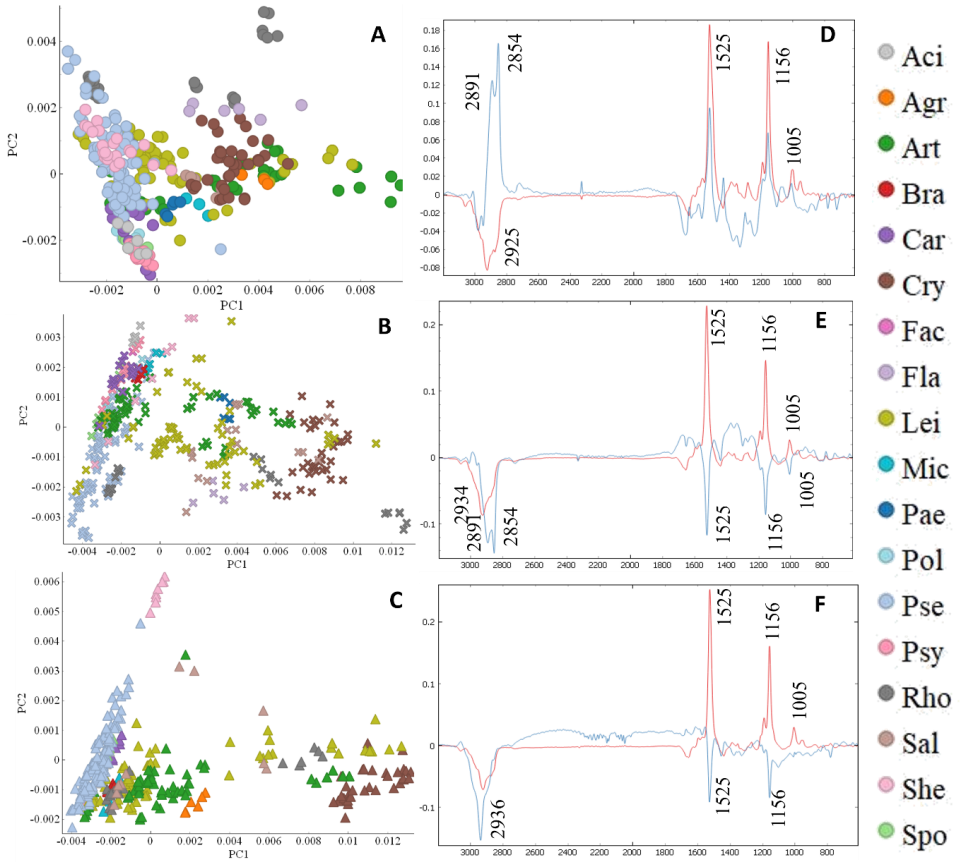

Figure S3. Principal component analysis (PCA) of the preprocessed FT-Raman spectra of bacteria grown at different temperatures ('●' – 5°C, '✖' – 15°C and '▲' – 25°C). A, B and C – score plot of PC1 and PC2 components, colors represent genera: Genera: Fla-*Flavobacterium*, Agr-*Agrococcus*, Art-*Arthrobacter*, Bra-*Brachybacterium*, Cry-*Cryobacterium*, Lei-*Leifsonia*, Mic-*Micrococcus*, Pae-*Paeniglutamicibacter*, Rho-*Rhodococcus*, Sal-*Salinibacterium*, shapes represent cultivation temperatures. PC1 provided 56% of explained variance and PC2 provided 15% of explained variance at 5°C, PC1 provided 68% of explained variance and PC2 provided 13% of explained variance at 15°C, PC1 provided 76% of explained variance and PC2 provided 9% of explained variance at 25°; C D, E and G – loading plot of FT-Raman data with the main contributing peaks, PC1 (red) and PC2 (blue).

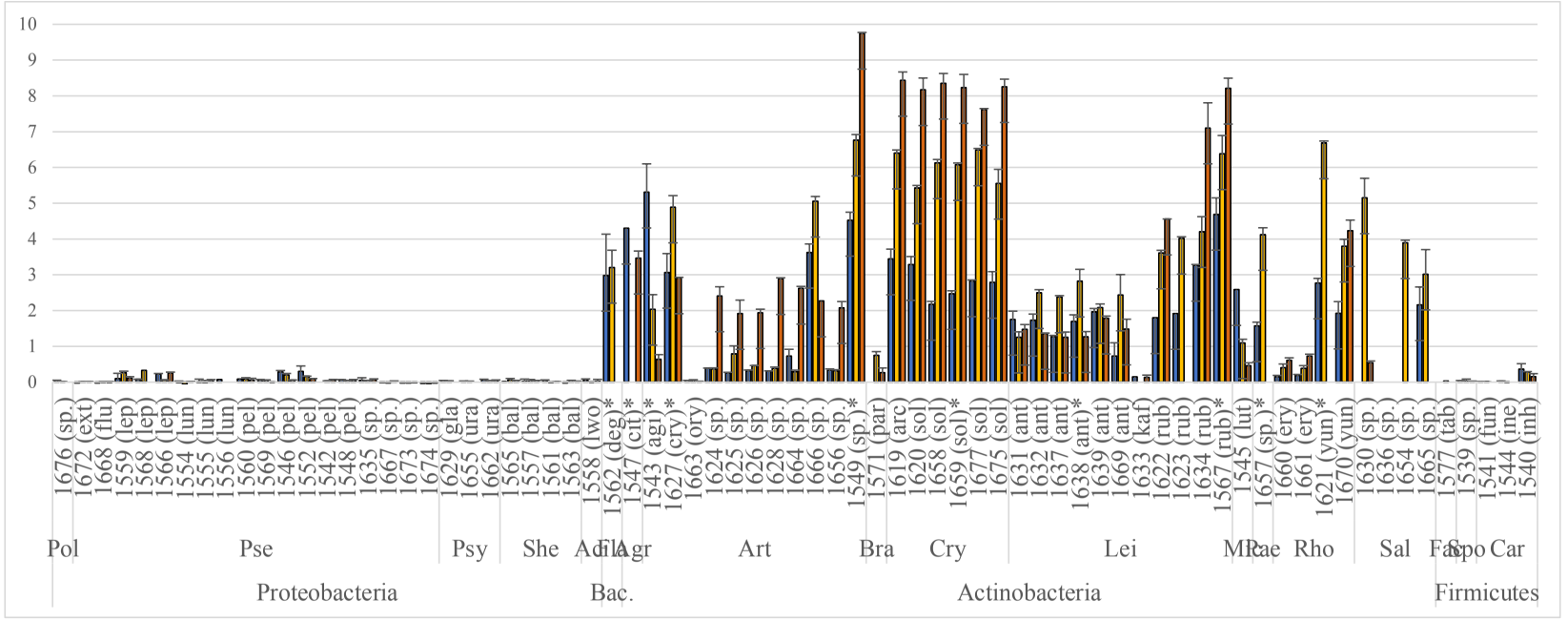

Figure S4. Ratiometric analysis (C/B ratio) of FT-Raman spectra of bacterial biomass obtained after cultivation at different temperatures (blue – 5°C, yellow – 15°C, and orange – 25°C). The standard deviation was calculated for genera that were represented by two or more strains. * - strains selected for further analysis. Genera: add here

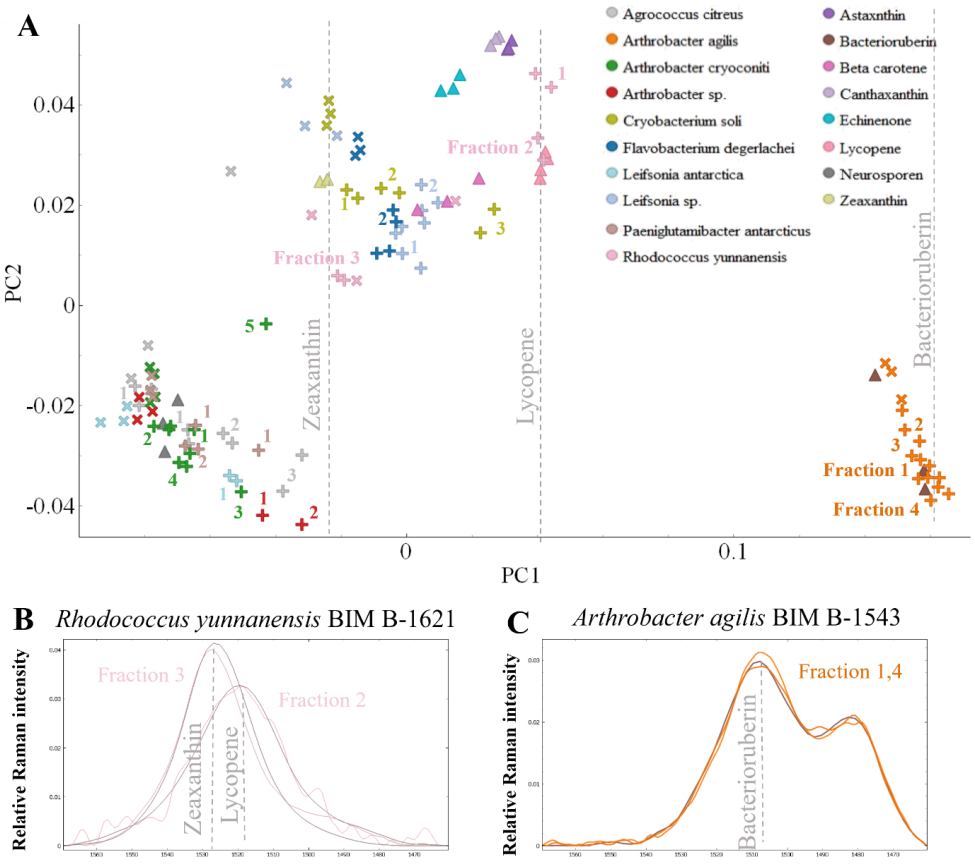

Figure S5. A – Score plot of PC1 and PC2 components where different colors represent genera and standards from the reference spectral library and shapes represent types of the sample: '✕' – bacterial pigment extracts, '▲' – pigment standards; ✚-purified pigments, numbers on the plot represent fractions (purifed pigments) after TLC of pigment extract. B– Representative spectra of the peak between 1600-1500 cm^{-1} related to C=C stretching vibrations in carotenoids of 2 different fractions from pigment extracts from *Rhodococcus yunnanensis* BIM B-1621 plotted with the spectra of two standards zeaxanthin and lycopene. C– Representative spectra of the peak between 1600-1500 cm^{-1} related to C=C stretching vibrations in carotenoids of 2 different fractions from pigment extracts from *Arthrobacter agilis* BIM B-1543 plotted with the spectra of one standard bacterioruberin

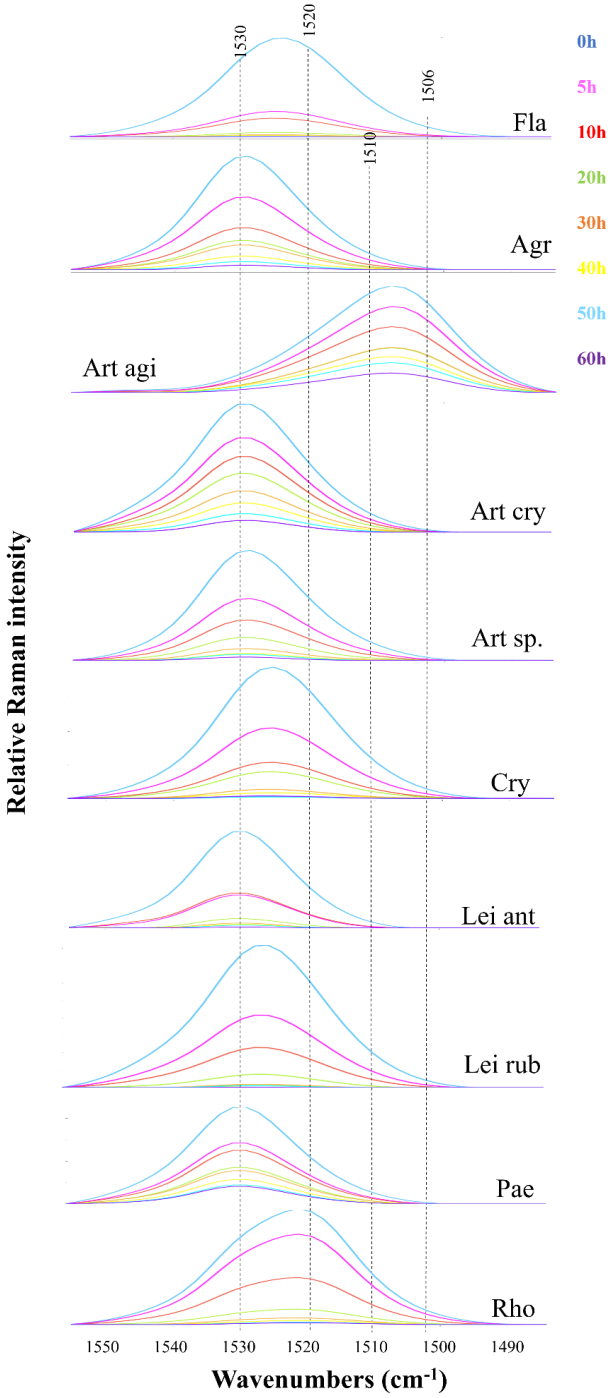

Figure S6. Raman shift after 0,5,10,20,30,40,50,60 hours of light explosion in the peak between 1600-1500 cm^{-1} related to C=C stretching vibrations in carotenoids.

Table S1. List of strains and GenBank accession number for the partial sequence of the ribosomal RNA gene of bacteria used in the study. ^{GS}– bacteria from green snow, ^{MP}– bacteria from temporary

meltwater ponds, * - strains selected for detail pigment analysis, evaluation of blue light effect on pigments production and photostability testing, gray color – no growth.

Genus	Strain name and collection №	Accession Number	Growth T°C		
Proteobacteria			**5**	**15**	**25**
***Pol**aromonas*	*Polaromonas* sp. BIM B-1676 [GS]	MT890199			
***Pse**udomonas*	*Pseudomona extremaustralis* BIM B-1672 [GS]	MT890192			
	Pseudomona fluorescens BIM B-1668 [GS]	MT89019			
	Pseudomona leptonychotis BIM B-1559[MP]	ON248066			
	Pseudomona leptonychotis BIM B-1568[MP]	ON248076			
	Pseudomona leptonychotis BIM B-1566[MP]	ON248077			
	Pseudomona lundensis BIM B-1554[MP]	ON248061			
	Pseudomonas lundensis BIM B-1555[MP]	ON248062			
	Pseudomonas lundensis BIM B-1556[MP]	ON248063			
	Pseudomonas peli BIM B-1560[MP]	ON248067			
	Pseudomonas peli BIM B-1569[MP]	ON248075			
	Pseudomonas peli BIM B-1546 [MP]	ON248078			
	Pseudomonas peli BIM B-1552[MP]	ON248080			
	Pseudomonas peli BIM B-1542[MP]	ON248083			
	Pseudomonas peli BIM B-1548[MP]	ON248084			
	Pseudomonas sp. BIM B-1635[GS]	MT890174			
	Pseudomonas sp. BIM B-1667[GS]	MT890189			
	Pseudomonas sp. BIM B-1673[GS]	MT890191			
	Pseudomonas sp. BIM B-1674[GS]	MT890193			
Psychrobacter	*Psychrobacter glacinicola* BIM B-1629[GS]	MT890168			
	Psychrobacter urativorans BIM B-1655 [GS]	MT890181			
	Psychrobacter urativorans BIM B-1662[GS]	MT890182			
Shewanella	*Shewanella baltica* BIM B-1565[MP]	ON248060			
	Shewanella baltica BIM B-1557[MP]	ON248064			
	Shewanella baltica BIM B-1561[MP]	ON248069			
	Shewanella baltica BIM B-1563[MP]	ON248072			
Acinetobacter	*Acinetobacter lwoffii* BIM B-1558[MP]	ON248065			
Bacteroidetes					
Flavobacterium	**Flavobacterium degerlachei* BIM B-1562[MP]	ON248071			
Actinobacteria					
Agrococcus	**Agrococcus citreus* BIM B-1547[MP]	ON248081			
Arthrobacter	**Arthrobacter agilis* BIM B-1543 [MP]	ON248082			
	**Arthrobacter cryoconiti* BIM B-1627[GS]	MT890166			
	Arthrobacter oryzae BIM B-1663[GS]	MT890183			
	Arthrobacter sp. BIM B-1624[GS]	MT890163			
	Arthrobacter sp. BIM B-1625 [GS]	MT890164			
	Arthrobacter sp. BIM B-1626[GS]	MT890165			
	Arthrobacter sp. BIM B-1628[GS]	MT890167			
	Arthrobacter sp. BIM B-1664[GS]	MT890186			
	Arthrobacter sp. BIM B-1666[GS]	MT890188			
	Arthrobacter sp. BIM B-1656[GS]	MT890194			
	**Arthrobacter* sp. BIM B-1549[MP]	ON248073			
Brachybacterium	*Brachybacterium paraconglomeratum* BIM B-1571 [MP]	ON248074			
Cryobacterium	*Cryobacterium arcticum* BIM B-1619 [GS]	MT890158			
	Cryobacterium soli BIM B-1620 [GS]	MT890159			
	Cryobacterium soli BIM B-1658[GS]	MT890196			
	**Cryobacterium soli* BIM B-1659[GS]	MT890197			
	Cryobacterium soli BIM B-1677[GS]	MT890198			
	Cryobacterium soli BIM B-1675[GS]	MT890200			
Leifsonia	*Leifsonia antarctica* BIM B-1631[GS]	MT890170			
	Leifsonia antarctica BIM B-1632[GS]	MT890171			
	Leifsonia antarctica BIM B-1637 [GS]	MT890176			
	**Leifsonia antarctica* BIM B-1638 [GS]	MT890177			
	Leifsonia antarctica BIM B-1639 [GS]	MT890178			
	Leifsonia antarctica BIM B-1669 [GS]	MT890179			

	Leifsonia antarctica BIM B-1671[GS]	MT890184			
	Leifsonia kafniensis BIM B-1633[GS]	MT890172			
	Leifsonia rubra BIM B-1622 [GS]	MT890161			
	Leifsonia rubra BIM B-1623 [GS]	MT890162			
	Leifsonia rubra BIM B-1634 [GS]	MT890173			
	**Leifsonia* sp. BIM B-1567[MP]	ON248088			
Micrococcus	*Micrococcus luteus* BIM B-1545[MP]	ON248079			
Paeniglutamicibacter	**Paeniglutamicibacter antarcticus* BIM B-1657[GS]	MT890195			
Rhodococcus	*Rhodococcus erythropolis* BIM B-1660[GS]	MT890201			
	Rhodococcus erythropolis BIM B-1661[GS]	MT890202			
	**Rhodococcus yunnanensis* BIM B-1621[GS]	MT890160			
	Rhodococcus yunnanensis BIM B-1670[GS]	MT890185			
Salinibacterium	*Salinibacterium* sp. BIM B-1630 [GS]	MT890169			
	Salinibacterium sp. BIM B-1636[GS]	MT890175			
	Salinibacterium sp. BIM B-1654[GS]	MT890180			
	Salinibacterium sp. BIM B-1665[GS]	MT890187			
Firmicutes					
Facklamia	*Facklamia tabacinasalis* BIM B-1577[MP]	ON248087			
Sporosarcina	*Sporosarcina* sp. BIM B-1539 [MP]	ON248068			
Carnobacterium	*Carnobacterium funditum* BIM B-1541[MP]	ON248085			
	Carnobacterium iners BIM B-1544[MP]	ON248086			
	Carnobacterium inhibens BIM B-1540[MP]	ON248070			

Table S2. Parameters for Find by Feature algorithm.

№	Parameter	Value
Elements and limits		
1	C	5-60
2	H	0-120
3	O	0-4
4	N	0
5	S	0-4
6	Cl	0
7	P	0-4
Charge carrier		
8	Positive ions	H, Na, K
9	Negative ions	None
10	Neutral looses	H_2O

Table S3. Parameters for Find by Formula algorithm.

№	Parameter	Value
Match tolerance		
1	Masses	+/- 15.00
2	Retention times	+/- 0.350
Result filters		
3	Warn if score	<20.00
4	Do not match if a score	<10.00
5	Maximum m/z differents, ppm	5.00
Charge carrier		
6	Positive ions	H, Na, K, NH_4, electron
7	Negative ions	None
8	Neutral losses	H_2O
9	Charge state range	2

10	Aggregates	Dimers

Table S4. Summary of electron spectroscopy for MeOH extracts.

Sample	Absorbance maxima, nm	A_{450}	Biomass color	Extract color	Remark
Flavobacterium degerlachei BIM B-1562	269, 335, 447, 474	0.538	Yellow	Extensive yellow	The sample is practically discolored
Arthrobacter sp. BIM B-1549	262, 335, 447, 467	0.137	Yellow	Extensive yellow	The sample is discolored
Agrococcus citreus BIM B-1547	263, 336, 439, 465	0.054	Yellow	Slightly yellow	The sample is practically discolored
Arthrobacter agilis BIM B-1543	260, 317, 386, 491, 522	0.096	Red	Extensive red	The sample is practically discolored
Leifsonia rubra BIM B-1567	262, 335, 450	0.288	Yellow	Extensive yellow	The sample is practically discolored
Rhodococcus yunnanensis BIM B-1621	261, 336, 450	0.464	Yellow	Extensive yellow	The sample is practically discolored
Arthrobacter cryoconiti BIM B-1627	263, 327, 417, 434, 467	0.277	Yellow	Extensive yellow	The sample is practically discolored
Leifsonia antarctica BIM B-1638	262, 412, 438, 468	0.013	Yellow	Slightly yellow	The sample is discolored
Paeniglutamicibacter antarcticus BIM B-1657	261, 412, 439, 467	0.127	Yellow	Extensive yellow	The sample is discolored
Cryobacterium soli BIM B-1659	260, 450, 469	0.065	Yellow	Extensive yellow	The sample is practically discolored

Table S5. Analysis of the extracted bacterial pigments by HPLC-MS and peaks maxima of the pigments measured by FT-Raman, Un. -unknown, *Standards added to the spectral library.

N	Name	HPLC-DAD-MS		FT-Raman		HPLC-MS (Peak area, 450 nm)									
		Brutto Formula	Absorption maximum, nm	c.d.b.	Main FT-Raman peaks maxima, cm^{-1}	*Flavobacterium degerlachei*	*Arthrobacter* sp.	*Arthrobacter cryoconiti*	*Arthrobacter agilis*	*Rhodococcus yunnanensis*	*Cryobacterium soli*	*Leifsonia antarctica*	*Leifsonia rubra*	*Agrococcus citreus*	*Paeniglutamicibacter antarcticus*
1	Farnesyl diphosphate (precursors)	$C_{15}H_{28}O_7P_2$	370, 460					**26**			**6**				
2	Geranylgeranyl diphosphate (precursors)	$C_{20}H_{36}O_7P_2$	441, 466, 498						**7**		**15**		**3**		**12**
3	Lycopene*	$C_{40}H_{56}$	296, 364, 447, 473, 504	11	1519,1158,1003					**14**	**138**		**873**		
4	beta-Carotene*	$C_{40}H_{56}$	278, 353, 429	11	1523,1158,1006	**17**									
5	Neurosporene*	$C_{40}H_{58}$	328, 413, 436, 465	9	1530,1158,1007		**4**					**22**			
6	zeta-Carotene	$C_{40}H_{60}$	295, 377, 398, 422	7		**11**									
7	Phytoene*	$C_{40}H_{64}$	276, 284, 294	3	Not detectable								**888**		
8	Echinenone*	$C_{40}H_{54}O$	460, 466	11	1523,1158,1006	**43**	**14**		**33**				**7**		
9	Canthaxanthin*	$C_{40}H_{52}O_2$	466, 476	11	1521,1158,1006	**43**				**365**					
10	Zeaxanthin*	$C_{40}H_{56}O_2$	275, 341, 429, 448, 473	11	1526,1158,1006	**21**	**14**			**124**					**18**
11	Nonaflavuxanthin	$C_{45}H_{64}O$	440, 468	11			**40**							**101**	**6**
12	Dihydroisopentenyldehydrorhodopin	$C_{45}H_{66}O$	457, 463, 484							**11**					
13	Bisanhydrobacterioruberin	$C_{50}H_{72}O_2$	370, 388, 465, 494, 527	13								**298**			
14	Flavuxanthin	$C_{50}H_{72}O_2$	416, 440, 468	11			**87**	**1007**				**23**	**82**	**21**	**3**
15	Decaprenoxanthin	$C_{50}H_{72}O_2$	428, 452, 482	11			**415**		**83**	**556**	**703**				
16	Dihydrobisanhydrobacterioruberin	$C_{50}H_{74}O_2$	416, 440, 469, 484	12		**21**	**290**	**378**	**63**						**184**
17	Monoanhydrobacterioruberin	$C_{50}H_{74}O_3$	–						**8**	**18**	**11**		**5**	**13**	
18	Bacterioruberin* (5Z)-Bacterioruberin (9Z)-Bacterioruberin (13Z)-Bacterioruberin 5Z.9'Z-bacterioruberin 9Z.9'Z-bacterioruberin	$C_{50}H_{76}O_4$	254, 329, 346, 365	16	1507/1482,1145,997	**11**									
Un.						**10**	**0**	**341**	**468**	**107**	**52**	**0**	**7**	**583**	**264**

1
2
3

ISBN: 978-82-575-2122-6
ISSN: 1894-6402

Norwegian University
of Life Sciences

Postboks 5003
NO-1432 Ås, Norway
+47 67 23 00 00
www.nmbu.no

119505 / MEDIEHUSET-ANDVORD.NO